Abstract of "Aspects of Scattering Amplitudes: Tensor Diagrams, Hyperbolic Volumes, and Celestial Sphere" by Lecheng Ren, Ph.D., Brown University, May 2024.

In this thesis, we present studies of the structures of loop-level amplitudes in planar $\mathcal{N} = 4$ supersymmetric Yang-Mills theory, via tensor diagrams and hyperbolic volumes, and singularity of scattering amplitudes in Yang-Mills and gravity from the celestial perspective.

First, we propose to use tensor diagrams and the Fomin-Pylyavskyy conjectures to explore the connection between symbol alphabets of n-particle amplitudes in planar $\mathcal{N} = 4$ super Yang-Mills theory and certain polytopes associated to the Grassmannian $G(4, n)$. We show how to assign a web (a planar tensor diagram) to each facet of these polytopes. These web diagrams encode all known rational letters, and all square roots of the known algebraic letters up to $n = 9$.

Second, we provide an explicit analytic result for the one-loop scalar n-gon Feynman integral in n dimensions, for even n, with massless or massive internal and external edges. The result can be represented by the volume of a hyperbolic object called orthoscheme. Furthermore, we evaluate the general six-dimensional hexagon integral in terms of classical polylogarithms.

Finally, we show that associativity of the tree-level OPE in a celestial CFT imposes constraints on the coupling constants of the corresponding bulk theory. The constrained theories are interesting as apparently well-defined celestial CFTs with a deformed $w_{1+\infty}$ symmetry algebra. We explicitly work out the ramifications of these constraints on scattering amplitudes and find that all n-point amplitudes constructible solely from holomorphic or anti-holomorphic three-point amplitudes vanish on the support of these constraints. We then studied the regular terms of the OPE of MHV amplitudes and the partial differential equations the MHV celestial amplitudes should satisfy. These PDEs originate from BCFW recursion of bulk amplitudes. We also investigate further structures of the celestial dual of planar $\mathcal{N} = 4$ SYM theory from dual superconformal symmetry.

Aspects of Scattering Amplitudes: Tensor Diagrams, Hyperbolic Volumes, and Celestial Sphere

by

Lecheng Ren

A dissertation submitted in partial fulfillment of the
requirements for the Degree of Doctor of Philosophy
in the Department of Physics at Brown University

Providence, Rhode Island
May 2024

This dissertation by Lecheng Ren is accepted in its present form by the Department of Physics as satisfying the dissertation requirement for the degree of Doctor of Philosophy.

Date ______________ ______________________________
Anastasia Volovich, Advisor

Recommended to the Graduate Council

Date ______________ ______________________________
Anastasia Volovich, Reader

Date ______________ ______________________________
Antal Jevicki, Reader

Date ______________ ______________________________
JiJi Fan, Reader

Approved by the Graduate Council

Date ______________ ______________________________
Thomas A. Lewis
Dean of the Graduate School

Lecheng Ren | *Curriculum Vitae*

lecheng_ren@brown.edu

Department of Physics, Brown University, Providence RI 02912

Education

Bachelor's degree in Physics — Beijing Normal University
September 2015 – June 2019

Undergraduate Exchange Program in Physics — College of William and Mary
July 2017 – August 2017

Undergraduate research program — ITP, CAS
May 2018 – June 2019 — Professor: Song He

PhD in Physics (candidate) — Brown University
September 2019 – — Professor: Anastasia Volovich

Publications

1. "Notes on polytopes, amplitudes and boundary configurations for Grassmannian string integrals," JHEP 04 (2020) 140 [arXiv:2001.09603], with S. He and Y. Zhang.
2. "Symbol alphabets from tensor diagrams," JHEP 12 (2021) 079 [arXiv:2106.01405], with M. Spradlin and A. Volovich.
3. "Celestial dual superconformal symmetry, MHV amplitudes and differential equations," JHEP 12 (2021) 171 [arXiv:2106.16111], with Y. Hu, A. Y. Srikant, and A. Volovich.
4. "Deformed $w_{1+\infty}$ Algebras in the Celestial CFT," SIGMA 19 (2023) 044 [arXiv:2111.11356], with J. Mago, A. Y. Srikant, and A. Volovich.
5. "On effective field theories with celestial duals," JHEP 08 (2022) 251 [arXiv:2206.08322], with M. Spradlin, A. Y. Srikant, and A. Volovich.
6. "Loop-level gluon OPEs in celestial holography," JHEP 11 (2022) 171 [arXiv:2208.14416], with R. Bhardwaj, L. Lippstreu, M. Spradlin, A. Y. Srikant and A. Volovich.
7. "All-order celestial OPE from on-shell recursion," JHEP 10 (2023) 080 [arXiv:2305.11851], with A. Schreiber, A. Sharma, and D. Wang.
8. "One-loop Integrals from Volumes of Orthoschemes," [arXiv:2306.04630], with M. Spradlin, C. Vergu, and A. Volovich.
9. "A double copy from twisted (co)homology at genus one," [arXiv:2312.02148], with R. Bhardwaj, A. Pokraka, and C. Rodriguez.
10. "Five-dimensional spinor helicity for all masses and spins," *to appear*, with A. Pokraka, S. Rajan, M. Spradlin, and A. Volovich.

Presentations

1. Short Talk, "Symbol Alphabets from Tensor Diagrams," Mainz Institute for Theoretical Physics, June 2021.

2. Gong Show, "Deformed $w_{1+\infty}$ Algebras in the Celestial CFT," Princeton Center for Theoretical Science, Princeton University, February 2022.
3. "On Effective field theory with celestial dual," Possible and Impossible in Effective Field Theory: From the S-Matrix to the Swampland, IAS, May 2022.
4. Gong Show, "All-order OPE expansion from MHV amplitudes," Joint BHI/CMSA Conference on Flat Holography, CMSA, Harvard University, June 2022.
5. Poster Presentation, "Deformed $w_{1+\infty}$ Algebras in the Celestial CFT," String 2022, University of Vienna, July 2022.
6. Poster Presentation, "Deformed $w_{1+\infty}$ Algebras in the Celestial CFT," Amplitudes 2022, Charles University, August 2022.
7. Invited talk, "On Effective field theory with celestial dual," Tianjin University, June 2023.
8. Invited talk, "On Effective field theory with celestial dual," Beijing Normal University, June 2023.
9. Invited talk, "On Effective field theory with celestial dual," ITP CAS, June 2023.
10. Invited talk, "One-loop Integrals from Volumes of Orthoschemes," ITP CAS, June 2023.
11. "On structures of celestial OPE and algebras," Amplifying Gravity at All Scales, Nordita, July 2023.
12. Gong show, "One-loop Integrals from Volumes of Orthoschemes," Amplitudes School 2023, CERN, August 2023.
13. Poster Presentation, "The twisted cohomology of Riemann-Wirtinger integrals," Amplitudes 2023, CERN, August 2023.
14. Invited talk, "The one-loop six-dimensional hexagon integral," Amplitudes Seminar, Bonn University, November 2023.

Conferences and Workshops Attended

1. The Ninth New England String Meeting, Brown University (virtual), April 2020.
2. Amplitudes 2020, Brown University (virtual), May 2020.
3. "Positive Geometries in Scattering Amplitudes and Beyond" workshop, Mainz Institute for Theoretical Physics, Johannes Gutenberg University (virtual), June 2021.
4. "Celestial Amplitudes and Flat Space Holography" workshop, Corfu Summer Institute (virtual), August 2021.
5. Amplitudes 2021, Niels Bohr Institute (virtual), August 2021.
6. Celestial holography workshop, Princeton University (virtual), February 2022.
7. Research visiting, IAS, March 2022.
8. "Possible and Impossible in Effective Field Theory: From the S-Matrix to the Swampland" workshop, IAS, May 2022.
9. Joint BHI/CMSA Conference on Flat Holography, CMSA, Harvard University, June 2022.
10. String 2022, University of Vienna, July 2022.
11. "Novel Developments in Scattering Amplitudes" workshop, MIAPbP, July – August 2022.
12. Amplitudes 2022, Charles University, August 2022.

13. The Tenth New England String Meeting, Brown University, April 2023.
14. “Amplifying Gravity at All Scales” workshop, Nordita, July 2023.
15. “From Amplitudes to Gravitational Waves” conference, Nordita, July 2023.
16. Amplitudes School 2023, CERN, August 2023.
17. Amplitudes 2023, CERN, August 2023.
18. “Brin MRC Workshop on Polylogarithms, Cluster Algebras, and Scattering Amplitudes”, University of Maryland, September 2023.
19. “Celestial kickoff Workshop”, Harvard University, October 2023.
20. “Solving $\mathcal{N}=4$ super-Yang-Mills theory via Scattering Amplitudes”, Simons Center for Geometry and Physics, January — February 2024.
21. “Positive Geometry in Particle Physics and Cosmology” ERC kickoff workshop, MPI MiS, February 2024.

Fellowship and Awards

Galkin Foundation Fellowship
Department of Physics, Brown University — 2023 - 2024

Teaching Experience

Basic Physics A — Teaching Assistant
Main work: Giving lectures in the lab sections and grading lab reports — Fall 2019

Instruction to Relativity, Waves and Quantum Mechanics — Teaching Assistant
Main work: Giving lectures in the lab sections and grading lab reports — Spring 2020

Foundation of Electromagnetism and Modern Physics — Teaching Assistant
Main work: Giving lectures in the lab sections and grading lab reports — Spring 2020

Basic Physics A — Teaching Assistant
Main work: Supervising problem session and grading exams — Autumn 2020

Statistical Mechanics — Teaching Assistant
Main work: Holding problem session, grading homework and exams — Spring 2021

Quantum Mechanics — Teaching Assistant
Main work: Holding problem session, grading homework and exams — Autumn 2022

Electrodynamics — Teaching Assistant
Main work: Holding problem session, grading homework and exams — Spring 2023

Preface

This thesis is based on the following works:

One-loop Integrals from Volumes of Orthoscheme
L.Ren, M. Spradlin, C.Vergu, A. Volovich
In review at JHEP [arXiv:2306.04630]

All-order celestial OPE from on-shell recursion
L. Ren, A. Schreiber, A. Sharma, D. Wang
JHEP 10 (2023) 080 [arXiv:2305.11851]

On effective field theories with celestial duals
L. Ren, M. Spradlin, A. Y. Srikant, A. Volovich
JHEP 08 (2022) 251 [arXiv:2206.08322]

Deformed $w_{1+\infty}$ Algebras in the Celestial CFT
J. Mago, L. Ren, A. Y. Srikant, A. Volovich
SIGMA 19 (2023) 044 [arXiv:2111.11356]

Celestial dual superconformal symmetry, MHV amplitudes and differential equations
Y. Hu, L. Ren, A. Y. Srikant, A. Volovich
JHEP 12 (2021) 171 [arXiv:2106.16111]

Symbol alphabets from tensor diagrams
L. Ren, M. Spradlin, A. Volovich
JHEP 12 (2021) 079 [arXiv:2106.01405]

Acknowledgments

First and foremost, I am deeply grateful to my advisor, Anastasia Volovich, for her incredible guidance, support, and patience throughout my PhD. Her mentorship has been essential to my growth in academia. I'll always value her teachings in physics, her insights into nature, and her significant role in my development toward becoming a proficient physicist. I'm also sincerely grateful to Marcus Spradlin, who acts like a second advisor of mine, for his invaluable advice and encouragement in my research. Professor Spradlin is always patient with all my questions, no matter how straightforward they might be.

I am also grateful to the entire high energy theory group faculty, including Stephon Alexander, JiJi Fan, Jim Gates, Antal Jevicki, Savvas Koushiappas, and David Lowe. Their extensive knowledge and engaging physics discussions have greatly contributed to my learning and research. I would like to especially thank Professor Jevicki and Professor Fan for taking the time to read my thesis.

I would like to thank Song He for his warm hospitality when I was back in China and for his generous support through the recommendation letters he has written on my behalf. I am also grateful to Akshay Yelleshpur and Andrzej Pokraka for all their patience and invaluable guidance. Their willingness to invest time in clarifying my confusion has improved my knowledge and research skills. I would also thank my collaborators, Rishabh Bhardwaj, Yangrui Hu, Luke Lippstreu, Jorge Mago, Carlos Rodriguez, Anders Schreiber, Atul Sharma, Cristian Vergu, Diandian Wang, and Yong Zhang, for their camaraderie, stimulating discussions, and shared moments that have enriched my research experience.

I would like to thank all my other colleagues in Brown high energy theory group, Adam Ball, Shounak De, Konstantinos Koutrolikos, Chang Liu, Xianlong Liu, Sze-Ning Hazel Mak, Giulio Salvatori, Marcos Skowronek, Stefan Stanojevic, He-Chen Weng, and Junjie Zheng, for enriching this experience with their friendship and academic solidarity, making my path through PhD both memorable and rewarding.

I'm thankful to my friends for providing a much-needed balance to my life, offering both distractions and support when most needed. Thank you, James, Michael, Hao-Lan, Lingfeng, Shannon, Tianyu, Xiangcheng, Xiazi, Yibo, and Zack for all the unforgettable moments of fun.

Last but not least, I must extend my profound appreciation to my family for their love, patience, and confidence in me. I am especially grateful for the mutual exchange of strength and comfort, and the support and solace we've shared during the most challenging time.

Contents

List of Figures

Chapter 1

Introduction

The Standard Model of particle physics describes three of the four fundamental forces of nature – electromagnetic, weak, and strong. It is based on quantum mechanics and special relativity, wedded to a powerful mathematical framework called quantum field theory (QFT). It has been used to make remarkably precise predictions of the cross-sections that are measured in particle experiments, notably those conducted at the Large Hadron Collider (LHC). The computation of cross sections is based on a physical quantity called *scattering amplitudes*. The most widely used method to compute scattering amplitudes in quantum field theories since the 1950s is the *Feynman path integral* [7]. For generic quantum field theories, Feynman path integral can only be computed via perturbation theory at weak coupling, where amplitudes can be represented by the summation of *Feynman diagrams*. The Feynman diagram is a highly efficient and visualized way of computing the amplitudes of a scattering process and plays a fundamental role in the construction of the Standard model.

However, the computation via Feynman integral will become drastically cumbersome as the loop level or multiplicity increases. For example, the number of Feynmann diagrams contributing to n-gluon tree-level amplitudes in pure Yang-Mill (YM) theory is:

n	3	4	5	6	7	8	9	$\cdots$
number of diagrams	1	3	10	38	154	654	2871	$\cdots$

On the other hand, after summing up these huge number of diagrams, dramatic simplification may occur and the amplitudes can be represented by only a few terms. For example, the tree-level gluon amplitudes in the maximally-helicity-violating (MHV) sector of YM theory are given by the famous Parke-Taylor formula [8]:

$$A(1^-2^-3^+\cdots n^+) = \frac{\langle 12\rangle^4}{\langle 23\rangle\langle 34\rangle\cdots\langle n1\rangle}\,. \tag{1.1}$$

Therefore, one would expect a novel way to obtain (1.1) without the tiring computation in the traditional Feynman method. More explicitly speaking, this method would derive the amplitudes directly from the basic principle of quantum field theories — locality and unitarity — bypassing the complexities on the detour going through the Lagrangian formalism and Feynman path integral.

The answer to this is *on-shell recursion*. The idea is performing a complex shift by a parameter z on external momenta, and the full amplitudes — as a rational function of external kinematics — can be obtained from collecting all the residues on poles of the amplitudes by Cauchy theorem. According to locality, each pole should correspond to a factorization channel of the amplitudes. Also, by unitarity, the residue on each pole — where the propagator goes on-shell – should correspond to subamplitudes that the full amplitudes factorize into. Therefore the n-point amplitude is completely determined in terms of lower-point on-shell amplitudes as

$$A_n = \sum_I \hat{A}_{\mathrm{L}}(z_I)\frac{1}{P_I}\hat{A}_{\mathrm{R}}(z_I)\,, \tag{1.2}$$

where $\hat{A}$ denotes shifted amplitudes, and the sum is over all possible factorization channels I.

The first and the most famous example of on-shell recursion relation is the so-called Britto-Cachazo-Feng-Witten (BCFW) recursion [9, 10], which applies a specific type of momentum shift on only two external momenta (called BCFW shift). The BCFW recursion relation provides a way to systematically construct higher point amplitudes from lower point amplitudes iteratively without having to write down all Feynman diagrams from scratch. For example, using BCFW recursion one can inductively prove the Parke-Taylor formula (1.1) for tree-level gluon amplitudes in the MHV sector.

Beyond the MHV sector, one can also use BCFW recursion to compute all n-point tree-level amplitudes in pure YM theory. Additionally, there is another type of on-shell recursion relation, which applies all-line shift [11] to external momenta. Such recursion leads to the representation of N^KMHV amplitudes by $(K+1)$ MHV subamplitudes. This construction is known as MHV expansion or Cachazo-Svrcek-Witten (CSW) expansion [12].

BCFW recursion relation and CSW expansion gave a nice and elegant way of understanding tree-level amplitudes. This success leads to the question of whether similarly straightforward methods exist for constructing loop amplitudes, suggesting for further exploration to simplify and better understand the calculations within quantum field theory.

We would concentrate on amplitudes in the planar maximally supersymmetric Yang-Mills theory ($\mathcal{N} = 4$ SYM), as it is one of the simplest theories to develop new tools for understanding the dynamics of 4-dimensional quantum field theories. One perspective of simplicity originates from its infinitely dimensional symmetry hidden from Lagrangian formalism. To represent the symmetry manifestly, one has to perform a reparametrization of external kinematics. Consider scattering amplitudes of n massless particles, labeled by momenta p_i. The dual momenta is defined as:

$$y_i^\mu - y_{i+1}^\mu = p_i^\mu\,. \tag{1.3}$$

The next step is to introduce another new variable via incidence relations:

$$[\mu_i^a| := \langle i|_{\dot{a}} y_i^{\dot{a}a} = \langle i|_{\dot{a}} y_{i+1}^{\dot{a}a}\,. \tag{1.4}$$

Note that the second equality is because all momenta are massless. We then pair the μ variables with half of the spinor helicity formalism into a four-vector:

$$Z_i^I := \left(|i\rangle^{\dot{a}}, [\mu_i|^a\right), \tag{1.5}$$

where $I = (\dot{a}, a)$ as an $SU(2,2)$ index. This new four-component variables Z_i^I are called *momentum twistors* [13]. According to [14], the planar $\mathcal{N}=4$ SYM theory enjoys the *dual conformal symmetry*, which acts as $GL(4)$ transformations on momentum twistors. We can construct dual conformal invariants from the $SU(2,2)$ Levi-Civita symbol,

$$\langle ijkl\rangle := \varepsilon_{IJKL} Z_i^I Z_j^J Z_k^K Z_l^L\,. \tag{1.6}$$

When $\mathcal{N}=4$ supersymmetry is imposed, the amplitudes of all the states in the supermultiplet combine into a superamplitude, and the momentum twistors and dual conformal symmetry can be promoted into *momentum supertwistors* denoted by $\mathcal{Z}$ and the $SU(2,2|4)$ *dual superconformal symmetry* [14] respectively. Note that $\mathcal{N}=4$ SYM also enjoys the $SU(2,2|4)$ superconformal symmetry from Lagrangian formalism. If we combine the generators in these two symmetries, we can obtain an infinite-dimensional symmetry called *Yangian symmetry* [15].

Yangian symmetry plays a crucial role in planar $\mathcal{N}=4$ SYM theory and one can construct all loop amplitudes from Yangian invariant functions. The n-point all loop N^KMHV superamplitude is conventionally written by factoring out the tree-level MHV amplitude:

$$\mathcal{A}_n^{\mathrm{N}^K\mathrm{MHV}} = \mathcal{A}_{n,\mathrm{tree}}^{\mathrm{MHV}}\,\mathcal{P}_n^{\mathrm{N}^K\mathrm{MHV}}(\epsilon)\,, \tag{1.7}$$

where ϵ is the regulator controlling the IR divergence. The IR divergence and dual conformal anomalies of $\mathcal{N}=4$ SYM amplitudes are captured by 1-loop MHV amplitudes via the BDS Ansatz [16]

$$\mathcal{P}_n^{\mathrm{MHV(BDS)}}(\epsilon) = \exp\left[\sum_{L=1}^{\infty}\lambda^L\left(f^{(L)}(\epsilon)\mathcal{P}_{n,1}^{\mathrm{MHV}}(L\epsilon) + C^{(L)} + O(\epsilon)\right)\right], \tag{1.8}$$

where $\lambda = g_{\mathrm{YM}}^2 N_c/(16\pi^2)$ is the 't Hooft coupling, and the functions $f^{(L)}$ are of the form $f^{(L)}(\epsilon) = f_0^{(L)} + \epsilon f_1^{(L)} + \epsilon^2 f_2^{(L)}$. The constants $f_\bullet^{(L)}$ and $C^{(L)}$ are independent of the number of external legs n. Therefore one can represent the amplitudes by BDS normalization:

$$\mathcal{A}_n^{\mathrm{N}^K\mathrm{MHV}} = \mathcal{A}_{n,\mathrm{tree}}^{\mathrm{MHV}}\,\mathcal{P}_n^{\mathrm{MHV(BDS)}}(\epsilon)\,R_{n,K} \tag{1.9}$$

where $R_{n,K}$ is called *ratio function* or *BDS-substracted amplitudes*. The ratio functions are IR finite and strictly speaking it is these ratio functions that respect the Yangian symmetry. One can then perform the following expansion

$$R_{n,K} = \sum_{\sigma_1,\cdots,\sigma_K} Y_n^{\sigma_1} Y_n^{\sigma_2}\cdots Y_n^{\sigma_K}\cdot V_{n,K}^{\{\sigma_i\}}\,. \tag{1.10}$$

The Y functions are conventionally called *Yangian invariants* and can be represented in terms of Grassmannian integrals [17, 18]. The functions V are dual conformal invariant and can then be expanded in loop order as

$$V_{n,K} = 1 + \sum_{L=1}^{\infty}\lambda^L V_{n,K}^{(L)}\,. \tag{1.11}$$

In particular, $V_{n,0}^{(1)} = 0$ and $R_{n,0}^{(1)} = 1$ since all the information of 1-loop MHV amplitudes has been absorbed in the BDS ansatz. In general, the functions $V_{n,K}^{(L)}$ are highly nontrivial transcendental functions of weight $2L$. Over the past decades, numerous elegant mathematical structures of loop amplitudes have been discovered. These structures have led to the development of techniques that have largely simplified the computation and deepened our understanding of loop amplitudes. In the next two sections, we will introduce several techniques on loop amplitudes of $\mathcal{N} = 4$ SYM that were studied in papers that this thesis is based on.

1.1 Symbol alphabets in $\mathcal{N} = 4$ SYM theory

As previously noted, the loop amplitudes in $\mathcal{N} = 4$ SYM include highly nontrivial transcendental functions. In this thesis, we would only concentrate on the simplest type of these — the *multiple polylogarithms* (MPL).

One technique to study MPL is known as *symbols* [19], which is a map from MPLs to a tensor product of *symbol alphabets*. For the ratio functions in loop amplitudes, these symbol alphabets are homogeneous polynomials of the four-brackets given in (1.6) due to dual conformal invariance. The symbols uncover the branch points, discontinuities, and differential structures of MPLs, and more importantly, make highly nontrivial identities between MPLs manifest. In physics literature, the symbol technique has been used to reduce the 6-point 2-loop MHV ratio function from a 17-page-long formula [20] into only a few lines [21]. This success raises our old question of whether new, straightforward methods can be developed to derive these simple results more directly.

The first understanding of the structure of the ratio functions was via the anomaly function of dual superconformal symmetry, namely the $\bar{Q}$ equations [22],. Perturbatively, the $\bar{Q}$ equations express the derivatives of L-loop n-point amplitudes in terms of one-fold integrals of $(L-1)$-loop $(n+1)$-point amplitudes, thus is a powerful tool to compute the higher loop level amplitudes. So far, the $\bar{Q}$ equations have been used to compute the symbol of loop amplitudes up to 3-loop 8-point in the MHV sector, and 2-loop 9-point in NMHV sector [22, 23, 24, 25, 26].

Another approach to deriving symbols loop amplitudes is known as *cluster bootstrap program* [27]. The general idea of the program is to find the elements in the space of tensor products of symbol alphabets that satisfy a series of restrictions from physics. In the end, it is believed that one can obtain a unique element that meets all the physical conditions. The first step and the key to this method is finding a proper list of symbol alphabets as the input of the bootstrap. So far there is only an effective conjecture up to 7 points, suggesting the symbol alphabets are *cluster $\mathcal{X}$-coordinates* in cluster algebra [28]. For amplitudes within 7 points, there are only finitely many of these coordinates, therefore one can always perform the bootstrapping program. However, for 8-point and beyond there exist infinitely many such coordinates. Since the ratio function is finite, we have to select a finite subset of these infinitely many coordinates. However, there is still a lack of data on the pattern of the symbol alphabets appearing, except by direct computation from Feynman integrals. Therefore one has to find an algorithm to truncate the infinite cluster algebra to "predict" the symbol alphabets.

There has been several approaches so far including Landau analysis [29, 30], tropical Grassmannian [31, 32, 33], and Shubert analysis [34]. Here we will discuss an approach involving *Grassmannian string integrals* and *tensor diagrams*. In [35], we defined a map from finitely many boundary configurations of Grassmannian string integrals to a specific type of cluster coordinates of momentum twistors. These cluster coordinates can be nicely organized into an object called tensor diagrams. However, the set of symbol alphabets we obtained from tensor diagrams is still larger than the actual data computed from $\bar{Q}$ equations in [24, 25, 26]. This discrepancy hints at the requirement for refining our method, with the hope of developing a more precise approach for predicting symbol alphabets in future investigations.

In Chapter 2 we will show how this approach can be used to truncate the infinite cluster algebra and produce a finite list of symbol alphabets. We will also see how these symbol alphabets can be nicely organized into tensor diagrams which also help visualize and simplify the calculus of cluster coordinates.

1.2 One loop amplitudes and hyperbolic orthoscheme

Having discussed the abundant story on symbols of loop amplitudes, it's still necessary to elevate the full functions from its symbols, since amplitude is always a function that yields specific numerical values, instead of an abstract tensor product. However, there are no sufficiently powerful mathematical tools that could obtain a full function from its symbol.

In [36] we took one step towards addressing this question. In particular, we studied the class of MPLs that appear in the most generic one-loop Feynman integrals of n-gon in n-dimension. For odd n the integral can be represented by m-gon integrals in m-dimension with even m and $m < n$ via a generalized version of Gauss-Bonnet theorem [37, 38]. One key and beautiful mathematical fact about the n-gon is that the same integral computes the volume of a simplex in $(n-1)$-dimensional hyperbolic space whose shape is set by the (Euclidean) kinematic data and propagator masses [39, 40].

Based on this connection, we provided the explicit formula for the integral in terms of MPLs in our paper. Our work was made possible by a recent mathematical breakthrough due to Rudenko, who provided an explicit formula for the volume of any (odd-dimensional) hyperbolic orthoscheme in terms of a class of functions called alternating polylogarithms [41]. Orthoschemes are generalizations of right triangles and we found an algorithm to express the volume of any simplex — and hence any (even) n-gon integral — by recursively expressing the volume of the simplex as a sum of volumes of orthoschemes. In Chapter 3, we will talk more about Rudenko's contribution on orthoschemes and how to triangulate an arbitrary hyperbolic simplex into orthoschemes to make use of Rudenko's formula.

1.3 Singularities in celestial amplitudes

While the Standard Model has been remarkably successful in making precise predictions for particle experiments, it is still regarded as an incomplete story of nature, primarily due to its inability to incorporate gravity. One basic idea to understand and construct the quantum theory of gravity is the holography principle, based on a dual theory that lives in fewer spacetime dimensions. The best understood and most successful example of this approach is the AdS/CFT correspondence [42]. It is conjectured that all observables in Anti de-Sitter (AdS) spacetime can be computed from a conformal field theory (CFT) living on its lower-dimensional boundary. Over the last 25 years, numerous complex calculations have lent substantial support to this AdS/CFT conjecture, providing compelling evidence for its validity. More recently, celestial holography [43], which is an attempt to apply the holography principle in asymptotically flat spacetimes, has offered a new perspective on quantum gravity. The key step is to express scattering amplitudes on the basis of boost eigenstates, which are known as *celestial amplitudes*. It is conjectured that the celestial amplitudes are correlators in a two-dimensional CFT on the celestial sphere, namely the *celestial CFT* (CCFT).

Following the celestial holography principle, many properties of the correlators in CCFT follow directly from the properties of scattering amplitudes. In particular, the operator product expansion (OPE) in the dual CFT is controlled by the collinear limits of scattering amplitudes. In the papers that are included in this thesis [44, 45, 46, 47], we primarily delved into such correspondence. In principle, a fundamental property of any CFT is the existence of an associative OPE. In [44, 45], we showed that for a generic EFT with arbitrary higher-dimension operators, the associativity might be violated. Therefore, demanding associativity imposes non-trivial constraints on the spectrum and Wilson coefficients of the "bulk" spacetime theory. Such constraints also have a very interesting effect on bulk theory amplitudes. My work presented a criterion for general effective field theories that are allowed to have a standard dual theory on the celestial sphere, through the behavior of scattering amplitudes. We found that for CSW-constructible amplitudes, we require that all the contributions from that only CSW-expanding three-point MHV (or $\overline{\text{MHV}}$) vertices have to vanish. Roughly speaking, each MHV (or $\overline{\text{MHV}}$) three-vertex would correspond to a chiral OPE on the celestial sphere, so associativity of the OPE would correspond to summing over all the factorization channels into three vertices in the space-time EFT. In Chapter 5 and Chapter 6, we will elaborate on how the associativity of celestial OPE affects the behaviors of spacetime EFT.

In Chapter 7, we also compute the all-order OPE in celestial YM and Einstein gravity at tree level in the MHV sector. We found that the regular terms in OPE are contributed by soft and conformal descendants of primary operators. Moreover, in Chapter 4, we will study the celestial theory dual to $\mathcal{N} = 4$ SYM in the bulk based on the emergent dual conformal symmetry discussed in the previous sections.

Chapter 2

Symbol Alphabets from Tensor Diagrams

This Chapter is based on [35].

The perturbative n-particle scattering amplitudes of planar maximally supersymmetric Yang-Mills (SYM) theory are a remarkable collection of functions that reflect deep but still partially mysterious mathematical structure. A prime example of this structure is the apparent connection [28] between their physical singularities, which for certain amplitudes (those of polylogarithmic type) are encoded in symbol letters [21] indicating where the amplitudes have logarithmic branch points, and the mathematics of cluster algebras [1]. All evidence available to date is consistent with the hypothesis that the symbol letters of all $6,7$-particle amplitudes (see [27] for a recent review) are cluster variables of the $\mathrm{G}(4,n)$ cluster algebra, whereas for $n \geq 8$ it is known that certain algebraic functions of cluster variables also appear as symbol letters (see Table 2.2)[1].

Recently this connection has been approached [50, 31, 32, 51] via the study of certain fans one can naturally associate to the tropical positive Grassmannian $\mathrm{Trop}_{>0}\,\mathrm{G}(4,n)$ (generalizing the construction of [52]) or (dually) certain "$\mathrm{G}(4,n)$-polytopes" one can associate to $\mathrm{G}(4,n)$ using the construction of [53][2]. This approach is appealing because for $n \geq 7$ the $\mathrm{G}(4,n)$-polytopes are different than cluster polytopes [58] in a way that makes them seem to more faithfully encode the symbol alphabets of SYM theory[3]. In particular, while the $\mathrm{G}(4,n)$ cluster algebra is infinite for $n \geq 8$, these polytopes are finite for any n, which matches the supposition [60] that the symbol alphabet of n-particle amplitudes might be finite for any fixed n. Moreover, while many facets of the relevant polytopes are naturally associated to certain finite subsets of cluster variables (many of which are known to appear as symbol letters of amplitudes), for $n \geq 8$ there are also "exceptional"

[1] The connection between cluster algebras and singularities of amplitudes could extend well beyond SYM theory [48, 49].

[2] The very same polytopes also appear in the study of $\mathbb{P}^{k-1}$-generalized scattering equations for biadjoint amplitudes [54, 55, 56, 57].

[3] Some finer aspects of this encoding for $n = 7$ are discussed in [32, 59].

facets that are not associated to any cluster variable. Consequently the $\mathrm{G}(4,n)$-polytopes may have room to "explain" the algebraic symbol letters that appear in $n \geq 8$-particle amplitudes[4].

There have been several different but related suggestions for how, precisely, algebraic letters are encoded in the structure of polytopes. Here we follow the framework proposed in [50], where partial information about algebraic letters is encoded in certain formal power series associated to exceptional facets. In that paper the authors studied a polytope called $\mathcal{C}^\dagger(4,8)$ (its definition is reviewed in Section 2.6.4), finding that the cluster variables associated to its 272 non-exceptional facets include the 172 (non-frozen) cluster variables known to appear as symbol letters of $n = 8$-particle amplitudes. Moreover they conjectured a formula for the series associated to its 2 exceptional facets based on explicit computation of the first three nontrivial terms in the associated series, extending the results of [6] (whose method they used), and showed that it was consistent with the expected square root of four-mass box type. Together, this was taken as evidence supporting the notion that $\mathcal{C}^\dagger(4,8)$ encodes information about the $n = 8$ symbol alphabet (see also [32], and [31, 51] which went further, fully reproducing all known algebraic letters). Unfortunately the computational complexity of the series introduced in [50] is such that computing higher order terms for $n = 8$, or any nontrivial terms for $n > 8$, seems vastly out of reach.

In this paper we bring new mathematical technology to bear on this problem: the "web diagrams" (called webs for short) and web invariants that star in the beautiful Fomin-Pylyavskyy (FP) conjectures [3]. We propose an algorithm for assigning webs to facets of $\mathrm{G}(k,n)$-polytopes. FP conjectured that the invariant associated to a web is a cluster variable if the web can be rearranged into a tree using certain graphical moves (in which case it is called "arborizable"). Exceptional facets therefore correspond to non-arborizable webs. To "almost arborizable webs" (those with only a single inner loop) we are able to associate a formal power series of webs whose invariants we can compute exactly, using a graphical recursion. In this manner we are able to compute the complete series associated to the exceptional facets of $\mathcal{C}^\dagger(4,8)$, confirming the conjecture of [50] (albeit in a slightly different basis; see Section 2.1.2).

A prime motivation for this work was to construct and study the polytope $\mathcal{C}^\dagger(4,9)$ as a candidate for encoding information about the $n = 9$ symbol letters known from [25]. We find that 3078 of its 3429 facets are associated with arborizable webs, and their invariants include all of the 522 (non-frozen) cluster variables known to appear in the $n = 9$ symbol alphabet. We find that 324 facets are associated to almost arborizable webs, and compute their web series exactly. These encode the expected 9 square roots of four-mass box type that appear in [25], as well as 315 additional, more complicated square roots. The apparent overabundance of facets suggests that $\mathcal{C}^\dagger(4,9)$ might be more complicated than needed to describe 9-particle amplitudes, although more complicated cluster variables and square roots could certainly be discovered in future computations at higher loop.

Some recent papers [63, 64, 65, 66] have explored the connection between symbol alphabets and plabic graphs [67, 68], and have in particular shown that the complete symbol alphabets for

[4] It is an interesting open question whether any information about the more complicated analytic structure of non-polylogarithmic amplitudes (that are known to appear for $n \geq 10$ [61, 62]) is encoded in polytopes.

$n = 6, 7, 8$ (including the $n = 8$ algebraic letters) can be "derived" by solving certain polynomial equations associated to plabic graphs. It is intriguing to note that the webs appearing prominently in this paper bear superficial resemblance to plabic graphs (compare for example Figure 2.6(b) with Fig 5.1 of [63]), and it would be interesting to see if the approach to symbol alphabets taken here could be connected to that of [63, 64, 65]. We note that a connection between webs and plabic graphs is known in the math literature; see Example 4.3 and Theorem 4.4 of [69].

The outline of this paper is as follows. In Section 2.1 we briefly review basic information about $\mathrm{G}(k, n)$-polytopes, cluster series, and symbol letters, and in Section 2.2 we review necessary details about webs and the FP conjectures. Section 2.3 explains our main algorithm for associating webs to the facets of $\mathrm{G}(k, n)$-polytopes. In Section 2.4 we define and compute the web series for almost arborizable webs. The results of our computations for (k, n) up to $(3, 10)$ and $(4, 9)$, and the implications thereof for symbol alphabets, are summarized in Section 2.5.

Node Added. After this paper was completed, we learned from G. Muller of the paper [70] by L. Lamberti, which considers $\mathfrak{sl}_3$ web series of the type we employ in Section 2.4.

2.1 Outline of the Paper

The central objects of study in this paper are certain $d = (k-1)(n-k-1)$-dimensional polytopes associated to the Grassmannian $\mathrm{G}(k, n)$. In particular we are interested in the apparent connection (for $k = 4$) between their facets and the symbol alphabet of n-particle amplitudes in SYM theory. Our main result, which we apply to some polytopes associated to $\mathrm{G}(3, n \leq 10)$ and $\mathrm{G}(4, n \leq 9)$, is a new algorithm to address the problem:

> *How can one efficiently extract the symbol alphabet data associated to a given* $\mathrm{G}(k, n)$*-polytope?*

The computational complexity of existing algorithms for answering this question is reviewed in Figure 2.2 and Section 2.6.3. In this section we very briefly review key features of these polytopes and the relations between the structures associated to their facets, enabling us to outline our new algorithm in Figure 2.2.

2.1.1 Warm-Up: The Polytope $\mathcal{C}(3, 5)$

In order to illustrate some key terminology we begin by considering the 2-dimensional polytope called $\mathcal{C}(3, 5)$ in [50]. It is equivalent to the associahedron [71, 72] K_4 as constructed in [73] and can

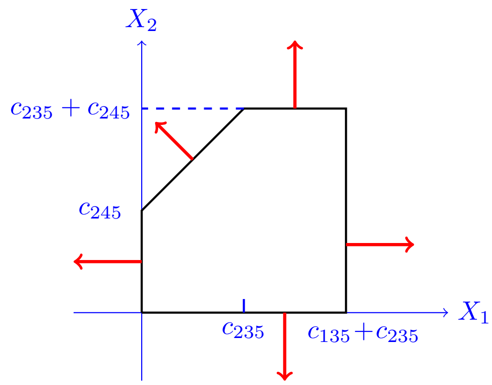

Figure 2.1: The polytope $\mathcal{C}(3,5)$, combinatorially equivalent to the exchange graph [1] of the G$(3,5)$ (or A_2) cluster algebra.

be realized in $\mathbb{R}^2$ with coordinates (X_1, X_2) by the inequalities

$$\begin{aligned} X_1 &\geq 0\,, \\ X_2 &\geq 0\,, \\ c_{135} + c_{235} - X_1 &\geq 0\,, \\ c_{235} + c_{245} - X_2 &\geq 0\,, \\ c_{245} + X_1 - X_2 &\geq 0\,, \end{aligned} \tag{2.1}$$

where the c's are positive constants (see Figure 2.1).

There are three natural structures we can use to label each facet $\mathcal{F}$ of this polytope:

1. the function in (2.1) that vanishes on $\mathcal{F}$ (and is positive inside the polytope),
2. the generator of the ray normal to $\mathcal{F}$ (we always choose the generator to be the first integer point along the *outward* pointing normal ray),
3. or the G$(3,5)$ cluster variable whose **g**-vector [74] is normal to $\mathcal{F}$.

The correspondence between these structures for the five facets of $\mathcal{C}(3,5)$ is shown in Table 2.1. Note that by convention we always fix the overall normalization of each kinematic function so that the coefficients of the X's match the components of (the negative of) the corresponding generator.

2.1.2 Cluster Series

The G(k,n) cluster algebra [1, 75] is finite if and only if $n{+}1 > d = (k{-}1)(n{-}k{-}1)$. For polytopes associated to these algebras, it has been found (by explicit computation in all cases studied so far) that the generator of each normal ray is a **g**-vector of the cluster algebra. It is this fact that allowed us to fill in the third column in Table 2.1. In contrast, [31, 50, 32] studied polytopes associated to the infinite algebra G$(4,8)$ having a facet normal to

$$(-1, 1, 0, 1, 0, -1, 0, -1, 1)\,, \tag{2.2}$$

kinematic function	generator	cluster variable
$s_{125} = c_{135} + c_{235} - X_1$	$(1,0)$	$\langle 1\,2\,4\rangle$
$s_{234} = c_{235} + c_{245} - X_2$	$(0,1)$	$\langle 1\,3\,4\rangle$
$s_{145} = c_{245} + X_1 - X_2$	$(-1,1)$	$\langle 1\,3\,5\rangle$
$s_{123} = X_1$	$(-1,0)$	$\langle 2\,3\,5\rangle$
$s_{345} = X_2$	$(0,-1)$	$\langle 2\,4\,5\rangle$

Table 2.1: The correspondence between kinematic functions, generators, and cluster variables for the $\mathcal{C}(3,5)$ polytope. Our conventions are summarized in Section 2.6, where we also review the definition and properties of the generalized Mandelstam variables s_{ijk}.

which is known to not be a $\mathbf{g}$-vector of $\mathrm{G}(4,8)$ (moreover, it is known to not even be inside the cluster fan [6]). For this reason we call (2.2) an *exceptional generator*. All exceptional generators of the polytopes studied in [31, 50, 32] are related to (2.2) by an element of the cluster modular group[5].

Since it is not possible to assign a cluster variable to exceptional facets, [50] suggested instead to assign to each ray $\mathbb{R}^+\mathbf{y}$ the (formal) *cluster series* (called a cluster algebraic function in [50]) defined by

$$f_{\mathbf{y}}(t) = \sum_{m\geq 0} \mathcal{B}(m\mathbf{y})t^m \,, \tag{2.3}$$

where $\mathcal{B}(\mathbf{y})$ is a cluster algebra basis element associated to the lattice point $\mathbf{y} \in \mathbb{Z}^d$.

In [50] it was conjectured that the cluster series associated to the ray generated by (2.2) takes the form

$$\frac{1}{1 - A\,t + B\,t^2} \tag{2.4}$$

in the canonical basis [77], where

$$\begin{aligned} A &= \langle 1\,2\,5\,6\rangle\langle 3\,4\,7\,8\rangle - \langle 1\,2\,7\,8\rangle\langle 3\,4\,5\,6\rangle - \langle 1\,2\,3\,4\rangle\langle 5\,6\,7\,8\rangle\,, \\ B &= \langle 1\,2\,3\,4\rangle\langle 3\,4\,5\,6\rangle\langle 5\,6\,7\,8\rangle\langle 1\,2\,7\,8\rangle\,. \end{aligned} \tag{2.5}$$

This conjecture was checked through $\mathcal{O}(t^3)$ by explicit computation using the character formula of [6].

In general $f_{\mathbf{g}}(t)$ may depend on the choice of basis for the cluster algebra, but we expect that certain important properties of $f_{\mathbf{g}}(t)$ are the same in any suitably reasonable basis. In particular, we expect that it is a rational function of t and that the locations of its poles (in t) are basis-independent and located on the positive t axis when the series is evaluated at any point in the positive Grassmannian $\mathrm{G}_{>0}(k,n)$.

In Section 2.4 of this paper we introduce a closely related *web series*. We conjecture that a web series exists for every ray, but we have not found the specific form of the series in general. However,

[5] In fact, (2.2) may be essentially unique in that all rays in $\mathbb{R}^9$ are either inside the $\mathrm{G}(4,8)$ cluster fan or related to the one generated by (2.2) by an element of the cluster modular group [76]. We thank C. Kalousios for providing some data that supports this hypothesis.

n-particle symbol data for $n =$	6	7	8	9
# of rational letters	9	42	172	522
# of algebraic letters	0	0	18	99
# of distinct square roots	0	0	2	9

$\mathcal{C}^\dagger(4,n)$ polytope data for $n =$	6	7	8	9
# of facets normal to **g**-vectors of $\mathrm{G}(4,n)$	9	42	272	3078
# of exceptional facets	0	0	2	351

Table 2.2: Summary of data about known symbol letters of n-particle amplitudes in SYM theory. On the top line we omit the n frozen variables of $\mathrm{G}(4,n)$.

for certain rays (those corresponding to almost arborizable webs; see Section 2.4) we prove, to all orders in t, that the web series takes the form

$$\frac{1 - B\,t^2}{1 - A\,t + B\,t^2}\,, \tag{2.6}$$

with A, B depending on the ray. In particular we prove that the web series associated to the ray generated by (2.2) takes the form (2.6) with A, B given by (2.5). Evidently our web series use a different basis than the one that gives the series (2.4), but is consistent with the abovementioned expectations (since it has the same poles, at $t = (A \pm \sqrt{A^2 - 4B})/(2B)$). We also prove that the web series has the form (2.6), and evaluate the corresponding A's and B's, for 324 normal rays of the polytope $\mathcal{C}^\dagger(4,9)$ that might be relevant to the symbol alphabet of 9-particle scattering amplitudes in SYM theory.

Finally let us note that if $\mathbf{g}$ is a $\mathbf{g}$-vector, then $\mathcal{B}(\mathbf{g})$ is the associated cluster variable and $\mathcal{B}(m\mathbf{g}) = \mathcal{B}(\mathbf{g})^m$ for any choice of basis, so the cluster series is basis-independent and geometric:

$$f_{\mathbf{g}}(t) = \frac{1}{1 - t\mathcal{B}(\mathbf{g})}\,. \tag{2.7}$$

In such cases the information content of knowing $f_{\mathbf{g}}(t)$ is the same as that of knowing the cluster variable $\mathcal{B}(\mathbf{g})$. This provides a sense in which it is reasonable—for infinite algebras—to generalize the third column "cluster variable" of Table 2.1 to "cluster series" as [50] did, or to "web series", as we shall do.

2.1.3 Symbol Letters

Finally let us briefly review the observed connection between the symbol alphabet of n-particle amplitudes in SYM theory and $\mathrm{G}(4,n)$-polytopes. All known symbol letters (see Section 2.7 for more details) fall into two classes: *rational* letters are cluster variables of $\mathrm{G}(4,n)$, and *algebraic* letters have the form[6] $\frac{a-\sqrt{b}}{a+\sqrt{b}}$ where a, b are polynomials in Plücker coordinates. Table 2.2 summarizes the number of each type of letter that is known to appear in various n-particle amplitudes, as well as

[6] All algebraic letters currently known have degree 2, but there is no reason to doubt that letters of arbitrarily high degree await discovery.

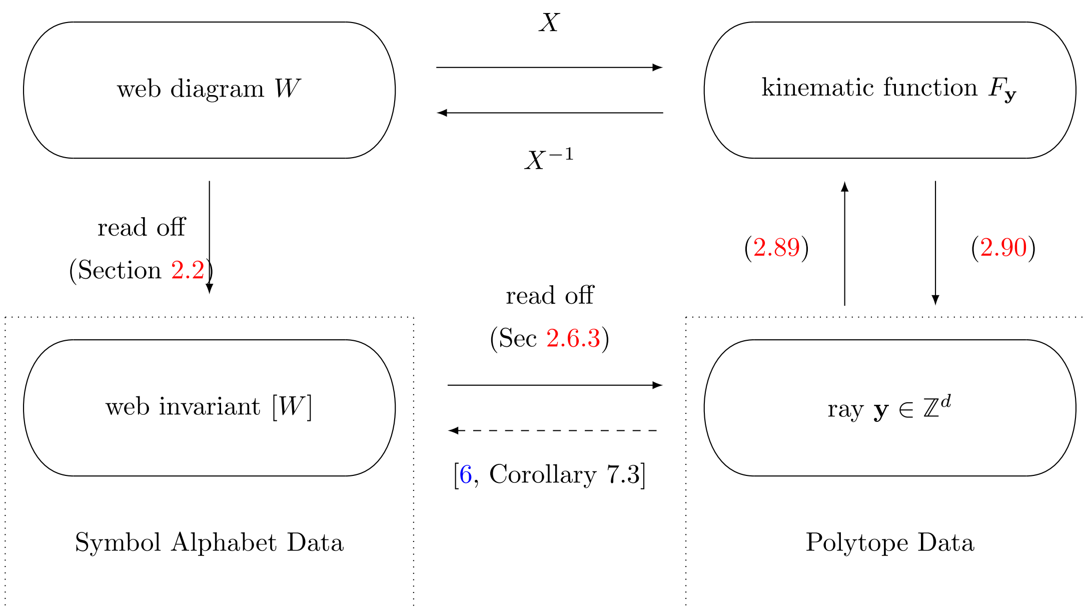

Figure 2.2: An outline of how our work fits into the literature. Recent studies have uncovered an apparent connection between data associated to the facets (with normal ray $\mathbf{y}$) of certain $\mathrm{G}(4,n)$-polytopes (indicated on the second column) and the symbol alphabet of n-particle amplitudes in SYM theory (left column). One route from the former to the latter [50] (the dotted line) uses the character formula of [6] and requires the series (2.3) to be computed term by term, with the m-th term having computational complexity $\mathcal{O}((mw)!)$, where w is an integer that depends on the facet. In this paper we employ web invariants and the Fomin-Pylyavskyy conjectures to provide an alternate route, indicated by the arrow labeled X^{-1}. Here X is a map from web invariants to kinematic functions that we define in Section 2.3. Its inverse X^{-1} can be computed in practice by scanning over a manifestly finite set of candidate preimages W for any given $F_{\mathbf{y}}$. Moreover, we provide a recursive (in m) all-order proof that for certain web invariants (those having a single closed loop), there is a web series that sums exactly to (2.6), with A, B depending on the facet. This proof applies to the exceptional $\mathrm{G}(4,8)$ generators encountered in [31, 50, 32], and here we show that it also applies to the generators of 324 facets of the $\mathcal{C}^{\dagger}(4,9)$ polytope, for which we compute the exact web series. Other alternate routes have been studied in [31, 51].

the number of distinct square roots (each $\sqrt{b}$ appears in several algebraic letters, i.e. paired with various different a's).

Table 2.2 also summarizes data about the facets of the polytopes called $\mathcal{C}^\dagger(4,n)$ in [53]. There (and also in [31, 32]) they were constructed and studied for $n \leq 8$, and found to contain information about the n-particle symbol alphabet in the following sense. First, the cluster variables associated to the **g**-vector facets (second to last line) include all known rational symbol letters (top line). For $n = 8$ it was further observed that the square roots appearing in the poles of the (conjectured) series (2.4) associated to the two exceptional facets (bottom line), given by $\sqrt{A^2 - 4B}$ in terms of (2.5) and its image under a $\mathbb{Z}_8$ cyclic shift, agree precisely with the two distinct square roots known to appear in algebraic symbol letters of 8-particle amplitudes (third line).

In this paper we extend this analysis to $n = 9$ using the algorithm summarized in Figure (2.2). We find that the polytope $\mathcal{C}^\dagger(4,9)$ has 3429 facets; 3078 are normal to **g**-vectors of $\mathrm{G}(4,9)$ while the other 351 are exceptional. The 3078 cluster variables associated to the former include the 522 (non-frozen) rational letters shown in Table 2.2. For 324 of the latter we prove that the web series has the form (2.6); the 324 distinct square roots of the form $\sqrt{A^2 - 4B}$ obtained in this way include the 9 counted in the third line of the table. The remaining 27 exceptional facets remain more mysterious. Although we expect that web series exist for them as well, we have not been able to find their explicit form.

As a further application of our technology we also define and study the polytopes $\mathcal{C}^\dagger(3,n)$. Interestingly we find that they do not have any exceptional facets for $n \leq 10$, which is as far as we have computed (see Section 2.5).

2.2 Review of Tensor Diagrams and the Fomin-Pylyavskyy Conjectures

In this section we review some basic facts about tensor diagrams, which provide a graphical way to encode data about the cluster structure of the Grassmannian. The connection between tensor diagrams and $\mathrm{G}(k,n)$ cluster algebras was first studied by Fomin and Pylyavskyy in [3]. The main elements of this connection are given by the Fomin-Pylyavskyy (FP) conjectures, which have been partly proved in [76]. Our work relies on the FP conjectures in a manner discussed in Section 2.5.

An $\mathfrak{sl}_k$ *tensor diagram* is a finite graph drawn inside a disk with n marked points (labeled $1,\ldots,n$ clockwise around its boundary) satisfying the requirements:

1. all boundary vertices are colored black, and may have arbitrary valence,
2. each internal vertex may be either black or white, but must have valence k,
3. and each edge of the graph must connect a black vertex to a white vertex.

A planar tensor diagram is called a *web*, and a tensor diagram with no closed loops (of internal vertices) is called a *tree*. If we glue all of the vertices and edges of two or more webs into the same disk, we get a *combination* of webs.

To each diagram D we can associate a *tensor invariant* $[D]$ constructed as follows. First, we associate to each boundary vertex i a k-component vector Z_i^a. (For $k = 4$ these are the familiar momentum twistor variables that encode massless n-particle kinematic data.) Then to each white vertex we associate $\epsilon^{a_1 \cdots a_k}$, to each internal black vertex we associate $\epsilon_{a_1 \cdots a_k}$, and we contract all indices as indicated by the edges of the graph. The resulting invariant is always a homogeneous polynomial in the Plücker coordinates

$$\langle i_1\, i_2\, \ldots\, i_k \rangle = \det(Z_{i_1} Z_{i_2} \cdots Z_{i_k}) \tag{2.8}$$

on $\mathrm{G}(k,n)$. This definition suffices for our purposes, but it is not precise because when k is even it leaves the overall sign of $[D]$ undetermined thanks to $\epsilon^{a_2 \cdots a_k a_1} = -\epsilon^{a_1 a_2 \cdots a_k}$. For a proper definition of tensor invariants, including a detailed discussion of how to fix this sign, we refer the reader to [78, 69]. In practice we will determine the "correct" overall sign for any invariant by requiring that it evaluates to a positive number when the $k \times n$ matrix Z_i^a is an element of the positive Grassmannian $\mathrm{G}_{>0}(k,n)$.

If W is a web satisfying certain additional conditions[7] we call $[W]$ a *web invariant*. If W is a combination of two or more webs $W_1, W_2, \ldots$ then $[W]$ is the product of the web invariants $[W_1], [W_2], \ldots$. If $[W]$ is not a product of two or more web invariants then we say that $[W]$ is *indecomposable*.

As their name suggests, tensor invariants are invariant under certain graphical moves known as *skein relations* (see Figure 2.5) [2, 79, 78, 3]. One important application of these relations is that they can sometimes be used to convert a web W with closed loops into a tree diagram D that is equivalent in the sense that $[D] = [W]$; if this is possible then the web W is called *arborizable* (note that D may or may not be a web, i.e. it may be non-planar).

The *Fomin-Pylyavskyy conjectures* [3] comprise several interesting connections between tensor invariants and cluster variables. These have been proven up to $\mathrm{G}(3,9)$ and $\mathrm{G}(4,8)$ in [76]. For our purposes the key conjecture is: *the set of cluster (and frozen) variables coincides with the set of indecomposable arborizable web invariants.* Henceforth we only consider indecomposable diagrams.

In order to better familiarize the reader with tensor diagrams let us now introduce some tricks for quickly reading off the invariants associated to certain diagrams.

2.2.1 $\mathfrak{sl}_2$ Tensor Diagrams

This case is rather trivial in an instructive way. The only structures an $\mathfrak{sl}_2$ tensor diagram can have are strands that begin and end on boundary vertices, passing along the way through an odd number of internal vertices alternating between white and black. All internal vertices except for a single white vertex on each strand can be removed by a skein relation ($\epsilon^{ab}\epsilon_{bc} = \delta^a_c$). The web invariants

[7] For $k = 3$ W must be *non-elliptic*, which means every pair of vertices is connected by at most one edge and each face formed by interior vertices has at least six sides [3]. For $k = 4$ W can have at most double edges and must have no 2-cycles [76].

have the form $[W_{ij}] = \langle i\, j \rangle$, corresponding to the web W_{ij} with a single strand connecting boundary vertices $1 \leq i < j \leq n$.

2.2.2 $\mathfrak{sl}_3$ Tensor Diagrams

The invariant for any $\mathfrak{sl}_3$ tree diagram D can be read out in a simple way [3]. First we choose any internal vertex of D to be the *central vertex* v and assign a direction to each edge in such a way that it points from the boundary of the diagram towards v; this assignment is unambiguous if D is a tree. Then at each internal vertex except v, there must be two inward pointing edges and one outward pointing edge. Having already assigned a vector Z_i to each boundary vertex i, we now assign to each internal vertex $v' \neq v$ the cross-product of the two vectors or covectors associated to the two inward edges at v'; this is a vector if v' is black and a covector if v' is white. Then the invariant of D is equal to the determinant of the three (co)vectors assigned to the three incoming edges at the central vertex v.

Some $\mathfrak{sl}_3$ webs and their corresponding invariants are shown in Figure 2.3. For example, let D be the diagram shown in Figure 2.3(b). If we choose the black vertex in the middle to be the central vertex, then the covectors assigned to the top, bottom right, and bottom left white vertices are respectively $Z_1 \times Z_2$ (which we immediately abbreviate to 1×2), 3×4, and 5×6, yielding the tensor invariant $[D] = \langle 1 \times 2, 3 \times 4, 5 \times 6 \rangle$ as indicated in the figure. We could also have chosen, say, the top white vertex as the center, in which case the invariant would have been computed as $[D]' = \langle 1, 2, (3 \times 4) \times (5 \times 6) \rangle$, but it is easy to check that $[D] = [D]'$.

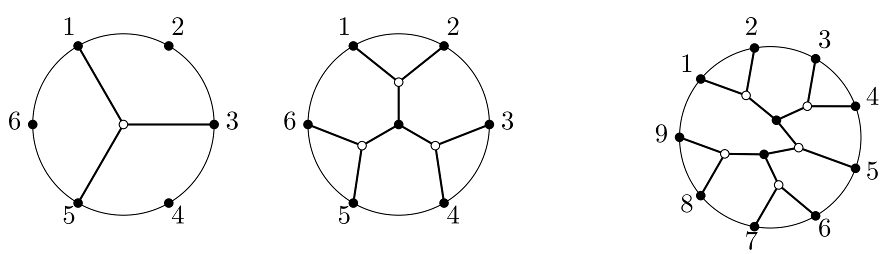

$\langle 1\,3\,5 \rangle$ $\quad$ $\langle 1 \times 2, 3 \times 4, 5 \times 6 \rangle$ $\quad$ $\langle (1 \times 2) \times (3 \times 4), 5, (6 \times 7) \times (8 \times 9) \rangle$

Figure 2.3: Examples of $\mathfrak{sl}_3$ webs and their corresponding invariants.

This shortcut for computing a tensor invariant $[D]$ can also be used if D is arborizable. For example, by choosing the white vertex adjacent to 3 as the center, the invariant associated to the diagram shown in Figure 2.4 evaluates to

$$\langle (7 \times 8) \times (1 \times 2), 3, (4 \times 5) \times (6 \times 8) \rangle \,. \tag{2.9}$$

2.2.3 $\mathfrak{sl}_4$ Tensor Diagrams

Again we emphasize that we have only explained how to compute tensor invariants mod sign when k is even. In order to formulate the skein relations for $\mathfrak{sl}_4$ tensor diagrams, it would be necessary

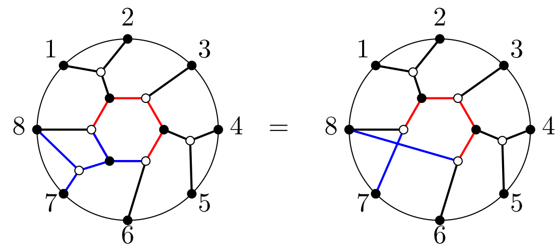

Figure 2.4: An example of arborization, where we break the inner hexagon on the left by applying the first and seventh skein relations shown in Figure 2.5 to the blue edges. (The blue and red colorings serve only to guide the eye.)

to be careful about the detailed sign convention explained in [79, 78]. In Figure 2.5 we show the equivalence relations (mod sign) that we require for the calculations in this paper.

Freed from having to worry about the sign, we can compute invariants for $\mathfrak{sl}_4$ trees in a similar manner to those of $\mathfrak{sl}_3$. If two vertices are connected by a pair of edges then we call the pair a *double edge*. After choosing a central vertex v and assigning to each edge a direction pointing towards v, every other internal vertex $v' \neq v$ has either a double or single outgoing edge, and the other two or three edges are incoming. Extending the $k = 3$ analysis in the obvious way, we now assign to v' the 1- or 2-index co- or contravariant tensor constructed by contracting ϵ^{abcd} (if v' is white) or ϵ_{abcd} (if v' is black) with the tensors associated to the incoming edges (multiplied by $\frac{1}{2}$ if there is a double edge). Finally, at the central vertex v all edges are incoming; contracting their indices with the appropriate ϵ computes the diagram's invariant (up to overall sign).

For example, if in the diagram

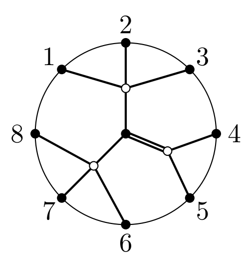

(2.10)

we choose the internal black vertex as the center, then the top, bottom right, and bottom left vertices are assigned (123), (45), and (678), respectively, where we use the shorthand

$$(ij) = \frac{1}{2}\epsilon_{abcd} Z_i^a Z_j^b \,, \qquad (ijk) = \epsilon_{abcd} Z_i^a Z_j^b Z_k^c \,. \tag{2.11}$$

Contracting indices at the central vertex computes the diagram's invariant, which can be expressed as $\langle 45(123) \cap (678) \rangle$ using the notation

$$\langle ab(cde) \cap (fgh) \rangle = \langle acde \rangle \langle bfgh \rangle - \langle bcde \rangle \langle afgh \rangle \,. \tag{2.12}$$

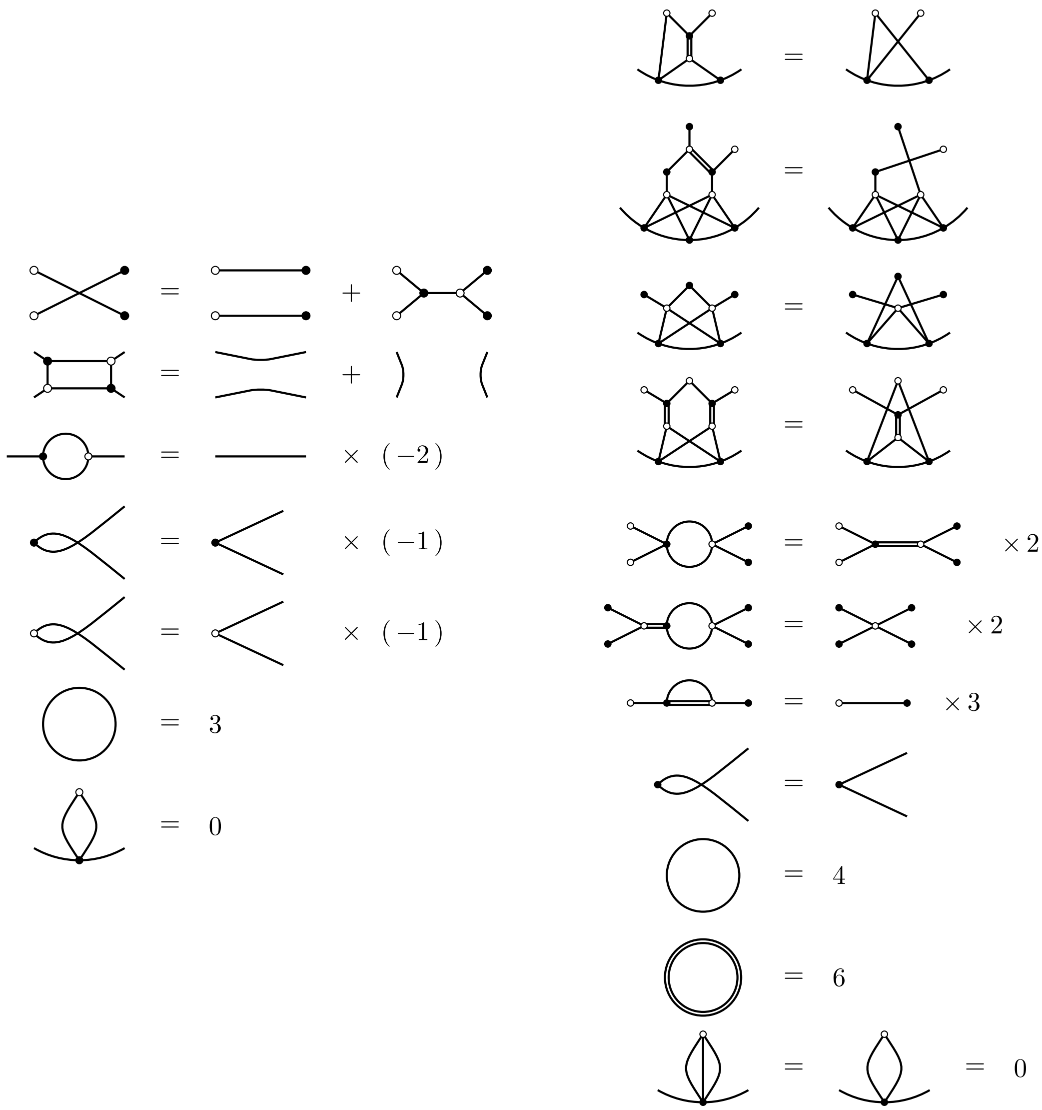

Figure 2.5: The skein relations for $\mathfrak{sl}_3$ and $\mathfrak{sl}_4$ tensor diagrams, adapted from [2, 3]. As mentioned in the text, the latter graphical relations are equivalences from skein relations between tensor invariants mod overall sign. Additionally, the $\mathfrak{sl}_4$ relations in the sixth and eighth lines hold with all colors exchanged. These relations are all derivable from identities for contractions of Levi-Civita tensors; for example the top relation on the left shows $\delta_b^d\delta_c^e = \delta_c^d\delta_b^e + \epsilon_{abc}\epsilon^{ade}$.

2.2.4 Non-Arborizable Web Invariants

According to the Fomin-Pylyavskyy conjectures, every cluster monomial (a product of compatible cluster variables) in $\mathrm{G}(k,n)$ is an n-point $\mathfrak{sl}_k$ web invariant. However, the converse is not true because of the existence of non-arborizable webs. Their invariants are multiplicatively independent of cluster variables and so indicate that bases for cluster algebras must (in general) have elements beyond cluster monomials (see Section III.A of [50] for an explicit example discussed in the physics literature). The simplest non-arborizable $\mathfrak{sl}_3$ webs appear at $n = 9$ and the simplest $\mathfrak{sl}_4$ webs appear at $n = 8$. These include for example [3, Figure 31] and [6, (8.2)], shown in Figure 2.6.

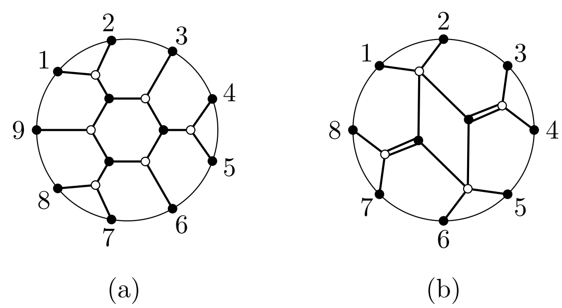

Figure 2.6: Two of the simplest non-arborizable webs, for (a) $\mathrm{G}(3,9)$ and (b) $\mathrm{G}(4,8)$.

2.3 From Tensor Diagrams to Kinematic Functions

In this section we study a map X that associates a kinematic function $F = X([D])$ to certain tensor invariants $[D]$. A key property we want the map to have is that if $[D]$ is a cluster variable, then $X([D])$ should be the kinematic function naturally associated to $[D]$ (in the same sense of association as between the first and third columns of Table 2.1).

More specifically, and more generally, X is defined as follows: if $[D]$ is a tensor invariant whose $\mathbf{g}$-vector (defined as reviewed in Section 2.6.3) is $\mathbf{y} \in \mathbb{Z}^d$, and if $\mathbf{y}$ is the first integer point along the ray $\mathbb{R}^+\mathbf{g}$ (in which case we say that $\mathbf{y}$ and $[D]$ are *primitive*), then $X([D])$ is the kinematic function $F_{\mathbf{y}}$ computed according to (2.89). These steps trace counterclockwise around Figure 2.2, when applied to a diagram that is not necessarily a web. In the rest of this section we present *conjectural* formulas that compute $X([D])$ for $k \leq 4$ directly, as opposed to tracing around the figure. We have confirmed that our formulas obey the defining property for all kinematic functions and web invariants that we have encountered in this work (summarized in Table 2.3), and conjecture them to be valid in general. In Section 2.4 we discuss web series, which extend this discussion to arbitrary integer points along $\mathbb{R}^+\mathbf{y}$.

It is sufficient to focus our attention on indecomposable invariants; more generally we have $X([D_1] \cdot [D_2] \cdots) = X([D_1]) + X([D_2]) + \cdots$. In order to make our results easily accessible to users of two different sets of conventions we study two distinct versions of the map: X_L and X_R. The former is attached to the conventions reviewed in Sections 2.6.1–2.6.4 (and used in the example of

Section 2.1.1), while the latter is attached to the "Langlands dual" convention where all arrows in Figure 2.7 are reversed (see Section 2.6.5).

For $k = 2$ it is possible to write down an explicit general formula for the X-map, exploiting the fact that every indecomposable $\mathfrak{sl}_2$ tensor invariant has the form $\langle i\,j\rangle$ for $i < j$ (see Section 2.2.1). The associated kinematic function, for the two choices of convention, is simply

$$\begin{aligned} X_L(\langle a\,b\rangle) &= \sum_{a+1\le i<j\le b} s_{ij}\,, \\ X_R(\langle a\,b\rangle) &= \sum_{a\le i<j\le b-1} s_{ij}\,. \end{aligned} \tag{2.13}$$

2.3.1 $\mathfrak{sl}_3$ Arborizable Invariants

For $k > 2$ we conjecture a recursive formula for the X-map, first for tree diagrams. In order to apply the recursion, $[D]$ must be written in the form obtained by reading it off from some diagram D as described in Section 2.2.2. If we are handed $[D]$ in some random form (as a polynomial in Plücker coordinates), we would first need to draw some tree diagram D whose invariant is $[D]$. Next, D must be put into *canonical order*, which means that all lines and vertices are placed so as to minimize the number of crossed lines but *without* producing or annihilating any lines or vertices. Specifically, all crossing structures of the type shown in the fourth and fifth lines of the $\mathfrak{sl}_3$ skein relations (Figure 2.5, left panel) should be cleared, but without using the moves shown on the first and second lines.

The recursion is seeded by the simplest possible $\mathfrak{sl}_3$ tensor diagrams: those with only a single internal vertex (see for example the left panel of Figure 2.3), for which we have

$$\begin{aligned} X_L(\langle a\,b\,c\rangle) &= S_{a+1,\ldots,b(b+1,\ldots,c)}\,, \\ X_R(\langle a\,b\,c\rangle) &= S_{(a,\ldots,b-1)b,\ldots,c-1}\,, \end{aligned} \tag{2.14}$$

using notation reviewed in Section 2.8.

For more general diagrams, our definition of the X-map is motivated by the $\mathrm{G}(3,6)$ "bipyramid relation" of [52] (see for example (6.10) of [56] for more specificity) which in our notation reads

$$S_{(12)34} + S_{12(34)} = S_{1234} + S_{3456} + S_{1256}\,. \tag{2.15}$$

Working for a moment with the "left" conventions, we can use (2.14) to rewrite all but the first term as X_L images of cluster variables:

$$S_{(12)34} + X_L(\langle 6\,2\,4\rangle) = X_L(\langle 6\,3\,4\rangle) + X_L(\langle 2\,5\,6\rangle) + X_L(\langle 4\,1\,2\rangle)\,. \tag{2.16}$$

We don't yet know what to do with the first term, but one can calculate that the **g**-vector of $S_{(12)34}$ is the same as that of the cluster variable $\langle 5\times 6, 1\times 2, 3\times 4\rangle$, which motivates us to *define*

$$X_L(\langle 5\times 6, 1\times 2, 3\times 4\rangle) := X_L(\langle 6\,3\,4\rangle) + X_L(\langle 2\,5\,6\rangle) + X_L(\langle 4\,1\,2\rangle) - X_L(\langle 6\,2\,4\rangle)\,. \tag{2.17}$$

Our recursive definition of X_L (and similar for X_R) is motivated by the desire to extend (2.17) to more general cases without having to rely on computing **g**-vectors at intermediate stages.

Therefore we now consider more complicated tensor diagrams whose invariants involve cross-products of the form $\langle a \times b,\, c \times d,\, e \times f\,\rangle$. Here $a, b, \ldots, f$ are either all vectors or all covectors (the expression makes no sense otherwise), and each could itself be a string of nested cross-products such as $a = (1 \times 2) \times (3 \times 4)$. The generalization of (2.17) is

$$\begin{aligned} X_L(\langle a \times b, c \times d, e \times f\rangle) &= X_L(\langle a, b, d\rangle) + X_L(\langle c, d, f\rangle) + X_L(\langle e, f, b\rangle) - X_L(\langle b, d, f\rangle)\,, \\ X_R(\langle a \times b, c \times d, e \times f\rangle) &= X_R(\langle a, c, d\rangle) + X_R(\langle c, e, f\rangle) + X_R(\langle e, a, b\rangle) - X_R(\langle a, c, e\rangle) \end{aligned} \tag{2.18}$$

for vectors and

$$\begin{aligned} X_L(\langle a \times b, c \times d, e \times f\rangle) &= X_L(\langle a, c, d\rangle) + X_L(\langle c, e, f\rangle) + X_L(\langle e, a, b\rangle) - X_L(\langle a, c, e\rangle)\,, \\ X_R(\langle a \times b,\, c \times d,\, e \times f\,\rangle) &= X_R(\langle a, b, d\rangle) + X_R(\langle c, d, f\rangle) + X_R(\langle e, f, b\rangle) - X_R(\langle b, d, f\rangle) \end{aligned} \tag{2.19}$$

for covectors.

The formulas (2.14), (2.18) and (2.19) provide a recursive formula for X_L and X_R for all $\mathfrak{sl}_3$ tree diagrams, but it may not immediately be clear how to apply the recursion to a diagram like the one in the right panel of Figure 2.3 because its invariant has no manifest cross-product in the middle entry. However, it is always possible to rewrite an invariant in an equivalent way that exposes a cross-product in each entry; in this case via the identity

$$\langle (1 \times 2) \times (3 \times 4), 5, (6 \times 7) \times (8 \times 9)\rangle = \langle 1 \times 2, 3 \times 4, 5 \times ((6 \times 7) \times (8 \times 9))\rangle\,, \tag{2.20}$$

to which one can now apply (2.19). In this example one has to perform further rearrangements at the next step in the recursion; the important point is that it is always possible to do so.

As emphasized above, although we have written the above recursion in a seemingly general way in terms of nested brackets, it will give inconsistent results unless $[D]$ is expressed as the invariant read off from a canonically ordered diagram. One obvious manifestation of the inconsistency for improper ordering is the fact that we clearly have

$$\langle 1 \times 2, 4 \times 3, 6 \times 5\rangle = \langle 1 \times 2, 3 \times 4, 5 \times 6\rangle\,, \tag{2.21}$$

but (2.18) and (2.19) are not invariant under $c \leftrightarrow d, e \leftrightarrow f$; the recursion must be applied only to the right-hand side of (2.21).

2.3.2 $\mathfrak{sl}_3$ Non-Arborizable Invariants

Now we propose recursion relations for computing $X([D])$ when $[D]$ is a non-arborizable invariant. The basic step is to “unroll” each internal loop by appropriately cutting one of its edges. Consider first the case when $[D]$ is the invariant of a diagram having a single internal loop. Then, for any choice of edge on the internal loop (shown in red) we define

$X_L\Bigg($ 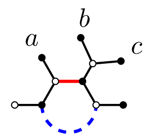

$\Bigg) = X_L\Bigg($ 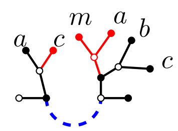

$\Bigg) - X_L\big(\langle m,a,c\rangle\big)\,,$

$X_R\Bigg($ 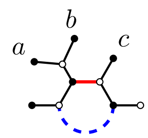

$\Bigg) = X_R\Bigg($ 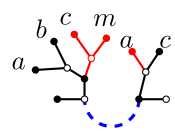

$\Bigg) - X_R\big(\langle a,c,m\rangle\big)\,,$ (2.22)

where we have removed the red edge of the loop and replaced it with the new red edges shown, the blue dashed lines denote an arbitrary (even) number of additional vertices on the inner loop, and m is an arbitrary reference point. One can check that all terms involving the reference point m cancel out when the recursion is applied and the right-hand sides are expanded out. We emphasize again that (2.22) is only valid when the diagram is drawn in canonical order, with minimal number of crossings.

To see an example of the recursion at work, let us compute the kinematic functions associated to Figure 2.6(a). Applying (2.22) and then (2.18), (2.19) we have

$X_L\Bigg($ 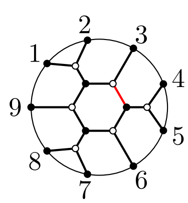

$\Bigg)$

$$\begin{aligned}
&= X_L\Big(\Big\langle \big((m\times 3)\times(4\times 5)\big)\times 6,\ 7\times 8,\ 9\times\big((1\times 2)\times(3\times 5)\big)\Big\rangle\Big) - X_L(\langle m,3,5\rangle) \qquad (2.23)\\
&= X_L(\langle m\times 3,\ 4\times 5,\ 6\times 8\rangle) + X_L(\langle 7\times 8,\ 1\times 2,\ 3\times 5\rangle) + X_L(\langle 6\times 9,\ 1\times 2,\ 3\times 5\rangle)\\
&\qquad - X_L(\langle 6\times 8,\ 1\times 2,\ 3\times 5\rangle) - X_L(\langle m,3,5\rangle)\\
&= X_L(\langle 1,2,5\rangle) + X_L(\langle 4,5,8\rangle) + X_L(\langle 7,8,2\rangle) + X_L(\langle 2,6,9\rangle) + X_L(\langle 3,5,9\rangle)\\
&\qquad + X_L(\langle 3,6,8\rangle) - X_L(\langle 2,5,9\rangle) - X_L(\langle 2,6,8\rangle) - X_L(\langle 3,5,8\rangle)\,,
\end{aligned}$$

and similarly

$$X_R\left(\vphantom{\Big|}\right.$$ 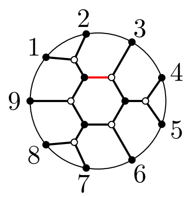 $$\left.\vphantom{\Big|}\right)$$

$$\begin{aligned}
&= X_R\Big(\Big\langle \big((1\times 3)\times(4\times 5)\big)\times 6,\ 7\times 8,\ 9\times\big((1\times 2)\times(3\times m)\big)\Big\rangle\Big) - X_R(\langle 1,3,m\rangle) \\
&= X_R(\langle 1\times 3,\ 4\times 5,\ 7\times 8\rangle) + X_R(\langle 7\times 9,\ 1\times 2,\ 3\times m\rangle) + X_R(\langle 1\times 3,\ 4\times 5,\ 6\times 9\rangle) \\
&\quad - X_R(\langle 1\times 3,\ 4\times 5,\ 7\times 9\rangle) - X_L(\langle 1,3,m\rangle) \\
&= X_R(\langle 7,1,2\rangle) + X_R(\langle 1,4,5\rangle) + X_R(\langle 4,7,8\rangle) + X_R(\langle 4,6,9\rangle) + X_R(\langle 3,7,9\rangle) \\
&\quad + X_R(\langle 1,3,6\rangle) - X_R(\langle 4,7,9\rangle) - X_R(\langle 1,3,7\rangle) - X_R(\langle 1,4,6\rangle)\,.
\end{aligned} \tag{2.24}$$

A diagram with $\ell > 1$ inner loops can be treated similarly, by recursively unrolling each loop via introduction of a new reference point. All ℓ reference points will disappear in the final result.

Of course, some diagrams with internal loops are equivalent to trees by the skein relations and it is important to check that the recursion relations we have given respect this equivalence. To see this we must look at the two types of arborization processes. First we consider

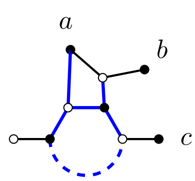

$$\longrightarrow$$

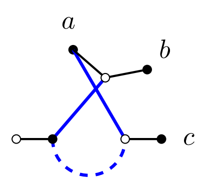

(2.25)

Applying X_L to the left-hand side and using (2.22) gives

$$X_L\left(\vphantom{\Big|}\right.$$ 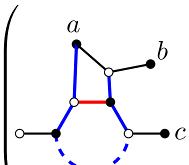 $$\left.\vphantom{\Big|}\right) = X_L\left(\vphantom{\Big|}\right.$$ 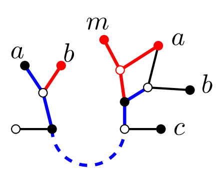 $$\left.\vphantom{\Big|}\right) - X_L\big(\langle m,a,b\rangle\big). \tag{2.26}$$

The first term on the right has the form $X_L(\langle m\times a, a\times b, c\times\cdots\rangle)$ where "$\cdots$" stands for everything along the dotted blue semicircle and to its left in the figure. Then using (2.18) we have

$$\begin{aligned}
(2.26) &= X_L(\langle m,a,b\rangle) + X_L(\langle a,b,\cdots\rangle) + X_L(\langle c,\cdots,a\rangle) - X_L(\langle a,b,\cdots\rangle) - X_L(\langle m,a,b\rangle) \\
&= X_L(\langle a,c,\cdots\rangle)\,,
\end{aligned} \tag{2.27}$$

but this is the same as X_L applied to the right-hand side of (2.25), as required.

Next consider applying X_L to the left-hand side of

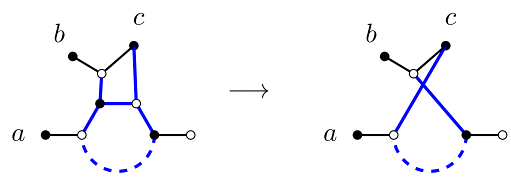

(2.28)

which by (2.22) gives

X_L 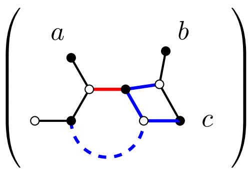

$= X_L$ 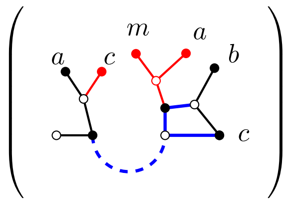

$- X_L\big(\langle m, a, c\rangle\big)$

$$\begin{aligned}
&= X_L(\langle m \times a, b \times c, c \times \cdots\rangle) - X_L(\langle m, a, c\rangle\rangle \\
&= X_L(\langle m, a, c\rangle) + X_L(\langle b, c, \cdots\rangle) + X_L(\langle c, \cdots, a\rangle) - X_L(\langle a, c, \cdots\rangle) - X_L(\langle m, a, c) \\
&= X_L(\langle b, c, \cdots\rangle)\,,
\end{aligned} \tag{2.29}$$

which again is the required answer: X_L applied to the right-hand side of (2.28).

We omit the proof for X_R, which is essentially the same, and instead illustrate with the example shown in Figure 2.4:

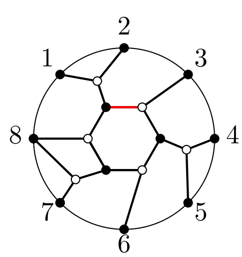

$=$
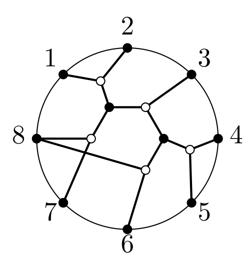

$= \langle (7 \times 8) \times (1 \times 2), 3, (4 \times 5) \times (6 \times 8)\rangle$

(2.30)

Using (2.22) to unroll the red edge on the inner loop of the left diagram gives

$$\begin{aligned}
&X_R(\langle((1 \times 3) \times (4 \times 5)) \times 6,\ 7 \times 8,\ 8 \times ((1 \times 2) \times (3 \times m))\rangle) - X_R(\langle 1, 3, m\rangle) \\
&\quad = X_R(\langle 7, 1, 2\rangle) + X_R(\langle 1, 4, 5\rangle) + X_R(\langle 4, 6, 8\rangle) + X_R(\langle 3, 7, 8\rangle) \\
&\qquad + X_R(\langle 1, 3, 6\rangle) - X_R(\langle 1, 3, 7\rangle) - X_R(\langle 1, 4, 6\rangle).
\end{aligned} \tag{2.31}$$

On the other hand, the right diagram in (2.30) is a tree; according to (2.19) its image under the X_R map is

$$\begin{aligned}
&X_R(\langle(7 \times 8) \times (1 \times 2), 3, (4 \times 5) \times (6 \times 8)\rangle) \\
&\quad = X_R(\langle 7, 1, 2\rangle) + X_R(\langle 1, 4, 5\rangle) + X_R(\langle 4, 6, 8\rangle) + X_R(\langle 3, 7, 8\rangle) + X_R(\langle 1, 3, 6\rangle) \\
&\qquad - X_R(\langle 1, 3, 7\rangle) - X_R(\langle 1, 4, 6\rangle)\,,
\end{aligned} \tag{2.32}$$

in agreement with (2.31).

2.3.3 $\mathfrak{sl}_4$ Arborizable Invariants

For $k = 4$ the recursion for calculating the X-map is seeded by

$$\begin{aligned} X_L(\langle a\,b\,c\,d\rangle) &= \mathbf{S}_{a+1,\ldots,b[b+1,\ldots,c(c+1,\ldots,d)]}\,, \\ X_R(\langle a\,b\,c\,d\rangle) &= \mathbf{S}_{[(a,\ldots,b-1)b,\ldots,c-1]c,\ldots,d-1}\,, \end{aligned} \tag{2.33}$$

using notation reviewed in Section 2.8.

There are two basic types of structures that can appear in place of simple vectors a, b, c, d in (2.33) when we look at more general tree invariants. We must describe separately how to recursively handle each type of structure.

The first type of structure that can appear in place of a vector is a tensor product involving 5 points:

$$[(ab) \cap (cde)]^\mu := \left(\frac{1}{2} a^\nu b^\rho \epsilon_{\nu\rho\sigma\tau}\right)\left(c^\alpha d^\beta e^\gamma \epsilon_{\alpha\beta\gamma\delta}\right)\epsilon^{\sigma\tau\delta\mu} \tag{2.34}$$

where all Greek subscripts and superscripts run from 1 to 4 and ϵ is the antisymmetric Levi-Civita symbol with $\epsilon_{1234} = \epsilon^{1234} = 1$; recall (2.11). For invariants involving one of these we have

$$\begin{aligned} X_L(\langle a, b, c, (d, e) \cap (f, g, h)\rangle) &= X_L(\langle a, b, c, e\rangle) + X_L(\langle d, e, g, h\rangle) \\ &\quad + X_L(\langle f, g, h, c\rangle) - X_L(\langle c, e, g, h\rangle)\,, \\ X_R(\langle a, b, c, (d, e) \cap (f, g, h)\rangle) &= X_R(\langle a, b, d, e\rangle) + X_R(\langle d, f, g, h\rangle) \\ &\quad + X_R(\langle f, a, b, c\rangle) - X_R(\langle a, b, d, f\rangle)\,. \end{aligned} \tag{2.35}$$

We could also have a structure like (2.34) but with a lower μ index—as would be the case for example if all of $a, \ldots, e$ were not individual vectors but triple-products like $a_\mu = \epsilon_{\mu\nu\rho\sigma} a_1^\nu a_2^\rho a_3^\sigma$ for some a_i. (Note that a_μ represents the plane in $\mathbb{P}^3$ containing the three a_i.). In this case we would have

$$\begin{aligned} X_L(\langle a, b, c, (d, e) \cap (f, g, h)\rangle) &= X_L(\langle a, b, d, e\rangle) + X_L(\langle d, f, g, h\rangle) \\ &\quad + X_L(\langle f, a, b, c\rangle) - X_L(\langle a, b, d, f\rangle)\,, \\ X_R(\langle a, b, c, (d, e) \cap (f, g, h)\rangle) &= X_R(\langle a, b, c, e\rangle) + X_R(\langle d, e, g, h\rangle) \\ &\quad + X_R(\langle f, g, h, c\rangle) - X_R(\langle c, e, g, h\rangle)\,. \end{aligned} \tag{2.36}$$

The second type of structure that can appear in tree invariants is a tensor product involving 9 points:

$$\begin{aligned} &[(a_1 a_2 a_3)(b_1 b_2 b_3)(c_1 c_2 c_3)]^\mu := \\ &\qquad (a_1^{\nu_1} a_2^{\nu_2} a_3^{\nu_3} \epsilon_{\nu_1\nu_2\nu_3\nu_4})(b_1^{\rho_1} b_2^{\rho_2} b_3^{\rho_3} \epsilon_{\rho_1\rho_2\rho_3\rho_4})(c_1^{\tau_1} c_2^{\tau_2} c_3^{\tau_3} \epsilon_{\tau_1\tau_2\tau_3\tau_4})\epsilon^{\nu_4\rho_4\tau_4\mu}\,, \end{aligned} \tag{2.37}$$

which can appear in combinations of the form (again recall (2.11))

$$C_{abc} := \langle (a_1 a_2 a_3), (b_1 b_2 b_3), (c_1 c_2 c_3), (d_1 d_2 d_3)\rangle = \langle a_1, a_2, a_3, (b_1 b_2 b_3)(c_1 c_2 c_3)(d_1 d_2 d_3)\rangle\,. \tag{2.38}$$

For this kind of invariant we have

$$\begin{aligned}
X_L(C_{abc}) &= X_L(\langle a_1,a_2,a_3,b_3\rangle) + X_L(\langle b_1,b_2,b_3,c_3\rangle) + X_L(\langle c_1,c_2,c_3,d_3\rangle) \\
&\quad + X_L(\langle d_1,d_2,d_3,a_3\rangle) + X_L(\langle a_2,a_3,c_2,c_3\rangle) + X_L(\langle b_2,b_3,d_2,d_3\rangle) \\
&\quad - X_L(\langle a_2,a_3,b_3,c_3\rangle) - X_L(\langle b_2,b_3,c_3,d_3\rangle) - X_L(\langle c_2,c_3,d_3,a_3\rangle) \\
&\quad - X_L(\langle d_2,d_3,a_3,b_3\rangle) + X_L(\langle a_3,b_3,c_3,d_3\rangle)\,, \\
X_R(C_{abc}) &= X_R(\langle a_1,b_1,b_2,b_3\rangle) + X_R(\langle b_1,c_1,c_2,c_3\rangle) + X_R(\langle c_1,d_1,d_2,d_3\rangle) \\
&\quad + X_R(\langle d_1,a_1,a_2,a_3\rangle) + X_R(\langle a_1,a_2,c_1,c_2\rangle) + X_R(\langle b_1,b_2,d_1,d_2\rangle) \\
&\quad - X_R(\langle a_1,b_1,c_1,c_2\rangle) - X_R(\langle b_1,c_1,d_1,d_2\rangle) - X_R(\langle c_1,d_1,a_1,a_2\rangle) \\
&\quad - X_R(\langle d_1,a_1,b_1,b_2\rangle) + X_R(\langle a_1,b_1,c_1,d_2\rangle)\,.
\end{aligned} \tag{2.39}$$

Alternatively, in the contravariant case (that is, when each of the nine entries in (2.37) represents a plane) we have

$$\begin{aligned}
X_L(C_{abc}) &= X_L(\langle a_1,b_1,b_2,b_3\rangle) + X_L(\langle b_1,c_1,c_2,c_3\rangle) + X_L(\langle c_1,d_1,d_2,d_3\rangle) \\
&\quad + X_L(\langle d_1,a_1,a_2,a_3\rangle) + X_L(\langle a_1,a_2,c_1,c_2\rangle) + X_L(\langle b_1,b_2,d_1,d_2\rangle) \\
&\quad - X_L(\langle a_1,b_1,c_1,c_2\rangle) - X_L(\langle b_1,c_1,d_1,d_2\rangle) - X_L(\langle c_1,d_1,a_1,a_2\rangle) \\
&\quad - X_L(\langle d_1,a_1,b_1,b_2\rangle) + X_L(\langle a_1,b_1,c_1,d_2\rangle)\,, \\
X_R(C_{abc}) &= X_R(\langle a_1,a_2,a_3,b_3\rangle) + X_R(\langle b_1,b_2,b_3,c_3\rangle) + X_R(\langle c_1,c_2,c_3,d_3\rangle) \\
&\quad + X_R(\langle d_1,d_2,d_3,a_3\rangle) + X_R(\langle a_2,a_3,c_2,c_3\rangle) + X_R(\langle b_2,b_3,d_2,d_3\rangle) \\
&\quad - X_R(\langle a_2,a_3,b_3,c_3\rangle) - X_R(\langle b_2,b_3,c_3,d_3\rangle) - X_R(\langle c_2,c_3,d_3,a_3\rangle) \\
&\quad - X_R(\langle d_2,d_3,a_3,b_3\rangle) + X_R(\langle a_3,b_3,c_3,d_3\rangle)\,.
\end{aligned} \tag{2.40}$$

All of the above relations are valid only when each invariant is read off from a tree diagram drawn in canonical order, as in the previous subsection.

2.3.4 $\mathfrak{sl}_4$ Non-Arborizable Invariants

Here we consider only inner loops which have no double edges. We have found this to be sufficient to analyze the $\mathcal{C}(4,8)$ and $\mathcal{C}^\dagger(4,9)$ polytopes (see Section 2.5); it would be interesting to formulate a recursive rule for more general diagrams. We find that single-edged inner loops of $\mathfrak{sl}_4$ diagrams can be unrolled with the rule

X_L 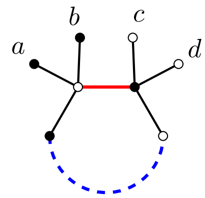

$= X_L$ 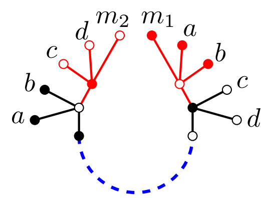

$- X_L\Big(\Big\langle m_1, a, b, (c,d) \cap m_2 \Big\rangle\Big)\,,$

X_R 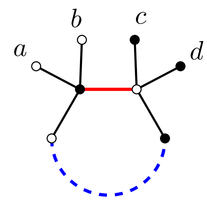

$= X_R$ 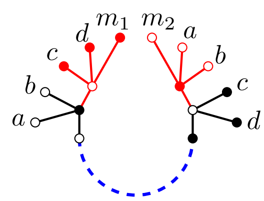

$- X_R\Big(\Big\langle m_2 \cap (a,b), c, d, m_1 \Big\rangle\Big)\,.$

(2.41)

Here we need two reference points m_1, m_2 for each unrolled loop. Actually, since m_2 is associated to a white vertex, it is better thought of as a reference plane, i.e. a triple of reference points. All dependence on these reference points drops out of any invariant. Of course, as always, the recursion rule can only be applied to canonically ordered diagrams.

By way of example let us apply X_L to the non-arborizable G(4, 8) web shown in Figure 2.6(b):

X_L 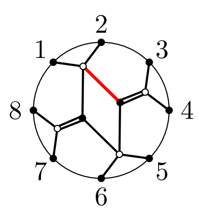

$$
\begin{aligned}
&= X_L\Big(\Big\langle (m_1 12) \cap (34), 5, 6, (78) \cap \big(1, 2, (34) \cap (m_2)\big) \Big\rangle\Big) - X_L(\langle m_1, 1, 2, (34) \cap (m_2) \rangle) \qquad (2.42)\\
&= X_L\big(\langle (m_1 12) \cap (34) \rangle,\ 5,\ 6,\ 8\big) + X_L\big(\langle 7,\ 8,\ 2,\ (34) \cap (m_2) \rangle\big) \\
&\qquad + X_L\big(\langle 6, 1, 2, (34) \cap (m_2) \rangle\big) - X_L\big(\langle 6, 8, 2, (34) \cap (m_2) \rangle\big) \\
&\qquad - X_L\big(\langle m_1, 1, 2, (34) \cap (m_2) \rangle\big) \\
&= X_L(\langle 1246 \rangle) + X_L(\langle 3468 \rangle) + X_L(\langle 5682 \rangle) + X_L(\langle 7824 \rangle) - 2 X_L(\langle 2468 \rangle)\,,
\end{aligned}
$$

which shows the cancellation of the reference points.

Like we discussed for the $\mathfrak{sl}_3$ case, it is of course important that the recursive relations we have given for the $k = 4$ X-map respect the skein equivalences shown in Figure 2.5, in particular applied to the arborization of an inner loop. The proof is similar to the $k = 3$ case but there are more cases of the equivalence to check. We omit the details here and instead consider the illustrative example

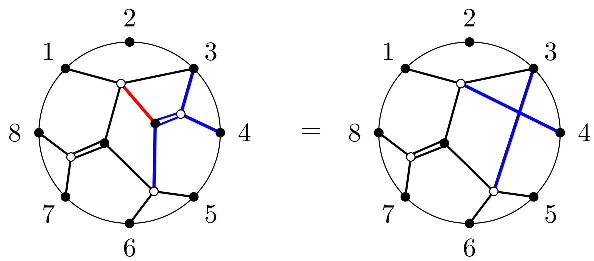

$$. \tag{2.43}$$

According to (2.41), the X_L image of the web on the left is

$$\begin{aligned} &X_L(\langle 1346\rangle) + X_L(\langle 3468\rangle) + X_L(\langle 5683\rangle) + X_L(\langle 7834\rangle) - 2X_L(\langle 3468\rangle) \\ &\qquad = X_L(\langle 1346\rangle) + X_L(\langle 5683\rangle) + X_L(\langle 7834\rangle) - X_L(\langle 3468\rangle)\,, \end{aligned} \tag{2.44}$$

which agrees as required with the X_L image of the web on the right computed from (2.35).

2.3.5 General Relations Between X_L and X_R

Here we point out a few general relations between X_L and X_R that can be derived from the above definitions. First, for $k = 3$, it follows from (2.18) and (2.19) that

$$X_L(W) = X_R(W^{\sharp_3})\,, \tag{2.45}$$

where W is any web invariant, either arborizable or non-arborizable, and $W^{\sharp_3}$ is obtained from W by the replacement

$$a \to (a{+}1) \times (a{+}2) \tag{2.46}$$

(which exchanges vectors and covectors). Note that if W involves something like $b \times (b{+}1)$ then according to (2.46) we have

$$b \times (b{+}1) \to [(b{+}1) \times (b{+}2)] \times [(b{+}2) \times (b{+}3)] = \langle b{+}1, b{+}2, b{+}3\rangle (b{+}2)\,. \tag{2.47}$$

Apart from a trivial overall factor of the frozen variable $\langle b{+}1, b{+}2, b{+}3\rangle$ we can effectively regard the above transformation as

$$b \times (b{+}1) \to b{+}2\,. \tag{2.48}$$

One can check that this makes sense because for both X_L and X_R it follows from (2.18) and (2.19) that

$$X_L(\langle ..., [(b{+}1) \times (b{+}2)] \times [(b{+}2) \times (b{+}3)], ...\rangle) = X_L(\langle ..., b{+}2, ...\rangle)\,, \tag{2.49}$$

$$X_R(\langle ..., [(b{+}1) \times (b{+}2)] \times [(b{+}2) \times (b{+}3)], ...\rangle) = X_R(\langle ..., b{+}2, ...\rangle)\,. \tag{2.50}$$

Therefore we can phrase the inverse of (2.45) and (2.46) as

$$X_R(W) = X_L(W^{\flat_3})\,, \tag{2.51}$$

where $W^{\flat_3}$ is obtained from W by taking

$$a \to (a{-}2) \times (a{-}1)\,. \tag{2.52}$$

Another relation between X_L and X_R involves reflection. For an arbitrary web invariant W, either arborizable or non-arborizable, we have

$$\mathbf{Ref}_s(X_L(W)) = X_R(\mathbf{Ref}(W))\,, \tag{2.53}$$

where **Ref** relabels the external vertices of W according to $a \to n{+}1{-}a$, and $\mathbf{Ref}_s$ acts on kinematic space by $s_{a,b,c} \to s_{n+1-c,n+1-b,n+1-a}$. By combining (2.45) and (2.53) we can also say that

$$\mathbf{Ref}_s(X_L(W)) = X_R(\mathbf{Ref}(W)) = X_L(\mathbf{Ref}(W)^{\flat_3}) = X_L(\mathbf{Ref}(W^{\sharp_3}))\,. \tag{2.54}$$

Analogous relations also exist for $k = 4$. First we have

$$\begin{aligned} X_L(W) &= X_R(W^{\sharp_4})\,, \\ X_R(W) &= X_L(W^{\flat_4})\,, \end{aligned} \tag{2.55}$$

where $W^{\sharp_4}$ and $W^{\flat_4}$ are defined respectively by

$$a \to (a{+}1,\, a{+}2,\, a{+}3) \tag{2.56}$$

and

$$a \to (a{-}3,\, a{-}2,\, a{-}1)\,. \tag{2.57}$$

The composition of $\sharp_4$ and $\flat_4$ is again equivalent to the identity transformation, up to overall factors of frozen variables. For $k = 4$ we again have

$$\mathbf{Ref}_s(X_L(W)) = X_R(\mathbf{Ref}(W)) \tag{2.58}$$

(where $\mathbf{Ref}_s$ acts in the obvious way on indices of Mandelstam variables) and hence

$$\mathbf{Ref}_s(X_L(W)) = X_R(\mathbf{Ref}(W)) = X_L(\mathbf{Ref}(W)^{\flat_4}) = X_L(\mathbf{Ref}(W^{\sharp_4}))\,. \tag{2.59}$$

2.3.6 Kinematic Length

It is intuitively clear that “more complicated” webs have “more complicated” invariants, and are assigned by the X-map to ”more complicated” kinematic functions. In this section we formalize this notion of complexity in a way that will play an important role in Section 2.5. To that end we first define two bases [80] of the generalized kinematic space $\mathcal{K}_{k,n}$ (different from the ABHY basis constructed in Section 2.6.2). The *left kinematic basis* is the set $\{X_L(p) : p \text{ is a non-frozen Plücker coordinate}\}$, and the *right kinematic basis* is defined analogously using X_R. Note that each set contains $\binom{n}{k} - k$ elements, the same as the dimension of $\mathcal{K}_{k,n}$, and it has been shown in [80] that they are linearly independent in $\mathcal{K}_{k,n}$, so each is indeed a basis.

We define the *left (right) kinematic length* of a kinematic function F as the sum of the coefficients of F when expressed in the left (right) kinematic basis. Next, we define the *cluster length* of a web invariant $[W]$ to be equal to $1/k$ times the number of external legs of the associated web; this is the same as the degree of $[W]$ when expressed as a polynomial in $\mathrm{G}(k,n)$ Plücker coordinates.

Now the notion that more complicated invariants are associated to more complicated kinematic functions is formalized in the statement that the left (or right) kinematic length of $X_L([W])$ (or $X_R([W])$) is equal to the cluster length of $[W]$. It is easy to verify that this statement is true by recursion. If p is a non-frozen Plücker coordinate then by definition its cluster length is 1 and the left (or right) kinematic length of $X_L(p)$ (or $X_R(p)$) is 1. For more complicated invariants, we note that in all of the recursive definitions (2.18), (2.19), (2.36), (2.39) and (2.40), each side is linear in both kinematic and cluster length; this establishes the equality.

2.4 Web Series

A *web series* $\mathcal{W}$ is a formal power series of webs $W_1, W_2, \ldots$

$$\mathcal{W} = 1 + \sum_{m=1}^{\infty} t^m W_m \,, \tag{2.60}$$

to which we associate the invariant

$$[\mathcal{W}] = 1 + \sum_{m=1}^{\infty} t^m [W_m] \,. \tag{2.61}$$

We are interested in web series whose invariants are cluster series of the type reviewed in Section 2.1.2. Once a cluster algebra basis is specified (for example, the one provided by the character formula of [6]), then each such series is (in principle) completely determined by its first nontrivial term W_1. Therefore, we are interested to study natural ways to associate an entire web series $\mathcal{W}(W)$ to a single web W, with $W_1 = W$ and with the higher-order terms $W_2, W_3, \ldots$ being determined from W in some manner.

One simple way to do this is via the "web thickening" procedure of [3, Definition 10.8]. If W is any web and we take W_m to be the combination of m copies of W, then $[W_m] = [W]^m$ and the web series invariant is geometric:

$$1 + \sum_{m=1}^{\infty} t^m [W_m] = \frac{1}{1 - t[W]} \,, \tag{2.62}$$

just like the series (2.7) for cluster variables. According to the FP conjectures, $[W]$ is a cluster variable precisely when W is an indecomposable arborizable web, so for such W we define the web series $\mathcal{W}(W)$ by the aforementioned thickening procedure.

However if W is a non-arborizable web we seek a different definition of the web series $\mathcal{W}(W)$ because we want its invariant to not be geometric, but rather to evaluate to more complicated rational functions such as (2.4) or (2.6). In Section 2.4.3 we provide such a definition for a class of indecomposable webs that we call *almost arborizable*—these are non-arborizable webs that can be converted, via skein relations, to tensor diagrams (possibly non-planar) with a single closed inner loop. (For $k > 3$ we further require every edge of that closed inner loop to be a single line.) We leave for future work the study of web series associated to more complicated non-arborizable webs. In order to connect to the notation used in Section 2.1.2 let us define $A(W) = [W]$, the usual web invariant, and now take a short diversion to define a new type of invariant $B(W)$ that we can associate to certain almost arborizable webs.

2.4.1 $\mathfrak{sl}_3$ Almost Arborizable Webs

Let W be an almost arborizable $\mathfrak{sl}_3$ web and let D be the equivalent tensor diagram with exactly one inner loop. We first define $B_1(W)$ and $B_2(W)$ as follows:

- (a) Starting with D, delete all the edges on the loop that go in clockwise order from a white vertex to a black vertex.
- (b) Now all vertices originally on the loop are divalent. Delete those vertices, fusing the two edges at each vertex into a single edge.
- (c) Now we have a new tensor diagram where all inner vertices are trivalent, and all edges connect a black vertex with a white vertex. Define $B_1(W)$ to be the invariant of this diagram.
- (d) Repeat steps (a)–(c) but delete edges that go from white vertices to black vertices in counter-clockwise order. Define $B_2(W)$ to be the invariant of this diagram.

Then define $B(W) = B_1(W)B_2(W)$. As an example let $W^{(1)}$ be our old friend, Figure 2.6(a), whose invariant is

$$A(W^{(1)}) = \langle 145\rangle\langle 278\rangle\langle 369\rangle - \langle 245\rangle\langle 178\rangle\langle 369\rangle - \langle 123\rangle\langle 456\rangle\langle 789\rangle - \langle 129\rangle\langle 345\rangle\langle 678\rangle \,. \tag{2.63}$$

To compute $B_1(W^{(1)})$ we delete the edges shown here as dotted red lines, and then remove the divalent vertices, which gives:

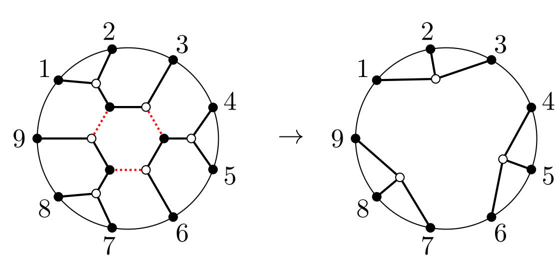

(2.64)

Similarly for $B_2(W^{(1)})$ we look at

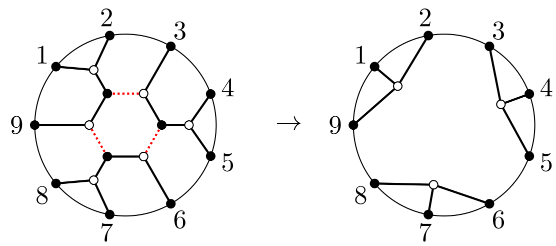

(2.65)

and so we can read off

$$B(W^{(1)}) = \langle 123\rangle\langle 456\rangle\langle 789\rangle\langle 345\rangle\langle 678\rangle\langle 129\rangle\,. \tag{2.66}$$

To see a less trivial example, we move on to $n = 10$ and consider the web $W^{(2)}$ given by

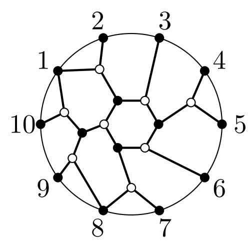

(2.67)

whose invariant is

$$\begin{aligned} A(W^{(2)}) = \langle 3\times 6, 8\times 9, 10\times 1\rangle\langle 1\times 2, 4\times 5, 7\times 8\rangle - \langle 1,2,3\rangle\langle 4,5,6\rangle\langle 7,8,9\rangle\langle 1,8,10\rangle \\ - \langle 3,4,5\rangle\langle 6,7,8\rangle\langle 1,8,9\rangle\langle 1,2,10\rangle\,. \end{aligned} \tag{2.68}$$

To compute $B_1(W^{(2)})$ we look at

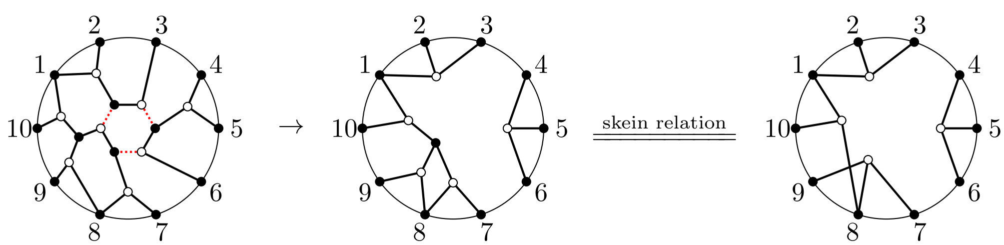

(2.69)

and to compute $B_2(W^{(2)})$ we look at

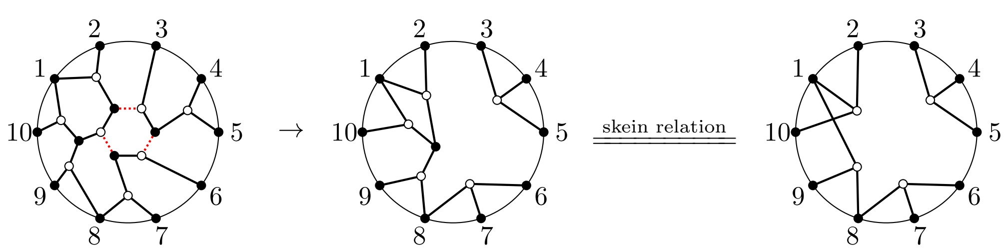

(2.70)

from which we read off

$$B(W^{(2)}) = \langle 1,2,3\rangle\langle 4,5,6\rangle\langle 7,8,9\rangle\langle 1,8,10\rangle\langle 1,2,10\rangle\langle 3,4,5\rangle\langle 6,7,8\rangle\langle 1,8,9\rangle\,. \tag{2.71}$$

2.4.2 $\mathfrak{sl}_4$ Almost Arborizable Webs

Let W be an almost arborizable $\mathfrak{sl}_4$ web and let D be the equivalent tensor diagram with exactly one inner loop. As mentioned above, require that all edges on the inner loop of D are single lines; this is sufficient to cover all webs we encounter in Section 2.5. In such cases we define $B_1(W)$ and $B_2(W)$ as follows:

- (a) Starting with D, delete all the edges on the loop that go in clockwise order from a white vertex to a black vertex.
- (b) If there were initially e edges on the inner loop, then there are now $e/2$ pairs of connected trivalent vertices where the loop used to be. For each pair of vertices we add another edge, giving altogether $e/2$ 2-cycles, and then multiply each new 2-cycle by a factor of $1/2$.
- (c) Then use the skein relations to cancel each 2-cycle, which removes the factors of $1/2$ introduced in the previous step.
- (d) At this stage we have a valid $\mathfrak{sl}_4$ tensor diagram (all inner vertices are quadrivalent, and all edges connect a black vertex to a white vertex). Define B_1 to be the invariant of this diagram.
- (e) Repeat steps (a)–(d) but delete edges that go from white vertices to black vertices in counter-clockwise order. Define $B_2(W)$ to be the invariant obtained in this way.

Then define $B(W) = B_1(W)B_2(W)$. To illustrate these definitions let $W^{(3)}$ be our other friend, Figure 2.6(b), whose invariant is

$$A(W^{(3)}) = \langle 1\,2\,5\,6\rangle\langle 3\,4\,7\,8\rangle - \langle 1\,2\,7\,8\rangle\langle 3\,4\,5\,6\rangle - \langle 1\,2\,3\,4\rangle\langle 5\,6\,7\,8\rangle\,. \tag{2.72}$$

Then to compute B_1 we look at

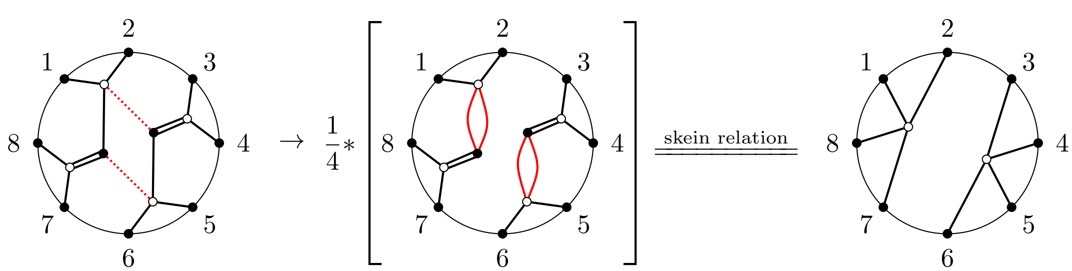

(2.73)

and to compute B_2 we look at

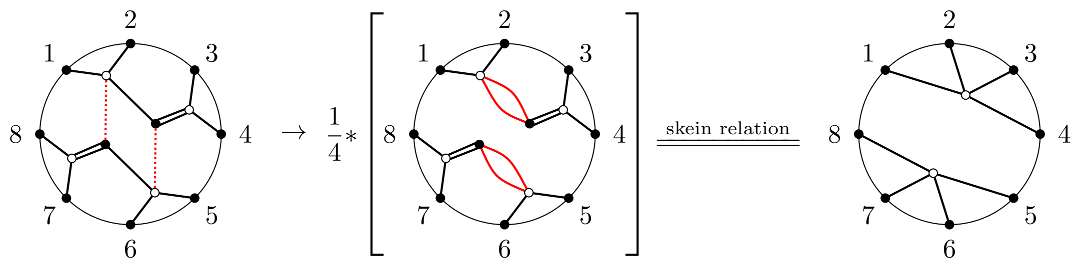

(2.74)

from which we see that

$$B(W^{(3)}) = \langle 1\,2\,3\,4\rangle\langle 5\,6\,7\,8\rangle\langle 1\,2\,7\,8\rangle\langle 3\,4\,5\,6\rangle\,. \tag{2.75}$$

Note that (2.72) and (2.75) agree with (2.5).

2.4.3 A Web Series for Almost Arborizable Webs

We now define a web series $\mathcal{W}(W)$ associated to every almost-arborizable web W via a slight modification of the thickening procedure of [3]. Let W be a given almost-arborizable web and let D be a tensor diagram with a single inner loop such that $[D] = [W]$. To define the $\mathcal{O}(t^2)$ term $W_{(2)}$ in the web series we first draw a combination of two copies of D and then connect the two inner loops by twisting any pair of edges. For example, if the inner loop is a hexagon then we take

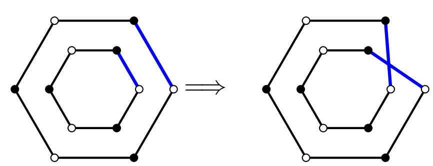

(2.76)

where we suppress the rest of the diagram, showing only the internal loop. The generalization is clear: $W_{(m)}$ is defined by combining m copies of W, cutting one identical edge on each of the m inner loops, and gluing them back together after a (cyclic) "shift-by-one" permutation. This was called the bracelet operation in [70], where web series and invariants constructed in this way were studied for $\mathfrak{sl}_3$.

Using skein relations and the definitions given in the previous two subsections, it is easy to see that

$$\begin{aligned} [W_{(2)}] &= A(W)^2 - 2\,B(W)\,, \\ [W_{(m)}] &= A(W)\,[W_{(m-1)}] - B(W)\,[W_{(m-2)}] \qquad m > 2\,, \end{aligned} \tag{2.77}$$

where $A(W) = [W]$ is the web invariant we start with and $B(W) = B_1(W)B_2(W)$. Thanks to (2.77), the invariant of the web series $\mathcal{W}(W)$ can be written in the form of (2.6):

$$[\mathcal{W}(W)] = \frac{1 - B(W)\,t^2}{1 - A(W)\,t + B(W)\,t^2}\,. \tag{2.78}$$

To summarize: we have shown that there is a natural web series $\mathcal{W}(W)$ one can associate to any almost arborizable web W, and that the invariant of this series evaluates to (2.78) in terms of the usual web invariant $A(W) = [W]$ and a second quantity $B(W)$ that admits a simple diagrammatic definition. (The definition of the web series can be considered to include arborizable webs as a special case for which $B(W) = 0$.)

We conjecture that for any almost arborizable W, $A(W)$ and $B(W)$ agree with the quantities A and B appearing in the series (2.4) associated (via the character formula of [6]) to the ray $\mathbb{R}^+\mathbf{y}$, where $\mathbf{y}$ is the $\mathbf{g}$-vector of $[W]$. It is furthermore natural to speculate that more complicated webs (that are not almost arborizable) are associated to series with higher-order polynomials in their denominators. We leave such questions to future work.

2.5 Results and Discussion

Now that all the pieces are finally in place we detail the application of our algorithm to the polytopes $\mathcal{C}(3, n \leq 10)$, $\mathcal{C}^\dagger(3, n \leq 10)$, $\mathcal{C}(4, n \leq 8)$ and $\mathcal{C}^\dagger(4, n \leq 9)$, the definitions of which are reviewed in Section 2.6.4. All of these have been constructed or analyzed in the literature, to varying degrees, and by various methods, although only the $k = 4$ polytopes are of direct relevance to SYM theory. In particular, the cluster variables associated to $\mathcal{C}(4, 8)$ and $\mathcal{C}^\dagger(4, 8)$ were determined in [31, 50, 32] and the cluster series associated to them were determined in [50]. These prior results serve as checks on the correctness of our methods; however our results for $\mathcal{C}(3, 10)$, $\mathcal{C}^\dagger(3, 10)$ and $\mathcal{C}^\dagger(4, 9)$ are genuinely new[8].

For each polytope $\mathcal{P}$ on the above list, our algorithm (summarized in Figure 2.2) proceeds as follows. Let $i = 1, 2, \ldots$ index the facets of $\mathcal{P}$, with $\mathbf{y}_i$ being the generator of the ray normal to facet i[9] and $F_{\mathbf{y}_i}$ being the associated kinematic function. Our first goal is to assign a web W_i to each facet such that $X_R(W_i) = F_{\mathbf{y}_i}$[10]. A priori it is not guaranteed that it always possible to find such a W_i. In practice, searching for W_i is feasible since for any given $F_{\mathbf{y}_i}$, we only need to scan over a manifestly finite set of sufficiently simple candidate webs—specifically, those whose length (defined in Section 2.3.6) is at most that of $F_{\mathbf{y}_i}$. Actually we can exploit the general relations derived in Section 2.3.5 for considerable simplification: for each facet i we only need to scan up to the length set by the *shortest* image of i under the D_n dihedral group. In this manner we have found webs associated to all facets of $\mathcal{C}(3, 10)$, $\mathcal{C}^\dagger(3, 10)$ and $\mathcal{C}^\dagger(4, 9)$ by scanning webs of length up to 7, 5, and 6, respectively.

The webs W_i we encounter fall into three types:

1. If W_i is arborizable, then (according to the FP conjectures) $\mathbf{y}_i$ is a $\mathbf{g}$-vector of the $\mathrm{G}(k, n)$ cluster algebra and $[W_i]$ is a cluster variable that we associate to facet i. (Equivalently, we

[8] We thank N. Henke for independently corroborating our results for $\mathcal{C}^\dagger(4, 9)$; see [33].

[9] This data, which is the "raw input" to our computation, was first computed in [52] for $(3, 6)$ and $(3, 7)$ (see also [81]), [50, 82] for $(3, 8)$, [82] for $(3, 9)$, [56, 31, 50, 32, 82] for $(4, 8)$, [83] for $(3, 10)$ and [82] for (4,9).

[10] We choose X_R to match the conventions of [6], following [50].

web type: cluster series type:	(1) arborizable (2.7) (i.e., cluster variable)	(2) almost arborizable (2.78)	(3) neither unknown
$\mathcal{C}(3,5) = \mathcal{C}^\dagger(3,5)$	5	0	0
$\mathcal{C}(3,6)$, $\mathcal{C}^\dagger(3,6)$	16	0	0
$\mathcal{C}(3,7)$, $\mathcal{C}^\dagger(3,7)$	42	0	0
$\mathcal{C}^\dagger(3,8)$	112	0	0
$\mathcal{C}(3,8)$	120	0	0
$\mathcal{C}^\dagger(3,9)$	327	0	0
$\mathcal{C}(3,9)$	468	3	0
$\mathcal{C}^\dagger(3,10)$	1060	0	0
$\mathcal{C}(3,10)$	2860	280	0
$\mathcal{C}^\dagger(4,6)$, $\mathcal{C}(4,6)$	9	0	0
$\mathcal{C}^\dagger(4,7)$, $\mathcal{C}(4,7)$	42	0	0
$\mathcal{C}^\dagger(4,8)$	272	2	0
$\mathcal{C}(4,8)$	356	4	0
$\mathcal{C}^\dagger(4,9)$	3078	324	27

Table 2.3: The number of facets of types (1), (2) and (3) (defined in the text) for various polytopes. Note that the facets of $\mathcal{C}^\dagger(k,n)$ are always (by construction) a subset of those of $\mathcal{C}(k,n)$. The set of facets associated to each polytope is closed under the action of the $\mathbb{Z}_n$ cyclic group, and for the $\mathcal{C}^\dagger$ polytopes they are closed under the full D_n dihedral group as well as under parity (see Appendix A of [28] for a discussion of parity symmetry.)

associate to facet i the cluster series $1/(1-t[W_i])$).

2. If W_i is almost arborizable, then we can compute $A(W_i)$ and $B(W_i)$ as described in Section 2.4 and the cluster series associated to facet i is $(1 - B(W_i)\,t^2)/(1 - A(W_i)\,t + B(W_i)\,t^2)$.

3. In other cases we don't yet know how to associate a web series to W_i, although we conjecture that there exists a natural way to do so; the cluster series associated to these facets may have polynomials of degree higher than 2 in their denominators.

We summarize the number of facets of each type for various polytopes in Table 2.3. We also include ancillary files that list, for each of these polytopes, the kinematic function $F_{\mathbf{y}_i}$ and web invariant $[W_i]$ associated to each facet. For each almost arborizable web we also include the A and B invariants appearing in the associated series (2.78).

A few important comments about our algorithm are in order. First of all, we cannot exclude in generality the possibility that there might exist two webs W_1, W_2 with $[W_1] \neq [W_2]$ that have the same image $X_R(W_1) = X_R(W_2) = F$. If this were to happen for a kinematic function F associated to some facet of a polytope of interest, then we would not know which web to assign to that facet. However, we have not encountered such a situation as far as we have computed: for given F, we have always found there is (up to skein relations, of course) precisely one web W such that $X_R(W) = F$ (among all possible webs below the maximum lengths we have checked).

Second, we must of course mention the possibility that the FP conjectures could be wrong for $(k,n) = (3,10)$ or $(4,9)$. Then we would have to worry that there could be some web W and some non-web D such that (1) $X_R(W) = X_R(D) = F$ and (2) $[D]$ is a cluster variable but $[W]$ is not. In such a case our algorithm would suggest associating W to the facet F, when it might be more appropriate to associate D instead. The fact that we have not encountered any apparent inconsistency in our calculations for $\mathcal{C}^\dagger(4,9)$, which furthermore are corroborated by the independent work of [33], suggests that such worries may be postponed to higher (k,n), if not indefinitely.

Next let us comment on a few interesting features of our results. First of all we note that while $\mathcal{C}(3,n)$ has facets associated to non-arborizable webs for $n = 9, 10$ (and, presumably, for all $n \geq 9$), these are absent from the $\mathcal{C}^\dagger(3,n)$ polytopes that we have studied: all facets of $\mathcal{C}^\dagger(3, n \leq 10)$ are associated to cluster variables. It would be interesting to see if this continues to hold for higher n.

The 3 non-arborizable webs associated to $\mathcal{C}(3,9)$ are the three cyclic images of Figure 2.6(a) and the 4 non-arborizable webs associated to $\mathcal{C}(4,8)$ are the four cyclic images of Figure 2.6(b). Out of the 324 almost arborizable webs associated to $\mathcal{C}^\dagger(4,9)$, 315 have an inner quadrilateral loop and 9 have an inner hexagon. The latter are the cyclic images of

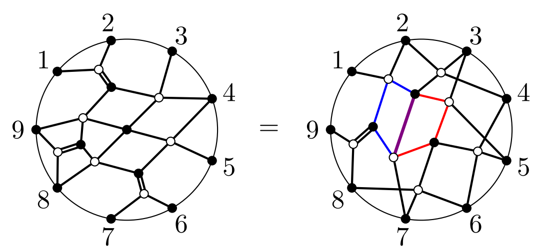

, (2.79)

which are skein equivalent. The figure on the left is a web with many inner loops which is almost arborizable, as apparent by the skein-equivalent figure on the right where the inner hexagon is highlighted in red.

The 27 webs of type (3) listed for $\mathcal{C}^\dagger(4,9)$ fall into three cyclic classes. Instead of drawing the (very complicated) webs, we display here a 2-loop non-planar tensor diagram for one representative of each cyclic class:

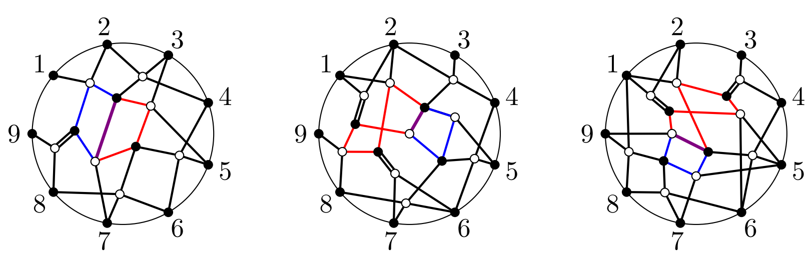

(2.80)

where we highlight the two loops in color. Each of these is skein-equivalent to a valid web (that means, with no 2-cycles or triple edges; see footnote 7).

As already noted above, it would be very interesting to find a natural web series to associate to these more complicated webs; the corresponding invariants might evaluate to rational functions with higher (than quadratic) order polynomials in their denominators. It is interesting to note that the approaches of [31, 51] also seem to encounter some difficulty when passing from $\mathrm{G}(4,8)$

to G$(4,9)$, for essentially the same reason: Whereas the G$(4,8)$ cluster algebra has finite mutation type [84], and all exceptional rays can be asymptotically approached by repeated mutation on some quiver containing an $A_{1,1}$ subalgebra, G$(4,9)$ does not have finite mutation type and has arbitrarily complicated quivers. It would be interesting to more precisely understand how (if at all) this fact relates to webs of the type shown in (2.80).

2.6 Appendix: Conventions

2.6.1 Web Variables

We begin by reviewing the web variables of [52]. First consider the $k \times n$ *web matrix*

$$\begin{pmatrix} 1_{k\times k} & \mathcal{W} \end{pmatrix} \tag{2.81}$$

where $\mathcal{W}$ is the $k \times (n-k)$ matrix constructed as follows. Draw a $(k-1)\times(n-k-1)$ array with faces labeled by *web variables* x_1 through x_d (reading down each column, from left to right). Label the horizontal lines $1,\ldots,k$ from top to bottom and the vertical lines $k+1,\ldots,n$ from left to right. Give each horizontal edge a rightward orientation and each vertical edge an upward orientation. To each path p through the diagram we associate the product of all web variables above p, which we denote by $p(x)$. Then the i,j element of $\mathcal{W}$ is given by

$$\mathcal{W}_{ij} = (-1)^{k-i} \sum_{p: i \to j+k} p(x)\,. \tag{2.82}$$

For example, for $k=3$ the array looks like

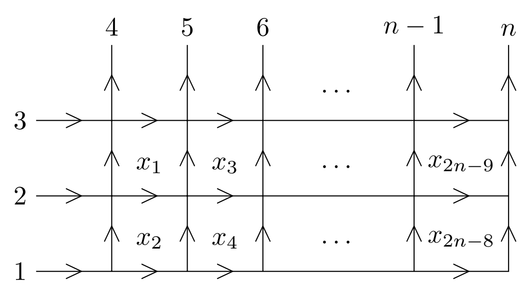

from which we can read off the G$(3,n)$ web matrix

$$\begin{pmatrix} 1 & 0 & 0 & 1 & 1{+}x_1{+}x_1x_2 & 1{+}x_1{+}x_1x_2{+}x_1x_3{+}x_1x_2x_3{+}x_1x_2x_3x_4 & \cdots \\ 0 & 1 & 0 & -1 & -1{-}x_1 & -1{-}x_1{-}x_1x_3 & \cdots \\ 0 & 0 & 1 & 1 & 1 & 1 & \cdots \end{pmatrix}. \tag{2.83}$$

The web matrix associated to G(k,n) provides a parameterization of G$_+(k,n)/T$ as the d web variables range over $\mathbb{R}^d_{>0}$, and (importantly for our purposes) the web variables are precisely the cluster $\mathcal{X}$-coordinates associated to the initial seed of G(k,n) shown in Figure 2.7. Specifically: when evaluated on the web matrix (2.81), the cluster $\mathcal{X}$-coordinate (see Section 2.6.3) attached to any mutable node of the initial quiver is equal to the web variable x that appears in the same position of the web array described above.

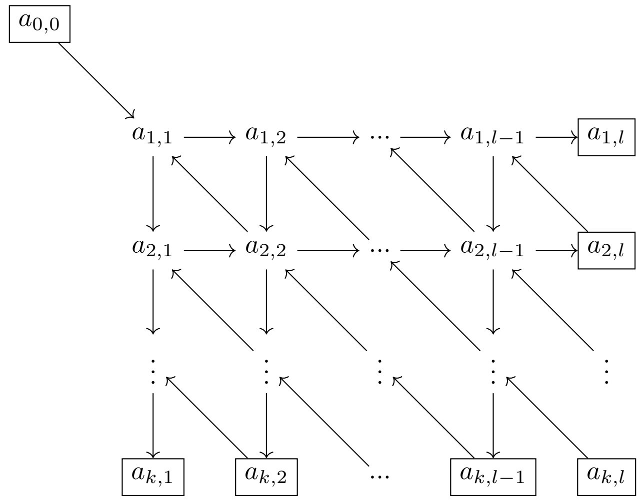

Figure 2.7: Initial seed for the $\mathrm{G}(k,n)$ cluster algebra [4, 5], where $l = n - k$ and $a_{x,y}$ denotes the Plücker coordinate $\langle 1,\ldots,k{-}x,k{+}y{-}x{+}1,\ldots,k{+}y\rangle$. The arrows here are reversed (and the figure is transposed) with respect to that used in [6]; see the discussion in Section 2.6.5.

2.6.2 Kinematic Space and Kinematic Functions

Next we review the planar kinematic variables first employed for $k = 2$ in the construction of [73]. We introduce $\binom{n}{k}$ (generalized) *Mandelstam variables* [54] $s_{i_1,i_2,\ldots,i_k}$, fully symmetric in all indices, subject to the "on-shell" condition $s_{i,i,\ldots} = 0$ and the "momentum conservation" condition

$$\sum_{\{i_2,\cdots,i_k\}\subset\{1,\cdots,n\}\setminus\{i_1\}} s_{i_1,i_2,\cdots,i_k} = 0 \quad \forall i_1\,. \tag{2.84}$$

The resulting $\binom{n}{k} - n$-dimensional space spanned by these variables is called the *kinematic space* $\mathcal{K}_{k,n}$.

Since the Mandelstam variables are not linearly independent, our next step is to define a particular basis for $\mathcal{K}_{k,n}$ [53]. To that end we consider

$$R_{k,n} = \prod_{1\le i_1<i_2<\cdots<i_k\le n} \langle i_1,i_2,\ldots,i_k\rangle^{\alpha' s_{i_1,i_2,\ldots,i_k}} \tag{2.85}$$

where α' is a positive constant that is irrelevant for our purposes. Note that thanks to (2.84), $R_{k,n}$ is invariant under the torus action that rescales each Z_i^a independently, and therefore is well-defined on $\mathrm{G}(k,n)/T$.

Something remarkable happens when $R_{k,n}$ is evaluated on the $\mathrm{G}(k,n)$ web matrix. The $\binom{n}{k}$ minors fall into two categories. First, there are $n + d$ *trivial minors* that evaluate to 1 or to monomials in web variables; these include the n frozen variables

$$\langle 1,2,\ldots,k\rangle, \langle 2,3,\ldots,k{+}1\rangle, \quad \ldots, \quad \langle 1,2,\ldots,k{-}1,n\rangle \tag{2.86}$$

as well as the d non-frozen variables of the form

$$\langle 1,2,\ldots,j,l,l{+}1,\ldots\, l{+}k{-}j{-}1\rangle \quad 1\le k,\ j+1\le l\le n-(k-j-1)\,. \tag{2.87}$$

Each of the remaining $\binom{n}{k} - n - d$ minors $\langle I \rangle$ factors into a monomial in web variables times a single polynomial $P_I(x)$ that is unique to each minor. Moreover, each of these polynomials is subtraction free and has constant term 1. By collecting all of the overall monomials from both the trivial and non-trivial minors, we can rewrite [53]

$$R_{n,k}(x_1, \ldots, x_d) = \prod_{a=1}^{d} x_a^{\alpha' X_a} \prod_I P_I(x)^{-\alpha' c_I}\,, \tag{2.88}$$

where the product runs over all non-trivial minors, the power of each overall x_a is α' times some linear combination of Mandelstam variables that we denote X_a, and we set $s_I = -c_I$. Altogether the total number of X_a and c_I variables is $\binom{n}{k} - n$, and they provide the desired basis for $\mathcal{K}_{k,n}$.

Here we explain the *kinematic functions* that first appeared in Section 2.1.1. We associate to any point $\mathbf{y} = (y_1, \ldots, y_d)$ in the integer lattice $\mathbb{Z}^d$ the function $F_{\mathbf{y}}$ on kinematic space defined by

$$F_{\mathbf{y}} = \frac{1}{\alpha'} \operatorname*{Res}_{\epsilon=0} d\log R_{k,n}(\epsilon^{-y_1}, \ldots, \epsilon^{-y_d})\,. \tag{2.89}$$

The properties of $R_{n,k}$ ensure that $F_{\mathbf{y}}$ is always an integer linear combination of the X_a and c_I. In fact the coefficient of X_a is just y_a, so we have

$$\mathbf{y} = -(\partial_{X_1} F_{\mathbf{y}}, \ldots, \partial_{X_d} F_{\mathbf{y}})\,. \tag{2.90}$$

Using (2.89) and (2.90) we can pass back and forth between $\mathbf{y}$ and $F_{\mathbf{y}}$ at ease. The two vertical arrows on the right side of Figure 2.2 apply this correspondence to the case when $\mathbf{y}$ is taken to be the generator $\mathbf{y}$ of an outward-pointing normal ray to a $\mathrm{G}(k,n)$-polytope.

For example, for $\mathrm{G}(3,5)$ a simple calculation reveals that

$$R_{3,5}(x_1, x_2) = x_1^{\alpha' X_1} x_2^{\alpha' X_2} (1 + x_1)^{-\alpha' c_{135}} (1 + x_2)^{-\alpha' c_{245}} (1 + x_1 + x_1 x_2)^{-\alpha' c_{235}} \tag{2.91}$$

where $X_1 = s_{123}$ and $X_2 = s_{345}$, and it is also easy to check that (2.89) computes the first column of Table 2.1 from the data given in the second column.

Note it is manifest (by homogeneity) that $F_{m\mathbf{y}} = m F_{\mathbf{y}}$ for any non-negative integer m. This bears resemblance to the statement about cluster algebra bases that $\mathcal{B}(m\mathbf{y}) = \mathcal{B}(\mathbf{y})^m$, but the former holds for any lattice point $\mathbf{y}$ while the latter holds only if $\mathbf{y}$ is inside the cluster fan.

2.6.3 g-Vectors

Next we review the horizontal arrows at the bottom of Figure 2.2. We order the $d+n$ cluster variables ($\mathcal{A}$-coordinates) appearing in the initial quiver (Figure 2.7) $a_1, a_2, \ldots, a_{d+n}$, first reading the mutable variables down each column from left to right, and then the frozen variables counterclockwise starting from $a_{0,0}$. Next recall that the associated exchange matrix is given by $B_{ij} = (\#\text{arrows } i \to j) - (\#\text{arrows } j \to i)$ where i, j run over the nodes, and the cluster $\mathcal{X}$-coordinate associated to node i is related to the $\mathcal{A}$-coordinates of its neighbors by $x_i = \prod_j a_j^{B_{ji}}$.

To any monomial $\prod_i a_i^{g_i}$ we associate the vector of powers $\mathbf{g} = (g_1, \ldots, g_{d+n})$. We introduce a partial order on such vectors by saying that $\mathbf{g}' \preceq \mathbf{g}$ iff $\mathbf{g}' - \mathbf{g}$ is a non-negative linear combination of the first d columns of B (the columns corresponding to mutable nodes). If a is a sum of monomials in the a_i we define the $\mathbf{g}$-vector of a to be that of the term whose $\mathbf{g}$-vector is largest with respect to $\preceq$ (if such a term exists). It is always sufficient to truncate $\mathbf{g}$ to its first d components. If a is a cluster variable of $\mathrm{G}(k,n)$, then the $\mathbf{g}$-vector of a exists and it is said to be a $\mathbf{g}$-vector of the cluster algebra.

We have therefore explained the upward pointing arrow in Figure 2.2. For example, for $\mathrm{G}(3,5)$ we have

$$B^{\mathrm{T}} = \left(\begin{array}{cc:ccccc} 0 & -1 & 1 & 0 & 0 & 1 & -1 \\ 1 & 0 & 0 & -1 & 1 & -1 & 0 \end{array}\right), \tag{2.92}$$

the initial cluster variables (given in the caption) are

$$(a_1, \ldots, a_7) = (\langle 1\,2\,4\rangle, \langle 1\,3\,4\rangle, \langle 1\,2\,3\rangle, \langle 2\,3\,4\rangle, \langle 3\,4\,5\rangle, \langle 1\,4\,5\rangle, \langle 1\,2\,5\rangle)\,, \tag{2.93}$$

and the remaining three cluster variables are given in terms of these by

$$\begin{aligned} \langle 2\,3\,5\rangle &= \frac{a_3 a_5}{a_2} + \frac{a_3 a_4 a_6}{a_1 a_2} + \frac{a_4 a_7}{a_1}\,, \\ \langle 2\,4\,5\rangle &= \frac{a_1 a_5}{a_2} + \frac{a_4 a_6}{a_2}\,, \\ \langle 1\,3\,5\rangle &= \frac{a_3 a_6}{a_1} + \frac{a_2 a_7}{a_1}\,. \end{aligned} \tag{2.94}$$

Here we have written the terms in each sum in increasing order with respect to $\preceq$ so it is easy to read off, from the last term in each line, the $\mathbf{g}$-vectors $(-1,0)$, $(0,-1)$ and $(-1,1)$, as shown in Table 2.1.

Going the other way, down the dotted arrow in Figure 2.2 to compute the cluster variable (or more general basis element) associated to a given lattice vector $\mathbf{x}$, is not so simple. In practice one often resorts to a computer search by repeatedly mutating away from the initial seed until one has the fortune to chance upon a cluster variable whose $\mathbf{g}$-vector is $\mathbf{x}$. Of course for infinite algebras this algorithm may take an indefinite amount of time. Even worse, $\mathbf{x}$ may lie outside the cluster fan in which case one will never find a match.

One alternative, suggested in [50], is to read Corollary 7.3 of [6] as providing an explicit formula for an element of the canonical basis [77] associated to every $\mathbf{g}$ that agrees with the usual cluster algebraic definition when $\mathbf{g}$ lies inside the cluster fan. Although the required computation is manifestly finite for any $\mathbf{g}$, its enormous computational complexity makes it impractical in many cases of interest.

2.6.4 $\mathrm{G}(k,n)$-Polytopes

Before ending this section, we are finally in a position to review the construction of the $\mathrm{G}(k,n)$-*polytopes* of interest, which generalize the well-known Stasheff polytope [71, 72] building on a construction introduced in [73]. These polytopes lie in the d-dimensional subspace $\mathcal{H}_{k,n}$ of $\mathcal{K}_{k,n}$ obtained by setting all of the c_I to positive constants. Here we see that the purpose of defining $X_1, \ldots, X_d$ in the previous subsection is that we can take these as coordinates on $\mathcal{H}_{k,n}$.

The polytope called $\mathcal{C}(k,n)$ in [50] (called $\mathcal{P}(k,n)$ or dual Trop $\mathrm{G}(k,n)$ in some other references) is defined by taking the Minkowski sum of the Newton polytopes (with respect to $x_1,\ldots,x_d$) associated to the polynomials P_I appearing in (2.88). Other polytopes can be constructed by only including proper subsets of the P_I in the Minkowski sum. For example, of particular interest is the polytope called $\mathcal{C}^\dagger(4,n)$ in [50] (also studied in [31, 32]). It is defined as the polytope obtained by including only polynomials associated to $\langle I\rangle$'s of the form $\langle i\,i{+}1\,j\,j{+}1\rangle$ or $\langle i{-}1\,i\,i{+}1\,j\rangle$, and may be obtained from $\mathcal{C}(4,n)$ by setting to zero all c_I except those corresponding to these I's. Here we define $\mathcal{C}^\dagger(3,n)$ to be the polytope obtained by keeping only $\langle I\rangle$'s of the form $\langle i\,i{+}1\,j\rangle$.

More general polytopes of the same basic type can be constructed by including other proper subsets of the P_I in the Minkowski sum, or by including polynomials obtained by evaluating more complicated $\mathrm{G}(k,n)$ cluster variables on the web matrix. An example of the latter was considered in [31].

2.6.5 Langlands Dual Conventions

Because our work touches on a wide range of previous work in the physics and math literature, we find it helpful to clearly connect to two different choices of convention that are related to each other by what could be called "Langlands duality" (see Remark 7.15 of [74]). By this we mean performing the following compatible set of changes:

1. inverting each $x_i \to 1/x_i$ in the web parameterization of Section 2.6.1,
2. reversing each arrow in Figure 2.7,
3. and, correspondingly, changing the sign of the B-matrix with respect to which $\mathbf{g}$-vectors are computed as described in Section 2.6.3.

The conventions outlined in Section 2.6.1 through Section 2.6.3 correspond to what we call the "left" convention starting in Section 2.3. To illustrate the different conventions we present in Table 2.4 the "right" convention version of the $\mathrm{G}(3,5)$ data from Table 2.1. Note that the form of the equations (2.94) is the same for both choices, and while the "left" $\mathbf{g}$-vectors shown in Table 2.1 can be read off from the last term in each line, we can similarly read off the "right" $\mathbf{g}$-vectors (shown in Table 2.4) from the first term on each line. We explain a general relation between the two conventions, at the level of our X-map applied to general tensor diagrams, in Section 2.3.5.

2.7 Appendix: Summary of Known Symbol Letters

Here we summarize what is known about the symbol alphabet S_n of n-particle amplitudes in SYM theory. In this discussion we of course restrict our attention to those amplitudes which are of polylogarithmic type, and so have conventionally-defined symbols.

Let us begin with the rational letters. All currently known rational letters are cluster coordinates of $\mathrm{G}(4,n)$, which (according to the FP conjectures) means that we can represent them as arborizable

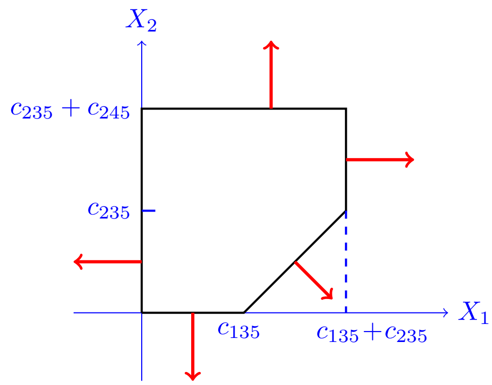

Figure 2.8: The polytope $\mathcal{C}(3,5)$ according to the "right" conventions; see Table 2.4 and contrast with Figure 2.1.

kinematic function	generator	cluster variable
$s_{123} = c_{135} + c_{235} - X_1$	$(1,0)$	$\langle 1\,2\,4\rangle$
$s_{345} = c_{235} + c_{245} - X_2$	$(0,1)$	$\langle 1\,3\,4\rangle$
$s_{125} = X_1$	$(-1,0)$	$\langle 1\,3\,5\rangle$
$s_{234} = X_2$	$(0,-1)$	$\langle 2\,3\,5\rangle$
$s_{145} = c_{135} - X_1 + X_2$	$(1,-1)$	$\langle 2\,4\,5\rangle$

Table 2.4: The correspondence between kinematic functions, generators, and cluster variables for the $\mathcal{C}(3,5)$ polytope according to the "right" conventions, shown in Figure 2.8, in contrast to Table 2.1 which shows the correspondence for the "left" conventions.

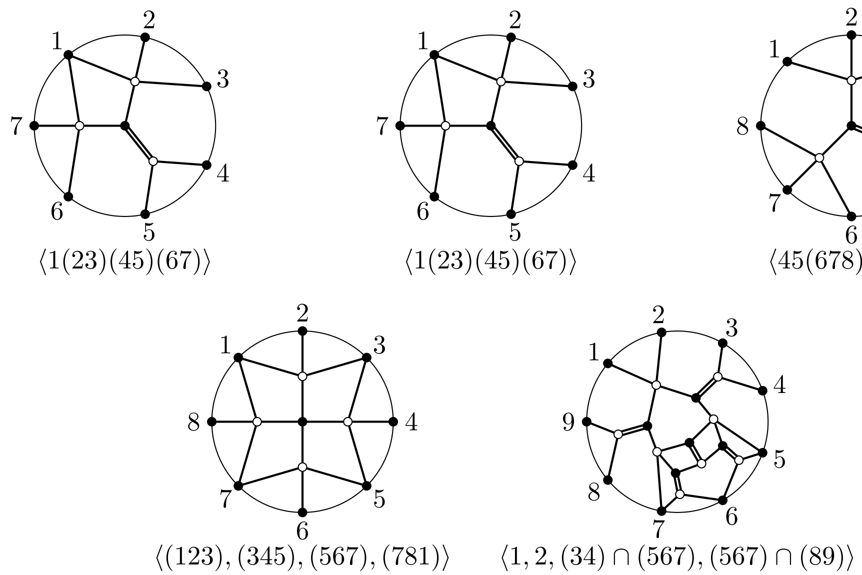

Figure 2.9: Examples of webs, and their corresponding invariants (cluster variables), for the five different basic types (defined in the text) of rational symbol letters that are known to appear in SYM theory.

webs. It expected that the n-particle symbol alphabet is a strict subset of the n'-particle symbol alphabet for all $n' > n$, which corresponds to the fact that we can always make a valid n'-particle web by adding $n' - n$ boundary vertices, with no edges attached, to an n-particle web. Therefore it is convenient to categorize different types of symbol letters according to the smallest value of n at which they first appear; we also categorize them by Plücker degree. In this way we encounter five basic types of rational letters for $n \leq 9$:

(1) $S_{n\geq 6}$ contains the Plücker coordinates of the form $\langle 1\,2\,a\,b\rangle$ for $3 \leq a < b \leq n$, and their cyclic images. (For $n < 8$ all Plücker coordinates are of this type.)

(2) $S_{n\geq 7}$ contains letters that are quadratic in Plücker coordinates having the form $\langle a(b\,c)(d\,e)(f\,g)\rangle :=$

n	(1)	(2)	(3)	(4)	(5)	References
6	15	0	0	0	0	[85, 86, 21, 87, 88, 89, 27]
7	35	14	0	0	0	[85, 90, 91, 92, 93, 94]
8	68	88	8	16	0	[85, 95, 96, 91, 97]
9	117	270	63	72	9	[85, 95, 96, 91, 25]

Table 2.5: Enumeration of rational symbol letters of n-particle amplitudes in SYM, based on the results of all explicit computations available to date, and categorized according to the five types defined in the text. The lines $n = 6, 7$ are believed to be complete (see [60]), comprising the 15 and 49 cluster variables of $\mathrm{G}(4,6)$ and $\mathrm{G}(4,7)$, respectively. For $n > 7$ the counts may grow as computations are pushed to higher order in the future; additional types of rational letters may also appear.

$\langle a\,b\,d\,e\rangle\langle a\,c\,f\,g\rangle - \langle a\,b\,f\,g\rangle\langle a\,c\,d\,e\rangle$. Specifically, S_7 contains the 14 non-Plücker cluster variables of $\mathrm{G}(4,7)$: $\langle 1(23)(45)(67)\rangle$, $\langle 1(72)(34)(56)\rangle$ and their cyclic images. The letters of this type for $n = 8, 9$ are listed in [97, 25].

(3) $S_{n\geq 8}$ contains additional quadratic letters having the form (2.12); specifically $\langle 12(abc)\cap(def)\rangle$ for $3 \leq a < b < c < d < e < f \leq n$ and their cyclic images.

(4) $S_{n\geq 8}$ also contains certain cubic letters listed for $n = 8, 9$ in [97, 25].

(5) For $n \geq 9$ S_n contains a second type of cubic letter; see [25].

In Table 2.5 we tabulate the number of cluster variables of each type that appear in the $n \leq 9$-particle amplitudes whose symbols have been explicitly computed to date. For $n \geq 8$ the numbers are expected to grow as higher-loop calculations are carried out, and there is no reason to expect that more complicated types will not be encountered. However, some evidence suggests that for every fixed value of n, the total number of symbol letters (at arbitrary finite order in perturbation theory) might be finite [60] (unlike the number of cluster variables, which is infinite).

Next we turn to the algebraic letters that are known to start appearing in S_n for $n \geq 8$. The two-loop NMHV amplitudes have 18, 99 multiplicatively independent algebraic letters respectively for $n = 8, 9$ [97, 25]. As reviewed in Table 2.2, these respectively involve 2, 9 distinct square roots of Plücker polynomials; all are of four-mass box type, having the form $\sqrt{A^2 - 4B}$ in terms of (2.5), or cyclic images thereof. In our approach, as we found in Section 2.4, each of these arises from a web series associated to (a cyclic image of) the almost arborizable web shown in Figure 2.6(b) (or, for $n = 9$, the same web but with a ninth boundary point added anywhere in the diagram).

2.8 Appendix: Some Notation for Kinematic Functions

In this appendix we collect some notation, originally introduced in [83], to efficiently encode certain kinematic functions. If A is a subset of $\{1, \ldots, n\}$, we define

$$S_A = \sum_{a_1 < a_2 < a_3 \in A} s_{a_1 a_2 a_3}\,. \tag{2.95}$$

If A, B are two subsets, then we define

$$S_{A(B)} = S_{(B)A} = S_A + S_{(B)} + S_{A|B} \quad \text{where} \quad S_{A|B} = \sum_{a_1 < a_2 \in A, b \in B} s_{a_1 a_2 b} \tag{2.96}$$

and, on the right-hand side, (B) means the complement of B in $\{1, \ldots, n\}$.

For $k = 4$ we require some additional notation. If A, B and C are subsets of $\{1, \ldots, n\}$ then we define

$$\boldsymbol{S}_{A[B(C)]} = \boldsymbol{S}_{[(C)B]A} = \boldsymbol{S}_A + \boldsymbol{S}_{[B(C)]} + \sum_{\substack{a_1 < a_2 < a_3 \in A \\ i \in B \cup C}} s_{a_1 a_2 a_3 i} + \sum_{\substack{a_1 < a_2 \in A \\ b_1 < b_2 \in B}} s_{a_1 a_2 b_1 b_2} + \sum_{\substack{a_1, a_2 \in A \\ b \in B, c \in C}} s_{a_1 a_2 b c} \tag{2.97}$$

where

$$\boldsymbol{S}_{[B(C)]} = \boldsymbol{S}_{[B]} + \boldsymbol{S}_{(C)} + \sum_{\substack{b_1 < b_2 \in B \\ c \in C, i \notin B \cup C}} s_{b_1 b_2 c i} + \sum_{\substack{b_1 < b_2 < b_3 \in B \\ c \in C}} s_{b_1 b_2 b_3 c} + \sum_{\substack{b_1 < b_2 \in B \\ c_1 < c_2 \in C}} s_{b_1 b_2 c_1 c_2} \tag{2.98}$$

and

$$
\begin{aligned}
\boldsymbol{S}_A &= \sum_{a_1<a_2<a_3<a_4\in A} s_{a_1a_2a_3a_4}\,, \\
\boldsymbol{S}_{[B]} &= \sum_{b_1<b_2<b_3<b_4\in B} 2s_{b_1b_2b_3b_4} + \sum_{\substack{b_1<b_2<b_3\in B\\ i\notin B}} s_{b_1b_2b_3i}\,, \\
\boldsymbol{S}_{(C)} &= \sum_{c_1<c_2<c_3<c_4\in C} 3s_{c_1c_2c_3c_4} + \sum_{\substack{c_1<c_2<c_3\in C\\ i\notin C}} 2s_{c_1c_2c_3i} + \sum_{\substack{c_1<c_2\in C\\ i,j\notin C}} s_{c_1c_2ij}\,.
\end{aligned}
\tag{2.99}
$$

Chapter 3

One-loop Integrals from Volumes of Orthoschemes

This Chapter is based on [36].

It is well known that Feynman integrals exhibit remarkable mathematical properties. Even the humblest one-loop integrals, which are not only the most relevant for collider physics computations but also feed their structure into higher loop order through differential equations, still have mysteries awaiting discovery. In this paper, we focus on a particularly famous class of one-loop integrals: the scalar n-gons in n dimensions. These integrals have seen so much attention that it may be surprising to hear that there is yet more to say.

The box integral has a history stretching back over 60 years; see in particular [98, 99, 100, 101]. The (five-dimensional) pentagon, in contrast, has been evaluated only much more recently [102, 103]. One key and beautiful mathematical fact about the n-gon is that the same integral computes the volume of a simplex in $(n-1)$-dimensional hyperbolic space whose shape is set by the (Euclidean) kinematic data and propagator masses [39, 40]. The box integral was revisited in this context in [103], making use of the Murakami-Yano formula for the volume of a hyperbolic tetrahedron [104]. Other papers that have made use of this correspondence include [37, 105, 106, 107], and the simplicity of the n-gon in Mellin space was pointed out in [108].

Around a decade ago there was a brief flurry of interest in the hexagon integral [20, 109, 110, 111, 112], due in part to the fact that (for special kinematics) it is related by differential equations to some one- and two-loop integrals that appear in planar $\mathcal{N} = 4$ super-Yang Mills theory. Also, the time was ripe for progress on loop integrals since the symbol calculus for polylogarithm functions had recently been introduced to the physics literature [21]. However, while its symbol was certainly known [112], the problem of explicitly evaluating the fully general hexagon integral remained unsolved, and seemed exceedingly difficult since the symbol involves 16 distinct square roots of 9 independent kinematic cross-ratios. Today the hexagon integral continues to play a starring role in developments at the forefront of multi-loop integration, in part because it is related by a simple differential equation [108] to the elliptic polylogarithmic double box integral which has received considerable recent attention [62, 113, 114, 115, 116, 117, 118, 119]. The (IR-divergent) massless hexagon has been evaluated to $\mathcal{O}(\epsilon)$ in dimensional regularization in [120].

In this paper, we provide an explicit analytic formula for the hexagon integral with arbitrary internal and external masses, for Euclidean kinematics, in terms of the functions log, Li_2 and Li_3 with algebraic functions of cross-ratios as their arguments. Our work was made possible by a recent mathematical breakthrough due to Rudenko, building on the classic work of Coxeter and Böhm [121, 122, 123, 124], who provided an explicit formula for the volume of any (odd-dimensional) hyperbolic orthoscheme in terms of a class of functions called alternating polylogarithms [41]. Orthoschemes are generalizations of right triangles and we can compute the volume of any simplex—and hence any (even) n-gon integral—by recursively expressing the volume of the simplex as a sum[1] of volumes of orthoschemes. Rudenko's construction works for any even n, but $n = 2, 4, 6$ are special because only in these cases can the answer be expressed in terms of the classical polylogarithm functions[2], and we have invested considerable effort in doing so.

Scientific progress is often nonlinear, and it was only during the course of our work that we learned of a 1995 paper in which Kellerhals provided an explicit formula (as a one-fold integral of weight-2 polylogarithms) for the volume of a doubly-asymptotic hyperbolic orthoscheme in 5 dimensions [125]. Doubly-asymptotic means having at least two vertices on the boundary, so combined with our triangulation algorithm, this is enough to compute the hexagon integral for massless internal propagators but still arbitrary external kinematics—a paper that should have been written a decade ago during the hexagon's brief heyday.

Before jumping into the details of our calculation let us make two remarks. First, it is interesting to note that the so-called antipodal map, which reverses the order of the entries in a symbol and has made an interesting appearance in the recent literature [126, 127], pops up in our work in two seemingly unrelated ways. The symbol of the n-gon integral is reversed if one exchanges the Gram matrix Q (see Section 3.1) associated to a simplex with Q^{-1}, and the "real period" map [19] reviewed in Appendix 3.6 has the effect of reversing the symbol of a function.

Second, it is worth emphasizing that even after the present work, the story of the n-gon integral is certainly not yet fully told. For one thing, in order to cautiously establish a foothold in uncharted territory we restrict our attention to the safe harbor of Euclidean kinematics, but it would certainly be interesting to better understand the structure of the alternating polylogarithm representation in other regions and kinematic signatures (see [103] for a nice discussion, and [128, 129] for a bootstrap approach to computing integrals where understanding various kinematic regions plays a crucial role). Moreover, although our triangulation algorithm gets the job done, it necessarily mangles some of the

[1] As we explain in Section 3.2.2, this is not a dissection since some components may lie outside the original simplex and therefore contribute to the volume with a minus sign. It is a conjecture of Hadwiger that any simplex can be dissected into orthoschemes.

[2] Interestingly the 7- and 9-gon integrals (with massless propagators) should also be classical; we leave these as exercises for the enthusiastic reader.

n-gon integral's structure: in particular, our result is not manifestly cyclically invariant. We hope and anticipate that the full structure of the n-gon integral will be better elucidated in the future.

This paper is structured as follows. In Section 3.1 we very briefly review the relation between n-gon integrals and the volumes of hyperbolic $(n-1)$-simplices. In Section 3.2 we describe the main ideas behind Rudenko's construction and explain our triangulation algorithm which leads to our main result (3.23). In Section 3.3 we review Kellerhals's formula, and in several appendices we compile various necessary technical details.

3.1 The one-loop n-gon integral as a hyperbolic volume

We begin by briefly reviewing the well-known correspondence between one-loop Feynman integrals and volumes of hyperbolic simplices [39, 40] (see also [103] for a nice review and many additional details). The one-loop n-gon scalar Feynman integral in n-dimensional Euclidean space, with propagators having arbitrary masses, is written in terms of dual (or region) momenta as

$$I_n(x_1,\ldots,x_n) = \int \frac{d^n x}{\pi^{n/2}} \prod_{i=1}^{n} \frac{1}{(x-x_i)^2 + m_i^2}\,. \tag{3.1}$$

After introducing Feynman parameters and integrating out x, this can be expressed as

$$I_n(G_{ij}) = \Gamma\left(\frac{n}{2}\right) \int_0^\infty \prod_{i=1}^{n} d\alpha_i\, \delta(\alpha_n - 1) \left(\sum_{i,j=1}^{n} G_{ij}\alpha_i\alpha_j\right)^{-n/2} \tag{3.2}$$

in terms of the quadratic form $G_{ij} = \frac{1}{2}((x_i - x_j)^2 + m_i^2 + m_j^2)$. Henceforth we view I_n as a function of the quadratic form G directly, instead of as a function of the x_i and m_i.

Next, we turn our attention to hyperbolic volumes. Consider the $(n-1)$-dimensional hyperboloid defined by the equation

$$y_1^2 + y_2^2 + \cdots + y_{n-1}^2 - y_n^2 = -1 \tag{3.3}$$

in n-dimensional Euclidean space. An alternate representation of this hyperboloid, called the *projective model*, associates to every point

$$y = (y_1,\ldots,y_{n-1},\sqrt{1+y_1^2+\cdots+y_{n-1}^2}) \tag{3.4}$$

on the upper branch of the hyperboloid the point p in the unit $(n-1)$-dimensional ball given by

$$p = (p_1,\ldots,p_{n-1}) \qquad \text{with} \qquad p_i = y_i/\sqrt{1+y_1^2+\cdots+y_{n-1}^2}\,. \tag{3.5}$$

Equivalently we could view $y_i = p_i/\sqrt{1-p_1^2-\cdots-p_{n-1}^2}$ with the convention $p_n = 1$. We denote the inner product of two points in the projective model by

$$\langle p, q\rangle := 1 - \sum_{i=1}^{n-1} p_i q_i\,. \tag{3.6}$$

For any point p we have $0 \leq \langle p, p \rangle \leq 1$, with $\langle p, p \rangle = 0$ if and only if p lies on the S^{n-2} boundary of the unit ball.

Now consider a geodesic simplex in the hyperboloid with vertices $v_1, \ldots, v_n$. We define the *Gram matrix* Q associated to the simplex by

$$Q_{ij} = \langle v_i, v_j \rangle \,. \tag{3.7}$$

The volume of this hyperbolic simplex depends only on the quadratic form Q and can be represented by the integral

$$\mathrm{Vol}(Q) = \sqrt{|\det Q|} \int_0^\infty \prod_{i=1}^n d\alpha_i \, \delta(\alpha_n - 1) \left(\sum_{i,j=1}^n Q_{ij} \alpha_i \alpha_j \right)^{-n/2} . \tag{3.8}$$

Note that this is manifestly invariant under rescaling $Q_{ij} \to Q_{ij} \lambda_i \lambda_j$; all calculations below will only involve ratios that are invariant under such scalings. By comparing (3.2) to (3.8) we see that the one-loop n-point integral in n dimensions can be expressed as

$$I_n(Q) = \Gamma\left(\frac{n}{2}\right) \frac{\mathrm{Vol}(Q)}{\sqrt{|\det Q|}} \qquad \text{with} \qquad Q_{ij} = \frac{(x_i - x_j)^2 + m_i^2 + m_j^2}{2} \,. \tag{3.9}$$

Note that the Q_{ij} appearing here is not the Gram matrix of any simplex computed from (3.7), but can be brought to such a form by an appropriate rescaling. However, the presentation (3.9) has the virtue of making the massless limit more transparent: the diagonal entries are now $Q_{ii} = m_i^2$, so an integral with all massless propagators computes the volume of a simplex with all vertices on the boundary, which is called an *ideal* simplex.

3.2 Volumes of hyperbolic simplices

In order to compute the volume of the hyperbolic simplex appearing in (3.9) we proceed in two steps. First, we review the recent mathematical breakthrough [41] that expresses the volume of a special class of simplices, called *hyperbolic orthoschemes*, in terms of alternating multiple polylogarithms. Then in Section 3.2.2 we explain a recursive procedure for dividing any simplex into orthoschemes, thereby allowing us to compute (3.9) for any Q. In this section, we use Q ($\mathcal{Q}$) interchangeably to refer either to a simplex (orthoscheme) or to its associated Gram matrix.

3.2.1 Volumes of orthoschemes

An $(n-1)$-dimensional hyperbolic orthoscheme is a hyperbolic simplex for which the bounding hyperplanes H_i can be ordered $(H_1, \ldots, H_n)$ in such a way that H_i is orthogonal to H_j for $|i - j| > 1$. An equivalent definition is that there exists an ordering of the vertices $(v_1, \ldots, v_n)$ of the orthoscheme so that the edges (v_1, v_2), (v_2, v_3), …, (v_{n-1}, v_n) are mutually orthogonal. The equivalence of these two definitions can be seen by taking the hyperplane H_i to be the convex hull of all vertices except v_i.

A *subscheme* of an orthoscheme is the convex hull of an arbitrary subset of its vertices, denoted by $\langle I\rangle = \mathrm{conv}\{v_i | \, i \in I\}$ with I being an ordered subset of $\{1, \ldots, n\}$. One can show that any subscheme of an orthoscheme is again an orthoscheme.

It was shown in [122] that there is a bijection between $(n-1)$-dimensional orthoschemes and configurations $z = (z_0, z_1, \ldots, z_{n+1}) \in \mathcal{M}_{0,n+2}$, the moduli space of $n+2$ points in $\mathbb{P}^1$. Under this bijection the Gram matrix of the orthoscheme is expressed as [41, (6.4), Example 6.6]

$$\mathcal{Q}_{i,j} = \mathcal{Q}_{j,i} = \lambda_i \lambda_j (z_0 - z_i)(z_j - z_{n+1}) \,, \qquad 1 \leq i \leq j \leq n \,, \tag{3.10}$$

where the λ_i are free parameters (associated to rescaling the Feynman parameters, as discussed in the previous section). The condition for the orthoscheme to be hyperbolic is

$$\mathcal{Q}_{i,j}^2 > \mathcal{Q}_{i,i} \mathcal{Q}_{j,j} \tag{3.11}$$

for each $i \neq j$, which we henceforth assume. (This will always be true when we study the n-gon integral in generic Euclidean kinematics [103].) In addition one can immediately see that (3.10) satisfies

$$\mathcal{Q}_{i,j} \mathcal{Q}_{j,k} = \mathcal{Q}_{i,k} \mathcal{Q}_{j,j} \,, \qquad i < j < k \,, \tag{3.12}$$

which is the hyperbolic Pythagorean theorem.

Inverting the relation (3.10) allows one to represent every cross-ratio of the configuration $z \in \mathcal{M}_{0,n+2}$ in terms of the Gram matrix $\mathcal{Q}$ of the corresponding hyperbolic orthoscheme:

$$\begin{aligned}
\frac{z_{0,a} z_{b,n+1}}{z_{0,n+1} z_{b,a}} &= \frac{\mathcal{Q}_{a,b}^2}{\mathcal{Q}_{a,b}^2 - \mathcal{Q}_{a,a} \mathcal{Q}_{b,b}} \,, \\
\frac{z_{0,a} z_{b,c}}{z_{0,c} z_{b,a}} &= -\frac{\mathcal{Q}_{a,b}^2 (\mathcal{Q}_{b,c}^2 - \mathcal{Q}_{b,b} \mathcal{Q}_{c,c})}{(\mathcal{Q}_{a,b}^2 - \mathcal{Q}_{a,a} \mathcal{Q}_{b,b}) \mathcal{Q}_{b,b} \mathcal{Q}_{c,c}} \,, \\
\frac{z_{a,b} z_{c,n+1}}{z_{a,n+1} z_{c,b}} &= -\frac{(\mathcal{Q}_{a,b}^2 - \mathcal{Q}_{a,a} \mathcal{Q}_{b,b}) \mathcal{Q}_{b,c}^2}{\mathcal{Q}_{a,a} \mathcal{Q}_{b,b} (\mathcal{Q}_{b,c}^2 - \mathcal{Q}_{b,b} \mathcal{Q}_{c,c})} \,, \\
\frac{z_{a,b} z_{c,d}}{z_{a,d} z_{c,b}} &= -\frac{\mathcal{Q}_{b,c}^2 (\mathcal{Q}_{a,b}^2 - \mathcal{Q}_{a,a} \mathcal{Q}_{b,b})(\mathcal{Q}_{c,d}^2 - \mathcal{Q}_{c,c} \mathcal{Q}_{d,d})}{\mathcal{Q}_{b,b} \mathcal{Q}_{c,c} (\mathcal{Q}_{a,d}^2 - \mathcal{Q}_{a,a} \mathcal{Q}_{d,d})(\mathcal{Q}_{b,c}^2 - \mathcal{Q}_{b,b} \mathcal{Q}_{c,c})}
\end{aligned} \tag{3.13}$$

for $1 \leq a < b < c < d \leq n$, where $z_{i,j} = z_i - z_j$. After fixing the convenient gauge

$$z_0 = 0 \,, \qquad z_n = 1 \,, \qquad z_{n+1} = \infty \tag{3.14}$$

it follows from (3.13) that the remaining z_i can be expressed simply as

$$z_i = \frac{\mathcal{Q}_{i,n}^2}{\mathcal{Q}_{i,i} \mathcal{Q}_{n,n}} \,. \tag{3.15}$$

For our application to the n-gon integral in generic Euclidean kinematics, the z_i will always be ordered as $z_0 < z_n < z_{n-1} < \cdots < z_1 < z_{n+1}$, opposite (but equivalent) to the convention in (6.12) of [41]. The formulas (3.13) and (3.15) break down when a vertex of the orthoscheme is on the boundary, a situation that we will encounter unless all of the propagators in the integral are massive.

This indicates only an incompatibility with our gauge choice (3.14), not a breakdown of Rudenko's formula. In practice, we sidestep this problem by adding a mass ϵ to each propagator and then taking the limit $\epsilon \to 0$, under which everything is smooth for generic Euclidean kinematics, at the end of the calculation. (This limit can be taken analytically, and should therefore be thought of more as a bookkeeping trick; it does not require numerical extrapolation.)

Rudenko showed that the volume of any odd-dimensional orthoscheme can be expressed in terms of these cross-ratios on the corresponding moduli space. The explicit construction in [41] is rather involved, so we defer the details to Appendix 3.5 and simply quote here the results for the volume of a 3-dimensional orthoscheme relevant for the four-dimensional box integral (here and in the following we write $z_{i,j}$ as z_{ij} when no confusion can arise):

$$\begin{aligned}\mathrm{Vol}(\mathcal{Q}_{n=4}) = \frac{1}{2}\,\mathrm{per}\Bigg[&\mathrm{ALi}_{1,1}\left(-\frac{z_{01}z_{25}}{z_{05}z_{12}}, -\frac{z_{23}z_{45}}{z_{25}z_{34}}\right) - \mathrm{ALi}_{1,1}\left(-\frac{z_{01}z_{45}}{z_{05}z_{14}}, -\frac{z_{14}z_{23}}{z_{12}z_{34}}\right) \\ &+ \mathrm{ALi}_{1,1}\left(-\frac{z_{03}z_{45}}{z_{05}z_{34}}, -\frac{z_{01}z_{23}}{z_{03}z_{12}}\right)\Bigg],\end{aligned} \tag{3.16}$$

and for a 5-dimensional orthoscheme relevant for the six-dimensional hexagon integral:

$$\begin{aligned}\mathrm{Vol}(\mathcal{Q}_{n=6}) =\frac{1}{8}\,\mathrm{per}\Bigg[&\mathrm{ALi}_{1,2}\left(-\frac{z_{01}z_{67}}{z_{07}z_{16}}, \frac{z_{16}z_{23}z_{45}}{z_{12}z_{34}z_{56}}\right) - \mathrm{ALi}_{1,2}\left(-\frac{z_{01}z_{47}}{z_{07}z_{14}}, \frac{z_{14}z_{23}z_{45}z_{67}}{z_{12}z_{34}z_{47}z_{56}}\right) \\ &+ \mathrm{ALi}_{1,2}\left(-\frac{z_{03}z_{47}}{z_{07}z_{34}}, \frac{z_{01}z_{23}z_{45}z_{67}}{z_{03}z_{12}z_{47}z_{56}}\right) - \mathrm{ALi}_{1,2}\left(-\frac{z_{03}z_{67}}{z_{07}z_{36}}, \frac{z_{01}z_{23}z_{36}z_{45}}{z_{03}z_{12}z_{34}z_{56}}\right) \\ -&\mathrm{ALi}_{1,1,1}\left(-\frac{z_{01}z_{27}}{z_{07}z_{12}}, -\frac{z_{23}z_{47}}{z_{27}z_{34}}, -\frac{z_{45}z_{67}}{z_{47}z_{56}}\right) + \mathrm{ALi}_{1,1,1}\left(-\frac{z_{01}z_{27}}{z_{07}z_{12}}, -\frac{z_{23}z_{67}}{z_{27}z_{36}}, -\frac{z_{36}z_{45}}{z_{34}z_{56}}\right) \\ -&\mathrm{ALi}_{1,1,1}\left(-\frac{z_{01}z_{27}}{z_{07}z_{12}}, -\frac{z_{25}z_{67}}{z_{27}z_{56}}, -\frac{z_{23}z_{45}}{z_{25}z_{34}}\right) + \mathrm{ALi}_{1,1,1}\left(-\frac{z_{01}z_{47}}{z_{07}z_{14}}, -\frac{z_{14}z_{23}}{z_{12}z_{34}}, -\frac{z_{45}z_{67}}{z_{47}z_{56}}\right) \\ +&\mathrm{ALi}_{1,1,1}\left(-\frac{z_{01}z_{47}}{z_{07}z_{14}}, -\frac{z_{45}z_{67}}{z_{47}z_{56}}, -\frac{z_{14}z_{23}}{z_{12}z_{34}}\right) - \mathrm{ALi}_{1,1,1}\left(-\frac{z_{01}z_{67}}{z_{07}z_{16}}, -\frac{z_{16}z_{23}}{z_{12}z_{36}}, -\frac{z_{36}z_{45}}{z_{34}z_{56}}\right) \\ +&\mathrm{ALi}_{1,1,1}\left(-\frac{z_{01}z_{67}}{z_{07}z_{16}}, -\frac{z_{16}z_{25}}{z_{12}z_{56}}, -\frac{z_{23}z_{45}}{z_{25}z_{34}}\right) - \mathrm{ALi}_{1,1,1}\left(-\frac{z_{01}z_{67}}{z_{07}z_{16}}, -\frac{z_{16}z_{45}}{z_{14}z_{56}}, -\frac{z_{14}z_{23}}{z_{12}z_{34}}\right) \\ -&\mathrm{ALi}_{1,1,1}\left(-\frac{z_{03}z_{47}}{z_{07}z_{34}}, -\frac{z_{01}z_{23}}{z_{03}z_{12}}, -\frac{z_{45}z_{67}}{z_{47}z_{56}}\right) - \mathrm{ALi}_{1,1,1}\left(-\frac{z_{03}z_{47}}{z_{07}z_{34}}, -\frac{z_{45}z_{67}}{z_{47}z_{56}}, -\frac{z_{01}z_{23}}{z_{03}z_{12}}\right) \\ +&\mathrm{ALi}_{1,1,1}\left(-\frac{z_{03}z_{67}}{z_{07}z_{36}}, -\frac{z_{01}z_{23}}{z_{03}z_{12}}, -\frac{z_{36}z_{45}}{z_{34}z_{56}}\right) + \mathrm{ALi}_{1,1,1}\left(-\frac{z_{03}z_{67}}{z_{07}z_{36}}, -\frac{z_{36}z_{45}}{z_{34}z_{56}}, -\frac{z_{01}z_{23}}{z_{03}z_{12}}\right) \\ -&\mathrm{ALi}_{1,1,1}\left(-\frac{z_{05}z_{67}}{z_{07}z_{56}}, -\frac{z_{01}z_{25}}{z_{05}z_{12}}, -\frac{z_{23}z_{45}}{z_{25}z_{34}}\right) + \mathrm{ALi}_{1,1,1}\left(-\frac{z_{05}z_{67}}{z_{07}z_{56}}, -\frac{z_{01}z_{45}}{z_{05}z_{14}}, -\frac{z_{14}z_{23}}{z_{12}z_{34}}\right) \\ -&\mathrm{ALi}_{1,1,1}\left(-\frac{z_{05}z_{67}}{z_{07}z_{56}}, -\frac{z_{03}z_{45}}{z_{05}z_{34}}, -\frac{z_{01}z_{23}}{z_{03}z_{12}}\right)\Bigg].\end{aligned} \tag{3.17}$$

These are expressed in terms of the alternating multiple polylogarithm defined by

$$\mathrm{ALi}_{m_1,\ldots,m_k}(\varphi_1,\ldots,\varphi_k) := \sum_{\epsilon_1,\ldots,\epsilon_k\in\{-1,1\}} \left(\prod_{i=1}^{k}\frac{\epsilon_i}{2}\right) \mathrm{Li}_{m_1,\ldots,m_k}(\epsilon_1\sqrt{\varphi_1},\ldots,\epsilon_k\sqrt{\varphi_k})\,, \tag{3.18}$$

and the function "per" appearing above is the *real period* reviewed in Appendix 3.6; there we also provide explicit formulas for the real periods of all multiple polylogarithms of weight up to 3.

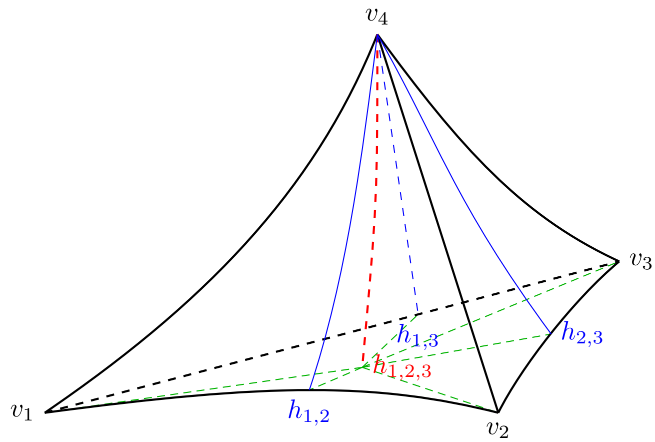

Figure 3.1: Triangulation of a hyperbolic tetrahedron into six orthoschemes. The point h_I denotes the point where the altitude from v_4 intersects the boundary $\langle I\rangle$, defined as the convex hull of vertices $\{v_i|\, i \in I\}$. The six orthoschemes are $\{\mathrm{conv}(v_4, h_{1,2,3}, h_{i,j}, v_i)|\, i, j \in \{1, 2, 3\},\ i \neq j\}$.

3.2.2 Triangulating a simplex into orthoschemes

In this section we discuss a triangulation of hyperbolic simplices into orthoschemes, beginning with the case of a hyperbolic tetrahedron as an example. The triangulation, shown in Figure 3.1, proceeds as follows. Let the vertices be (v_1, v_2, v_3, v_4). First we find the altitude (shown in red) from the vertex v_4 to the plane (v_1, v_2, v_3), and then the altitudes (shown in blue) from v_4 to the edges (v_1, v_2), (v_2, v_3) and (v_1, v_3). Then the tetrahedron has been divided into six simplices as shown in the figure: the convex hulls of $(v_4, h_{1,2,3}, h_{2,3}, v_3)$, $(v_4, h_{1,2,3}, h_{2,3}, v_2)$, $(v_4, h_{1,2,3}, h_{1,3}, v_1)$, $(v_4, h_{1,2,3}, h_{1,3}, v_3)$, $(v_4, h_{1,2,3}, h_{1,2}, v_2)$ and $(v_4, h_{1,2,3}, h_{1,2}, v_1)$. One can show that these simplices are all orthoschemes.

This algorithm generalizes recursively. Starting with an $(n-1)$-dimensional simplex with vertices $(v_1, \ldots, v_n)$, we first draw the altitudes from v_n to each boundary of dimension ≥ 1. Each boundary is a convex hull of some subset of (at least two of) the vertices $(v_1, \ldots, v_{n-1})$ and we denote these subsimplices by

$$\langle I\rangle := \mathrm{conv}(\{v_i|\, i \in I\}) \tag{3.19}$$

for any ordered subset I of $(v_1, \ldots, v_{n-1})$ of cardinality $2 \leq |I| \leq n-1$. We also denote the altitude from v_n to $\langle I\rangle$ by h_I.

Then for every permutation σ of $\{1, \ldots, n-1\}$ there is an orthoscheme

$$\begin{aligned} \mathcal{Q}^\sigma := \mathrm{conv}(&v_{\sigma(1)},\, h_{\sigma(1),\sigma(2)},\, h_{\sigma(1),\sigma(2),\sigma(3)},\, \ldots,\, h_{\sigma(1),\sigma(2),\cdots,\sigma(n-2)}, \\ &h_{\sigma(1),\sigma(2),\cdots,\sigma(n-1)} = h_{1,2,\cdots,n-1}, v_n)\,. \end{aligned} \tag{3.20}$$

These $(n-1)!$ orthoschemes do not always provide a dissection because some components may lie outside the original simplex. Such components contribute to the total volume with a minus sign, which we will account for shortly.

Next we discuss how to represent the cross-ratios associated to each orthoscheme in terms of the Gram matrix Q associated to the initial simplex. For any subset I of $\{1, \ldots, n\}$, we denote by $Q[I]$

the submatrix of Q obtained by keeping the rows and columns indexed by the elements of I. Using this notation, the moduli space coordinates $z^\sigma = (z_0^\sigma, \ldots, z_{n+1}^\sigma)$ associated to the orthoscheme $\mathcal{Q}^\sigma$ are given by

$$z_i^\sigma = 1 - \frac{\det Q[\sigma(1), \ldots, \sigma(i), n]}{\det Q[\sigma(1), \ldots, \sigma(i)]\, Q_{n,n}}\,, \qquad 1 \le i \le n-1\,, \tag{3.21}$$

with $z_0^\sigma = 0$, $z_n^\sigma = 1$, and $z_{n+1}^\sigma = \infty$ for each σ (according to our choice of gauge). Then the volume of $\mathcal{Q}^\sigma$ is given by evaluating Rudenko's formula (3.47) on (3.21):

$$\mathrm{Vol}(\mathcal{Q}^\sigma) = (\text{eq. } 3.47)\Big|_{\text{eq. } (3.21)}\,. \tag{3.22}$$

As mentioned above, in general it can happen that some orthoschemes fall outside the original simplex and therefore contribute negatively to the volume. This can be accounted for by comparing the sign of the determinant of the Gram matrix of each orthoscheme $\mathcal{Q}^\sigma$ to that of the original simplex. Altogether, the complete formula for the volume of any odd-dimensional hyperbolic simplex Q may be written as

$$\boxed{\mathrm{Vol}(Q) = \sum_{\sigma \in S_{n-1}} \frac{\mathrm{sgn}(\sigma)\,\mathrm{sgn}(\det \mathcal{Q}^\sigma)}{\mathrm{sgn}(\det Q)}\,(\text{eq. } 3.47)\Big|_{\text{eq. } (3.21)}} \tag{3.23}$$

where $\mathrm{sgn}(\sigma)$ denotes the signature of the permutation σ. The determinant $\det \mathcal{Q}^\sigma$ can also be computed recursively according to our triangulation algorithm, although the full result is a bit lengthy so we will not write it here. Plugging (3.23) into (3.9) completes our calculation of the scalar n-dimensional n-gon integral (for even n), for arbitrary internal and external masses, in terms of the Gram matrix Q given in (3.9).

3.3 An alternative formula for the hexagon with massless propagators

According to the discussion in the previous sections, Rudenko's formula can be used to compute the one-loop scalar n-gon Feynman integral in n dimensions for any even n. It applies for general Euclidean kinematics, including arbitrary internal and external masses, but is rather complicated to use in practice. For example, for $n = 6$ one has to combine (3.17), (3.21), (3.23), and (3.55)–(3.58). However, if we take all of the propagators to be massless (but still with arbitrary external momenta), a simpler formula for $n = 6$ is available thanks to a 1995 result due to Kellerhals [125], which we now describe.

A massless propagator in the Feynman integral corresponds to a point on the boundary of the hyperboloid. When all propagators are massless, the corresponding hyperbolic simplex is therefore ideal. When we triangulate a simplex using the algorithm described in Section 3.2.2, the first and last vertices of every orthoscheme are always vertices of the original simplex. Therefore, every orthoscheme appearing in the triangulation of an ideal simplex is *doubly asymptotic*, which means having (at least) two vertices on the boundary.

The volume of doubly asymptotic simplices in 5 dimensions was computed by Kellerhals in [125]. The volume is expressed in terms of the dihedral angles

$$\alpha_i := \angle(H_i, H_{i+1}) \,, \quad i \in \{1,2,3,4,5\} \,. \tag{3.24}$$

For a generic orthoscheme the five dihedral angles are independent. However, for a doubly asymptotic orthoscheme, the dihedral angles satisfy the relation

$$\tan\alpha_1 \cot\alpha_4 = \cot\alpha_2 \tan\alpha_5 = \cot\alpha_0 \tan\alpha_3 = \tan\Theta =: \lambda \tag{3.25}$$

where we have introduced two new angles α_0 and Θ and one more parameter λ for later convenience, with $0 \le \alpha_0 \le \frac{\pi}{2}$, $0 \le \Theta \le \frac{\pi}{2}$, and $\lambda \ge 0$.

Kellerhals's formula for the volume of a double asymptotic 5-dimensional orthoscheme is

$$\begin{aligned}
\mathrm{Vol}(\mathcal{Q}^{\mathrm{da}}_{n=6}) = -\frac{1}{8}\Big\{ & I\left(\lambda^{-1},0;\alpha_1\right) + \frac{1}{2} I\left(\lambda,0;\alpha_2\right) - I\left(\lambda^{-1},0;\frac{\pi}{2}-\alpha_0\right) \\
& + \frac{1}{2} I\left(\lambda,0;\alpha_4\right) + I\left(\lambda^{-1},0;\alpha_5\right) \Big\} \\
+ \frac{1}{32}\Big\{ & I\left(\lambda,-\left(\frac{\pi}{2}+\alpha_1\right);\frac{\pi}{2}+\alpha_1+\alpha_2\right) + I\left(\lambda,-\left(\frac{\pi}{2}-\alpha_1\right);\frac{\pi}{2}-\alpha_1+\alpha_2\right) - \\
& - I\left(\lambda,-\left(\frac{\pi}{2}+\alpha_1\right);\pi+\alpha_1\right) - I\left(\lambda,-\left(\frac{\pi}{2}-\alpha_1\right);\pi-\alpha_1\right) - \\
& - I\left(\lambda,-\left(\frac{\pi}{2}+\alpha_5\right);\pi+\alpha_5\right) - I\left(\lambda,-\left(\frac{\pi}{2}-\alpha_5\right);\pi-\alpha_5\right) + \\
& + I\left(\lambda,-\left(\frac{\pi}{2}+\alpha_5\right);\frac{\pi}{2}+\alpha_5+\alpha_4\right) + I\left(\lambda,-\left(\frac{\pi}{2}-\alpha_5\right);\frac{\pi}{2}-\alpha_5+\alpha_4\right)\Big\}
\end{aligned} \tag{3.26}$$

where I is the weight 3 polylogarithm function defined by

$$\begin{aligned}
I(a,b;x) &:= \frac{1}{4i}\int_{\frac{\pi}{2}}^{x} \left(\mathrm{Li}_2(e^{2iy}) - \mathrm{Li}_2(e^{-2iy})\right) d\arctan(a\tan(b+y)) \\
&= \frac{1}{8}\Bigg[\mathrm{Li}_{2,1}\left(\frac{a-1}{a+1}e^{-2ib}, \frac{a+1}{a-1}e^{2i(b+x)}\right) - \mathrm{Li}_{2,1}\left(\frac{a-1}{a+1}e^{-2ib}, -\frac{a+1}{a-1}e^{2ib}\right) \\
&\quad - \mathrm{Li}_{2,1}\left(\frac{a+1}{a-1}e^{-2ib}, \frac{a-1}{a+1}e^{2i(b+x)}\right) + \mathrm{Li}_{2,1}\left(\frac{a+1}{a-1}e^{-2ib}, -\frac{a-1}{a+1}e^{2ib}\right) \\
&\quad + \mathrm{Li}_{2,1}\left(\frac{a-1}{a+1}e^{2ib}, \frac{a+1}{a-1}e^{-2i(b+x)}\right) - \mathrm{Li}_{2,1}\left(\frac{a-1}{a+1}e^{2ib}, -\frac{a+1}{a-1}e^{-2ib}\right) \\
&\quad - \mathrm{Li}_{2,1}\left(\frac{a+1}{a-1}e^{2ib}, \frac{a-1}{a+1}e^{-2i(b+x)}\right) + \mathrm{Li}_{2,1}\left(\frac{a+1}{a-1}e^{2ib}, -\frac{a-1}{a+1}e^{-2ib}\right)\Bigg] .
\end{aligned} \tag{3.27}$$

To express Kellerhals's formula (3.26) in terms of the Gram matrix Q of the full simplex, we can first write the dihedral angles in terms of the cross-ratios and then use (3.21). According to the hyperbolic geometry identities reviewed in Appendix 3.4, the map from moduli space to the dihedral angle can be expressed as

$$\begin{aligned}
\alpha_i &= \arccos\sqrt{\frac{z_{i-1,i}z_{i+1,i+2}}{z_{i-1,i+1}z_{i,i+2}}} \,, \quad 1 \le i \le n-1 \,, \\
\alpha_0 &= \arctan\sqrt{-\frac{z_{0,1}z_{2,5}z_{6,7}}{z_{1,2}z_{5,6}z_{0,7}}} \,, \\
\Theta &= \arctan\sqrt{-\frac{z_{1,2}z_{3,4}z_{5,6}z_{0,7}}{z_{0,1}z_{2,3}z_{4,5}z_{6,7}}} \,.
\end{aligned} \tag{3.28}$$

With all ingredients in place, we conclude that the volume of an ideal simplex in hyperbolic 5-space, (the type corresponding to the hexagon integral in six dimensions with massless internal propagators) is

$$\boxed{\mathrm{Vol}(Q_{n=6}^{\mathrm{ideal}}) = \sum_{\sigma \in S_{n-1}} \frac{\mathrm{sgn}(\sigma)\,\mathrm{sgn}(\det \mathcal{Q}^{\sigma})}{\mathrm{sgn}(\det Q)} (\text{eq. } 3.26)\Big|_{\text{eq. } (3.28)}\Big|_{\text{eq. } (3.21)}\,.} \tag{3.29}$$

In practice this formula is significantly simpler than (3.23) when Q is ideal.

3.4 Appendix: Some hyperbolic geometry

Since an orthoscheme is defined by a sequence of planes $(H_1, \ldots, H_n)$ such that H_i and H_j are orthogonal if $|i-j| \geq 2$, only the dihedral angle α_i between adjacent planes H_i and H_{i+1} can be nontrivial. This angle is given by

$$\cos^2 \alpha_i = \frac{(\mathcal{Q}^{-1}_{i,i+1})^2}{\mathcal{Q}^{-1}_{i,i}\,\mathcal{Q}^{-1}_{i+1,i+1}}\,, \qquad 1 \leq i \leq n-1\,, \tag{3.30}$$

where $\mathcal{Q}^{-1}$ denotes the inverse of the matrix $\mathcal{Q}$. Writing these out explicitly in terms of the entries of $\mathcal{Q}$ and using (3.13) one can also express the dihedral angles as

$$\cos^2 \alpha_i = \frac{z_{i-1,i} z_{i+1,i+2}}{z_{i-1,i+1} z_{i,i+2}}\,, \qquad 1 \leq i \leq n-1\,. \tag{3.31}$$

The relation (3.31) generalizes to cross-ratios of four arbitrary points as follows. For four vertices v_a, v_b, v_c, v_d satisfying $1 \leq b \leq c \leq d$, consider the subscheme $\langle a,b,c,d\rangle$. Denote by $\langle v_b,\, v_c\rangle_{\langle a,b,c,d\rangle}$ the dihedral angle between the planes of $\langle a,b,c,d\rangle$ which are opposite to vertices v_b and v_c, and similarly for $\langle v_a,\, v_b\rangle_{\langle a,b,c,d\rangle}$ and $\langle v_c,\, v_d\rangle_{\langle a,b,c,d\rangle}$. (Note that in this manner of notation $\langle v_a,\, v_c\rangle_{\langle a,b,c,d\rangle} = \langle v_b,\, v_d\rangle_{\langle a,b,c,d\rangle} = \langle v_a,\, v_d\rangle_{\langle a,b,c,d\rangle} = 0$.) Then we have the relations

$$\begin{aligned}
\cos^2\left(\langle v_b,\, v_c\rangle_{\langle a,b,c,d\rangle}\right) &= \frac{z_{a,b} z_{c,d}}{z_{a,c} z_{b,d}}\,, \\
\cos^2\left(\langle v_c,\, v_d\rangle_{\langle a,b,c,d\rangle}\right) &= \frac{z_{b,c} z_{d,n+1}}{z_{b,c} z_{c,n+1}}\,, \quad 1 \leq a \leq b-1\,, \\
\cos^2\left(\langle v_a,\, v_b\rangle_{\langle a,b,c,d\rangle}\right) &= \frac{z_{0,a} z_{b,c}}{z_{0,b} z_{a,c}}\,, \qquad c+1 \leq d \leq n\,.
\end{aligned} \tag{3.32}$$

We see that cross-ratios of the configuration of the z_i in $\mathcal{M}_{0,n+2}$ can be interpreted as (squares of) cosines of dihedral angles of the orthoscheme. The only exception is when z_0 and z_{n+1} are both among the four points, in which case we have the special cross-ratio

$$\cosh^2 l_{a,b} = \frac{z_{0,a} z_{b,n+1}}{z_{0,b} z_{a,n+1}}\,, \qquad 1 \leq a < b \leq n \tag{3.33}$$

where $l_{a,b}$ is the hyperbolic length of the edge between v_a and v_b.

One can generalize the relations (3.32) even further. For any subscheme $\langle I\rangle$ (defined in Section 3.2.2), where $I = \{\rho_1, \rho_2, \ldots, \rho_m\}$ is ordered and $3 \leq m \leq n$, we have

$$\cos^2\left(\langle v_{\rho_i},\, v_{\rho_{i+1}}\rangle|_{\langle I\rangle}\right) = \frac{z_{\rho_{i-1},\rho_i}\, z_{\rho_{i+1},\rho_{i+2}}}{z_{\rho_{i-1},\rho_{i+1}}\, z_{\rho_i,\rho_{i+2}}}\,, \qquad 1 \leq i \leq m-1\,, \tag{3.34}$$

with boundary cases $\rho_0 := 0$ and $\rho_{m+1} := n+1$.

3.5 Appendix: Details on Rudenko's volume formula

In this section we review the key ingredients from [41] that are needed to write down the explicit formula for the volume of an odd-dimensional orthoscheme. The final result is given in (3.47) but we begin with several key definitions.

A *weighted alphabet* is a set of *weighted letters* $[\varphi, m]$ where φ is an arbitrary function and m is a positive integer, called its weight. In the following few paragraphs we define an algebra on weighted alphabets.

We can use *concatenation* of letters to define words which we denote by any one of $[\varphi_1, m_1][\varphi_1, m_1]$, $[\varphi_1, m_1] \otimes [\varphi_1, m_1]$, or $[\varphi_1, m_1|\varphi_1, m_1]$ without distinction. The concatenation of a sequence of weighted alphabets is called a *word*. The empty word is denoted by 1.

The *product* of two weighted letters is defined by

$$[\varphi_1, m_1] \cdot [\varphi_1, m_1] := [\varphi_1\varphi_2, m_1 + m_2]\,. \tag{3.35}$$

The product of a weighted letter and a word is defined by $[\varphi, m] \cdot 1 := 0$ and

$$[\varphi_1, m_1] \cdot [\varphi_2, m_2|\cdots|\varphi_k, m_k] := [\varphi_1\varphi_2, m_1 + m_2|\cdots|\varphi_k, m_k]\,, \tag{3.36}$$

and we extend these definitions to the vector space of (formal) linear combinations of words in the obvious way.

The *quasi-shuffle product*, or the *star product* of two words is defined by

$$[\varphi, m] \star 1 = 1 \star [\varphi, m] := [\varphi, m] \tag{3.37}$$

and

$$\begin{aligned}([\varphi_1, m_1] \otimes \omega_1) \star ([\varphi_2, m_2] \otimes \omega_2) &:= [\varphi_1, m_1] \otimes ((\omega_1) \star ([\varphi_2, m_2] \otimes \omega_2)) \\ &+ [\varphi_2, m_2] \otimes (([\varphi_1, m_1] \otimes \omega_1) \star (\omega_2)) + ([\varphi_1, m_1] \cdot [\varphi_2, m_2]) \otimes (\omega_1 \star \omega_2)\,, \end{aligned} \tag{3.38}$$

where ω_1 and ω_2 denote words of arbitrary length.

The cross-ratio of four points is denoted

$$[z_0,\, z_1,\, z_2,\, z_3] := \frac{z_{01}z_{23}}{z_{03}z_{21}}\,. \tag{3.39}$$

More generally, consider any even number of points $z = (z_0, z_1, \ldots, z_{n+1})$ in $\mathbb{P}^1$. For any (ordered) even subset of the points $z_P = \{z_{p_0}, z_{p_1} \ldots, z_{p_{2k+1}}\}$ with $p_0 < p_1 < \cdots < p_{2k+1}$, the generalized cross-ratio is defined as

$$\mathrm{cr}(z_P) := \begin{cases} \displaystyle\prod_{i=1}^{k} [z_{p_0},\, z_{p_{2i-1}},\, z_{p_{2i}},\, z_{p_{2i+1}}] & \text{if } p_0 \text{ is even,} \\ \displaystyle\prod_{i=1}^{k} [z_{p_0},\, z_{p_{2i-1}},\, z_{p_{2i}},\, z_{p_{2i+1}}]^{-1} & \text{if } p_0 \text{ is odd.} \end{cases} \tag{3.40}$$

One can recursively define a map T (called *arborification*) from z and any even subset $\{p_0, \ldots, p_{2k+1}\}$ of the ordered set $\{0, 1, \ldots, n+1\}$ to the set of words by

$$T_P(z) = \begin{cases} \displaystyle\sum_{\substack{0<i<j<2n+1 \\ i \text{ is odd} \\ j \text{ is even}}} T_{(0,i,j,2n+1)} \otimes \left(T_{(0\cdots i)} \star T_{(i\cdots j)} \star T_{(j\cdots 2n+1)}\right) & \text{if } p_0 \text{ is even,} \\ \displaystyle\sum_{\substack{1<i<j<2n+2 \\ i \text{ is even} \\ j \text{ is odd}}} \Big\{T_{(1,i,j,2n+2)} \otimes \left(T_{(1\cdots i)} \star T_{(i\cdots j)} \star T_{(j\cdots 2n+2)}\right) & \\ \qquad + T_{(1,i,j,2n+2)} \cdot \left(T_{(1\cdots i)} \star T_{(i\cdots j)} \star T_{(j\cdots 2n+2)}\right)\Big\} & \text{if } p_0 \text{ is odd,} \end{cases} \tag{3.41}$$

where

$$\begin{aligned} T_{(p_0,p_1,p_2,p_3)}(z) &= \begin{cases} -\left[\dfrac{z_{p_0,p_1} z_{p_2,p_3}}{z_{p_0,p_3} z_{p_2,p_1}}, 1\right] & \text{if } p_0 \text{ is even,} \\ \left[\dfrac{z_{p_0,p_3} z_{p_2,p_1}}{z_{p_0,p_1} z_{p_2,p_3}}, 1\right] & \text{if } p_0 \text{ is odd} \end{cases} \\ T_{(p_0,p_1)}(z) &= 1\,. \end{aligned} \tag{3.42}$$

As an example, consider $P = (0, 1, 2, 3, 4, 5)$, which gives

$$T_P(x) = \left[\frac{z_{01}z_{25}}{z_{05}z_{21}}, 1 \,\middle|\, \frac{z_{23}z_{45}}{z_{25}z_{43}}, 1\right] - \left[\frac{z_{01}z_{45}}{z_{05}z_{41}}, 1 \,\middle|\, \frac{z_{14}z_{32}}{z_{12}z_{34}}, 1\right] + \left[\frac{z_{03}z_{45}}{z_{05}z_{43}}, 1 \,\middle|\, \frac{z_{01}z_{23}}{z_{03}z_{21}}, 1\right]. \tag{3.43}$$

On the other hand for $P = (1, 2, 3, 4, 5, 6)$, we have

$$\begin{aligned} T_P(z) = &\left[\frac{z_{16}z_{32}}{z_{12}z_{36}}, 1 \,\middle|\, \frac{z_{36}z_{54}}{z_{34}z_{56}}, 1\right] - \left[\frac{z_{16}z_{52}}{z_{12}z_{56}}, 1 \,\middle|\, \frac{z_{23}z_{45}}{z_{25}z_{43}}, 1\right] \\ &+ \left[\frac{z_{16}z_{54}}{z_{14}z_{56}}, 1 \,\middle|\, \frac{z_{14}z_{32}}{z_{12}z_{34}}, 1\right] + \left[\frac{z_{16}z_{23}z_{45}}{z_{12}z_{34}z_{56}}, 2\right]. \end{aligned} \tag{3.44}$$

The *alternating multiple polylogarithm* associated to a word is defined by

$$\mathrm{ALi}([\varphi_1, m_1|\cdots|\varphi_k, m_k]) := \sum_{\epsilon_1,\ldots,\epsilon_k\in\{-1,1\}} \left(\prod_{i=1}^{k} \frac{\epsilon_i}{2}\right) \mathrm{Li}_{m_1,\ldots,m_k}(\epsilon_1\sqrt{\varphi_1}, \ldots, \epsilon_k\sqrt{\varphi_k}) \tag{3.45}$$

in terms of the familiar multiple polylogarithms (specifically, using the conventions of, for example, [130]). This definition extends to linear combinations of words (with coefficients ± 1, which is all that is needed) by

$$\mathrm{ALi}(\omega_1 \pm \omega_2) = \mathrm{ALi}(\omega_1) \pm \mathrm{ALi}(\omega_2)\,. \tag{3.46}$$

With all that preparation, we are now ready to present Rudenko's formula for the volume of the $(n-1)$-dimensional hyperbolic orthoscheme $\mathcal{Q}$ corresponding to the configuration $z = (z_0, \ldots, z_{n+1})$ of $n+2$ points in $\mathbb{P}^1$:

$$\mathrm{Vol}(\mathcal{Q}) = \frac{1}{2^{\frac{n}{2}-1}\Gamma(\frac{n}{2})} \mathrm{per}\left(\mathrm{ALi}\big(T_{(0,\ldots,n+1)}(z)\big)\right), \tag{3.47}$$

where per is the real period defined in [19] and reviewed in the next appendix.

3.6 Appendix: Real periods

In this section we give some examples for the real period map, which was first introduced in [19]. The definition of the real period is[3]

$$\mathrm{per}(G) := (2\pi)^{w(G)} \sum_{k=1}^{w(G)} \sum_{a_1+\cdots+a_k=w(G)} (-1)^{k-1}\, \nabla(\Delta_{a_1,\cdots,a_k}(G))\,, \tag{3.48}$$

where w denotes the weight, Δ is the coproduct (with $\Delta_{w(G)}(G) = G$), and ∇ is defined as

$$\nabla\left(\bigotimes_{i=1}^{m} f_i\right) := \mathrm{Re}\left(\prod_{i=1}^{m-1} \frac{f_i}{(2\pi i)^{w(f_i)}}\right) \mathrm{Im}\left(\frac{f_m}{(2\pi i)^{w(f_m)}}\right), \tag{3.49}$$

where we take $\mathrm{Im}(x+iy) = iy$. Note that despite the name, the real period is only real-valued for functions of odd weight; for even weight it is purely imaginary.

The real periods are closely related to the single-valued map [131] more widely known in the physics literature (see for example [132, 133]). Specifically, they are related by:

$$\mathrm{per}(G(\vec{a};z)) = \begin{cases} -\frac{i}{2}\ \mathrm{Re}\ \mathrm{sv}(G(\vec{a};z)), & w(G)\ \text{odd}, \\ -\frac{i}{2}\ \mathrm{Im}\ \mathrm{sv}(G(\vec{a};z)), & w(G)\ \text{even}. \end{cases} \tag{3.50}$$

Weight 1 The only weight 1 function is the logarithm $\log(x)$. It has only one non-vanishing coproduct component, $\Delta_1(\log(x)) = \log(x)$. Therefore, its real period reads

$$\mathrm{per}(\log(x)) = -2\pi\nabla(\log(x)) = 2\pi\ \mathrm{Im}\left(\frac{\log(x)}{2\pi i}\right) = -\,\mathrm{Re}(\log(x)) = -\log(|x|)\,. \tag{3.51}$$

Weight 2 Weight 2 functions are building blocks for the volumes of hyperbolic 3-simplices, and the box integral in 4 dimensions. We start with $\mathrm{Li}_2(x)$, whose coproduct components are

$$\Delta_2(\mathrm{Li}_2(x)) = \mathrm{Li}_2(x)\,, \qquad \Delta_{1,1}(\mathrm{Li}_2(x)) = \mathrm{Li}_1(x) \otimes \log(x)\,. \tag{3.52}$$

Therefore the real period of $\mathrm{Li}_2(x)$ is

$$\begin{aligned} \mathrm{per}(\mathrm{Li}_2(x)) &= 4\pi^2 \Big\{\nabla(\mathrm{Li}_2(x)) - \nabla\left(\mathrm{Li}_1(x)\otimes\log(x)\right)\Big\} \\ &= 4\pi^2 \left\{\mathrm{Im}\left(\frac{\mathrm{Li}_2(x)}{(2\pi i)^2}\right) - \mathrm{Re}\left(\frac{\mathrm{Li}_1(x)}{2\pi i}\right) \mathrm{Im}\left(\frac{\log(x)}{2\pi i}\right)\right\} \\ &= -\,\mathrm{Im}\ \mathrm{Li}_2(x) + \mathrm{Im}\ \mathrm{Li}_1(x)\ \mathrm{Re}\log(x) \end{aligned} \tag{3.53}$$

which is $((-1)$ times) the Bloch-Wigner function. Similarly it is easy to see that the real period of $\mathrm{Li}_{1,1}(x,y)$ is

$$\begin{aligned} \mathrm{per}(\mathrm{Li}_{1,1}(x,y)) = -\,\mathrm{Im}\ \mathrm{Li}_{1,1}(x,y) - \mathrm{Re}\ \mathrm{Li}_1(1/x)\ \mathrm{Im}\ \mathrm{Li}_1(xy) \\ + \mathrm{Im}\ \mathrm{Li}_1(y)\ \mathrm{Re}\ \mathrm{Li}_1(x) + \mathrm{Re}\ \mathrm{Li}_1(y)\ \mathrm{Im}\ \mathrm{Li}_1(xy)\,. \end{aligned} \tag{3.54}$$

[3]Here we use a definition different from that in [19] and that used in [41] by a factor of i^{m+1}, where m denotes the weight of the function. This is in order to make the volume in (3.47) always be a positive real number (for orthoschemes corresponding to Euclidean kinematics).

Weight 3 Here we tabulate the real periods for weight 3 (multiple) polylogarithms, relevant for the volumes of hyperbolic 5-simplices and the hexagon integral in 6 dimensions:

$$\mathrm{per}(\mathrm{Li}_3(x)) = \mathrm{Re}\ \mathrm{Li}_3(x) + (\mathrm{Re}\log(x))^2\ \mathrm{Re}\ \mathrm{Li}_1(x) - \mathrm{Re}\log(x)\ \mathrm{Re}\ \mathrm{Li}_2(x)\,, \tag{3.55}$$

$$\begin{aligned}
\mathrm{per}(\mathrm{Li}_{1,2}(x,y)) &= \mathrm{Re}\ \mathrm{Li}_{1,2}(x,y) + \mathrm{Re}\log(1/y)\ \mathrm{Re}\ \mathrm{Li}_{1,1}(x,y) \\
&- \mathrm{Im}\ \mathrm{Li}_1(1/x)\ \mathrm{Re}\log(1/y)\ \mathrm{Im}\ \mathrm{Li}_1(xy) + \mathrm{Im}\ \mathrm{Li}_1(y)\ \mathrm{Re}\log(1/y)\ \mathrm{Im}\ \mathrm{Li}_1(xy) \\
&+ \mathrm{Im}\ \mathrm{Li}_1(1/x)\ \mathrm{Im}\ \mathrm{Li}_1(xy)\ \mathrm{Re}\log(1/xy) - \mathrm{Im}\ \mathrm{Li}_2(1/x)\ \mathrm{Im}\ \mathrm{Li}_1(xy) \\
&+ \mathrm{Im}\ \mathrm{Li}_2(y)\ \mathrm{Im}\ \mathrm{Li}_1(xy) - \mathrm{Re}\ \mathrm{Li}_1(x)\ \mathrm{Re}\ \mathrm{Li}_2(y) + \mathrm{Re}\ \mathrm{Li}_1(1/x)\ \mathrm{Re}\ \mathrm{Li}_2(xy) \\
&- 2\ \mathrm{Re}\ \mathrm{Li}_1(x)\ \mathrm{Re}\ \mathrm{Li}_1(y)\ \mathrm{Re}\log(1/y) + \mathrm{Re}\ \mathrm{Li}_1(1/x)\ \mathrm{Re}\log(1/y)\ \mathrm{Re}\ \mathrm{Li}_1(xy) \\
&+ \mathrm{Re}\ \mathrm{Li}_1(1/x)\ \mathrm{Re}\ \mathrm{Li}_1(xy)\ \mathrm{Re}\log(1/xy) - \mathrm{Re}\ \mathrm{Li}_1(y)\ \mathrm{Re}\log(1/y)\ \mathrm{Re}\ \mathrm{Li}_1(xy)\,,
\end{aligned} \tag{3.56}$$

$$\begin{aligned}
\mathrm{per}(\mathrm{Li}_{2,1}(x,y)) &= \mathrm{Re}\ \mathrm{Li}_{2,1}(x,y) - \mathrm{Re}\log(1/y)\ \mathrm{Re}\ \mathrm{Li}_{1,1}(x,y) \\
&+ \mathrm{Re}\log(1/xy)\ \mathrm{Re}\ \mathrm{Li}_{1,1}(x,y) - \mathrm{Im}\ \mathrm{Li}_1(x)\ \mathrm{Im}\ \mathrm{Li}_1(y)\ \mathrm{Re}\log(1/y) \\
&+ \mathrm{Im}\ \mathrm{Li}_1(1/x)\ \mathrm{Re}\log(1/y)\ \mathrm{Im}\ \mathrm{Li}_1(xy) - \mathrm{Im}\ \mathrm{Li}_1(y)\ \mathrm{Re}\log(1/y)\ \mathrm{Im}\ \mathrm{Li}_1(xy) \\
&+ \mathrm{Im}\ \mathrm{Li}_1(x)\ \mathrm{Im}\ \mathrm{Li}_1(y)\ \mathrm{Re}\log(1/xy) + \mathrm{Im}\ \mathrm{Li}_1(1/x)\ \mathrm{Im}\ \mathrm{Li}_1(xy)\ \mathrm{Re}\log(1/xy) \\
&+ \mathrm{Im}\ \mathrm{Li}_2(x)\ \mathrm{Im}\ \mathrm{Li}_1(y) - \mathrm{Im}\ \mathrm{Li}_2(y)\ \mathrm{Im}\ \mathrm{Li}_1(xy) + \mathrm{Im}\ \mathrm{Li}_1(xy)\ \mathrm{Im}\ \mathrm{Li}_2(1/x) \\
&- \mathrm{Re}\ \mathrm{Li}_1(y)\ \mathrm{Re}\ \mathrm{Li}_2(xy) + \mathrm{Re}\ \mathrm{Li}_1(x)\ \mathrm{Re}\ \mathrm{Li}_1(y)\ \mathrm{Re}\log(1/y) \\
&- \mathrm{Re}\ \mathrm{Li}_1(x)\ \mathrm{Re}\ \mathrm{Li}_1(y)\ \mathrm{Re}\log(1/xy) - \mathrm{Re}\ \mathrm{Li}_1(1/x)\ \mathrm{Re}\log(1/y)\ \mathrm{Re}\ \mathrm{Li}_1(xy) \\
&+ \mathrm{Re}\ \mathrm{Li}_1(1/x)\ \mathrm{Re}\ \mathrm{Li}_1(xy)\ \mathrm{Re}\log(1/xy) + \mathrm{Re}\ \mathrm{Li}_1(y)\ \mathrm{Re}\log(1/y)\ \mathrm{Re}\ \mathrm{Li}_1(xy) \\
&- 2\ \mathrm{Re}\ \mathrm{Li}_1(y)\ \mathrm{Re}\ \mathrm{Li}_1(xy)\ \mathrm{Re}\log(1/xy)\,,
\end{aligned} \tag{3.57}$$

$$
\begin{aligned}
\mathrm{per}(\mathrm{Li}_{1,1,1}(x,y,z)) = {} & \mathrm{Im}\ \mathrm{Li}_1(z)\ \mathrm{Im}\ \mathrm{Li}_{1,1}(x,y) - \mathrm{Im}\ \mathrm{Li}_{1,1}\left(y,1/xy\right)\ \mathrm{Im}\ \mathrm{Li}_1(xyz) \\
& + \mathrm{Im}\ \mathrm{Li}_{1,1}(y,z)\ \mathrm{Im}\ \mathrm{Li}_1(xyz) + \mathrm{Re}\ \mathrm{Li}_1\left(1/y\right)\ \mathrm{Re}\ \mathrm{Li}_{1,1}(x,yz) \\
& - \mathrm{Re}\ \mathrm{Li}_1(z)\ \mathrm{Re}\ \mathrm{Li}_{1,1}(x,yz) - \mathrm{Re}\ \mathrm{Li}_1(x)\ \mathrm{Re}\ \mathrm{Li}_{1,1}(y,z) \\
& + \mathrm{Re}\ \mathrm{Li}_1\left(1/x\right)\ \mathrm{Re}\ \mathrm{Li}_{1,1}(xy,z) - \mathrm{Re}\ \mathrm{Li}_1(y)\ \mathrm{Re}\ \mathrm{Li}_{1,1}(xy,z) + \mathrm{Re}\ \mathrm{Li}_{1,1,1}(x,y,z) \\
& + \mathrm{Im}\ \mathrm{Li}_1(z)\ \mathrm{Re}\ \mathrm{Li}_1\left(1/x\right)\ \mathrm{Im}\ \mathrm{Li}_1(xy) - \mathrm{Im}\ \mathrm{Li}_1(y)\ \mathrm{Im}\ \mathrm{Li}_1(z)\ \mathrm{Re}\ \mathrm{Li}_1(x) \\
& - \mathrm{Im}\ \mathrm{Li}_1\left(1/x\right)\ \mathrm{Re}\ \mathrm{Li}_1\left(1/y\right)\ \mathrm{Im}\ \mathrm{Li}_1(xyz) \\
& + \mathrm{Re}\ \mathrm{Li}_1\left(1/y\right)\ \mathrm{Im}\ \mathrm{Li}_1(yz)\ \mathrm{Im}\ \mathrm{Li}_1(xyz) - \mathrm{Im}\ \mathrm{Li}_1(z)\ \mathrm{Re}\ \mathrm{Li}_1(y)\ \mathrm{Im}\ \mathrm{Li}_1(xy) \\
& + \mathrm{Re}\ \mathrm{Li}_1(y)\ \mathrm{Im}\ \mathrm{Li}_1\left(1/xy\right)\ \mathrm{Im}\ \mathrm{Li}_1(xyz)\ - \mathrm{Im}\ \mathrm{Li}_1(z)\ \mathrm{Re}\ \mathrm{Li}_1(y)\ \mathrm{Im}\ \mathrm{Li}_1(xyz) \\
& + \mathrm{Im}\ \mathrm{Li}_1\left(1/x\right)\ \mathrm{Re}\ \mathrm{Li}_1\left(1/xy\right)\ \mathrm{Im}\ \mathrm{Li}_1(xyz) - \mathrm{Re}\ \mathrm{Li}_1(z)\ \mathrm{Im}\ \mathrm{Li}_1(yz)\ \mathrm{Im}\ \mathrm{Li}_1(xyz) \\
& + \mathrm{Re}\ \mathrm{Li}_1(x)\ \mathrm{Re}\ \mathrm{Li}_1(y)\ \mathrm{Re}\ \mathrm{Li}_1(z) - \mathrm{Re}\ \mathrm{Li}_1\left(1/x\right)\ \mathrm{Re}\ \mathrm{Li}_1(z)\ \mathrm{Re}\ \mathrm{Li}_1(xy) \\
& + \mathrm{Re}\ \mathrm{Li}_1(y)\ \mathrm{Re}\ \mathrm{Li}_1(z)\ \mathrm{Re}\ \mathrm{Li}_1(xy) - 2\ \mathrm{Re}\ \mathrm{Li}_1(x)\ \mathrm{Re}\ \mathrm{Li}_1\left(1/y\right)\ \mathrm{Re}\ \mathrm{Li}_1(yz) \\
& + 2\ \mathrm{Re}\ \mathrm{Li}_1(x)\ \mathrm{Re}\ \mathrm{Li}_1(z)\ \mathrm{Re}\ \mathrm{Li}_1(yz) + \mathrm{Re}\ \mathrm{Li}_1\left(1/x\right)\ \mathrm{Re}\ \mathrm{Li}_1\left(1/y\right)\ \mathrm{Re}\ \mathrm{Li}_1(xyz) \\
& - \mathrm{Re}\ \mathrm{Li}_1(y)\ \mathrm{Re}\ \mathrm{Li}_1\left(1/xy\right)\ \mathrm{Re}\ \mathrm{Li}_1(xyz) \\
& + \mathrm{Re}\ \mathrm{Li}_1\left(1/x\right)\ \mathrm{Re}\ \mathrm{Li}_1\left(1/xy\right)\ \mathrm{Re}\ \mathrm{Li}_1(xyz) \\
& - 2\ \mathrm{Re}\ \mathrm{Li}_1\left(1/x\right)\ \mathrm{Re}\ \mathrm{Li}_1(z)\ \mathrm{Re}\ \mathrm{Li}_1(xyz) + \mathrm{Re}\ \mathrm{Li}_1(y)\ \mathrm{Re}\ \mathrm{Li}_1(z)\ \mathrm{Re}\ \mathrm{Li}_1(xyz) \\
& - \mathrm{Re}\ \mathrm{Li}_1\left(1/y\right)\ \mathrm{Re}\ \mathrm{Li}_1(yz)\ \mathrm{Re}\ \mathrm{Li}_1(xyz) + \mathrm{Re}\ \mathrm{Li}_1(z)\ \mathrm{Re}\ \mathrm{Li}_1(yz)\ \mathrm{Re}\ \mathrm{Li}_1(xyz)\,.
\end{aligned}
\tag{3.58}
$$

3.7 Appendix: Explicit formula for the box integral in terms of alternating polylogs

In this section, we give the explicit formula for the volume of a hyperbolic 3-simplex, related to the box integral by (3.9). Combining (3.16), (3.21), and (3.54), one obtains

$$
\begin{aligned}
\mathrm{Vol}(Q_{n=4}) = \frac{1}{2}\Bigg\{ & \mathrm{sgn}\left(\frac{(Q_{1,2}Q_{1,4}-Q_{1,1}Q_{2,4})\bar{Q}_{3,4}}{(Q_{1,2}Q_{1,4}-Q_{2,2}Q_{1,4}-Q_{1,1}Q_{2,4}+Q_{1,2}Q_{2,4})(\bar{Q}_{1,4}+\bar{Q}_{2,4}+\bar{Q}_{3,4})}\right) \\
& \times \mathrm{per}\Bigg(\mathrm{ALi}_{1,1}\left[1-\frac{Q_{4,4}\bar{Q}_{4,4}}{\Delta^2}, \frac{Q_{1,4}^2\bar{Q}_{3,4}^2}{(Q_{1,2}Q_{1,4}-Q_{1,1}Q_{2,4})^2(\Delta^2-Q_{4,4}\bar{Q}_{4,4})}\right] \\
& +\mathrm{ALi}_{1,1}\left[\frac{Q_{1,4}^2(Q_{1,2}^2-Q_{1,1}Q_{2,2})}{(Q_{1,2}Q_{1,4}-Q_{1,1}Q_{2,4})^2}, \frac{\bar{Q}_{3,4}^2}{\Delta^2(Q_{1,2}^2-Q_{1,1}Q_{2,2})}\right] \\
& -\mathrm{ALi}_{1,1}\left[\frac{Q_{1,4}^2}{Q_{1,4}^2-Q_{1,1}Q_{4,4}}, \frac{(Q_{1,4}^2-Q_{1,1}Q_{4,4})\bar{Q}_{3,4}^2}{\Delta^2(Q_{1,2}Q_{1,4}-Q_{1,1}Q_{2,4})^2}\right]\Bigg)\Bigg\} \\
& + (\text{perm } 1,2,3)\,,
\end{aligned}
\tag{3.59}
$$

where

$$
\bar{Q}_{i,j} := (-1)^{i+j}\det Q[1\cdots\hat{\imath}\cdots n; 1\cdots\hat{\jmath}\cdots n]\,, \quad \Delta := \det Q\,. \tag{3.60}
$$

Now let us consider the massless limit, for which $Q_{i,i} \to 0$. In this limit, (3.59) simplifies to

$$\mathrm{Vol}(Q^{\mathrm{ideal}}_{n=4}) = \frac{1}{2}\left\{ \mathrm{sgn}\left(\frac{Q_{1,4}\bar{Q}_{3,4}}{(Q_{1,4}+Q_{2,4})(\bar{Q}_{1,4}+\bar{Q}_{2,4}+\bar{Q}_{3,4})}\right) \mathrm{per}\left(\mathrm{ALi}_{1,1}\left[1, \frac{\bar{Q}^2_{3,4}}{Q^2_{1,2}\,\Delta}\right]\right)\right\} \tag{3.61}$$
$$+(\text{perm } 1,2,3)\,.$$

After using (3.18) and computing the real period of $\mathrm{Li}_{1,1}$ via (3.54) and using the identity

$$\mathrm{Li}_{1,1}\left(a_1, a_2\right) = \mathrm{Li}_2\left(\frac{1-a_1}{1-a_2^{-1}}\right) - \mathrm{Li}_2\left(\frac{a_2}{a_2-1}\right) - \mathrm{Li}_2\left(a_1 a_2\right), \tag{3.62}$$

one can check that (3.61) finally evaluates to the familiar four-mass box function

$$\frac{1}{i}\left[\mathrm{Li}_2\left(\frac{w+v-u+\sqrt{\Delta}}{w+v-u-\sqrt{\Delta}}\right) - \mathrm{Li}_2\left(\frac{w+v-u-\sqrt{\Delta}}{w+v-u+\sqrt{\Delta}}\right)\right] + (\text{cyclic } u, v, w) \tag{3.63}$$

where

$$u = Q_{1,2}Q_{3,4}\,, \quad v = Q_{1,4}Q_{2,3}\,, \quad w = Q_{1,3}Q_{2,4}\,, \quad \Delta = u^2+v^2+w^2-2(uv+uw+vw)\,. \tag{3.64}$$

Chapter 4

Celestial Dual Superconformal Symmetry, MHV Amplitudes and Differential Equations

This chapter is based on [134].

The quest for flat space holography has recently received a boost owing to the realization [135, 136, 137, 138, 43, 139, 140, 141] that scattering amplitudes in 4D flat spacetime can be recast as correlation functions of a 2D conformal field theory living on the celestial sphere. The appearance of the 2D conformal symmetry is due to the fact that the Lorentz group $\mathrm{SL}(2,\mathbb{C})$ acting at null infinity of 4D Minkowski spacetime is mapped to the global conformal group acting on the celestial sphere. Such a theory, dubbed celestial CFT (CCFT), is a potential candidate for a holographic description of the flat space S-matrix. Unsurprisingly, it has been the subject of intense study for the past few years. However, our understanding of CCFTs remains primitive, and in particular, a dictionary similar to the one for the AdS/CFT correspondence remains elusive.

A path towards a better understanding of CCFTs can be forged by generating more "data". This involves translating well understood aspects of momentum space amplitudes into statements about celestial correlators, as well as mapping momentum space amplitudes onto the celestial sphere providing us with explicit examples of celestial amplitudes. The last few years have seen a lot of progress on both accounts. Soft and collinear theorems have been studied in [142, 143, 144, 145, 146, 147, 148, 149, 150, 151, 152]. The factorization of gauge theory amplitudes into "hard" and "soft/collinear" factors has been extended to and interpreted on the celestial sphere [153, 154, 155]. Attempts have been made to demonstrate the existence of celestial double copy relations [156, 157]. Several momentum space amplitudes have been mapped onto the celestial sphere including tree-level gluon amplitudes [139, 158], one-loop amplitudes in scalar [159] and gauge theories [160], all-loop four-point amplitudes [161] and string amplitudes [162]. A parallel path towards the same goal is to leverage symmetries to directly obtain constraints on CCFTs along the lines of [163, 164, 165, 166, 167, 168, 169, 170, 171, 172].

Theories with a large symmetry group are amenable to both lines of attack. Recently celestial superconformal symmetry of $\mathcal{N}=4$ Yang-Mills has been studied in [173, 174]. In this paper, we study the celestial avatar of the dual superconformal symmetry [14]. Celestial n-point tree-level MHV amplitudes have been computed in [158] and found to be Aomoto-Gelfand hypergeometric functions, which satisfy a known set of differential equations [175]. We identify these equations as arising from momentum conservation and $GL(n-4)$ transformations. Another set of differential equations for the full MHV amplitude has been found in [164]. We derive versions of these equations satisfied by colour ordered amplitudes and generalize them. We rewrite them in momentum space and identify them as encoding properties of amplitudes under BCFW shifts. Tree-level amplitudes in other helicity sectors and loop amplitudes are generalized hypergeometric functions satisfying more complex differential equations. Celestial graviton amplitudes are also known to satisfy differential equations [165]. While we have restricted ourselves to MHV gluon amplitudes in this work, we hope to return to these topics in the future [176].

This paper is organized as follows. In Section 4.1, we quickly review superamplitudes and their celestial counterparts. We then discuss dual conformal symmetry of momentum space amplitudes in Section 4.2.1 and present its celestial counterpart in Section 4.2.2. In Section 4.3.1, we derive momentum space generalizations of the differential equations found in [164] by connecting them to the behaviour of amplitudes under BCFW shifts and in Section 4.3.2, we provide physical interpretations for the hypergeometric equations satisfied by the celestial MHV tree-level amplitudes. Finally, in Section 4.3.3, we discuss the relation between these differential equations.

4.1 Superamplitudes and celestial superamplitudes

Amplitudes in supersymmetric theories, particularly in planar $\mathcal{N}=4$ Yang-Mills have been the focus of a lot of recent work. The field content of $\mathcal{N}=4$ Yang-Mills can be packaged into an on-shell superfield defined by

$$\begin{aligned}\Psi(p_i) =& G^+(p_i) + \eta_i^A \Gamma_A(p_i) + \frac{1}{2!}\eta_i^A\eta_i^B\Phi_{AB}(p_i) + \frac{1}{3!}\epsilon_{ABCD}\eta_i^A\eta_i^B\eta_i^C\bar{\Gamma}^D(p_i) \\ &+ \frac{1}{4!}\epsilon_{ABCD}\eta_i^A\eta_i^B\eta_i^C\eta_i^D G^-(p_i) \quad .\end{aligned} \tag{4.1}$$

Here $G^{\pm}$ are the $\pm$ helicity gluons, Γ^D are the gluinos and Φ_{AB} are the scalars. $A, B, \ldots$ are $SU(4)$ R-symmetry indices. For more details, refer to [177] and [178]. The natural states to scatter in this theory are $\Psi(p_i)$ and the corresponding scattering amplitudes are called superamplitudes $\mathcal{A}_n$[1].

[1] We will focus on the colour ordered superamplitudes in the planar limit and denote them by $\mathcal{A}_n$. An ordering will be specified only when necessary.

These amplitudes can be expanded as polynomials in the Grassmann variables η_i as

$$\mathcal{A}_n = \sum_{k=0}^{n-4} \mathcal{A}_{n,k} \quad , \tag{4.2}$$

where $\mathcal{A}_{n,k}$ is the N^{k}MHV amplitude and has $4(k+2)$ Grassmann variables. The tree-level MHV amplitude can be compactly written as

$$\mathcal{A}_{n,0} \;=\; \frac{\delta^{(8)}\,(Q)}{\langle 12\rangle\langle 23\rangle\cdots\langle n1\rangle}\delta^{(4)}\left(\sum_{i=1}^{n} p_i\right) \;=\; \frac{\frac{1}{2^4}\prod_{A=1}^{4}\sum_{i,j=1}^{n}\langle ij\rangle\eta_i^A\eta_j^A}{\langle 12\rangle\langle 23\rangle\cdots\langle n1\rangle}\delta^{(4)}\left(\sum_{i=1}^{n} p_i\right). \tag{4.3}$$

Here λ_i, λ_j are the usual spinor helicity variables and they appear in (4.3) in the following Lorentz invariant combinations,

$$\langle ij\rangle = \epsilon_{\alpha\,\beta}\lambda_i^{\alpha}\,\lambda_j^{\beta} \qquad , \qquad [ij] = -\epsilon_{\dot\alpha\,\dot\beta}\tilde\lambda_i^{\dot\alpha}\,\tilde\lambda_j^{\dot\beta} \quad . \tag{4.4}$$

The MHV gluon amplitude[2] (with particles s and t having negative helicity and the remaining $n-2$ having positive helicity), which we denote by $\mathcal{M}_n$, is contained in (4.3) as the coefficient of $(\eta_s)^4(\eta_t)^4$

$$\mathcal{M}_n \;=\; \frac{\langle st\rangle^4\,\delta^{(4)}\,(\sum_{i=1}^{n} p_i)}{\langle 12\rangle\langle 23\rangle\cdots\langle n1\rangle} \quad . \tag{4.5}$$

Mapping these amplitudes to the celestial sphere requires the following parametrization of momenta

$$\begin{aligned} p_i^{\mu} \;&=\; \epsilon_i\,\omega_i\,q^{\mu}(z_i,\,\bar z_i) \qquad i=1,\,\ldots,\,n \\ &=\; \epsilon_i\,\omega_i\,(1+z_i\bar z_i,\,(z_i+\bar z_i),\,-i(z_i-\bar z_i),\;1-z_i\bar z_i) \quad , \end{aligned} \tag{4.6}$$

with $\epsilon_i = 1, -1$ for outgoing and incoming particles respectively. The spinor helicity variables, the angle and square brackets can all be written in terms of $z_i, \bar z_i, \omega_i$ as

$$\begin{aligned} \lambda_i^{\alpha} \;&=\epsilon_i\sqrt{2\omega_i}\begin{pmatrix}1\\ z_i\end{pmatrix} \quad , \quad \lambda_{i,\alpha} \;=\; \epsilon_i\sqrt{2\omega_i}\begin{pmatrix}-z_i\\ 1\end{pmatrix} \quad , \\ \tilde\lambda_{i,\dot\alpha} \;&=\sqrt{2\omega_i}\begin{pmatrix}-\bar z_i\\ 1\end{pmatrix} \quad , \quad \tilde\lambda_i^{\dot\alpha} \;=\; \sqrt{2\omega_i}\begin{pmatrix}1\\ \bar z_i\end{pmatrix} \quad , \end{aligned} \tag{4.7}$$

and

$$\langle i\,j\rangle \;=\; -\,2\epsilon_i\epsilon_j\sqrt{\omega_i\omega_j}\,z_{ij} \quad , \quad [i\,j] \;=\; 2\sqrt{\omega_i\omega_j}\,\bar z_{ij} \quad . \tag{4.8}$$

The celestial superamplitude $\tilde{\mathcal{A}}_n$ is the Mellin transform of the superamplitude w.r.t. to ω_i,

$$\tilde{\mathcal{A}}_n(J_i,\Delta_i,z_i,\bar z_i) \;=\; \int\left[\prod_{i=1}^{n}\frac{d\omega_i}{\omega_i}\,\omega_i^{\Delta_i}\right]\mathcal{A}_n(h_i,\omega_i,z_i,\bar z_i) \quad , \tag{4.9}$$

with similar definitions for $\tilde{\mathcal{A}}_{n,k}$. For more details, see [173, 174]. Here $\Delta_i = 1+i\lambda_i$ is the conformal dimension and the 2D spin J_i is identified as the 4D helicity of particle i, h_i.

[2] We will denote superamplitudes by $\mathcal{A}_{n,k}$ and the MHV gluon amplitude by $\mathcal{M}_n$.

In this paper, we will focus only on the celestial MHV amplitudes for which we can use the expression in (4.3) and (4.5) to write

$$\begin{aligned}\tilde{\mathcal{A}}_{n,0} \;&=\; \int \left[\prod_{i=1}^{n} \frac{d\omega_i}{\omega_i}\,\omega_i^{\Delta_i}\right] \frac{\prod_{A=1}^{4}\sum_{i,j=1}^{n}\sqrt{\omega_i\,\omega_j}\,\epsilon_i\,\epsilon_j\,z_{ij}\eta_i^A\eta_j^A}{(-2)^n\,\omega_1\,\ldots\omega_n\,z_{12}\,\ldots\,z_{n1}}\,\delta^{(4)}\left(\sum_{n=1}^{n}\epsilon_i\,\omega_i\,q_i\right)\\ &=\; \mathcal{H}_{st}\int\left[\prod_{i=1}^{n}\frac{d\omega_i}{\omega_i}\,\omega_i^{\Delta_i}\right]\mathcal{M}_n \;=\; \mathcal{H}_{st}\,\tilde{\mathcal{M}}_n \quad ,\end{aligned} \tag{4.10}$$

with

$$\mathcal{H}_{st} = \frac{1}{z_{st}^4\,2^4}\prod_{A=1}^{4}\sum_{i,j=1}^{n}(\epsilon_i\,\epsilon_j\,z_{ij})\,\eta_i^A\eta_j^A e^{\frac{1}{2}\left(\frac{\partial}{\partial\Delta_i}+\frac{\partial}{\partial\Delta_j}-\frac{\partial}{\partial\Delta_s}-\frac{\partial}{\partial\Delta_t}\right)} \quad . \tag{4.11}$$

$\tilde{\mathcal{M}}_n$ has already been computed in [158]. We will revisit this in Section 4.3.2 in greater detail.

4.2 Dual superconformal symmetry

4.2.1 Dual superconformal symmetry of momentum space amplitudes

The remarkable simplicity of scattering amplitudes in $\mathcal{N}=4$ Yang-Mills theory and our ability to compute them stem partly from the symmetries of the theory. It is now well known that in addition to the conventional superconformal symmetry $PSU(2,2|4)$, tree-level amplitudes of the theory are invariant under dual superconformal symmetry [14, 15] which can be easily seen if we define dual momentum and supermomentum variables

$$(p_i)_{\alpha\,\dot\alpha} \;=\; -\,\lambda_{i\,\alpha}\,\tilde\lambda_{i\,\dot\alpha} \;:=\; (x_i - x_{i+1})_{\alpha\,\dot\alpha} \qquad i = 1\,\ldots,\,n \quad , \tag{4.12}$$

$$q_{i\,\alpha}^A \;=\; \lambda_{i\,\alpha}\eta_i^A \;:=\; (\theta_i - \theta_{i+1})_\alpha^A \qquad i = 1\,\ldots,\,n \quad . \tag{4.13}$$

Dual superconformal symmetry is ordinary superconformal symmetry in variables (x_i, θ_i). The amplitudes are covariant under this symmetry and the generators do not annihilate them. However, we can modify these generators such that they annihilate the amplitudes and express them in terms of λ_i, $\tilde\lambda_i$, see [14, 15] for more details. All the generators except $K^{\alpha\dot\alpha}$ and S_α^A either act trivially on the amplitude or are equal to one of their conformal counterparts. Hence, we only present expressions for $K^{\alpha\dot\alpha}$ and S_α^A here.

Let us first rewrite the expression for the generators $K^{\alpha\dot\alpha}$ given in [15] in a more compact form

$$\begin{aligned}\mathcal{K}^{\alpha\dot\alpha} &= -\sum_{i=1}^{n}\left[\sum_{j=1}^{i-1}\lambda_j^\beta\tilde\lambda_j^{\dot\alpha}\lambda_i^\alpha\frac{\partial}{\partial\lambda_i^\beta} + \sum_{j=1}^{i}\lambda_j^\alpha\tilde\lambda_j^{\dot\beta}\tilde\lambda_i^{\dot\alpha}\frac{\partial}{\partial\tilde\lambda_i^{\dot\beta}} + \sum_{j=1}^{i}\tilde\lambda_i^{\dot\alpha}\lambda_j^\alpha\eta_j^A\frac{\partial}{\partial\eta_i^A} + \sum_{j=1}^{i-1}\lambda_j^\alpha\tilde\lambda_j^{\dot\alpha}\right]\\ &= -\sum_{i<j}\left(\tilde\lambda_i^{\dot\alpha}\lambda_j^\alpha D_{j,i} + \lambda_i^\alpha\tilde\lambda_i^{\dot\alpha}\right) \quad ,\end{aligned} \tag{4.14}$$

where we have made use of momentum conservation and also introduced the operator

$$D_{i,j} \;=\; \lambda_j^\alpha\,\frac{\partial}{\partial\lambda_i^\alpha} \;-\; \tilde\lambda_{i,\dot\beta}\frac{\partial}{\partial\tilde\lambda_{j,\dot\beta}} \;-\; \sum_A \eta_i^A\frac{\partial}{\partial\eta_j^A} \quad , \tag{4.15}$$

which will play an additional role in Section 4.3.

Similar manipulations on $\mathcal{S}_\alpha^A$ lead to

$$\begin{aligned}\mathcal{S}_\alpha^A &= -\sum_{i=1}^{n}\left[\sum_{j=1}^{i-1}\lambda_j^\beta\eta_j^A\lambda_{i,\alpha}\frac{\partial}{\partial\lambda_i^\beta}+\sum_{j=1}^{i}\lambda_{j,\alpha}\tilde{\lambda}_j^{\dot\beta}\eta_i^A\frac{\partial}{\partial\tilde{\lambda}_i^{\dot\beta}}-\sum_{j=1}^{i}\lambda_{j,\alpha}\eta_j^B\eta_i^A\frac{\partial}{\partial\eta_i^B}+\sum_{j=1}^{i-1}\lambda_{j,\alpha}\eta_j^A\right]\\ &= -\sum_{i<j}\left(\lambda_{j,\alpha}\eta_i^A D_{j,i}+\lambda_{i,\alpha}\eta_i^A\right) \quad .\end{aligned} \tag{4.16}$$

4.2.2 Dual superconformal symmetry of celestial amplitudes

Symmetries have played a pivotal role in determining scattering amplitudes in $\mathcal{N}=4$ Yang-Mills. It is conceivable that understanding these symmetries on the celestial sphere will lead to some insight about the putative celestial conformal field theory governing these amplitudes. Several results have already been obtained along these lines for Poincaré [179], conformal and superconformal symmetries [180, 173, 174, 151]. Here we take the first steps towards an understanding of the implications of celestial dual superconformal symmetry by obtaining the form of the generators on the celestial sphere.

Let $\mathcal{O}$ be an operator acting on the amplitude. Then, the corresponding operator $\tilde{\mathcal{O}}$, which acts on the celestial amplitude is defined by

$$\tilde{\mathcal{O}}\tilde{\mathcal{A}}_n := \int\left(\prod_{i=1}^{n}\frac{d\omega_i}{\omega_i}\,\omega_i^{\Delta_i}\right)\mathcal{O}\mathcal{A}_n \quad . \tag{4.17}$$

Then the operator $D_{i,j}$ becomes

$$\tilde{D}_{i,j} \;=\; -\,\epsilon_i\epsilon_j\, e^{\frac{\partial}{2\partial\Delta_j}-\frac{\partial}{2\partial\Delta_i}}\left(\Delta_i+J_i+z_{ij}\frac{\partial}{\partial z_i}\right)+e^{\frac{\partial}{2\partial\Delta_i}-\frac{\partial}{2\partial\Delta_j}}\left(\Delta_j-J_j+\bar{z}_{ji}\frac{\partial}{\partial\bar{z}_j}\right)-\sum_A\eta_i^A\frac{\partial}{\partial\eta_j^A} \quad . \tag{4.18}$$

We can use this in (4.14) and (4.16) to work out the all the components of $\tilde{\mathcal{K}}^{\alpha\dot\alpha}$ and $\tilde{\mathcal{S}}_\alpha^A$ on the celestial sphere

$$\begin{aligned}\tilde{\mathcal{K}}^{\alpha\dot\alpha} =&\sum_{i<j}\left\{\begin{pmatrix}1 & \bar{z}_i\\ z_j & \bar{z}_i z_j\end{pmatrix}\left[2\epsilon_i e^{\frac{\partial}{\partial\Delta_i}}\left(\Delta_j+J_j-z_{ij}\frac{\partial}{\partial z_j}\right)+2\epsilon_j e^{\frac{\partial}{2\partial\Delta_i}+\frac{\partial}{2\partial\Delta_j}}\sum_A\eta_j^A\frac{\partial}{\partial\eta_i^A}\right.\right.\\ &\left.\left.-2\epsilon_j e^{\frac{\partial}{\partial\Delta_j}}\left(\Delta_i-J_i+\bar{z}_{ij}\frac{\partial}{\partial\bar{z}_i}\right)\right]-2\epsilon_i e^{\frac{\partial}{\partial\Delta_i}}\begin{pmatrix}1 & \bar{z}_i\\ z_i & z_i\bar{z}_i\end{pmatrix}\right\} \quad ,\end{aligned} \tag{4.19}$$

$$\begin{aligned}\tilde{\mathcal{S}}_\alpha^A =&\sqrt{2}\sum_{i<j}\left\{\begin{pmatrix}-z_j\\ 1\end{pmatrix}\left[\epsilon_i\eta_i^A e^{\frac{\partial}{2\partial\Delta_i}}\left(\Delta_j+J_j-z_{ij}\frac{\partial}{\partial z_j}\right)+\epsilon_j e^{\frac{\partial}{2\partial\Delta_j}}\eta_i^A\sum_B\eta_j^B\frac{\partial}{\partial\eta_i^B}\right.\right.\\ &\left.\left.-\epsilon_j\eta_i^A e^{\frac{\partial}{\partial\Delta_j}-\frac{\partial}{2\partial\Delta_i}}\left(\Delta_i-J_i+\bar{z}_{ij}\frac{\partial}{\partial\bar{z}_i}\right)\right]-\epsilon_i\eta_i^A e^{\frac{\partial}{2\partial\Delta_i}}\begin{pmatrix}-z_i\\ 1\end{pmatrix}\right\} \quad .\end{aligned} \tag{4.20}$$

We have explicitly checked that these generators annihilate the all tree-level celestial superamplitudes. Note that while the results of the next two sections will be specific to MHV amplitudes, the results of this section hold for all helicity sectors.

4.3 Differential equations for celestial MHV amplitudes

4.3.1 Generalized Banerjee-Ghosh equations

In [164], Banerjee and Ghosh derived a set of $n-2$ differential equations satisfied by celestial n-point MHV gluon amplitudes at tree-level. We refer to these as BG equations. While these equations are satisfied by the full amplitude, it is easier to work with the colour ordered amplitudes. We will use the equation derived in [164] to derive equations for colour ordered MHV amplitudes. Transforming to momentum space, we find that these equations encode the properties of the amplitude under an infinitesimal BCFW shift. We will then derive generalizations of these equations for MHV amplitudes.

Colour stripped amplitudes

It is well known that the tree-level n-gluon amplitude, M_n admits a colour decomposition

$$M_n = \sum_{\pi \in S_{n-1}} \mathcal{M}_n[1, \pi(2), \pi(3), \ldots, \pi(n)] \operatorname{Tr}[T^{a_1} T^{a_{\pi(2)}} \cdots T^{a_{\pi(n)}}] \quad , \tag{4.21}$$

where π is a permutation of $\{1, 2, \cdots, n\}$ with the requirement $\pi(1) = 1$. This decomposition trivially carries over to celestial amplitude,

$$\tilde{M}_n \ := \ \left\langle \mathcal{O}^{a_1}_{\Delta_1} \ldots \mathcal{O}^{a_n}_{\Delta_n} \right\rangle = \sum_{\pi \in S_{n-1}} \tilde{\mathcal{M}}_n[1, \pi(2), \pi(3), \ldots, \pi(n)] \operatorname{Tr}[T^{a_1} T^{a_{\pi(2)}} \cdots T^{a_{\pi(n)}}] \quad . \tag{4.22}$$

Here $\tilde{M}_n$ and $\tilde{\mathcal{M}}_n$ are the Mellin transforms of M_n and $\mathcal{M}_n$ respectively. All undefined symbols used for the remainder of this subsection will have the same meanings as in [164]. There the authors derived a differential equation for $\tilde{M}_n$. To do this, they imposed the constraints arising from the current algebra of the subleading soft modes of a gluon primary on the subleading singularities of the OPE between a gluon primary and a subleading soft mode. This leads to the identification of a null state, which when inserted into a correlation function of n gluon primaries, leads to a differential equation. We follow this route here albeit with minor modifications to arrive at differential equations for the colour ordered amplitude $\tilde{\mathcal{M}}_n\,(1, \ldots n)$.

We begin with equation (6.5) from [164], which after making the replacement $1 \to i$ is

$$\left[\delta^{a_i\, x} J^a_{-1} \, + \, i\, f^{a\, a_i\, x} L_{-1} P_i^{-1} - (\delta^{a\, x} \delta^{a_i\, y} - (\Delta_i - 1) \delta^{a\, y} \delta^{a_i\, x})\, j^y_{-1}\, P_i^{-1}\right] \, \mathcal{O}^x_{\Delta_i,+} = 0 \quad . \tag{4.23}$$

Shifting $\Delta_i \to \Delta_i + 1$, using $\mathcal{O}^x_{\Delta_i+1,+} = P_i \mathcal{O}^x_{\Delta_i,+}$ and inserting this into the MHV amplitude yields

$$\begin{aligned} &\left[\delta^{a_i\, x} J^a_{-1}(i)\, P(i) \ - \ (\delta^{a\, x} \delta^{a_i\, y} - \Delta_i \delta^{a\, y} \delta^{a_i\, x})\, j^y_{-1}(i)\right] \left\langle \mathcal{O}^{a_1}_{\Delta_1} \ldots \mathcal{O}^{x}_{\Delta_i} \ldots \mathcal{O}^{a_n}_{\Delta_n} \right\rangle \\ &\qquad\qquad + \ T^a(i) L_{-1}(i) \left\langle \mathcal{O}^{a_1}_{\Delta_1} \ldots \mathcal{O}^{a_i}_{\Delta_i} \ldots \mathcal{O}^{a_n}_{\Delta_n} \right\rangle \ = \ 0 \quad . \end{aligned} \tag{4.24}$$

Performing the appropriate OPEs, this turns into a differential equation for $\tilde{M}_n$

$$T_i^a \frac{\partial}{\partial z_i} \left\langle \mathcal{O}^{a_1}_{\Delta_1} \dots \mathcal{O}^{a_i}_{\Delta_i} \dots \mathcal{O}^{a_n}_{\Delta_n} \right\rangle \; - \; \sum_{j \neq i} \epsilon_i \epsilon_j \, \frac{\Delta_j - J_j - 1 + \bar{z}_{ji} \bar{\partial}_j}{z_{ji}} \, T_j^a \left\langle \mathcal{O}^{a_1}_{\Delta_1} \dots \mathcal{O}^{a_j}_{\Delta_{j-1}} \dots \mathcal{O}^{a_i}_{\Delta_{i+1}} \dots \mathcal{O}^{a_n}_{\Delta_n} \right\rangle$$
$$- \; \sum_{j \neq i} \frac{T_j^{a_i}}{z_{ji}} \left\langle \mathcal{O}^{a_1}_{\Delta_1} \dots \mathcal{O}^{a}_{\Delta_i} \dots \mathcal{O}^{a_n}_{\Delta_n} \right\rangle \; + \; \Delta_i \sum_{j \neq i} \frac{T_j^a}{z_{ji}} \left\langle \mathcal{O}^{a_1}_{\Delta_1} \dots \mathcal{O}^{a_i}_{\Delta_i} \dots \mathcal{O}^{a_n}_{\Delta_n} \right\rangle = 0 \quad . \tag{4.25}$$

This is true for each positive helicity gluon i. Thus we have a set of $(n-2)$ partial differential equations satisfied by $\tilde{M}_n$. We can now extract the equations satisfied by the colour ordered amplitudes. For the sake of concreteness, we will derive equations for the colour ordered celestial amplitude $\tilde{\mathcal{M}}_n\,(1\,2\,\dots n)$. The relevant contribution from the first term in (4.25) is

$$\begin{aligned} &\left(\frac{\partial}{\partial\, z_i} \tilde{\mathcal{M}}_n\,(1\,\dots\,n) \right) \, T_i^a \, \mathrm{Tr}[T^{a_1} \cdots T^{a_{i-1}} T^x T^{a_{i+1}} \cdots] \\ = &\left(\frac{\partial}{\partial\, z_i} \tilde{\mathcal{M}}_n\,(1\,\dots\,n) \right) \, i\, f^{a a_i x} \, \mathrm{Tr}[T^{a_1} \cdots T^{a_{i-1}} T^x T^{a_{i+1}} \cdots] \\ = &\left(\frac{\partial}{\partial\, z_i} \tilde{\mathcal{M}}_n\,(1\,\dots\,n) \right) \left(\mathrm{Tr}[T^{a_1} \cdots T^{a_{i-1}} T^a T^{a_i} T^{a_{i+1}} \cdots] \; - \; \mathrm{Tr}[T^{a_1} \cdots T^{a_{i-1}} T^{a_i} T^a T^{a_{i+1}} \cdots] \right) \quad . \end{aligned} \tag{4.26}$$

Looking at terms with the prefactor of $\mathrm{Tr}[T^{a_1} \cdots T^{a_{i-1}} T^a T^{a_i} T^{a_{i+1}} \cdots]$, we see that the next three terms in eq (4.25) contribute only when $j = i \pm 1$ yielding

$$\begin{aligned} &\left(\partial_i \; - \; \frac{\Delta_i}{z_{i-1,i}} \; - \; \frac{1}{z_{i+1,i}} \right) \tilde{\mathcal{M}}_n(1, \cdots, n) \\ &\quad + \; \left(\epsilon_i \epsilon_{i-1} \, \frac{\Delta_{i-1} - J_{i-1} - 1 + \bar{z}_{i-1,i} \bar{\partial}_{i-1}}{z_{i-1,i}} \, e^{\frac{\partial}{\partial \Delta_i} - \frac{\partial}{\partial \Delta_{i-1}}} \right) \tilde{\mathcal{M}}_n(1, \cdots, n) \; = \; 0 \quad , \end{aligned} \tag{4.27}$$

and another equation with $i{-}1 \leftrightarrow i{+}1$ if we look at terms with the prefactor of $\mathrm{Tr}[T^{a_1} \cdots T^{a_{i-1}} T^{a_i} T^a T^{a_{i+1}} \cdots]$.
The terms with the prefactor of
$\mathrm{Tr}[T^{a_1} \cdots T^{a_{i-1}} T^{a_i} T^{a_{i+1}} \cdots T^{a_{j-1}} T^a T^{a_j} T^{a_{j+1}} \cdots]$, in which the insertion T^a isn't adjacent to T^{a_i} imply

$$\begin{aligned} &\Bigg\{ - \epsilon_i \epsilon_j \, \frac{\Delta_j - J_j - 1 + \bar{z}_{j,i} \bar{\partial}_j}{z_{j,i}} \, e^{\frac{\partial}{\partial \Delta_i} - \frac{\partial}{\partial \Delta_j}} \; + \; \epsilon_i \epsilon_{j-1} \, \frac{\Delta_{j-1} - J_{j-1} - 1 + \bar{z}_{j-1,i} \bar{\partial}_{j-1}}{z_{j-1,i}} \, e^{\frac{\partial}{\partial \Delta_i} - \frac{\partial}{\partial \Delta_{j-1}}} \\ &\quad + \; \left(\frac{\Delta_i}{z_{j,i}} \; - \; \frac{\Delta_i}{z_{j-1,i}} \right) \Bigg\} \, \tilde{\mathcal{M}}_n[1, \cdots, i-1, i, i+1, \dots, j-1, j, \cdots] \\ &\qquad + \; \left(\frac{1}{z_{i-1,i}} \; - \; \frac{1}{z_{i+1,i}} \right) \tilde{\mathcal{M}}_n[1, \cdots, i-1, i+1, \dots, j-1, i, j, \cdots] = 0 \quad . \end{aligned} \tag{4.28}$$

Plugging in the form of the MHV celestial amplitude (4.42), it is easy to see that (4.28) is satisfied if (4.27) is true. Thus, we will take (4.27) to be the set of independent equations satisfied by the colour stripped amplitude.

Momentum space origin

We can recast (4.27) as an equation acting on the momentum space amplitude $\mathcal{M}_n$ to get

$$\left(\lambda^{\alpha}_{i-1}\frac{\partial}{\partial\lambda^{\alpha}_{i}} - \tilde{\lambda}^{\dot\alpha}_{i}\frac{\partial}{\partial\tilde{\lambda}^{\dot\alpha}_{i-1}}\right)\mathcal{M}_n = \frac{\langle i-1\, i+1\rangle}{\langle i+1\, i\rangle}\mathcal{M}_n \quad , \tag{4.29}$$

where i is a positive helicity gluon. We will now demonstrate that this equation follows simply from the properties of $\mathcal{M}_n$ under a BCFW shift and that we can generalize this equation to superamplitudes.

Consider the n-point MHV amplitude with negative helicity gluons s and t

$$\mathcal{M}_n[123\ldots n] \;=\; \frac{\langle st\rangle^4\,\delta^{(4)}\left(\sum_{i=1}^n p_i\right)}{\langle 12\rangle\langle 23\rangle\cdots\langle n1\rangle} \quad , \tag{4.30}$$

and the BCFW shift

$$\lambda_i \;\to\; \hat{\lambda}_i \;=\; \lambda_i + z\,\lambda_j \quad , \quad \tilde{\lambda}_j \;\to\; \hat{\tilde{\lambda}}_j \;=\; \tilde{\lambda}_j - z\,\tilde{\lambda}_i \quad . \tag{4.31}$$

For infinitesimal z, this shift is implemented on (4.30) by the operator

$$D_{i,j} \;=\; \lambda^{\alpha}_{j}\frac{\partial}{\partial\lambda^{\alpha}_{i}} \;-\; \tilde{\lambda}_{i,\dot\beta}\frac{\partial}{\partial\tilde{\lambda}_{j,\dot\beta}} \quad . \tag{4.32}$$

Note that this coincides with the LHS of (4.29) when $j = i-1$ and i corresponds to a negative helicity gluon. The RHS depends on the helicities of i, j and we tabulate the cases below.

1. When $(J_i,\, J_j) = (+,\pm),\,(-,\,-)$,

$$\begin{aligned}\hat{\mathcal{M}}_n[\ldots\hat{i}\ldots] \;&= \mathcal{M}_n\,\frac{1}{1+z\,\frac{\langle i-1,j\rangle}{\langle i-1,i\rangle}}\,\frac{1}{1+z\,\frac{\langle i+1,j\rangle}{\langle i+1,i\rangle}} \\ &= \mathcal{M}_n\left(1 - z\,\frac{\langle i-1,j\rangle}{\langle i-1,i\rangle} - z\,\frac{\langle i+1,j\rangle}{\langle i+1,i\rangle}\right) \;+\; \mathcal{O}(z^2) \quad .\end{aligned} \tag{4.33}$$

2. When $(J_i,\, J_j) = (-,\,+)$, consider $i = s$,

$$\begin{aligned}\hat{\mathcal{M}}_n[\ldots\hat{i}\ldots] \;&= \frac{(\langle it\rangle + z\,\langle jt\rangle)^4}{\langle 12\rangle\langle 23\rangle\cdots\langle n1\rangle}\,\frac{1}{1+z\,\frac{\langle i-1,j\rangle}{\langle i-1,i\rangle}}\,\frac{1}{1+z\,\frac{\langle i+1,j\rangle}{\langle i+1,i\rangle}} \\ &= \mathcal{M}_n\left(1 - z\,\frac{\langle i-1,j\rangle}{\langle i-1,i\rangle} - z\,\frac{\langle i+1,j\rangle}{\langle i+1,i\rangle} + 4z\,\frac{\langle j,t\rangle}{\langle i,t\rangle}\right) \;+\; \mathcal{O}(z^2) \quad .\end{aligned} \tag{4.34}$$

Both of these cases can be compactly summarized as

$$D_{i,j}\,\mathcal{M}_n \;=\; \mathcal{M}_n\left(-\frac{\langle i-1,j\rangle}{\langle i-1,i\rangle} - \frac{\langle i+1,j\rangle}{\langle i+1,i\rangle} + 4\,\frac{\langle j,t\rangle}{\langle i,t\rangle}\,\delta_{i,s} + 4\,\frac{\langle j,s\rangle}{\langle i,s\rangle}\,\delta_{i,t}\right) \quad , \tag{4.35}$$

which is a generalization of (4.29).

We can map this to the celestial sphere. Taking $J_i = +$, we get

$$\begin{aligned}&\left[-\left(\Delta_i + z_{ij}\frac{\partial}{\partial z_i}\right) \;+\; \frac{z_{i-1,j}}{z_{i-1,i}} \;+\; \frac{z_{i+1,j}}{z_{i+1,i}} \;-\; 1\right] \tilde{\mathcal{M}}_n \\ &\quad +\; \epsilon_i\epsilon_j \left(\Delta_j - J_j - 1 + \bar{z}_{ji}\frac{\partial}{\partial \bar{z}_j}\right) e^{\frac{\partial}{\partial\Delta_i} - \frac{\partial}{\partial\Delta_j}} \tilde{\mathcal{M}}_n \;=\; 0 \;\;,\end{aligned} \tag{4.36}$$

which generalizes (4.27).

Supersymmetric case

The discussion above readily generalizes to MHV superamplitudes. The super-BCFW shift

$$\lambda_i \;\to\; \lambda_i \;+\; z\,\lambda_j \;\;,\;\; \tilde{\lambda}_j \;\to\; \tilde{\lambda}_j \;-\; z\,\tilde{\lambda}_i \;\;,\;\; \eta_j^A \;\to\; \eta_j^A \;-\; z\,\eta_i^A \tag{4.37}$$

is generated by

$$D_{i,j} \;=\; \lambda_j^\alpha \frac{\partial}{\partial \lambda_i^\alpha} \;-\; \tilde{\lambda}_{i,\dot{\beta}} \frac{\partial}{\partial \tilde{\lambda}_{j,\dot{\beta}}} \;-\; \sum_A \eta_i^A \frac{\partial}{\partial \eta_j^A} \quad . \tag{4.38}$$

Recall that

$$\mathcal{A}_{n,0} \;=\; \frac{\frac{1}{2^4}\prod_{A=1}^4 \sum_{i,j=1}^n \langle ij\rangle \eta_i^A \eta_j^A}{\langle 12\rangle\langle 23\rangle\cdots\langle n1\rangle} \delta^{(4)}\left(\sum_{i=1}^n p_i\right) \quad . \tag{4.39}$$

Under the super-BCFW shift (4.37), the numerator of (4.39) is invariant and we have

$$D_{i,j}\,\mathcal{A}_{n,0} \;=\; -\,\mathcal{A}_{n,0}\left(\frac{\langle i-1,j\rangle}{\langle i-1,i\rangle} + \frac{\langle i+1,j\rangle}{\langle i+1,i\rangle}\right) \quad . \tag{4.40}$$

Note that the equation above is valid for arbitrary i and j.

Transforming (4.40) to the celestial sphere we get

$$\begin{aligned}&\left[-\left(\Delta_i + J_i + z_{ij}\frac{\partial}{\partial z_i}\right) \;+\; \frac{z_{i-1,j}}{z_{i-1,i}} \;+\; \frac{z_{i+1,j}}{z_{i+1,i}}\right] \tilde{\mathcal{A}}_{n,0} \\ &\quad -\; \epsilon_i\epsilon_j \left(\sum_A \eta_i^A \frac{\partial}{\partial \eta_j^A}\right) e^{\frac{1}{2}\frac{\partial}{\partial\Delta_i} - \frac{1}{2}\frac{\partial}{\partial\Delta_j}} \tilde{\mathcal{A}}_{n,0} \\ &\quad +\; \epsilon_i\epsilon_j \left(\Delta_j - J_j - 1 + \bar{z}_{ji}\frac{\partial}{\partial \bar{z}_j}\right) e^{\frac{\partial}{\partial\Delta_i} - \frac{\partial}{\partial\Delta_j}} \tilde{\mathcal{A}}_{n,0} \;=\; 0 \;\;,\end{aligned} \tag{4.41}$$

which is a generalization of (4.27) to celestial MHV superamplitudes.

4.3.2 Hypergeometric equations and their momentum space origin

The tree-level celestial MHV gluon n-point amplitudes have been computed in [158] and have been found to be Aomoto-Gelfand hypergeometric functions. It is well known that these functions satisfy a set of differential equations. We refer the reader to Appendix 4.4 for more details. In this section, we will motivate these differential equations from properties of amplitudes. The celestial tree-level MHV n-point amplitude is given by

$$\begin{aligned}
\tilde{\mathcal{M}}_n &= 2\pi \, \frac{z_{st}^4}{z_{12}z_{23}\dots z_{n1}} \frac{\delta\left(\sum_i(\Delta_i - 1)\right)}{2^{n-4}} \frac{1}{U} \prod_{a,b} \mathbf{1}\left(x_{a,b} > 0\right) \\
&\times \int \left(\prod_{c=1}^{n-4} \mathrm{d}u_c\right) \delta\left(1 - \sum_{d=1}^{n-4} u_d\right) \left(\prod_{a=1}^{n-4} u_a^{\Delta_a - J_a - 1}\right) \prod_{b=n-3}^{n} \left(\sum_{a=1}^{n-4} x_{a,b}u_a\right)^{\Delta_b - J_b - 1} \\
&:= \mathcal{N}\,\delta\left(\sum_i(\Delta_i - 1)\right) F\left(x_{a,\,b}, \Delta_i\right) \quad ,
\end{aligned} \tag{4.42}$$

where

$$\begin{aligned}
&U = \det\{q_{n-3}, q_{n-2}, q_{n-1}, q_n\}, \;\; U_{a,b} = \det\{q_{n-3}, q_{n-2}, q_{n-1}, q_n\}|_{b\to a} \quad , \\
&x_{a,b} = -\frac{\epsilon_a\, U_{a,b}}{\epsilon_b\, U} \quad ,
\end{aligned} \tag{4.43}$$

and F is the Aomoto-Gelfand hypergeometric function[175]. This is of the form given in (4.62) with

$$Z \;=\; \begin{pmatrix} 1 & 0 & 0 & \dots & 0 & x_{1,\,n-3} & x_{1,\,n-2} & x_{1,\,n-1} & x_{1,\,n} \\ 0 & 1 & 0 & \dots & 0 & x_{2,\,n-3} & x_{2,\,n-2} & x_{2,\,n-1} & x_{2,\,n} \\ \vdots & & & & & & & & \\ 0 & 0 & 0 & \dots & 1 & x_{n-4,\,n-3} & x_{n-4,\,n-2} & x_{n-4,\,n-1} & x_{n-4,\,n} \end{pmatrix} \quad , \tag{4.44}$$

which corresponds to setting (with $k = n - 4$ and $m = n$)

$$\begin{aligned}
z_{a,b} &= \delta_{a,b} \qquad 1 \le a,\, b \le n-4 \quad , \\
z_{a,b} &= x_{a,b} \qquad 1 \le a \le n-4 \quad , \quad n-3 \le b \le n \quad .
\end{aligned} \tag{4.45}$$

The polynomials ℓ_b are

$$\begin{aligned}
\ell_1 &= u_1, \qquad \dots , \qquad \ell_{n-4} \;=\; u_{n-4} \;, \\
\ell_b &= \sum_{a=1}^{n-4} x_{a,b}u_a \,, \qquad b \;=\; n-3, \dots, n \quad ,
\end{aligned} \tag{4.46}$$

and the exponents are given by

$$\alpha_j \;=\; \Delta_j - J_j - 1 \quad . \tag{4.47}$$

Momentum conservation is manifest in (4.9) due to the presence of the delta function in $\mathcal{A}_n$. However, in arriving at the expression in (4.42), we have used the delta function to eliminate $\omega_{n-3}, \dots, \omega_n$. The statement of momentum conservation can now be written as a differential equation on F. Let $\mathbb{P}^\mu$ be the total momentum operator acting on $\mathcal{M}_n$. The corresponding celestial operator, along the lines of (4.17) is

$$\tilde{\mathbb{P}}^\mu = \sum_{i=1}^{n} \epsilon_i \, q_i^\mu e^{\frac{\partial}{\partial \Delta_i}} \quad , \tag{4.48}$$

and we must have

$$\sum_{i=1}^{n} \epsilon_i\, q_i^\mu e^{\frac{\partial}{\partial \Delta_i}} \tilde{\mathcal{M}}_n = 0 \quad . \tag{4.49}$$

We can extract four independent conditions by contracting this with the four vectors v_b^μ, $b = \{n-3,\, n-2,\, n-1,\, n\}$ defined by

$$\begin{aligned} \epsilon_n\, v_n^\mu &= -\,\epsilon^{\mu\,\nu\,\rho\,\sigma} q_{n-3\,\nu} q_{n-2\,\rho} q_{n-1\,\sigma} \quad , \quad \epsilon_{n-3}\, v_{n-3}^\mu = \epsilon^{\mu\,\nu\,\rho\,\sigma} q_{n-2\,\nu} q_{n-1\,\rho} q_{n\,\sigma} \quad , \\ \epsilon_{n-2}\, v_{n-2}^\mu &= -\,\epsilon^{\mu\,\nu\,\rho\,\sigma} q_{n-1\,\nu} q_{n\,\rho} q_{n-3\,\sigma} \quad , \quad \epsilon_{n-1}\, v_{n-1}^\mu = \epsilon^{\mu\,\nu\,\rho\,\sigma} q_{n\,\nu} q_{n-3\,\rho} q_{n-2\,\sigma} \quad . \end{aligned} \tag{4.50}$$

Noting that $v_b^\mu\, \epsilon_a\, q_{a\mu} = -U x_{a,b}$, we get

$$\begin{aligned} &\left[-\sum_{a=1}^{n-4} x_{a,b}\, U\, e^{\frac{\partial}{\partial \Delta_a}} + U\, e^{\frac{\partial}{\partial \Delta_b}} \right] \tilde{\mathcal{M}}_n = 0 \\ &\implies \mathcal{N}\, \delta \left(1 + \sum_{i=1}^{n} (\Delta_i - 1) \right) e^{\frac{\partial}{\partial \Delta_b}} \left(-\sum_{a=1}^{n-4} \frac{1}{\alpha_b} x_{a,b} \frac{\partial}{\partial x_{a,b}} + 1 \right) F = 0 \quad , \end{aligned} \tag{4.51}$$

where we have used the fact that $e^{\frac{\partial}{\partial \Delta_a}} F = e^{\frac{\partial}{\partial \Delta_b}} \frac{1}{\alpha_b} \frac{\partial}{\partial x_{a,b}} F$. This gives us a set of differential equations

$$\sum_{a=1}^{n-4} x_{a,b} \frac{\partial F}{\partial x_{a,b}} = \alpha_b\, F \quad , \tag{4.52}$$

which correspond to eq (4.69).

The other set of differential equations eq (4.68) can be derived by noting that the form for $\tilde{\mathcal{M}}_n$ given in (4.42) corresponds to using the momentum conserving delta function to solve for $\omega_{n-3}, \ldots, \omega_n$. A different choice, say solving for $\omega_k, \ldots, \omega_{k+3}$ would lead to

$$\begin{aligned} \tilde{\mathcal{M}}_n \ &= 2\pi\, \frac{z_{s,t}^4}{z_{12} z_{23} \ldots z_{n1}} \frac{\delta\left(\sum_i (\Delta_i - 1)\right)}{2^{n-4}} \frac{1}{U'} \int \left[\prod_{c \neq \{k,\, \ldots,\, k+3\}} \mathrm{d}u_c \right] \delta \left(1 - \sum_{d \neq \{k,\, \ldots,\, k+3\}} u_d \right) \\ &\times \left[\prod_{b \neq \{k,\, \ldots,\, k+3\}} u_b^{\Delta_b - s_b - 1} \right] \prod_{b=k}^{k+3} \left(\sum_{a \neq \{k\, \ldots k+3\}} x'_{a,b} u_a \right)^{\Delta_b - s_b - 1} \quad , \end{aligned} \tag{4.53}$$

with

$$\begin{aligned} &U' = \det\{q_k, q_{k+1}, q_{k+2}, q_{k+3}\} \ , \ U'_{a,b} = \det\{q_k, q_{k+1}, q_{k+2}, q_{k+3}\}|_{b \to a} \quad , \\ &x'_{a,b} = -\frac{\epsilon_a\, U'_{a,b}}{\epsilon_b\, U'} \quad . \end{aligned} \tag{4.54}$$

This corresponds to an integral of the form given in (4.62) but with

$$Z \ = \ \begin{pmatrix} 1 & 0 & \ldots & x_{1,\,k} & x_{1,\,k+1} & x_{1,\,k+2} & x_{1,\,k+3} & \ldots & 0 \\ 0 & 1 & \ldots & x_{2,\,k} & x_{2,\,k+1} & x_{2,\,k+2} & x_{2,\,k+3} & \ldots & 0 \\ \vdots & & & & & & & & \\ 0 & 0 & \ldots & x_{n-4,\,k} & x_{n-4,\,k+1} & x_{n-4,\,k+2} & x_{n-4,\,k+3} & \ldots & 1 \end{pmatrix} \quad . \tag{4.55}$$

Both of these are equivalent representations of the celestial amplitude and Z is defined up to $GL(n-4)$ transformations acting on the left. These transformations correspond to a change of solved and unsolved variables. As shown in Appendix 4.4, this transformation property of $\tilde{\mathcal{M}}_n$ gives rise to the differential equation (4.68).

$$\sum_{j=1}^{n} z_{a,b}\frac{\partial F}{\partial z_{c,b}} \;=\; -\,\delta_{a,c}\,F \qquad 1 \leq a,\, c \leq n-4 \quad . \tag{4.56}$$

We need to make sense of the differentials of the gauge fixed $z_{i,j}$. To do this, we first differentiate the function F as in (4.62) and then set $z_{i,\,j}$ to the corresponding gauge fixed values. In particular, $z_{a,b}\frac{\partial F}{\partial z_{c,b}} = \delta_{a,b}\,\alpha_a e^{\frac{\partial}{\partial \Delta_c}-\frac{\partial}{\partial \Delta_a}}F$ for $a,\, b,\, c \in \{1, \ldots n-4\}$. We can now write (4.56) in terms of the $x_{a,b}$.

$$\alpha_a F + \sum_{b=n-3}^{n} x_{a,b}\frac{\partial F}{\partial x_{a,b}} \;=\; -\,F \quad , \tag{4.57}$$

$$\alpha_a e^{\frac{\partial}{\partial \Delta_c}-\frac{\partial}{\partial \Delta_a}} F + \sum_{b=n-3}^{n} x_{a,b}\frac{\partial F}{\partial\, x_{c,b}} \;=\; 0 \qquad c \neq a \quad . \tag{4.58}$$

It can be shown that (4.58) can be derived from the rest and isn't independent.

4.3.3 Relation between differential equations

Finally, we make a comment here about the relationship between the colour stripped BG equations (4.27) and the hypergeometric PDEs. Recall that the celestial MHV amplitude

$$\tilde{\mathcal{M}}_n \;= \mathcal{N}\,\delta\left(\sum_i (\Delta_i - 1)\right) F\left(x_{a,\,b}, \Delta_i\right) \quad , \tag{4.59}$$

where F is a hypergeometric function. To compare the two sets of equations, we rewrite the BG equations as equations for F in terms of the variables $x_{a,\,b}$ in (4.43). Without loss of generality, we choose $i = 1$. After some manipulation, it can be brought to the form

$$\begin{aligned}\Bigg[\left(\alpha_1 + 1 + \sum_{b=n-3}^{n} x_{1,b}\frac{\partial}{\partial x_{1,b}}\right) - \sum_b \frac{\epsilon_2}{\epsilon_1}\left(x_{2,b} + \bar{z}_{1,2}\frac{\partial x_{2,b}}{\partial \bar{z}_2}\right)\left(\frac{\partial}{\partial x_{1,b}} - \frac{\partial}{\partial x_{2,b}} e^{\frac{\partial}{\partial \Delta_1}-\frac{\partial}{\partial \Delta_2}}\right) \\ -\frac{\epsilon_2}{\epsilon_1} e^{\frac{\partial}{\partial \Delta_1}-\frac{\partial}{\partial \Delta_2}}\left(\alpha_2 + 1 + \sum_b x_{2,b}\frac{\partial}{\partial x_{2,b}}\right)\Bigg] F = 0 \quad ,\end{aligned} \tag{4.60}$$

which shows that the BG equations reduce to combinations of the hypergeometric equations.

4.4 Appendix: Aomoto-Gelfand hypergeometric functions

The Aomoto-Gelfand hypergeometric functions [175] are associated to Grassmannians. In this section, we will make this connection explicit and derive the differential equations associated to them.

For a quick introduction, see [181] from which most of this section is adopted (with cosmetic changes).

Let Z be a $k \times m$ matrix,

$$Z = \begin{pmatrix} z_{1,1} & z_{1,2} & \dots & z_{1,m} \\ \vdots & & & \\ z_{k,1} & z_{l,2} & \dots & z_{k,m} \end{pmatrix} \quad . \tag{4.61}$$

The hypergeometric function associated to this matrix is

$$F(Z) = \int \prod_{b=1}^{m} \ell_b(u)^{\alpha_b} \frac{du_1 \dots du_k}{\text{Vol GL}(1)} \quad , \tag{4.62}$$

where $\ell_b(u) = \sum_{a=1}^{k} u_a \, z_{a,b}$ and $u = (u_1, \dots u_k) \in \mathbb{CP}^k$. The polynomials $\ell_1, \dots, \ell_m$ can be collectively written as

$$\ell = (\ell_1, \dots \ell_m) = u \cdot Z \quad . \tag{4.63}$$

A point in the Grassmannian $G(k, m)$ is defined modulo $GL(k)$ transformations. We would like to understand how the function $F(Z)$ behaves under such transformations. A $GL(k)$ transformation, G, acts by left multiplication on the matrix Z as $Z \to G \cdot Z$ and we have,

$$\ell \to \ell' = u \cdot G \, Z \quad . \tag{4.64}$$

We see that the effect on $F(Z)$ is a change of variables from $u \to u'$ leading to

$$F(G \cdot Z) = \det(G)^{-1} F(Z) \quad . \tag{4.65}$$

We can also rescale each column separately. This is effected through right multiplication by an $m \times m$ diagonal matrix $S = \text{diag}\,(s_0, \dots s_m)$.

$$Z \to Z \cdot S = \begin{pmatrix} s_1 \, z_{1,1} & s_2 \, z_{1,2} & \dots & s_m \, z_{1,m} \\ \vdots & & & \\ s_1 \, z_{k,1} & s_2 \, z_{l,2} & \dots & s_m \, z_{k,m} \end{pmatrix} \quad . \tag{4.66}$$

The polynomials transform in a simple manner as $\ell_i \to s_i \, \ell_i$ resulting in

$$F(Z \cdot S) = F(Z) \prod_{b=1}^{m} s_b^{\alpha_b} \quad . \tag{4.67}$$

The transformation properties in (4.65) and (4.67) lead to the following set of differential equations [175], [181]

$$\sum_{b=1}^{m} z_{a,b} \frac{\partial F}{\partial z_{c,b}} = -\delta_{a,c} \, F \qquad 1 \leq a, \, c \leq k \quad , \tag{4.68}$$

$$\sum_{a=1}^{k} z_{a,b} \frac{\partial F}{\partial \, z_{a,b}} = \alpha_b \, F \qquad 1 \leq b \leq m \quad . \tag{4.69}$$

Chapter 5

Deformed $w_{1+\infty}$ Algebras in the Celestial CFT

This chapter is based on [44].

Symmetries have played a central role in shaping our understanding of fundamental physics. They often hint towards simpler or alternate formulations of theories. The Lorentz group SO(3,1) of 4D flat spacetime acts as the conformal group $SL(2,\mathbb{C})$ on the 2D celestial sphere at null infinity. Any theory living on the celestial sphere naturally inherits this conformal symmetry. S-matrix elements, typically evaluated in a basis of momentum eigenstates, can be rewritten in a basis of boost eigenstates via a Mellin transform (for massless particles) [43, 182, 139]. The resulting amplitudes transform as correlation functions of a 2D conformal field theory on the celestial sphere. It is conjectured that a suitable theory on the 2D celestial sphere, called Celestial CFT (CCFT), is the holographic dual to gauge and gravity theories in 4D flat spacetime (see [183, 184, 185] for reviews).

Celestial CFTs have additional symmetries beyond the usual 2D conformal symmetry which follow from leading and subleading soft gluon theorems and leading, subleading and subsubleading soft graviton theorems (see [186] for a review). Remarkably, these symmetries completely fix the leading celestial operator product expanstion (OPE) of conformal primary gluons and gravitons on the celestial sphere in terms of the Euler beta function [187]. These OPEs have been also derived in [144] by Mellin transforming the collinear limits of amplitudes. The Euler beta function has an infinite sequence of poles at integer conformal weights, associated with conformally soft currents: the first pole corresponds to the conformally soft current, the second to the subleading soft current, and so on[1]. The OPEs between the conformally soft positive-helicity gluon and graviton currents have been obtained in [196] by taking appropriate residues of the results of [187]. These OPEs can then be used to compute the commutation relations of the modes of the soft currents [197]. Remarkably, it was recently shown by Strominger [168] that the resulting algebra is the wedge algebra of $w_{1+\infty}$

[1] Soft theorems in the 4D bulk translate into conformally soft theorems on the celestial sphere in which the conformal dimensions of external particles take on specific integer values [188, 189, 190, 191, 144, 192, 193]. The infinite tower of soft theorems has been discussed in [194, 195].

algebra which has been extensively studied in the 90s (see [198, 199, 200, 201, 202, 203, 204]). This $w_{1+\infty}$ structure of the symmetry algebra holds for all spins and in the presence of supersymmetry [196, 205, 206]. Additionally, it has also been derived from the worldsheet perspective [207, 208]. The effect of loop corrections and higher derivative interactions on conventional soft theorems has been studied in [209, 210, 211, 212, 213, 214]. It is interesting to understand their corresponding celestial versions and their implications for the $w_{1+\infty}$ structure.

In this paper, we consider the effect of non-minimal couplings in the bulk on the OPEs of soft currents in the CCFT. We compute the corresponding modifications to the symmetry algebra, and find that while the modified algebra bears some semblance to the well-known $W_{1+\infty}$ [200], it differs from $W_{1+\infty}$ in crucial ways. We find that the Jacobi identity imposes constraints on the spectrum and couplings of the theory. The rest of the paper is organized as follows. We review the OPEs of soft currents in the presence of non-minimal couplings in Section 5.1. We compute the algebra in a simplified form and demand the closure of Jacobi identities in Section 5.2. In Appendix 5.3, we demonstrate the structure of soft current operators directly from well-known scattering amplitudes. Appendix 5.4 provides an alternate derivation of the gluon soft current OPEs from double soft limits of scattering amplitudes. Finally, in Appendix 5.6, we comment on an alternate definition of the commutator for soft currents.

5.1 Soft current OPEs

The OPE for two operators of arbitrary spins, s_1, s_2 and conformal dimensions Δ_1, Δ_2 in CCFT is heavily constrained. They have been determined from collinear limits of scattering amplitudes [144] and separately from asymptotic symmetries [187]. The contribution to the OPE from a three-point interaction with bulk dimension $p+4$ was worked out in full generality in [196] and takes the form[2]

$$\mathcal{O}_{h_1,\bar{h}_1}(z_1,\bar{z}_1)\,\mathcal{O}_{h_2,\bar{h}_2}(z_2,\bar{z}_2) \sim \frac{1}{z_{12}}\sum_{\alpha=0}^{\infty} C_p^{(\alpha)}\left(\bar{h}_1,\bar{h}_2\right) \bar{z}_{12}^{p+\alpha}\bar{\partial}^{\alpha}\mathcal{O}_{h_1+h_2-1,\bar{h}_1+\bar{h}_2+p}(z_2,\bar{z}_2)\,, \tag{5.1}$$

where $(h,\bar{h}) = \left(\frac{\Delta+s}{2}, \frac{\Delta-s}{2}\right)$ are the conformal weights. The OPE in (5.1) gets modified slightly if both operators carry a color index. In this case the right hand side must include an appropriate group theoretical factor. In the rest of this paper, we will avoid writing color indices explicitly unless necessary. The OPE coefficient $C_p^{(\alpha)}\left(\bar{h}_1,\bar{h}_2\right)$ is completely determined by the three-point amplitude of massless particles with helicities $s_1, s_2, -s_I$ (where $s_I = s_1+s_2-p-1$ is the spin of the intermediate particle in the collinear factorization channel) to be [196]

$$C_p^{(\alpha)}\left(\bar{h}_1,\bar{h}_2\right) = -\frac{1}{2}\kappa_{s_1,s_2,-s_I}\frac{1}{\alpha!}B\left(2\bar{h}_1+p+\alpha, 2\bar{h}_2+p\right), \tag{5.2}$$

where $B(a,b)$ is the Euler beta function, $\kappa_{s_1,s_2,-s_I}$ is the coupling constant of the relevant three-point amplitude which has mass dimension $-p$ which can include contributions from multiple terms

[2] We are only considering the holomorphic collinear pole. Depending on s_1, s_2, there could be an additional anti-holomorphic pole.

in the Lagrangian. As an example, $\kappa_{2,2,2}$ comes from various higher derivative terms with different R^3 type contractions. Discounting the existence of massless higher spin particles in the bulk, there are only a finite number of interactions which contribute to this OPE and we must sum over all allowed values of p. It is apparent from (5.2) that the OPE coefficient has poles in Δ corresponding to conformally soft limits. The soft current with dimension k for a particle with spin s is defined by the limit

$$H^{k,s} = \lim_{\Delta \to k} (\Delta - k)\, \mathcal{O}_{\frac{k+s+\epsilon}{2}, \frac{k+\epsilon-s}{2}} = \lim_{\epsilon \to 0} \epsilon \mathcal{O}_{\frac{k+s+\epsilon}{2}, \frac{k+\epsilon-s}{2}} \tag{5.3}$$

where $k = 2, 1, 0, -1, -2, \ldots$ for gravitons, $k = 1, 0, -1, \ldots$ for gluons and $k = 0, -1, -2, \ldots$ for scalars[3]. Again, it is understood that missing color indices are restored in the appropriate cases. Appendix 5.3 contains more details on the derivation and structure of these soft currents. Using this definition of soft currents and the limit

$$\lim_{\epsilon \to 0} \frac{\epsilon}{2} \frac{\Gamma\left(2\bar{h}_1 + p + \alpha + \epsilon\right) \Gamma\left(2\bar{h}_2 + p + \epsilon\right)}{\Gamma\left(2\bar{h}_1 + 2\bar{h}_2 + 2p + \alpha + 2\epsilon\right)} = \binom{-2\bar{h}_1 - 2\bar{h}_2 - 2p - \alpha}{-2\bar{h}_2 - p}, \tag{5.4}$$

we obtain the soft current OPE [196]

$$\begin{aligned} &H^{k_1,s_1}(z_1,\bar{z}_1)\, H^{k_2,s_2}(z_2,\bar{z}_2) \sim \\ &-\sum_p \frac{\kappa_{s_1,s_2,-s_I}}{2} \frac{1}{z_{12}} \sum_{\alpha=0}^{\infty} \frac{(\bar{z}_{12})^{\alpha+p}}{\alpha!} \binom{-2\bar{h}_1 - 2\bar{h}_2 - 2p - \alpha}{-2\bar{h}_2 - p} \bar{\partial}^\alpha H^{k_1+k_2+p-1, s_1+s_2-p-1}. \end{aligned} \tag{5.5}$$

The OPE of two positive helicity gravitons includes the term with $p = 1$, which is the contribution from the usual MHV amplitude with coupling $\kappa_{-2,2,2}$, $p = 3$ which is the contribution from a graviton-graviton-scalar coupling $\kappa_{0,2,2}$, and $p = 5$ which is the contribution from a non-minimal R^3 coupling $\kappa_{2,2,2}$. The roster of soft currents considered in this paper is

- Soft graviton currents $H^{k,\pm 2}$
- Soft gluon currents $H^{k,\pm 1,a}$
- Two kinds of soft scalar currents $H^{k,0,a}$ (colored) and $H^{k,0}$ (uncolored).

For the sake of clarity, we explicitly write out two OPEs involving operators of color. The OPE of two positive helicity gluons is

$$\begin{aligned} &H^{k_1,+1,a}(z_1,\bar{z}_1)\, H^{k_2,+1,b}(z_2,\bar{z}_2) \sim \\ &-if^{abc} \sum_{p=0,2} \frac{\kappa_{1,1,p-1}}{2} \frac{1}{z_{12}} \sum_{\alpha} \frac{(\bar{z}_{12})^{\alpha+p}}{\alpha!} \binom{-2\bar{h}_1 - 2\bar{h}_2 - 2p - \alpha}{-2\bar{h}_2 - p} \bar{\partial}^\alpha H^{k_1+k_2+p-1, 1-p, c} \\ &-\frac{\delta^{ab}}{N_c} \frac{\kappa_{1,1,0}}{2} \frac{1}{z_{12}} \sum_{\alpha} \frac{(\bar{z}_{12})^{\alpha+1}}{\alpha!} \binom{-2\bar{h}_1 - 2\bar{h}_2 - 2 - \alpha}{-2\bar{h}_2 - 1} \bar{\partial}^\alpha H^{k_1+k_2,0} \\ &-d^{abc} \frac{\kappa_{1,1,0}}{2} \frac{1}{z_{12}} \sum_{\alpha} \frac{(\bar{z}_{12})^{\alpha+1}}{\alpha!} \binom{-2\bar{h}_1 - 2\bar{h}_2 - 2 - \alpha}{-2\bar{h}_2 - 1} \bar{\partial}^\alpha H^{k_1+k_2,0,c}, \end{aligned} \tag{5.6}$$

[3] Note that the $k = 0$ term is non trivial for scalars in the adjoint representation.

where f^{abc} is the structure of constant and accompanies gluon operators, δ^{ab} accompanies uncolored scalars, N_c is the number of colors and d^{abc} is a total symmetric tensor defined by $d_{abc} := 2\mathrm{Tr}\left[\left\{T^a, T^b\right\} T^c\right]$ which accompanies colored scalars.

Finally, the OPE of a gluon and a colored scalar is

$$\begin{aligned}
&H^{k_1,+1,a}\left(z_1,\bar{z}_1\right) H^{k_2,0,b}\left(z_2,\bar{z}_2\right) \sim \\
&-if^{abc}\frac{\kappa_{0,0,1}}{2}\frac{1}{z_{12}}\sum_{\alpha}\frac{\left(\bar{z}_{12}\right)^{\alpha}}{\alpha!}\begin{pmatrix}-2\bar{h}_1-2\bar{h}_2-\alpha\\-2\bar{h}_2\end{pmatrix}\bar{\partial}^{\alpha}H^{k_1+k_2-1,0,c}\\
&-d^{abc}\frac{\kappa_{0,1,1}}{2}\frac{1}{z_{12}}\sum_{\alpha}\frac{\left(\bar{z}_{12}\right)^{\alpha+1}}{\alpha!}\begin{pmatrix}-2\bar{h}_1-2\bar{h}_2-2-\alpha\\-2\bar{h}_2-1\end{pmatrix}\bar{\partial}^{\alpha}H^{k_1+k_2,-1,c},
\end{aligned} \tag{5.7}$$

Note that this time f^{abc} accompanies colored scalars while d^{abc} accompanies gluons and that we have no δ^{ab} term. We will find that the algebra of soft currents involving gravitons and gluons does not satisfy the Jacobi identity unless we include additional scalars (see Section 5.2.2).

5.2 Algebras

The OPEs obtained in the previous sections can be used to compute the commutators of the modes of soft currents. Following the suggestion in Appendix 5.3 we have

$$H^{k,s}\left(z,\bar{z}\right)=\sum_{\bar{m}=-\infty}^{-\bar{h}}\frac{1}{\bar{z}^{\bar{m}+\bar{h}}}H^{k,s}_{\bar{m}}\left(z\right). \tag{5.8}$$

The modes can also be extracted from the current by the contour integral

$$H^{k,s}_{\bar{m}}\left(z\right)=\oint\limits_{|\bar{z}|=\epsilon}\frac{\mathrm{d}\bar{z}}{2\pi i}\bar{z}^{\bar{m}+\bar{h}-1}H^{k,s}(z,\bar{z}). \tag{5.9}$$

We define a 2D commutator as

$$\left[H^{k_1,s_1}_{\bar{m}_1},H^{k_2,s_2}_{\bar{m}_2}\right]\left(z_2\right)=\oint\limits_{\mathcal{C}}\frac{dz_1}{2\pi i}\frac{d\bar{z}_1}{2\pi i}\bar{z}_1^{\bar{m}_1+\bar{h}_1-1}\frac{d\bar{z}_2}{2\pi i}\bar{z}_2^{\bar{m}_2+\bar{h}_2-1}H^{k_1,s_1}\left(z_1,\bar{z}_1\right)H^{k_2,s_2}\left(z_2,\bar{z}_2\right), \tag{5.10}$$

where the contour $\mathcal{C}$ is defined by the conditions $z_1=z_2, |\bar{z}_1|=\epsilon, |\bar{z}_2|=\epsilon$ with ϵ infinitesimal. The OPE of soft currents with opposite spin involves both holomorphic and anti-holomorphic poles. The commutator defined above captures the residue on the holomorphic poles only. We can alternatively define a commutator which is sensitive to both sets of poles. However, this definition would lead to a violation of the Jacobi identity as we will see in Appendix 5.6. A particularly striking consequence of the definition (5.10) is

$$\left[H^{k_1,s_1}_{\bar{m}_1},H^{k_2,s_2}_{\bar{m}_2}\right]\left(z_2\right)=0 \qquad \text{if} \qquad s_1<0,s_2<0, \tag{5.11}$$

since the OPE of two negative helicity soft currents only involves anti-holomorphic poles. The algebra of the modes of the soft currents is determined by the OPE (5.5) to be

$$\left[H^{k_1,s_1}_{\bar{m}_1}, H^{k_2,s_2}_{\bar{m}_2}\right] = -\sum_p \frac{\kappa_{s_1,s_2,-s_I}}{2} \sum_{\alpha=0}^{\infty} \binom{-2\bar{h}_1 - 2\bar{h}_2 - 2p - \alpha}{-2\bar{h}_2 - p} \oint \frac{d\bar{z}_1}{2\pi i}\frac{d\bar{z}_2}{2\pi i} \bar{z}_1^{\bar{m}_1+\bar{h}_1-1} \bar{z}_2^{\bar{m}_2+\bar{h}_2-1} \frac{(\bar{z}_{12})^{\alpha+p}}{\alpha!} \bar{\partial}_2^{\alpha} H^{k_1+k_2+p-1,s_1+s_2-p-1}(z_2,\bar{z}_2)\,. \tag{5.12}$$

Performing the $\bar{z}_1$ integral we get,

$$\left[H^{k_1,s_1}_{\bar{m}_1}, H^{k_2,s_2}_{\bar{m}_2}\right] = -\sum_p \frac{\kappa_{s_1,s_2,-s_I}}{2} \sum_{\alpha=0}^{\infty} \binom{-2\bar{h}_1 - 2\bar{h}_2 - 2p - \alpha}{-2\bar{h}_2 - p} \binom{p+\alpha}{-\bar{m}_1 - \bar{h}_1} \frac{1}{\alpha!}(-1)^{\alpha+p+\bar{m}_1+\bar{h}_1} \tag{5.13}$$

$$\oint \frac{d\bar{z}_2}{2\pi i} \bar{z}_2^{p+\alpha+\bar{m}_1+\bar{h}_1+\bar{m}_2+\bar{h}_2-1} \bar{\partial}_2^{\alpha} H^{k_1+k_2+p-1,s_1+s_2-p-1}(z_2,\bar{z}_2)\,. \tag{5.14}$$

We can perform the last integral by using the mode expansion of $H^{k_1+k_2+p-1,s_1+s_2-p-1}(z_2,\bar{z}_2)$ in (5.8). The result is

$$\left[H^{k_1,s_1}_{\bar{m}_1}, H^{k_2,s_2}_{\bar{m}_2}\right] = -\sum_p \frac{\kappa_{s_1,s_2,-s_I}}{2} \sum_{\alpha=0}^{\infty} \binom{-2\bar{h}_1 - 2\bar{h}_2 - 2p - \alpha}{-2\bar{h}_2 - p} \binom{p+\alpha}{-\bar{m}_1 - \bar{h}_1} \frac{(-1)^{\alpha+p+\bar{m}_1+\bar{h}_1}}{\alpha!} \frac{(-\bar{m}_1 - \bar{m}_2 - \bar{h}_1 - \bar{h}_2 - p)!}{(-\bar{m}_1 - \bar{m}_2 - \bar{h}_1 - \bar{h}_2 - p - \alpha)!} H^{k_1+k_2+p-1,s_1+s_2-p-1}_{\bar{m}_1+\bar{m}_2}\,. \tag{5.15}$$

It is useful to rewrite the above expression using the identity

$$\frac{(p+\alpha)!}{(-\bar{m}_1-\bar{h}_1)!\,(\alpha+p+\bar{m}_1+\bar{h}_1)!\,\alpha!} = \sum_{x=0}^{p} \binom{p}{x} \frac{1}{(-\bar{m}_1-\bar{h}_1-x)!\,(\alpha+x+\bar{m}_1+\bar{h}_1)!}. \tag{5.16}$$

The commutation relation (5.15) now becomes

$$\left[H^{k_1,s_1}_{\bar{m}_1}, H^{k_2,s_2}_{\bar{m}_2}\right] = -\sum_p \frac{\kappa_{s_1,s_2,-s_I}}{2} \sum_{x=0}^{p} \binom{p}{x} \sum_{\alpha=0}^{\infty} \binom{-2\bar{h}_1 - 2\bar{h}_2 - 2p - \alpha}{-2\bar{h}_2 - p} (-1)^{\alpha+p+\bar{m}_1+\bar{h}_1} \frac{(-\bar{m}_1 - \bar{m}_2 - \bar{h}_1 - \bar{h}_2 - p)!\; H^{k_1+k_2+p-1,s_1+s_2-p-1}_{\bar{m}_1+\bar{m}_2}}{(-\bar{m}_1 - \bar{m}_2 - \bar{h}_1 - \bar{h}_2 - p - \alpha)!\,(-\bar{m}_1-\bar{h}_1-x)!\,(\alpha+x+\bar{m}_1+\bar{h}_1)!}\,. \tag{5.17}$$

This allows us to perform the sum over α more easily to get

$$\left[H^{k_1,s_1}_{\bar{m}_1}, H^{k_2,s_2}_{\bar{m}_2}\right] = -\sum_p \sum_{x=0}^{p} \left[\frac{\kappa_{s_1,s_2,-s_I}}{2}(-1)^{p-x}\binom{p}{x}\binom{\bar{m}_1+\bar{m}_2-\bar{h}_1-\bar{h}_2-p}{\bar{m}_1-\bar{h}_1-p+x} \times \binom{-\bar{m}_1-\bar{m}_2-\bar{h}_1-\bar{h}_2-p}{-\bar{m}_1-\bar{h}_1-x}\right] H^{k_1+k_2+p-1,s_1+s_2-p-1}_{\bar{m}_1+\bar{m}_2}. \tag{5.18}$$

Restricting the sum over p to only include particles with helicities between -2 and 2 implies that $p \in (\mathrm{Max}(s_1+s_2-3,0), \mathrm{Max}(s_1+s_2+1,0))$. However, some values of p in this range might still be forbidden if the corresponding amplitude does not exist. The introduction of color indices modifies this formula in a manner analogous to the modification of the OPE.

5.2.1 W_∞-like currents

It is useful to define new currents which are light-transforms of the soft currents. These have simplified the algebra and revealed its w_∞ structure in [168, 196, 205]. Let[4]

$$W^{q,s}(z,\bar{z}) = \Gamma(2q)\,\bar{\mathbf{L}}\left[H^{s+2(1-q),s}(z,\bar{z})\right], \tag{5.19}$$

where $q = 1, \frac{3}{2}, 2, \dots$ and

$$\bar{\mathbf{L}}\left[\mathcal{O}_{h,\bar{h}}(z,\bar{z})\right] = \int_{\mathbb{R}} \frac{d\bar{w}}{(\bar{z}-\bar{w})^{2-2\bar{h}}}\mathcal{O}_{h,\bar{h}}(z,\bar{w}). \tag{5.20}$$

The conformal weights of $W^{q,s}$ are $(s+1-q, 1-q)$. Applying this definition to the mode expansion (5.8) we get,

$$W^{q,s}(z,\bar{z}) = \sum_{\bar{m}=-\infty}^{\bar{m}=-\bar{h}} (-\bar{m}+q-1)!\,(\bar{m}+q-1)!\frac{1}{\bar{z}^{\bar{m}+q}} H_{\bar{m}}^{s+2(1-q),s}(z) \tag{5.21}$$

which implies the following mode expansion

$$W^{q,s}(z,\bar{z}) = \sum_{\bar{m}=-\infty}^{q-1} W_{\bar{m}}^{q,s}(z)\frac{1}{\bar{z}^{\bar{m}+q}} \tag{5.22}$$

with[5]

$$W_{\bar{m}}^{q,s}(z) = (-\bar{m}+q-1)!\,(\bar{m}+q-1)! H_{\bar{m}}^{s+2(1-q),s}(z). \tag{5.23}$$

The commutator (5.18) takes the simplified form

$$\begin{aligned}
\left[W_{\bar{m}_1}^{q_1,s_1}, W_{\bar{m}_2}^{q_2,s_2}\right] &= -\sum_p \sum_{x=0}^{p} \frac{\kappa_{s_1,s_2,-s_I}}{2}(-1)^{p-x}\binom{p}{x}[\bar{m}_1+q_1-1]_{p-x}[-\bar{m}_1+q_1-1]_x \\
&\qquad \times [\bar{m}_2+q_2-1]_x[-\bar{m}_2+q_2-1]_{p-x}\, W_{\bar{m}_1+\bar{m}_2}^{q_1+q_2-p-1,s_1+s_2-p-1} \\
&\equiv -\sum_{p=\mathrm{Max}(s_1+s_2-3,0)}^{\mathrm{Max}(s_1+s_2+1,0)} \frac{\kappa_{s_1,s_2,-s_I}}{2} N(q_1,q_2,\bar{m}_1,\bar{m}_2,p)\, W_{\bar{m}_1+\bar{m}_2}^{q_1+q_2-p-1,s_1+s_2-p-1}
\end{aligned} \tag{5.24}$$

where $[a]_n := a(a-1)\cdots(a-n+1)$ is the descending Pochhammer symbol and

$$\begin{aligned}
N(q_1,q_2,\bar{m}_1,\bar{m}_2,p) = \sum_{x=0}^{p}(-1)^{p-x}\binom{p}{x}[\bar{m}_1+q_1-1]_{p-x}[-\bar{m}_1+q_1-1]_x \\
\times\, [\bar{m}_2+q_2-1]_x[-\bar{m}_2+q_2-1]_{p-x}.
\end{aligned} \tag{5.25}$$

While p generically ranges between $\mathrm{Max}(s_1+s_2-3,0)$ and $\mathrm{Max}(s_1+s_2+1,0)$, some values of p are forbidden because the corresponding amplitudes do not exist. Note that $N(q_1,q_2,\bar{m}_1,\bar{m}_2,p)$ is

[4] As usual color indices are suppressed.

[5] The expression as written is valid only for modes in the range $1-q \leq \bar{m} \leq q-1$. Similar expressions can be written for modes outside this range.

symmetric under the exchange of $q_1 \leftrightarrow q_2, \bar{m}_1 \leftrightarrow \bar{m}_2$ for even p while it is antisymmetric for odd p. Thus, when both $W^{q_1,s_1}_{\bar{m}_1}$ and $W^{q_2,s_2}_{\bar{m}_2}$ have no color indices, the commutator is antisymmetric under the exchange only for odd values of p. When we include colored particles, the allowed values of p depend on the group theoretical structure. For example, the commutator involving two gluons then reads (note that $N(q_1, q_2, \bar{m}_1, \bar{m}_2, 0) = 1$)

$$\begin{aligned}
&\left[W^{q_1,s_1,a}_{\bar{m}_1},\, W^{q_2,s_2,b}_{\bar{m}_2}\right] \\
&= -\, i f^{abc} \sum_{\substack{p=\mathrm{Max}(s_1+s_2-2,0)\\ p \text{ even}}}^{\mathrm{Max}(s_1+s_2,0)} \frac{\kappa_{s_1,s_2,-s_I}}{2} N\left(q_1, q_2, \bar{m}_1, \bar{m}_2, p\right) W^{q_1+q_2-1,s_1+s_2-p-1,c}_{\bar{m}_1+\bar{m}_2} \\
&\quad - \frac{\delta^{ab}}{N_c} \sum_{\substack{p=\mathrm{Max}(s_1+s_2-3,0)\\ p \text{ odd}}}^{\mathrm{Max}(s_1+s_2+1,0)} \frac{\kappa_{s_1,s_2,-s_I}}{2} N\left(q_1, q_2, \bar{m}_1, \bar{m}_2, p\right) W^{q_1+q_2-p-1,s_1+s_2-p-1}_{\bar{m}_1+\bar{m}_2} \\
&\quad - d^{abc} \sum_{\substack{p=\mathrm{Max}(s_1+s_2-2,0)\\ p \text{ odd}}}^{\mathrm{Max}(s_1+s_2,0)} \frac{\kappa_{s_1,s_2,-s_I}}{2} N\left(q_1, q_2, \bar{m}_1, \bar{m}_2, p\right) W^{q_1+q_2-p-1,s_1+s_2-p-1,c}_{\bar{m}_1+\bar{m}_2},
\end{aligned} \tag{5.26}$$

while the commutator of a gluon (or colored scalar) with a graviton or scalar reads

$$\begin{aligned}
&\left[W^{q_1,s_1,a}_{\bar{m}_1},\, W^{q_2,s_2}_{\bar{m}_2}\right] \\
&= - \sum_{\substack{p=\mathrm{Max}(s_1+s_2-2,0)\\ p \text{ odd}}}^{\mathrm{Max}(s_1+s_2,0)} \frac{\kappa_{s_1,s_2,-s_I}}{2} N\left(q_1, q_2, \bar{m}_1, \bar{m}_2, p\right) W^{q_1+q_2-p-1,s_1+s_2-p-1,a}_{\bar{m}_1+\bar{m}_2}.
\end{aligned} \tag{5.27}$$

5.2.2 Jacobi identity

We must now demand that these commutators satisfy the Jacobi identity. To this end, we compute the double commutator from (5.24). After some algebra, we have

$$\begin{aligned}
&\left[\left[W^{q_1,s_1}_{\bar{m}_1}, W^{q_2,s_2}_{\bar{m}_2}\right], W^{q_3,s_3}_{\bar{m}_3}\right] + \text{cyclic} \\
&= \sum_{\substack{l=s_1+s_2+s_3-4\\ l \text{ even}}}^{s_1+s_2+s_3} \sum_{\substack{r=0\\ r \text{ odd}}}^{l} \frac{\kappa_{s_1,s_2,1+l-r-s_1-s_2}}{2} \frac{\kappa_{s_1+s_2-l-1+r,s_3,l+2-s_1-s_2-s_3}}{2} \\
&\qquad \times N\left(q_1, q_2, \bar{m}_1, \bar{m}_2, l-r\right) N\left(q_1+q_2-l-1+r, q_3, \bar{m}_1+\bar{m}_2, \bar{m}_3, r\right) \\
&\qquad \times W^{q_1+q_2+q_3-l-2,s_1+s_2+s_3-l-2}_{\bar{m}_1+\bar{m}_2+\bar{m}_3} \qquad + \text{cyclic}.
\end{aligned} \tag{5.28}$$

We find that the coupling constants are highly constrained by the Jacobi identities.[6] The Jacobi identity for $s_1 = s_2 = s_3 = 2$ requires

$$\left(\kappa_{-2,2,2} - \kappa_{0,0,2}\right) \kappa_{0,2,2} = 0 \qquad 3\kappa_{0,2,2}^2 = 10\kappa_{-2,2,2}\, \kappa_{2,2,2} \tag{5.29}$$

[6] After the first version of this paper was published, [215] showed that in order for the Jacobi identity to be satisfied, only the soft generators inside the wedge $\bar{h} \leq \bar{m} \leq -\bar{h}$ are allowed.

and the one for $s_1 = s_2 = 2, s_3 = 0$ also requires

$$(\kappa_{-2,2,2} - \kappa_{0,0,2})\,\kappa_{0,0,2} = 0\,. \tag{5.30}$$

Adding on the gluons, the Jacobi identity for $s_1 = s_2 = 2, s_3 = 1$ requires

$$(\kappa_{-2,2,2} - \kappa_{-1,1,2})\,\kappa_{-1,1,2} = 0 \qquad \kappa_{-2,2,2}\,\kappa_{1,1,2} = \kappa_{-1,1,2}\,\kappa_{1,1,2} = \kappa_{0,2,2}\,\kappa_{0,1,1}\,, \tag{5.31}$$

the one for $s_1 = 2, s_2 = 1, s_3 = 0$ requires

$$(\kappa_{0,0,2} - \kappa_{-1,1,2})\,\kappa_{0,1,1} = 0\,, \tag{5.32}$$

the one for $s_1 = 2, s_2 = s_3 = 1$ requires

$$\kappa_{-1,1,2}\,\kappa_{1,1,1} = 3\kappa_{1,1,2}\,\kappa_{-1,1,1}\,, \tag{5.33}$$

the one for $s_1 = +2, s_2 = 1, s_3 = -1$ requires

$$(\kappa_{-1,1,2} - \kappa_{-2,2,2})\,\kappa_{-1,1,2} = 0\,, \tag{5.34}$$

the one for $s_1 = s_2 = 1, s_3 = 0$ requires

$$(\kappa_{-1,1,1} - \kappa_{0,0,1})\,\kappa_{0,0,1} = 0 \qquad (\kappa_{-1,1,1} - \kappa_{0,0,1})\,\kappa_{0,1,1} = 0\,, \tag{5.35}$$

and finally, the one for $s_1 = s_2 = s_3 = 1$ requires

$$\kappa_{0,1,1}^2 = 2\kappa_{-1,1,1}\,\kappa_{1,1,1}\,. \tag{5.36}$$

For the final case, the Jacobi identity involving just F^3 correction $\kappa_{1,1,1} \neq 0$ fails to close unless we include a colored scalar soft current *in addition* to the uncolored scalar, with the coefficient the same as that of uncolored scalar.

5.2.3 Relation to $W_{1+\infty}$

The algebra in (5.24) is a deformation of the $w_{1+\infty}$ algebra obtained in [168] in the absence of higher derivative corrections.[7] There, it was conjectured that quantization of the theory would deform $w_{1+\infty}$ to the well studied $W_{1+\infty}$ [198, 199, 200, 201, 202, 203, 204, 216]. This algebra was derived in [200, 204] by starting with a generic deformation with parameter λ of $w_{1+\infty}$

$$\left[V^{q_1}_{\bar{m}_1}, V^{q_2}_{\bar{m}_2}\right] := \sum_{r=0}^{\infty} \lambda^{2r} g^{q_1 q_2}_{2r}(\bar{m}_1, \bar{m}_2) V^{q_1+q_2-2r}_{\bar{m}_1+\bar{m}_2} + \lambda^{2q_1} c_{q_1}(\bar{m}) \delta^{q_1,q_2} \delta_{\bar{m}_1+\bar{m}_2,0}, \tag{5.37}$$

(here $\bar{m} = 0, 1, 2\ldots$ label the modes of V) and demanding that the central charge be non-vanishing, the structure constants satisfy the Jacobi identity while also enforcing the truncation of this algebra

[7] There are more generators in the algebra (5.24) than in $w_{1+\infty}$.

to a finite number of terms. In particular, $g_{2r}^{i\,j}(\bar{m}_1,\bar{m}_2,q_1,q_2)=0$ whenever $q_1+q_2-2r<0$. These conditions completely fix the central charge as well as the structure constants to

$$c_q=\frac{2^{2q-3}q!(q+2)!}{(2q+1)!!(2q+3)!!}c \qquad g_{2r}^{q_1q_2}(\bar{m}_1,\bar{m}_2)=\frac{\phi_{2r}^{q_1q_2}}{2(2r+1)!}N(q_1+2,q_2+2,\bar{m}_1,\bar{m}_2,2r+1)\,, \quad (5.38)$$

with

$$\phi_{2r}^{q_1q_2}=\sum_{a=0}^{r}\prod_{l=1}^{a}\frac{(2l-3)(2l+1)(2r-2l+3)(r-l+1)}{l(2q_1-2l+3)(2q_2-2l+3)(2q_1+2q_2-4r+2l+3)}. \quad (5.39)$$

Note that N in (5.38) is identical to the one appearing in (5.25). Note that when $\lambda=0$ the algebra goes back to $w_{1+\infty}$ algebra. The algebra obtained in this paper is similar to the algebra referred to as case (1) in [216]. The function $\phi_{2r}^{q_1q_2}$ which has non-trivial zeroes enforcing the truncation of the algebra is absent here. Here the truncation occurred naturally due to the absence of massless higher spin fields.[8]

It is important to understand how the algebra in (5.24) is further deformed by loop corrections. It seems plausible that they would lead to a central extension of the algebra. The scalar currents are forced to exist for the algebra to close in the presence of non-minimal couplings. Clarifying their origin, perhaps by linking them to the the spontaneous breaking of some symmetry would also be of interest. Finally, the constraints on the couplings imposed by the Jacobi identity are very restrictive. We leave a systematic study of the implications of these constraints to future work.

5.2.4 Simplest loop corrections and connection with the self-dual sector

One-loop corrections to gluon amplitudes are generically logarithmic and IR divergent. This poses a hurdle to defining a mode expansion of the soft factor. However, one-loop amplitudes involving only positive helicity gluons or only positive helicity gravitons[9] are purely algebraic and their effect on the algebra is easily determined. The one-loop all plus gluon amplitude is [218, 219]

$$A_{n;1}^{[1]}\left(1^+,2^+,\ldots,n^+\right)=-\frac{i}{48\pi^2}\sum_{1\leq i<j<k<l\leq n}\frac{[ij]\langle jk\rangle[kl]\langle li\rangle}{\langle 12\rangle\langle 23\rangle\cdots\langle n1\rangle}. \quad (5.40)$$

A similar expression can be obtained for the corresponding one-loop graviton amplitude [220]. Remarkably, the OPEs and algebra computed from the collinear limits of this amplitude are identical to the ones obtained from tree-level amplitudes. They leave the $w_{1+\infty}$ algebra undeformed.

This one-loop amplitude also happens to be the only non-zero amplitude in the self-dual sector of Yang-Mills theory. More precisely, the only non-zero amplitudes in self-dual Yang-Mills and self-dual gravity are the three-point tree-level amplitudes with two-positive and one-negative helicities, and

[8] During the preparation of the second version of this paper, [217] appeared with more detailed studies on this deformed algebra. [217] related the algebra in (5.24) with the loop algebra of a wedged-symplecton algebra, denoted by $LW_\wedge$. The symplecton algebra is a different deformation of $w_{1+\infty}$ from $W_{1+\infty}$ with exactly $\phi_{2r}^{q_1q_2}=1$ as we have in (5.24).

[9] These amplitudes vanish at tree-level.

the one-loop amplitudes with all positive helicities [221]. Consequently, we can only define collinear limits of positive helicity particles in the self-dual sector and the OPEs obtained from them agree with the OPEs of positive helicity particles obtained from the full theory. It would be interesting to analyze the effect of non-minimal couplings (obeying the self-duality condition) on the self-dual sector. Such a theory will naturally be free of anti-holomorphic poles and provides an alternate, and arguably more natural way to deform the $w_{1+\infty}$ algebra.

5.3 Appendix: Single soft factors

We start by recalling that the Mellin transform of the amplitude is interpreted as a correlation function of gluon primary operators [43, 139]. More specifically, we first decompose the amplitude in trace basis as

$$A_n\left(1,2,3\dots n\right)=\sum_{\sigma\in S_{n-1}}\mathrm{Tr}\left[T^{a_1}T^{a_{\sigma_2}}\dots T^{a_{\sigma_{n-1}}}\right]\mathcal{A}_n\left(1,2,3\dots n\right). \tag{5.41}$$

Amplitudes are usually expressed as a function of spinor helicity variables $p_{\alpha\dot{\alpha}}=\lambda_\alpha\tilde{\lambda}_{\dot{\alpha}}$. We parametrize these as

$$\lambda_i^\alpha=\varepsilon_i\sqrt{\omega_i}\,t_i\begin{pmatrix}1\\ z_i\end{pmatrix}\qquad \tilde{\lambda}_i^{\dot{\alpha}}=\sqrt{\omega_i}\,t_i^{-1}\begin{pmatrix}1\\ \bar{z}_i\end{pmatrix} \tag{5.42}$$

and Mellin transform the color-ordered amplitudes,

$$\tilde{\mathcal{A}}_n\left(1,2,3,\dots n\right):=\int d\omega_1\dots d\omega_n\,\omega_1^{\Delta_1-1}\dots\omega_n^{\Delta_n-1}\mathcal{A}_n\left(1,2,3,\dots n\right). \tag{5.43}$$

Then we have

$$\mathrm{Tr}\left[T^{a_1}T^{a_2}\dots T^{a_n}\right]\tilde{\mathcal{A}}_n\left(1,2,3\dots n\right)=\left\langle\mathcal{O}^{a_1}_{\Delta_1}(z_1,\bar{z}_1)\mathcal{O}^{a_1}_{\Delta_2}(z_2,\bar{z}_2)\dots\mathcal{O}^{a_n}_{\Delta_n}(z_n,\bar{z}_n)\right\rangle. \tag{5.44}$$

When particle 1 becomes soft, we can expand the amplitude in a Laurent series as

$$\mathcal{A}_n\left(1,2,\dots n\right)=\sum_{r=-\infty}^{1}\omega_1^{-r}\mathcal{A}_n^{\prime(r)} \tag{5.45}$$

where the coefficients $\mathcal{A}_n^{\prime(r)}$ are independent of ω_1. The conformally soft limit [188, 189] $\Delta_1\to k$, with $k=1,0,-1,\dots$ gives

$$\begin{aligned}&\lim_{\Delta_1\to k}(\Delta_1-k)\left\langle\mathcal{O}^{a_1}_{\Delta_1}(z_1,\bar{z}_1)\mathcal{O}^{a_2}_{\Delta_2}(z_2,\bar{z}_2)\dots\mathcal{O}^{a_n}_{\Delta_n}(z_n,\bar{z}_n)\right\rangle\\&=\mathrm{Tr}\left[T^{a_1}T^{a_2}\dots T^{a_n}\right]\int\frac{\mathrm{d}\omega_1}{\omega_1}(\Delta_1-k)\,\omega_1^{\Delta_1}\sum_{r=-\infty}^{1}\omega_1^{-r}\int\frac{\mathrm{d}\omega_2}{\omega_2}\dots\frac{\mathrm{d}\omega_n}{\omega_n}\,\omega_2^{\Delta_2}\dots\omega_n^{\Delta_n}\mathcal{A}_n^{\prime(r)}\\&=\mathrm{Tr}\left[T^{a_1}T^{a_2}\dots T^{a_n}\right]\int\frac{\mathrm{d}\omega_2}{\omega_2}\dots\frac{\mathrm{d}\omega_n}{\omega_n}\,\omega_2^{\Delta_2}\dots\omega_n^{\Delta_n}\mathcal{A}_n^{\prime(k)}\end{aligned} \tag{5.46}$$

where from the last but one line to the last line we are using the identity

$$\lim_{\epsilon\to 0} \epsilon\omega^{\epsilon-1} = \delta(\omega). \tag{5.47}$$

We interpret this soft expansion as defining the correlation function of soft currents, i.e.

$$\begin{aligned}
&\lim_{\Delta_1\to k}(\Delta_1-k)\left\langle \mathcal{O}^{a_1,+1}_{\Delta_1}(z_1,\bar z_1)\mathcal{O}^{a_2}_{\Delta_2}(z_2,\bar z_2)\dots\mathcal{O}^{a_n}_{\Delta_n}(z_n,\bar z_n)\right\rangle\\
&\qquad\qquad= \left\langle H^{k,+1,a_1}(z_1,\bar z_1)\,\mathcal{O}^{a_2}_{\Delta_2}(z_2,\bar z_2)\dots\mathcal{O}^{a_n}_{\Delta_n}(z_n,\bar z_n)\right\rangle\\
&\lim_{\Delta_1\to k}(\Delta_1-k)\left\langle \mathcal{O}^{a_1,-1}_{\Delta_1}(z_1,\bar z_1)\mathcal{O}^{a_2}_{\Delta_2}(z_2,\bar z_2)\dots\mathcal{O}^{a_n}_{\Delta_n}(z_n,\bar z_n)\right\rangle\\
&\qquad\qquad= \left\langle H^{k,-1,a_1}(z_1,\bar z_1)\,\mathcal{O}^{a_2}_{\Delta_2}(z_2,\bar z_2)\dots\mathcal{O}^{a_n}_{\Delta_n}(z_n,\bar z_n)\right\rangle
\end{aligned} \tag{5.48}$$

where $k = 1, 0, -1, \cdots$. All the dependence of the correlation function on the variables $z_1, \bar z_1$ is entirely due to the soft current operator. We can thus attempt to guess the structure of the soft current operators $H^{k,+1,a}$ by examining the functional dependence of the amplitudes on $z_1, \bar z_1$ in the soft limit. We first review the case of MHV amplitudes and see the polynomial structure of the currents. We will then move beyond MHV amplitudes and consider the structure of soft expansion of the 6-point NMHV amplitude and non-minimally coupled amplitudes.

5.3.1 MHV amplitudes

We are interested in the structure of amplitudes in the soft limit. The soft limits of negative helicity particles vanish in the MHV sector. Consider the following expression for $\mathcal{A}^{\mathrm{MHV}}_n(1,\dots n)$, obtained from a BCFW expansion using the shifts $\hat\lambda_1 = \lambda_1 + z\lambda_n$, $\hat{\tilde\lambda}_n = \tilde\lambda_n - z\tilde\lambda_1$,

$$\mathcal{A}^{\mathrm{MHV}}_n = \frac{\langle n2\rangle}{\langle n1\rangle\langle 12\rangle}\exp\left(\frac{\langle n1\rangle}{\langle n2\rangle}\tilde\lambda_1\frac{\partial}{\partial\tilde\lambda_2} + \frac{\langle 12\rangle}{\langle n2\rangle}\tilde\lambda_1\frac{\partial}{\partial\tilde\lambda_n}\right)\mathcal{A}^{\mathrm{MHV}}_{n-1}(2,\dots n). \tag{5.49}$$

Expressing this in terms of $\omega_i, z_i, \bar z_i, t_i$ using

$$\frac{\partial}{\partial\tilde\lambda^{\dot 1}_i} = \frac{1}{\sqrt{\omega_i}}\left(\omega_i\frac{\partial}{\partial\omega_i} - \bar z_i\frac{\partial}{\partial\bar z_i} - t_i\frac{\partial}{\partial t_i}\right),\qquad \frac{\partial}{\partial\tilde\lambda^{\dot 2}_i} = \frac{t}{\sqrt{\omega}}\frac{\partial}{\partial\bar z_i},\qquad t_i\frac{\partial}{\partial t_i}\tilde{\mathcal{A}}_{n-1} = -2s_i\tilde{\mathcal{A}}_{n-1}, \tag{5.50}$$

gives

$$\begin{aligned}
\mathcal{A}_n &= -\frac{1}{\omega_1}\frac{z_{n2}}{z_{n1}z_{12}}\exp\Bigg[\frac{z_{n1}}{z_{n2}}\frac{\omega_1}{\omega_2}\left(\omega_2\frac{\partial}{\partial\omega_2} + \bar z_{12}\frac{\partial}{\partial\bar z_2} - t_2\frac{\partial}{\partial t_2}\right)\\
&\qquad\qquad + \frac{z_{12}}{z_{1n}}\frac{\omega_1}{\omega_n}\left(\omega_n\frac{\partial}{\partial\omega_n} + \bar z_{1n}\frac{\partial}{\partial\bar z_n} - t_n\frac{\partial}{\partial t_n}\right)\Bigg]\mathcal{A}_{n-1}(2,\dots n)\\
&= -\frac{1}{\omega_1}\frac{z_{n2}}{z_{n1}z_{12}}\exp\Bigg\{\omega_1\Bigg[\left(\frac{z_{n1}}{z_{n2}}\frac{\partial}{\partial\omega_2} + \frac{z_{12}}{z_{n2}}\frac{\partial}{\partial\omega_n}\right) + \left(\frac{z_{n1}\bar z_{12}}{z_{n2}\omega_2}\frac{\partial}{\partial\bar z_2} + \frac{z_{12}\bar z_{1n}}{z_{n2}\omega_2}\frac{\partial}{\partial\bar z_n}\right)\\
&\qquad\qquad + \left(\frac{z_{n1}}{z_{n2}}\frac{2s_2}{\omega_2} + \frac{z_{12}}{z_{n2}}\frac{2s_n}{\omega_n}\right)\Bigg]\Bigg\}\mathcal{A}_{n-1}.
\end{aligned} \tag{5.51}$$

Using the definition in (5.48) and the relation (5.46), the correlation function of the soft current $H^{k_1,+1,a_1}$ is

$$\begin{aligned}
&\left\langle H^{k_1,+1,a_1}\left(z_1,\bar{z}_1\right)\mathcal{O}^{a_2}_{\Delta_2}(z_2,\bar{z}_2)\dots\mathcal{O}^{a_n}_{\Delta_n}(z_n,\bar{z}_n)\right\rangle \qquad (5.52)\\
=&\,\mathrm{Tr}\left[T^{a_1}T^{a_2}\dots T^{a_n}\right]\int\frac{\mathrm{d}\omega_2}{\omega_2}\dots\frac{\mathrm{d}\omega_n}{\omega_n}\,\omega_2^{\Delta_2}\dots\omega_n^{\Delta_n}\mathcal{A}_n^{\prime(k)}\frac{z_{n2}}{z_{n1}z_{12}}\\
=&\,-\,\mathrm{Tr}\left[T^{a_1}T^{a_2}\dots T^{a_n}\right]\int\frac{\mathrm{d}\omega_2}{\omega_2}\dots\frac{\mathrm{d}\omega_n}{\omega_n}\,\omega_2^{\Delta_2}\dots\omega_n^{\Delta_n}\\
&\times\left(\left[\frac{z_{n1}}{z_{n2}}\frac{\partial}{\partial\omega_2}+\frac{z_{12}}{z_{n2}}\frac{\partial}{\partial\omega_n}\right]+\left[\frac{z_{n1}\bar{z}_{12}}{z_{n2}\omega_2}\frac{\partial}{\partial\bar{z}_2}+\frac{z_{12}\bar{z}_{1n}}{z_{n2}\omega_2}\frac{\partial}{\partial\bar{z}_n}\right]+\left[\frac{z_{n1}}{z_{n2}}\frac{2s_2}{\omega_2}+\frac{z_{12}}{z_{n2}}\frac{2s_n}{\omega_n}\right]\right)^{1-k}\mathcal{A}_{n-1}\\
=&\,\mathrm{Tr}\left[T^{a_1}T^{a_2}\dots T^{a_n}\right]\sum_{\bar{m}=0}^{1-k}H^{k,+1,a_1}_{-\bar{m}-\frac{k-1}{2}}\left(z_1\right)\bar{z}_1^{\bar{m}}\tilde{\mathcal{A}}_{n-1},
\end{aligned}$$

which is a simple polynomial of degree $1-k$ in $\bar{z}_1$. A similar analysis has already been performed for gravity and can be found in [193].

5.3.2 NMHV and beyond

The factorization of the amplitude in (5.49) ceases to be valid beyond the MHV sector[10]. While the leading and subleading soft limits are universal [222, 223] , the remaining terms are specific to the amplitude in question. We examine the series expansion of the NMHV 6-point amplitude and show that the amplitude is no longer a finite polynomial in the $z,\bar{z}$ coordinates of the soft particle. This suggests that the polynomial structure of soft current breaks down in the presence of more than two negative helicity gluons. Consider the following expression for the 6-point NMHV (see for e.g [224])

$$\begin{aligned}
&\mathcal{A}_6\left(1^-,2^-,3^-,4^+,5^+,6^+\right) \qquad (5.53)\\
=&\frac{\langle 3|1+2|6]^3\,\delta^4\left(P\right)}{P^2_{126}\,[21]\,[16]\,\langle 34\rangle\,\langle 45\rangle\,\langle 5|1+6|2]}+\frac{\langle 1|5+6|4]^3\,\delta^4\left(P\right)}{P^2_{156}\,[23]\,[34]\,\langle 56\rangle\,\langle 61\rangle\,\langle 5|1+6|2]},
\end{aligned}$$

where $\delta^4\left(P\right)$ is the momentum conserving delta function. If particle 1 becomes soft, we can expand the amplitude as series around $\omega_1 = 0$. The coefficient of ω_1^k can then be identified with the correlation function of the soft current as seen from (5.46). The structure of these correlation

[10] Recently, an infinite number of soft theorems involving a part of the amplitude have been found in [194, 195]

functions is displayed below.

$$
\begin{aligned}
&\left\langle H^{k,-1,a_1}(z_1,\bar{z}_1)\,\mathcal{O}^{-,a_2}_{\Delta_2}(z_2,\bar{z}_2)\dots\mathcal{O}^{+,a_6}_{\Delta_6}(z_6,\bar{z}_6)\right\rangle\\
&=\begin{cases}
\dfrac{1}{(\bar{z}_1-\bar{z}_2)(\bar{z}_1-\bar{z}_6)}a_{0,0}\,, & k=1\\[2ex]
\dfrac{1}{(\bar{z}_1-\bar{z}_2)(\bar{z}_1-\bar{z}_6)}\displaystyle\sum_{i=0,j=0}^{i=1,j=1}a_{i,j}z_1^i\bar{z}_1^j\,, & k=0\\[2ex]
\dfrac{1}{(\bar{z}_1-\bar{z}_2)(\bar{z}_1-\bar{z}_6)}\dfrac{1}{(z_1-z_6)}\displaystyle\sum_{i=0,j=0}^{i=3,j=2}a_{i,j}z_1^i\bar{z}_1^j\,, & k=-1\\[2ex]
\dfrac{1}{(\bar{z}_1-\bar{z}_2)(\bar{z}_1-\bar{z}_6)}\dfrac{1}{(z_1-z_6)}\displaystyle\sum_{i=0,j=0}^{i=4,j=3}a_{i,j}z_1^i\bar{z}_1^j\,, & k=-2
\end{cases}
\end{aligned}
\tag{5.54}
$$

Repeating the same exercise for particle 2 yields,

$$
\begin{aligned}
&\left\langle \mathcal{O}^{-,a_1}_{\Delta_1}(z_1,\bar{z}_1)H^{k,-1,a_2}(z_2,\bar{z}_2)\dots\mathcal{O}^{+,a_6}_{\Delta_6}(z_6,\bar{z}_6)\right\rangle\\
&=\begin{cases}
\dfrac{1}{(\bar{z}_2-\bar{z}_1)(\bar{z}_2-\bar{z}_3)}a_{0,0}\,, & k=1\\[2ex]
\dfrac{1}{(\bar{z}_2-\bar{z}_1)(\bar{z}_2-\bar{z}_3)}\displaystyle\sum_{i=0,j=0}^{i=1,j=1}a_{i,j}z_1^i\bar{z}_1^j\,, & k=0\\[2ex]
\dfrac{1}{(\bar{z}_2-\bar{z}_1)(\bar{z}_2-\bar{z}_3)}\displaystyle\sum_{i=0,j=0}^{i=2,j=2}a_{i,j}z_1^i\bar{z}_1^j\,, & k=-1\\[2ex]
\dfrac{1}{(\bar{z}_2-\bar{z}_1)(\bar{z}_2-\bar{z}_3)}\displaystyle\sum_{i=0,j=0}^{i=3,j=3}a_{i,j}z_1^i\bar{z}_1^j\,, & k=-2
\end{cases}
\end{aligned}
\tag{5.55}
$$

where we have omitted writing the overall trace factor. The leading and subleading soft factors are universal as expected. However, the soft currents starting from $k=-1$ develop a pole in z as seen in (5.54). This is the pole which gives the collinear limit $1^-||6^+$. The full amplitude is a sum over all orderings and will consequently have poles in both z and $\bar{z}$.

5.3.3 Single soft factors in non-minimally coupled theories

We examine the structure of the soft currents when we include non-minimal couplings. In particular, we consider the example of Yang-Mills theory supplemented by an F^3 interaction. First order corrections to amplitude due to the F^3 operator have been computed in [225]. The 6-point NMHV amplitude, including the first order corrections is

$$
\begin{aligned}
&\mathcal{A}_6\left(1^+,2^+,3^+,4^-,5^-,6^-\right)\\
&=\frac{[3|1+2|6\rangle^3}{P_{126}^2\langle 21\rangle\langle 16\rangle[34][45][5|1+6|2\rangle}+\frac{[1|5+6|4\rangle^3}{P_{156}^2\langle 23\rangle\langle 34\rangle[56][61][5|1+6|2\rangle}\\
&\quad+\frac{\kappa_{F^3}}{2}\frac{\langle 45\rangle^2\langle 56\rangle^2\langle 64\rangle^2}{\langle 12\rangle\langle 23\rangle\langle 34\rangle\langle 45\rangle\langle 56\rangle\langle 61\rangle}+\frac{\kappa_{F^3}}{2}\frac{[12]^2[23]^2[31]^2}{[12][23][34][45][56][61]}.
\end{aligned}
\tag{5.56}
$$

Processing as in the previous sections, we obtain results similar to (5.54, 5.55) with coefficients $a_{i,j}$ receiving first order corrections. It is worth pointing out here that taking the collinear limit $1||2$ here will not produce only the $p=1$ term in the first line of (5.6). The $p=2$ term in the first line would arise only once we include second order corrections. The remaining terms would arise only if we include the contributions from the scalars.

Equations (5.54, 5.55) show that a general Ansatz for the soft current cannot be a finite polynomial in $z, \bar{z}$ (which holds only in the MHV sector as in [197]) and we must have

$$H^{k,s,a} = \sum_{\bar{m}=-\infty}^{-\bar{h}} \sum_{m=-\infty}^{-h} H^{k,s,a}_{m,\bar{m}} \frac{1}{z^{m+h}} \frac{1}{\bar{z}^{\bar{m}+\bar{h}}}. \tag{5.57}$$

For the purposes of this paper, we choose to explicitly write the mode expansion in $\bar{z}$ with the modes being a function of z as

$$H^{k,s,a} = \sum_{\bar{m}=-\infty}^{-\bar{h}} H^{k,s,a}_{\bar{m}}(z) \frac{1}{\bar{z}^{\bar{m}+\bar{h}}}. \tag{5.58}$$

5.4 Appendix: Gluon OPEs from double soft limits

In this section, we derive the soft current OPEs directly from *simultaneous* double soft limits of scattering amplitudes. We are mainly interested in the singular terms in the OPE and these correspond to taking holomorphic and anti-holomorphic collinear limits on the simultaneous double soft limit factor of n-gluon amplitudes. We can expand this amplitude in a basis of color-ordered amplitudes as in equation (5.41). Collinear poles $\frac{1}{z_{12}}$ or $\frac{1}{\bar{z}_{12}}$ can only occur in the color-ordered amplitudes when particles 1 and 2 are adjacent. We will restrict our attention to the color-ordered amplitude with the canonical ordering. A similar result holds for the remaining relevant orderings.

The simultaneous double soft limit of two positive helicity gluons has been derived in [226, 227]. Keeping only the singular term as $z_1 \to z_2$, we have

$$\mathcal{A}_n\left(1^+, 2^+, 3, \dots n\right) \xrightarrow{z_{12}\to 0} \frac{\langle n2\rangle}{\langle n1\rangle\langle 12\rangle} \exp\left(\frac{\langle n1\rangle}{\langle n2\rangle}\tilde{\lambda}_1^{\dot{\alpha}}\partial_{\tilde{\lambda}_2^{\dot{\alpha}}} + \frac{\langle 12\rangle}{\langle n2\rangle}\tilde{\lambda}_1^{\dot{\alpha}}\partial_{\tilde{\lambda}_n^{\dot{\alpha}}}\right)\mathcal{A}_{n-1}\left(2^+, \dots n\right). \tag{5.59}$$

We parametrize the spinors as in (5.42). In the collinear limit,

$$\begin{aligned} &\omega_1 = \tau\omega_p, \quad \omega_2 = (1-\tau)\,\omega_p, \quad z_1 = z_2 = z_p \qquad \bar{z}_p = \bar{z}_2 + \tau\bar{z}_{12}. \\ &\tilde{\lambda}_2 + \frac{\langle n1\rangle}{\langle n2\rangle}\tilde{\lambda}_1 = \sqrt{\frac{\omega_p}{1-\tau}}\begin{pmatrix}1\\ \bar{z}_p\end{pmatrix} = \frac{1}{\sqrt{1-\tau}}\tilde{\lambda}_p \end{aligned} \tag{5.60}$$

which then gives

$$\begin{aligned} \mathcal{A}_n\left(1^+, 2^+, 3, \dots n\right) \xrightarrow{z_{12}\to 0} &\frac{1}{z_{12}}\frac{1}{\tau\,\omega_p}\mathcal{A}_{n-1}\left(\left\{\sqrt{1-\tau}\lambda_p, \frac{1}{\sqrt{1-\tau}}\tilde{\lambda}_p\right\}, \dots \left\{\lambda_n, \tilde{\lambda}_n\right\}\right) \\ =&\frac{1}{z_{12}}\frac{1}{\tau(1-\tau)\,\omega_p}\mathcal{A}_{n-1}\left(\left\{\lambda_p, \tilde{\lambda}_p\right\}, \dots \left\{\lambda_n, \tilde{\lambda}_n\right\}\right). \end{aligned} \tag{5.61}$$

Recalling that particle labelled by p is soft, we can perform a soft expansion of the amplitude to get

$$\mathcal{A}_n\left(1^+,2^+,3,\dots n\right) \xrightarrow{z_{12}\to 0} \frac{1}{z_{12}}\frac{1}{\tau(1-\tau)}\sum_{m=-1}^{\infty}\omega_p^m H^{m,1}\left(z_2,\bar{z}_2+\tau\bar{z}_{12}\right)\mathcal{A}^{(m)}, \tag{5.62}$$

where $\mathcal{A}^{(-1)}=\mathcal{A}^{(0)}=\mathcal{A}_{n-2}\left(3,\dots n\right)$ are universal and the rest are specific to the amplitude. We can get the OPE by performing a Mellin transform. Recall that the celestial amplitude, which is the correlation function of primary gluon operators is

$$\begin{aligned}\tilde{A}_n\left(1^+,2^+,3,\dots n\right) &= \left\langle \mathcal{O}^{+,a_1}_{\Delta_1}(z_1,\bar{z}_1)\mathcal{O}^{+,a_2}_{\Delta_2}(z_2,\bar{z}_2)\dots\mathcal{O}^{s_n,a_n}_{\Delta_n}(z_n,\bar{z}_n)\right\rangle \\ &= \int \mathrm{d}\omega_1\dots\mathrm{d}\omega_n\,\omega_1^{\Delta_1-1}\dots\omega_n^{\Delta_n-1}\mathcal{A}_n\left(1^+,2^+,3,\dots n\right).\end{aligned} \tag{5.63}$$

The double soft limit is

$$\lim_{\epsilon\to 0}\epsilon^2\left\langle \mathcal{O}^{+,a_1}_{k+\epsilon}(z_1,\bar{z}_1)\mathcal{O}^{+,a_2}_{l+\epsilon}(z_2,\bar{z}_2)\dots\mathcal{O}^{s_n,a_n}_{\Delta_n}(z_n,\bar{z}_n)\right\rangle \qquad k,l=1,0,-1,\dots \tag{5.64}$$

Plugging in the double soft expansion from (5.62) and using the identity (5.47) we get

$$H^{k_1,+1,a_1}(z_1,\bar{z}_1)H^{k_2,+1,a_2}(z_2,\bar{z}_2)\sim -\frac{if^{a_1a_2b}}{z_{12}}\sum_{n=0}^{\infty}\begin{pmatrix}2-k_1-k_2-n\\ 1-k_2\end{pmatrix}\frac{\bar{z}_{12}^n}{n!}\bar{\partial}^n H^{k_1+k_2-1,+1,b}. \tag{5.65}$$

The simultaneous double soft limit in the mixed helicity case was also derived in [226, 227]. The singular terms in the collinear limit are given by

$$\begin{aligned}\mathcal{A}(1^+,2^-,3,...,n) &\xrightarrow{1\to 2}\frac{\langle n2\rangle}{\langle n1\rangle\langle 12\rangle}\exp\left(\frac{\langle n1\rangle}{\langle n2\rangle}\tilde{\lambda}_1^{\dot{\alpha}}\partial_{\tilde{\lambda}_2^{\dot{\alpha}}}\right)\mathcal{A}(2^-,...,n) \\ &+\frac{[13]}{[12]\,[23]}\exp\left(\frac{[23]}{[13]}\lambda_2^{\alpha}\partial_{\lambda_1^{\alpha}}\right)\mathcal{A}(1^+,...,n).\end{aligned} \tag{5.66}$$

We treat the holomorphic and anti-holomorphic collinear limits separately. In the $z_{12}\to 0$ case we use (5.60) and find

$$\begin{aligned}\mathcal{A}_n\left(1^+,2^-,3,\dots n\right) &\xrightarrow{z_{12}\to 0}\frac{1}{z_{12}}\frac{1}{\tau\,\omega_p}\mathcal{A}_{n-1}\left(\left\{\sqrt{1-\tau}\lambda_p,\frac{1}{\sqrt{1-\tau}}\tilde{\lambda}_p\right\},\dots\left\{\lambda_n,\tilde{\lambda}_n\right\}\right) \\ &=\frac{1}{z_{12}}\frac{1-\tau}{\tau\,\omega_p}\mathcal{A}_{n-1}\left(\left\{\lambda_p,\tilde{\lambda}_p\right\},\dots\left\{\lambda_n,\tilde{\lambda}_n\right\}\right).\end{aligned} \tag{5.67}$$

The procedure for performing the Mellin transform is the same as in the ++ case, we just need to account for the difference in powers of $1-\tau$ and that the soft particle p is now of negative helicity. We then find

$$\begin{aligned}&\left\langle H^{k_1,+1,a_1}(z_1,\bar{z}_1)H^{k_2,-1,a_2}(z_2,\bar{z}_2)\cdots\mathcal{O}^{s_n,a_n}_{\Delta_n}(z_n,\bar{z}_n)\right\rangle\xrightarrow{z_{12}\to 0} \\ &-if^{a_1a_2b}\frac{1}{z_{12}}\sum_{n=0}^{\infty}\begin{pmatrix}-k_1-k_2-n\\ -1-k_2\end{pmatrix}\frac{\bar{z}_{12}^n}{n!}\bar{\partial}^n H^{k_1+k_2-1,-1,b}(z_2,\bar{z}_2)\tilde{\mathcal{A}}^{(k_1+k_2-1)}.\end{aligned} \tag{5.68}$$

To take the anti-holomorphic collinear limit we take the following parametrization

$$\begin{aligned}&\omega_1=\tau\omega_p,\quad \omega_2=(1-\tau)\omega_p,\quad \bar{z}_1=\bar{z}_2=\bar{z}_p,\quad z_p=z_2+\tau z_{12}, \\ &\lambda_1+\frac{[23]}{[13]}\lambda_2=\sqrt{\frac{\omega_p}{\tau}}\begin{pmatrix}1\\ z_p\end{pmatrix}=\frac{1}{\sqrt{\tau}}\lambda_p,\end{aligned} \tag{5.69}$$

which gives

$$\begin{aligned}\mathcal{A}_n(1^+,2^-,3,...,n) &\xrightarrow{\bar{z}_{12}\to 0} \frac{1}{\bar{z}_{12}}\frac{1}{(1-\tau)\,\omega_p}\mathcal{A}_{n-1}\left(\left\{\frac{1}{\sqrt{\tau}}\lambda_p,\sqrt{\tau}\tilde{\lambda}_p\right\},...,\{\lambda_n,\tilde{\lambda}_n\}\right)\\ &= \frac{1}{\bar{z}_{12}}\frac{\tau}{(1-\tau)\omega_p}\mathcal{A}_{n-1}\left(\{\lambda_p,\tilde{\lambda}_p\},...,\{\lambda_n,\tilde{\lambda}_n\}\right).\end{aligned} \tag{5.70}$$

Taking the Mellin transform we find

$$\begin{aligned}&\left\langle H^{k,+1,a_1}(z_1,\bar{z}_1)H^{l,-1,a_2}(z_2,\bar{z}_2)\cdots\mathcal{O}^{s_n,a_n}_{\Delta_n}(z_n,\bar{z}_n)\right\rangle \xrightarrow{\bar{z}_{12}\to 0}\\ &\quad -if^{a_1a_2b}\frac{1}{\bar{z}_{12}}\sum_{n=0}^{\infty}\begin{pmatrix}-k-l-n\\ 1-l\end{pmatrix}\frac{z_{12}^n}{n!}\partial^n H^{k+l-1,+1,b}(z_2,\bar{z}_2)\tilde{\mathcal{A}}^{(k+l-1)}.\end{aligned} \tag{5.71}$$

The full OPE is then

$$\begin{aligned}H^{k,+1,a_1}(z_1,\bar{z}_1)H^{l,-1,a_2}(z_2,\bar{z}_2) \sim &-\frac{if^{a_1a_2b}}{z_{12}}\sum_{n=0}^{\infty}\begin{pmatrix}-k-l-n\\ -1-l\end{pmatrix}\frac{\bar{z}_{12}^n}{n!}\bar{\partial}^n H^{k+l-1,-1,b}\\ &-\frac{if^{a_1a_2b}}{\bar{z}_{12}}\sum_{n=0}^{\infty}\begin{pmatrix}-k-l-n\\ 1-l\end{pmatrix}\frac{z_{12}^n}{n!}\partial^n H^{k+l-1,+1,b}.\end{aligned} \tag{5.72}$$

5.5 Appendix: Examples for deriving constraints of coupling constants

In this appendix we show how we derive the constraint

$$3\kappa_{0,2,2}^2 = 10\kappa_{-2,2,2}\,\kappa_{2,2,2} \tag{5.73}$$

in (5.29). The other constraints can be derived similarly. Consider the double commutator (5.28). Take $s_1 = s_2 = s_3 = 2$. We then have:

$$\begin{aligned}&\left[\left[W^{q_1,2}_{\bar{m}_1},W^{q_2,2}_{\bar{m}_2}\right],W^{q_3,2}_{\bar{m}_3}\right]+\text{cyclic} \qquad (5.74)\\ &=\sum_{l=2,4,6}\sum_{\substack{r=0\\ r\text{ odd}}}^{l}\frac{\kappa_{2,2,l-r-3}}{2}\frac{\kappa_{3-l+r,2,l-4}}{2}\\ &\qquad\times N\left(q_1,q_2,\bar{m}_1,\bar{m}_2,l-r\right)N\left(q_1+q_2-l-1+r,q_3,\bar{m}_1+\bar{m}_2,\bar{m}_3,r\right)\\ &\qquad\times W^{q_1+q_2+q_3-l-2,4-l}_{\bar{m}_1+\bar{m}_2+\bar{m}_3}\qquad+\text{cyclic}.\end{aligned}$$

Here we are interested in the coefficients of the generator $W^{q_1+q_2+q_3-8,-2}$ on the RHS. These terms correspond to $l=6$, therefore r can only be 1,3,5 in the summation. In the end the total coefficient is

$$\sum_{r=1,3,5} \frac{\kappa_{2,2,3-r}}{2}\frac{\kappa_{r-3,2,2}}{2} N(q_1,q_2,\bar m_1,\bar m_2,6-r)N(q_1+q_2-7+r,q_3,\bar m_1+\bar m_2,\bar m_3,r) + \text{cyclic}$$

$$\begin{aligned}= \frac{\kappa_{-2,2,2}\kappa_{2,2,2}}{4}\Big(& N(q_1,q_2,\bar m_1,\bar m_2,1)N(q_1+q_2-2,\bar m_1+\bar m_2,\bar m_3,5) \\ &+ N(q_1,q_2,\bar m_1,\bar m_2,5)N(q_1+q_2-6,q_3,\bar m_1+\bar m_2,\bar m_3,1)\Big) \\ + \frac{\kappa_{0,2,2}^2}{4}& N(q_1,q_2,\bar m_1,\bar m_2,3)\,N(q_1+q_2-4,q_3,\bar m_1+\bar m_2,\bar m_3,3) \qquad + \text{cyclic}\,.\end{aligned} \tag{5.75}$$

The N polynomials satisfy the following identity:

$$\begin{aligned}&\frac{1}{5!}N(q_1,q_2,\bar m_1,\bar m_2,1)\,N(q_1+q_2-2,\bar m_1+\bar m_2,\bar m_3,5) \\ +&\frac{1}{5!}N(q_1,q_2,\bar m_1,\bar m_2,5)\,N(q_1+q_2-6,q_3,\bar m_1+\bar m_2,\bar m_3,1) \\ +&\frac{1}{3!^2}N(q_1,q_2,\bar m_1,\bar m_2,3)\,N(q_1+q_2-4,q_3,\bar m_1+\bar m_2,\bar m_3,3)\ + \text{cyclic}\ =\ 0\,.\end{aligned} \tag{5.76}$$

Therefore (5.75) becomes

$$\begin{aligned}\left(\frac{\kappa_{-2,2,2}\kappa_{2,2,2}}{4} - 3!^2\,\frac{\kappa_{0,2,2}^2}{4\times 5!}\right)\Big(& N(q_1,q_2,\bar m_1,\bar m_2,1)N(q_1+q_2-2,\bar m_1+\bar m_2,\bar m_3,5) \\ &+ N(q_1,q_2,\bar m_1,\bar m_2,5)N(q_1+q_2-6,q_3,\bar m_1+\bar m_2,\bar m_3,1)\Big) \\ &+ \text{cyclic} = 0\,.\end{aligned} \tag{5.77}$$

For arbitrary $q_1, q_2, \bar m_1, \bar m_2$, the quadratics of N polynomials shown above are all independent, therefore to make (5.75) vanishing, one get

$$\kappa_{-2,2,2}\kappa_{2,2,2} = \frac{3!^2}{5!}\kappa_{0,2,2}^2 = \frac{3\kappa_{0,2,2}^2}{10} \tag{5.78}$$

which is exactly the constraint (5.73).

5.6 Appendix: Alternate definition of commutators

$$H^{k,s}(z,\bar z) = \sum_{\bar m=-\infty}^{-\bar h}\sum_{m=-\infty}^{-h}\frac{1}{\bar z^{\bar m+\bar h} z^{m+h}} H^{k,s}_{m,\bar m} \tag{5.79}$$

$$H^{k,s}_{m,\bar m} = \oint \frac{\mathrm{d}z}{2\pi i}\oint\frac{\mathrm{d}\bar z}{2\pi i} z^{m+h-1}\bar z^{\bar m+\bar h-1} H^{k,s}(z,\bar z)\,. \tag{5.80}$$

Having defined this mode expansion, we can define the commutator

$$\left[H^{k_1,s_1}_{m_1,\bar m_1}, H^{k_2,s_2}_{m_2,\bar m_2}\right] := \oint_{z_1>z_2} \frac{dz_1}{2\pi i} \oint_{z_2=0} \frac{dz_2}{2\pi i} \oint_{\bar z_1>\bar z_2} \frac{d\bar z_1}{2\pi i} \oint_{\bar z_2=0} \frac{d\bar z_2}{2\pi i} H^{k_1,s_1}\left(z_1,\bar z_1\right) H^{k_2,s_2}\left(z_2,\bar z_2\right) \tag{5.81}$$
$$- \oint_{z_1=0} \frac{dz_1}{2\pi i} \oint_{z_2>z_1} \frac{dz_2}{2\pi i} \oint_{\bar z_1=0} \frac{d\bar z_1}{2\pi i} \oint_{\bar z_2>\bar z_1} \frac{d\bar z_2}{2\pi i} H^{k_2,s_2}\left(z_2,\bar z_2\right) H^{k_1,s_1}\left(z_1,\bar z_1\right)$$
$$= \oint_{z_1=z_2} \frac{dz_1}{2\pi i} \oint_{z_2=0} \frac{dz_2}{2\pi i} \oint_{\bar z_1>\bar z_2} \frac{d\bar z_1}{2\pi i} \oint_{\bar z_2=0} \frac{d\bar z_2}{2\pi i} H^{k_1,s_1}\left(z_1,\bar z_1\right) H^{k_2,s_2}\left(z_2,\bar z_2\right)$$
$$+ \oint_{z_1=0} \frac{dz_1}{2\pi i} \oint_{z_2>z_1} \frac{dz_2}{2\pi i} \oint_{\bar z_1=\bar z_2} \frac{d\bar z_1}{2\pi i} \oint_{\bar z_2=0} \frac{d\bar z_2}{2\pi i} H^{k_2,s_2}\left(z_2,\bar z_2\right) H^{k_1,s_1}\left(z_1,\bar z_1\right)$$

$$\begin{aligned}
&\left[H^{k_1,s_1}_{m_1,\bar m_1},\, H^{k_2,s_2}_{m_2,\bar m_2}\right] \\
&= -\sum_p \frac{\kappa_{s_1,s_2,-s_I}}{2} \sum_{x=0}^{p} \frac{(\bar m_1+\bar m_2-\bar h_1-\bar h_2-p)!(-\bar m_1-\bar m_2-\bar h_1-\bar h_2-p)!}{(\bar m_1-\bar h_1-p+x)!(-\bar m_1-\bar h_1-x)!(\bar m_2-\bar h_2-x)!(-\bar m_2-\bar h_2-p+x)!} \\
&\qquad \times (-1)^{p-x} \frac{p!}{x!(p-x)!} H^{k_1+k_2+p-1,s_1+s_2-p-1}_{m_1+m_2,\bar m_2+\bar m_2} \\
&\quad -\sum_p \frac{\bar\kappa_{s_1,s_2,-s_I}}{2} \sum_{x=0}^{p} \frac{(m_1+m_2-h_1-h_2-p)!(-m_1-m_2-h_1-h_2-p)!}{(m_1-h_1-p+x)!(-m_1-h_1-x)!(m_2-h_2-x)!(-m_2-h_2-p+x)!} \\
&\qquad \times (-1)^{p-x} \frac{p!}{x!(p-x)!} H^{k_1+k_2+p-1,s_1+s_2+p+1}_{m_1+m_2,\bar m_2+\bar m_2}\,.
\end{aligned} \tag{5.82}$$

The Jacobi identity for commutators involving both positive and negative helicity currents is violated.

Chapter 6

On Effective Field Theories with Celestial Dual

This chapter is based on [45].

The central tenet of celestial holography [43, 182, 139] is that a scattering amplitude of n massless particles, with momenta $\{p_i\}$ and helicities $\{s_i\}$, when recast in a basis of boost eigenstates, can be interpreted as a correlation function of n operators with conformal weights $(h_i, \bar{h}_i)$ in a two-dimensional celestial conformal field theory (CCFT). The four-dimensional helicity s_i of particle i is the same as the two-dimensional spin $s_i = h_i - \bar{h}_i$, and we use $\Delta_i = h_i + \bar{h}_i$.

This dictionary implies that the OPE of two operators in CCFT is determined by the collinear limit of the corresponding scattering amplitudes [144, 166, 196]. Specifically, the OPE is given by

$$\mathcal{O}_{h_1,\bar{h}_1}(z_1,\bar{z}_1)\mathcal{O}_{h_2,\bar{h}_2}(z_2,\bar{z}_2) \sim \frac{1}{z_{12}} \sum_p \sum_{m=0}^{\infty} C_p^{(m)}\left(\bar{h}_1,\bar{h}_2\right) \bar{z}_{12}^{p+m}\, \bar{\partial}^m \mathcal{O}_{h_1+h_2-1,\bar{h}_1+\bar{h}_2+p}(z_2,\bar{z}_2) \tag{6.1}$$

where $z_{ij} = z_i - z_j$ and the OPE coefficient $C_p^{(m)}\left(\bar{h}_1,\bar{h}_2\right)$ corresponding to the contribution of an operator with weights $(h_1+h_2-1, \bar{h}_1+\bar{h}_2+p+m)$ is given by [144, 166, 196]

$$C_p^{(m)}(\bar{h}_1,\bar{h}_2) = -\frac{1}{2}\kappa_{s_1,s_2,-s_I}\frac{1}{m!}B(2\bar{h}_1+p+m, 2\bar{h}_2+p), \tag{6.2}$$

where $B(a,b)$ is the Euler beta function and $\kappa_{s_1,s_2,-s_I}$ is the coupling constant appearing in the bulk three-point scattering amplitude of particles with helicities s_1, s_2 and $-s_I$, with $s_I = s_1+s_2-p-1$. Thus there is a direct link between the bulk three-point couplings and the celestial OPE. Restricting to tree-level and excluding massless higher spins leaves a finite roster of bulk three-point amplitudes which could potentially contribute to the sum in (6.1). These have been tabulated in [166].

It was observed in [170] that the OPE of conformally soft graviton operators (those with $\Delta_i = 2, 1, 0, -1, -2, \dots$), in the absence of higher derivative interactions in the bulk, forms a symmetry algebra. This algebra was identified as the Kac Moody algebra of the wedge subalgebra of $w_{1+\infty}$ in [168]. The inclusion of higher derivative interactions in the bulk deforms the algebra as demonstrated in [44]. In particular, note that for a given value of p, only the soft currents with $\Delta \geq p-1$

are modified. This implies that there is short list of operators that can modify the subleading and subsubleading soft currents. This is consistent with the results of [228, 229, 209]. In [44] it was also shown that the algebra of soft modes violates the Jacobi identity unless the bulk couplings satisfy certain particular constraints (reviewed in Section 6.1 below). In particular, this implies that the OPE of the soft modes is not associative for arbitrary couplings. It is natural to wonder about the implications of celestial OPE associativity on bulk scattering amplitudes. The purpose of this paper is to answer this question and to investigate the properties of amplitudes in theories which have an associative celestial OPE at tree level.

The paper is organized as follows. In Section 6.1 we briefly review the constraints obtained by imposing the Jacobi identity on the algebra of soft modes [44]. We then rephrase the question of tree-level associativity directly at the level of bulk scattering amplitudes in Section 6.2 and show that they yield the same constraints on the bulk couplings. In Section 6.3 we demonstrate that these constraints lead to the vanishing of certain four-point amplitudes and we work out the consequences on amplitudes of higher multiplicity. We close with a discussion of various open questions.

6.1 Review of the coupling constants constraints

We begin by listing all relevant three-point amplitudes and briefly reviewing the constraints among their couplings found in [44]. The most generic scenario involves a graviton, gluons and scalars. However, there are subsets of these particles which yield an associative OPE.

The first subset is the graviton-scalar sector, where we consider the usual Einstein-Hilbert term with coupling proportional to $\kappa_{-2,2,2}$, an R^3 interaction proportional to $\kappa_{2,2,2}$, an $R^2\phi$ interaction proportional to $\kappa_{0,2,2}$ and an $R\phi^2$ interaction proportional to $\kappa_{0,0,2}$. To be more precise, we specify this sector by the anti-holomorphic[1] three-point amplitudes

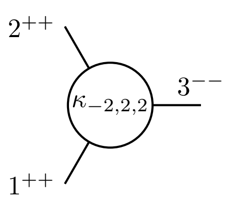

$$= \kappa_{-2,2,2}\frac{[12]^6}{[23]^2[13]^2}$$

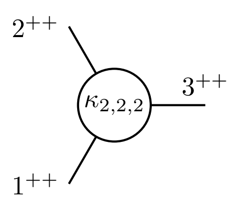

$$= \kappa_{2,2,2}[12]^2[23]^2[13]^2 \tag{6.3}$$

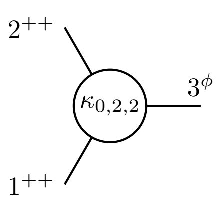

$$= \kappa_{0,2,2}[12]^4$$

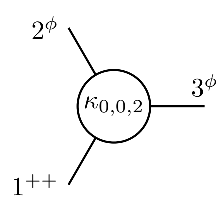

$$= \kappa_{0,0,2}\frac{[12]^2[13]^2}{[23]^2}$$

together with their holomorphic parity conjugates. Note that in this paper we don't equate the coupling constants of the parity conjugate amplitudes with those of the original amplitude. Namely we regard $\kappa_{s_1,s_2,s_3} \neq \kappa_{-s_1,-s_2,-s_3}$ in general. The OPE of conformally soft operators satisfies the

[1] We call $\mathcal{A}(1^{s_1}, 2^{s_2}, 3^{s_3})$ anti-holomorphic if $s_1 + s_2 + s_3 > 0$ and holomorphic if $s_1 + s_2 + s_3 < 0$; see (6.43).

Jacobi identity only if the couplings are related by

$$(\kappa_{-2,2,2} - \kappa_{0,0,2})\,\kappa_{0,2,2} = 0\,, \qquad (\kappa_{-2,2,2} - \kappa_{0,0,2})\,\kappa_{0,0,2} = 0\,, \tag{6.4}$$

$$3\kappa_{0,2,2}^2 = 10\,\kappa_{-2,2,2}\,\kappa_{2,2,2}\,. \tag{6.5}$$

In particular, note that the presence of a scalar is required if the R^3 interaction has a non-zero coefficient. The equivalence principle requires $\kappa_{-2,2,2} = \kappa_{0,0,2}$, which automatically ensures (6.4), but (6.5) is more nontrivial.

The second subset is the gluon-scalar sector defined by the three-point amplitudes

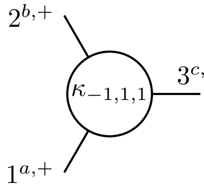

$$= if^{abc}\kappa_{-1,1,1}\frac{[12]^3}{[23][31]}$$

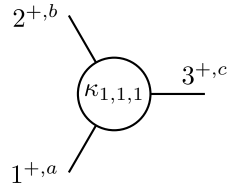

$$= if^{abc}\kappa_{1,1,1}[12][23][31]$$

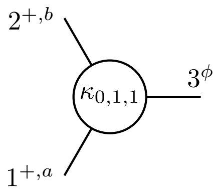

$$= \sqrt{\frac{2}{N_c}}\delta^{ab}\kappa_{0,1,1}[12]^2$$

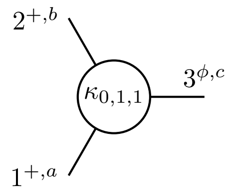

$$= d^{abc}\kappa_{0,1,1}[12]^2 \tag{6.6}$$

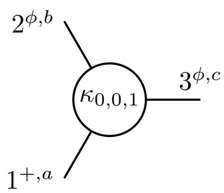

$$= if^{abc}\kappa_{0,0,1}\frac{[12][31]}{[23]}$$

and their parity conjugates. Here f^{abc} are the structure constants of the gauge group and $d^{abc} = 2\,\mathrm{Tr}[\{T^a, T^b\}T^c]$. Note that we have introduced two separate scalar fields—one adjoint and one singlet. In a general theory, the $\kappa_{0,1,1}$ coupling of the former could be considered independent of that of the latter. However, imposing the Jacobi identity on the OPE of soft modes requires the precise relative normalization already indicated in the two figures in the middle row above, and additionally requires

$$(\kappa_{-1,1,1} - \kappa_{0,0,1})\,\kappa_{0,0,1} = 0\,, \qquad (\kappa_{-1,1,1} - \kappa_{0,0,1})\,\kappa_{0,1,1} = 0\,, \tag{6.7}$$

$$\kappa_{0,1,1}^2 = 2\kappa_{-1,1,1}\,\kappa_{1,1,1}\,. \tag{6.8}$$

The constraints (6.7) are automatically satisfied when we impose $\kappa_{-1,1,1} = \kappa_{0,0,1}$ as required by gauge invariance (at the level of a Lagrangian this identity follows when the kinetic term is written as $(D\phi)^2$ where D is the gauge covariant derivative). However, the constraint (6.8) is novel.

Finally, we can couple the two sectors by introducing additional three-point amplitudes

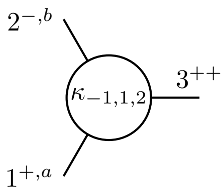

$$= \sqrt{\frac{2}{N_c}}\delta^{ab}\kappa_{-1,1,2}\frac{[13]^4}{[12]^2}$$

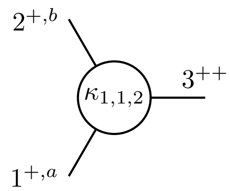

$$= \sqrt{\frac{2}{N_c}}\delta^{ab}\kappa_{1,1,2}[13]^2[23]^2 \tag{6.9}$$

and their parity conjugates. In addition to the constraints in (6.4), (6.5), (6.7), and (6.8), the celestial Jacobi identity also requires

$$(\kappa_{-2,2,2} - \kappa_{-1,1,2})\,\kappa_{-1,1,2} = 0\,, \qquad (\kappa_{-2,2,2} - \kappa_{-1,1,2})\,\kappa_{1,1,2} = 0\,, \tag{6.10}$$

$$\kappa_{-1,1,2}\,\kappa_{1,1,2} = \kappa_{0,2,2}\,\kappa_{0,1,1}\,, \qquad (\kappa_{0,0,2} - \kappa_{-1,1,2})\,\kappa_{0,1,1} = 0\,, \tag{6.11}$$

$$\kappa_{-1,1,2}\,\kappa_{1,1,1} = 3\kappa_{1,1,2}\,\kappa_{-1,1,1}\,. \tag{6.12}$$

Note that all of the constraints presented above are consistent with dimensional analysis since κ_{s_1,s_2,s_3} has mass dimension $1 - |s_1 + s_2 + s_3|$.

6.2 Tree-level OPE associativity from amplitudes

The standard way to check OPE associativity is to introduce a mode expansion of the participating operators and then compute their commutators using the OPE. If the OPE is associative, the commutator of these modes must satisfy the Jacobi identity. In the context of CCFT, the bulk interpretation of this procedure is opaque. Our goal in this paper is not just to check OPE associativity, but also to interpret the condition directly at the level of momentum space scattering amplitudes. To derive a more direct check of OPE associativity consider the following identity involving contour integrals[2]:

$$\begin{aligned}&\oint\limits_{|z_{13}|=2} \mathrm{d}z_1 \oint\limits_{|z_{23}|=1} \mathrm{d}z_2\, \langle \mathcal{O}_{\Delta_1,s_1}(z_1,\bar{z}_1)\dots\mathcal{O}_{\Delta_n,s_n}(z_n,\bar{z}_n)\rangle = \\ &\oint\limits_{|z_{23}|=2} \mathrm{d}z_2 \oint\limits_{|z_{13}|=1} \mathrm{d}z_1\, \langle \mathcal{O}_{\Delta_1,s_1}(z_1,\bar{z}_1)\dots\mathcal{O}_{\Delta_n,s_n}(z_n,\bar{z}_n)\rangle + \oint\limits_{|z_{23}|=2} \mathrm{d}z_2 \oint\limits_{|z_{12}|=1} \mathrm{d}z_1\, \langle \mathcal{O}_{\Delta_1,s_1}(z_1,\bar{z}_1)\dots\mathcal{O}_{\Delta_n,s_n}(z_n,\bar{z}_n)\rangle\,.\end{aligned} \tag{6.13}$$

This is valid as long as all of the (Δ_i, s_i) are such that the correlation functions are single-valued functions of z_i. Practically, we evaluate these integrals using the OPE. Thus the identity serves as a check on the OPE associativity. We can write this in a condensed form as

$$\left[\operatorname*{Res}_{2\to3}\operatorname*{Res}_{1\to2} - \operatorname*{Res}_{1\to3}\operatorname*{Res}_{2\to3} + \operatorname*{Res}_{2\to3}\operatorname*{Res}_{1\to3}\right] \langle \mathcal{O}_{\Delta_1,s_1}(z_1,\bar{z}_1)\dots\mathcal{O}_{\Delta_n,s_n}(z_n,\bar{z}_n)\rangle = 0\,. \tag{6.14}$$

[2]A similar analysis of the associativity of the one-loop OPE in self-dual Yang-Mills was performed in [230].

The correlator in (6.14) is nothing but the Mellin transform of the amplitude. If we parameterize the momenta of outgoing massless external particles as

$$p_i^\mu \sim \lambda_i \tilde{\lambda}_i \qquad \text{with} \qquad \lambda_i = \sqrt{2\omega_i}\begin{pmatrix}1\\ z_i\end{pmatrix} \qquad \text{and} \qquad \tilde{\lambda}_i = \sqrt{2\omega_i}\begin{pmatrix}1\\ \bar{z}_i\end{pmatrix}, \tag{6.15}$$

the transformation from momentum to boost eigenstates is implemented via the Mellin transform

$$\langle \mathcal{O}_{\Delta_1,s_1}(z_1,\bar{z}_1)\ldots\mathcal{O}_{\Delta_n,s_n}(z_n,\bar{z}_n)\rangle = \int \prod_{i=1}^{n} \frac{\mathrm{d}\omega_i}{\omega_i^{1-\Delta_i}} \mathcal{A}_n\left(\left\{\lambda_1,\tilde{\lambda}_1\right\}^{s_1},\left\{\lambda_2,\tilde{\lambda}_2\right\}^{s_2},\ldots,\left\{\lambda_n,\tilde{\lambda}_n\right\}^{s_n}\right). \tag{6.16}$$

Demanding

$$\left[\operatorname*{Res}_{2\to3}\operatorname*{Res}_{1\to2} - \operatorname*{Res}_{1\to3}\operatorname*{Res}_{2\to3} + \operatorname*{Res}_{2\to3}\operatorname*{Res}_{1\to3}\right] \mathcal{A}_n\left(\left\{\lambda_1,\tilde{\lambda}_1\right\}^{s_1},\left\{\lambda_2,\tilde{\lambda}_2\right\}^{s_2},\ldots,\left\{\lambda_n,\tilde{\lambda}_n\right\}^{s_n}\right) = 0 \tag{6.17}$$

ensures that the same is true of the correlator. The upshot is that we can check associativity of the celestial OPE by evaluating double residues directly on the amplitude rather than dealing with the celestial correlators.

The first step is to isolate the collinear limits. Bearing in mind that we will later be interested in examining the effects of (6.17) on amplitudes with various higher derivative corrections, we will analyze the collinear limit using the all-line shift recursion relations [12, 11], reviewed briefly in Appendix 6.5. We begin by using (6.42) to isolate the collinear channel as the momentum of particle one approaches that of particle two

$$\begin{aligned}&\mathcal{A}_n\left(\left\{\lambda_1,\tilde{\lambda}_1\right\}^{s_1},\left\{\lambda_2,\tilde{\lambda}_2\right\}^{s_2},\ldots,\left\{\lambda_n,\tilde{\lambda}_n\right\}^{s_n}\right)\\ =&\sum_{s_I}\hat{\mathcal{A}}_3\left(\left\{\hat{\lambda}_1,\tilde{\lambda}_1\right\}^{s_1},\left\{\hat{\lambda}_2,\tilde{\lambda}_2\right\}^{s_2},\left\{\hat{\lambda}_I,\hat{\tilde{\lambda}}_I\right\}^{-s_I}\right)\frac{1}{\langle 12\rangle\,[12]}\hat{\mathcal{A}}_{n-1}\left(\left\{\hat{\lambda}_I,\hat{\tilde{\lambda}}_I\right\}^{s_I},\ldots,\left\{\hat{\lambda}_n,\tilde{\lambda}_n\right\}^{s_n}\right)\\ &\qquad + \{\text{other channels}\}\,.\end{aligned} \tag{6.18}$$

In terms of these, the residue is

$$\operatorname*{Res}_{z_1\to z_2}\mathcal{A}_n = \sum_{s_I}\mathcal{A}_3\left(\tilde{\lambda}_1^{s_1},\tilde{\lambda}_2^{s_2},\tilde{\lambda}_I^{-s_I}\right)\frac{1}{2\sqrt{\omega_1\omega_2}\,[12]}\mathcal{A}_{n-1}\left(\left\{\lambda_I,\tilde{\lambda}_I\right\}^{s_I},\ldots,\left\{\lambda_n,\tilde{\lambda}_n\right\}^{s_n}\right) \tag{6.19}$$

where, on the right-hand side, in the limit $z_{12}=0$ we have

$$\lambda_1 = \sqrt{\frac{\omega_1}{\omega_1+\omega_2}}\lambda_I\,, \qquad \lambda_2 = \sqrt{\frac{\omega_2}{\omega_1+\omega_2}}\lambda_I\,, \qquad \tilde{\lambda}_I = \sqrt{\frac{\omega_1}{\omega_1+\omega_2}}\tilde{\lambda}_1 + \sqrt{\frac{\omega_2}{\omega_1+\omega_2}}\tilde{\lambda}_2\,. \tag{6.20}$$

In arriving at (6.19), we have made use of the fact that only anti-holomorphic three-point amplitudes contribute to the collinear limit (see Appendix 6.5) and that the terms from other channels drop out in this limit. Furthermore, the subamplitude $\mathcal{A}_{n-1}$ now depends only on the unshifted momenta as the deformation parameter α vanishes in the collinear limit (see (6.39)). Applying this formula a second time, to compute the double residue, therefore translates (6.17) into

$$\begin{aligned}\sum_{s_{I_1}}\Bigg[&\frac{1}{\bar{z}_{12}\bar{z}_{I_1 3}}\frac{1}{\omega_1+\omega_2}\mathcal{A}_3\left(\tilde{\lambda}_1^{s_1},\tilde{\lambda}_2^{s_2},\tilde{\lambda}_{I_1}^{-s_{I_1}}\right)\mathcal{A}_3\left(\tilde{\lambda}_{I_1}^{s_{I_1}},\tilde{\lambda}_3^{s_3},\tilde{\lambda}_{I_2}^{-s_{I_2}}\right)\\ &+\frac{1}{\bar{z}_{23}\bar{z}_{I_1 1}}\frac{1}{\omega_2+\omega_3}\mathcal{A}_3\left(\tilde{\lambda}_2^{s_2},\tilde{\lambda}_3^{s_3},\tilde{\lambda}_{I_1}^{-s_{I_1}}\right)\mathcal{A}_3\left(\tilde{\lambda}_{I_1}^{s_{I_1}},\tilde{\lambda}_1^{s_1},\tilde{\lambda}_{I_2}^{-s_{I_2}}\right)\\ &+\frac{1}{\bar{z}_{31}\bar{z}_{I_1 2}}\frac{1}{\omega_1+\omega_3}\mathcal{A}_3\left(\tilde{\lambda}_3^{s_3},\tilde{\lambda}_1^{s_1},\tilde{\lambda}_{I_1}^{-s_{I_1}}\right)\mathcal{A}_3\left(\tilde{\lambda}_{I_1}^{s_{I_1}},\tilde{\lambda}_2^{s_2},\tilde{\lambda}_{I_2}^{-s_{I_2}}\right)\Bigg]=0\end{aligned}\tag{6.21}$$

with $\bar{z}_{I_1}=\frac{\omega_1\bar{z}_1+\omega_2\bar{z}_2}{\omega_1+\omega_2}$. (We emphasize that this equation must hold for arbitrary s_{I_2}.) Using the three-point amplitudes defined in the previous section, it is now a straightforward (if slightly tedious) exercise to show that (6.21) is true only when the constraints (6.4), (6.5), (6.7), (6.8) and (6.10)–(6.12) are satisfied.

6.3 Amplitudes in EFTs with celestial dual

In this section, we will examine the properties of amplitudes in effective theories that satisfy (6.21) or equivalently, the constraints reviewed in Section 6.1.

6.3.1 Four-point amplitudes in the graviton-scalar sector

We start with amplitudes involving external gravitons, which were computed in [231, 232]. The amplitude involving four positive helicity gravitons is[3]

$$\mathcal{A}_4\left(1^{++},2^{++},3^{++},4^{++}\right)=$$

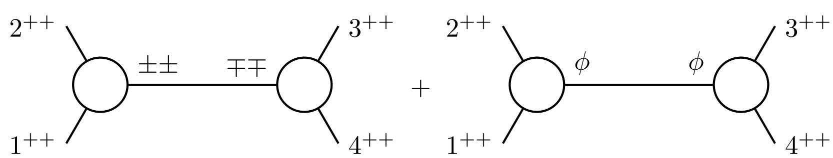

(6.22)

$+$ (cyclic of 1,2,3)

where (cyclic of 1,2,3) refers to the diagrams obtained by making the stated replacements. Evaluating the diagrams results in

$$\begin{aligned}\mathcal{A}_4\left(1^{++},2^{++},3^{++},4^{++}\right)&=\kappa_{-2,2,2}\kappa_{2,2,2}\left(\frac{[12]^5[34]^2}{\langle 12\rangle}\frac{\langle 1X\rangle^2\langle 2X\rangle^2}{\langle 3X\rangle^2\langle 4X\rangle^2}+\frac{[34]^5[12]^2}{\langle 34\rangle}\frac{\langle 3X\rangle^2\langle 4X\rangle^2}{\langle 1X\rangle^2\langle 2X\rangle^2}\right)\\ &\quad+\kappa_{0,2,2}^2\frac{[12]^4[34]^4}{s_{12}}+\ \text{(cyclic of 1,2,3)}\\ &=\left(10\kappa_{-2,2,2}\kappa_{2,2,2}-3\kappa_{0,2,2}^2\right)s_{12}s_{13}s_{23}\frac{[12][23][34][41]}{\langle 12\rangle\langle 23\rangle\langle 34\rangle\langle 41\rangle}\\ &=0\end{aligned}\tag{6.23}$$

[3] We will omit explicitly displaying the dependence of the amplitude on $\lambda,\tilde{\lambda}$ for brevity and only display the helicities.

where we used $s_{ij} = \langle ij\rangle\,[ij]$. In the last line, we have imposed the constraint in (6.5) to conclude that the amplitude vanishes.

The remaining four-graviton amplitudes $\mathcal{A}\left(1^{++},2^{++},3^{++},4^{--}\right)$, $\mathcal{A}\left(1^{++},2^{--},3^{--},4^{++}\right)$, and their parity conjugates are not all-line shift constructible since they violate the condition (6.37). Instead, they were computed in [231, 232, 233]:

$$\begin{aligned}\mathcal{A}\left(1^{++},2^{++},3^{++},4^{--}\right) &= \kappa_{2,2,2}\kappa_{-2,-2,2}(\langle 14\rangle[13]\langle 34\rangle)^2\frac{[12][23][31]}{\langle 12\rangle\langle 23\rangle\langle 31\rangle}\,,\\ \mathcal{A}\left(1^{++},2^{--},3^{--},4^{++}\right) &= \frac{\left(\langle 23\rangle\,[14]\right)^4}{s_{14}}\left(\kappa_{2,2,2}^2 s_{12}\,s_{13} - \kappa_{2,2,0}^2 + \kappa_{2,2,-2}^2\frac{1}{s_{12}\,s_{13}}\right)\,,\end{aligned} \tag{6.24}$$

and we note that these amplitudes are non-vanishing, even on the support of the associativity constraints.

Moving on to amplitudes involving external scalars in addition to gravitons, the only amplitude that is all-line shift constructible is

$\mathcal{A}_4\left(1^{++},2^{++},3^{++},4^{\phi}\right) =$ 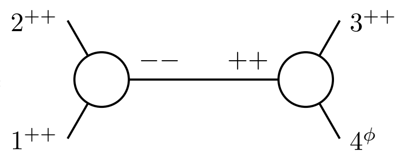

$+$ 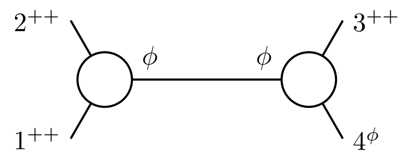

$$\begin{aligned}&+\ \text{(cyclic of 1,2,3)}\\ &= \kappa_{-2,2,2}\kappa_{2,2,0}\frac{[12]\,[34]^4}{\langle 12\rangle}\frac{\langle 4X\rangle^4}{\langle 1X\rangle^2\,\langle 2X\rangle^2} + \kappa_{2,2,0}\kappa_{0,0,2}\frac{[12]^3\,[34]^2}{\langle 12\rangle}\frac{\langle 4X\rangle^2}{\langle 3X\rangle^2}\\ &+\ \text{(cyclic of 1,2,3)}\\ &= 0\end{aligned} \tag{6.25}$$

and it vanishes on the support of the constraints (6.4).

6.3.2 Four-point amplitudes in the gluon-scalar sector

The situation in the gluon-scalar sector is similar: the constraints lead to the vanishing of all-line shift constructible amplitudes. In this sector the only all-line shift constructible all-gluon amplitude is

$\mathcal{A}_4\left(1^{+,a_1},2^{+,a_2},3^{+,a_3},4^{+,a_4}\right) =$ 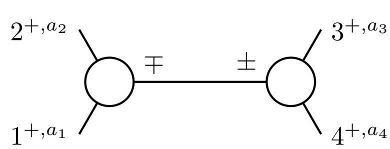

$+$ 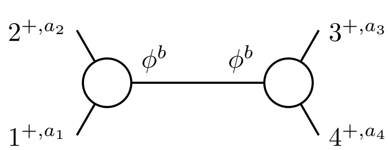

$+$ 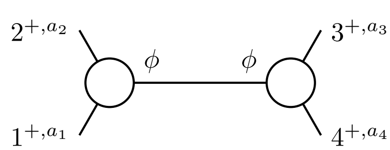

$+$ (cyclic of 1,2,3)

(6.26)

A straightforward calculation yields

$$
\begin{aligned}
&\mathcal{A}_4\left(1^{+,a_1},2^{+,a_2},3^{+,a_3},4^{+,a_4}\right)\\
&=-\,f^{a_1a_2e}f^{ea_3a_4}\,\kappa_{-1,1,1}\kappa_{1,1,1}\left(\frac{[12]^2[34]}{\langle 12\rangle}\frac{\langle 1X\rangle\langle 2X\rangle}{\langle 3X\rangle\langle 4X\rangle}+\frac{[34]^2[12]}{\langle 34\rangle}\frac{\langle 3X\rangle\langle 4X\rangle}{\langle 1X\rangle\langle 2X\rangle}\right)\\
&\quad+\frac{2\kappa_{0,1,1}^2}{N_c}\left(\delta^{a_1a_2}\delta^{a_3a_4}\frac{[12]^2[34]^2}{\langle 12\rangle\,[12]}\right)+\kappa_{0,1,1}^2\left(d^{a_1a_2b}d^{a_3a_4b}\frac{[12]^2[34]^2}{\langle 12\rangle\,[12]}\right)+(\text{cyclic of 1,2,3})\\
&=\left(4\kappa_{-1,1,1}\kappa_{1,1,1}-2\kappa_{0,1,1}^2\right)\frac{[13][24]^2}{\langle 13\rangle}\mathrm{Tr}[T^{a_1}T^{a_2}T^{a_3}T^{a_4}]+(\text{permutation of 1,2,3})\,.
\end{aligned}
\tag{6.27}
$$

Here we used properties of f^{abc} and d^{abc}, and in the last line the constraint $\kappa_{0,1,1}^2=2\kappa_{-1,1,1}\kappa_{1,1,1}$ from (6.8) to find that this amplitude vanishes as well. The remaining four-gluon amplitudes are not all-line shift constructible and are non-vanishing for generic couplings, even when all the constraints from Section 6.1 are imposed.

We also find that the four-point amplitude involving three positive helicity gluons and one scalar (either the adjoint or singlet) is vanishing. For the adjoint scalar, the full amplitude reads (here we omit on each line "+ cyclic(1,2,3)")

$\mathcal{A}_4\left(1^{+,a_1},2^{+,a_2},3^{+,a_3},4^{\phi,a_4}\right)$

$=$ 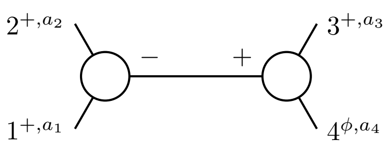

$+$ 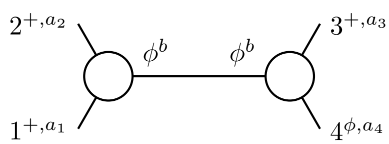

$$
\begin{aligned}
&=if^{a_1a_2b}d^{a_3a_4b}\kappa_{-1,1,1}\kappa_{0,1,1}\frac{[34]^2}{\langle 12\rangle}\frac{\langle 4X\rangle^2}{\langle 1X\rangle\langle 2X\rangle}+id^{a_1a_2b}f^{a_3a_4b}\kappa_{0,1,1}\kappa_{0,0,1}\frac{[12][34]}{\langle 12\rangle}\frac{\langle 4X\rangle}{\langle 3X\rangle}
\end{aligned}
\tag{6.28}
$$

$$
\begin{aligned}
&=if^{a_1a_2b}d^{a_3a_4b}\kappa_{-1,1,1}\kappa_{0,1,1}\frac{[34]^2}{\langle 12\rangle}\frac{\langle 4X\rangle^2}{\langle 1X\rangle\langle 2X\rangle}+\left(if^{a_2a_3b}d^{a_1a_4b}-if^{a_3a_1b}d^{a_2a_4b}\right)\kappa_{0,1,1}\kappa_{0,0,1}\frac{[12][34]}{\langle 12\rangle}\frac{\langle 4X\rangle}{\langle 3X\rangle}\\
&=if^{a_1a_2b}d^{a_3a_4b}\left(\kappa_{-1,1,1}\kappa_{0,1,1}\frac{[34]^2\langle 4X\rangle^2}{\langle 12\rangle\langle 1X\rangle\langle 2X\rangle}-\kappa_{0,1,1}\kappa_{0,0,1}\frac{[23][14]\langle 4X\rangle}{\langle 23\rangle\langle 1X\rangle}+\kappa_{0,1,1}\kappa_{0,0,1}\frac{[31][24]\langle 4X\rangle}{\langle 31\rangle\langle 2X\rangle}\right)\\
&=if^{a_1a_2b}d^{a_3a_4b}\left(\kappa_{-1,1,1}\kappa_{0,1,1}-\kappa_{0,1,1}\kappa_{0,0,1}\right)\frac{[34]^2\langle 4X\rangle^2}{\langle 12\rangle\langle 1X\rangle\langle 2X\rangle}\\
&=0
\end{aligned}
$$

on the support of the constraints (6.10), while the amplitude for the singlet scalar is:

$\mathcal{A}_4\left(1^{+,a_1},2^{+,a_2},3^{+,a_3},4^{\phi}\right)=$ 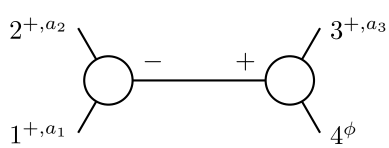

$+$ (cyclic of 1,2,3)

$$
\begin{aligned}
&=\ i\sqrt{\frac{2}{N_c}}\kappa_{-1,1,1}\kappa_{0,1,1}f^{a_1a_2b}\delta^{a_3b}\frac{[34]^2}{\langle 12\rangle}\frac{\langle 4X\rangle^2}{\langle 1X\rangle\langle 2X\rangle}\quad+\quad(\text{cyclic of 1,2,3})
\end{aligned}
\tag{6.29}
$$

$$
\begin{aligned}
&=\ i\sqrt{\frac{2}{N_c}}\kappa_{-1,1,1}\kappa_{0,1,1}f^{a_1a_2a_3}\left(\frac{[34]^2\langle 4X\rangle^2}{\langle 12\rangle\langle 1X\rangle\langle 2X\rangle}+\frac{[14]^2\langle 4X\rangle^2}{\langle 23\rangle\langle 2X\rangle\langle 3X\rangle}+\frac{[24]^2\langle 4X\rangle^2}{\langle 31\rangle\langle 3X\rangle\langle 1X\rangle}\right)\\
&=\ 0\,.
\end{aligned}
$$

6.3.3 Amplitudes of arbitrary multiplicity

We can now generalize the results of the previous sections to amplitudes of arbitrary multiplicity.

For amplitudes that are all-line shift constructible, the general statement is that all contributions that involve purely holomorphic (or purely anti-holomorphic) vertices to amplitudes must vanish due to the constraints. So, in particular, if an amplitude is all-line shift constructible and each term breaks down into only purely holomorphic or purely anti-holomorphic three-point building blocks, then the entire amplitude must vanish.

To see this, let us start by constructing an arbitrary four-point amplitude by using the all-line shift recursion relations to glue together two anti-holomorphic three-point amplitudes:

$$\mathcal{A}_4\left(\left\{\lambda_1,\tilde{\lambda}_1\right\}^{s_1},\left\{\lambda_2,\tilde{\lambda}_2\right\}^{s_2},\left\{\lambda_3,\tilde{\lambda}_3\right\}^{s_3},\left\{\lambda_4,\tilde{\lambda}_4\right\}^{s_4}\right)$$

$$=$$

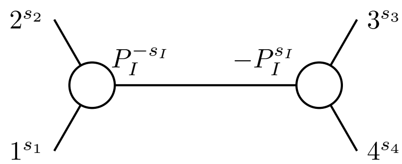

$$+ \quad \text{(cyclic of 1,2,3)} \tag{6.30}$$

$$=\sum_{s_I}\left[\mathcal{A}_3\left(\tilde{\lambda}_1^{s_1},\tilde{\lambda}_2^{s_2},\hat{\tilde{\lambda}}_I^{-s_I}\right)\frac{1}{\langle 12\rangle\,[12]}\mathcal{A}_3\left(\hat{\tilde{\lambda}}_I^{s_I},\tilde{\lambda}_3^{s_3},\tilde{\lambda}_4^{s_4}\right)+\text{(cyclic of 1,2,3)}\right].$$

Using momentum conservation, we can rewrite this as

$$\begin{aligned}\frac{[34]}{\langle 12\rangle}\sum_{s_I}\Bigg[&\mathcal{A}_3\left(\tilde{\lambda}_1^{s_1},\tilde{\lambda}_2^{s_2},\hat{\tilde{\lambda}}_I^{-s_I}\right)\frac{1}{[12]\,[34]}\mathcal{A}_3\left(\hat{\tilde{\lambda}}_I^{s_I},\tilde{\lambda}_3^{s_3},\tilde{\lambda}_4^{s_4}\right)\\&+\mathcal{A}_3\left(\tilde{\lambda}_1^{s_1},\tilde{\lambda}_3^{s_3},\hat{\tilde{\lambda}}_I^{-s_I}\right)\frac{1}{[31]\,[24]}\mathcal{A}_3\left(\hat{\tilde{\lambda}}_I^{s_I},\tilde{\lambda}_2^{s_2},\tilde{\lambda}_4^{s_4}\right)\\&+\mathcal{A}_3\left(\tilde{\lambda}_1^{s_1},\tilde{\lambda}_2^{s_4},\hat{\tilde{\lambda}}_I^{-s_I}\right)\frac{1}{[14]\,[23]}\mathcal{A}_3\left(\hat{\tilde{\lambda}}_I^{s_I},\tilde{\lambda}_3^{s_3},\tilde{\lambda}_4^{s_2}\right)\Bigg],\end{aligned} \tag{6.31}$$

which must hold for arbitrary s_4. This is precisely the double residue condition (6.21) on the support of four-point momentum conservation! Hence we conclude that tree-level associativity of the celestial OPE forces any four-point amplitude constructed solely from anti-holomorphic vertices to vanish[4].

The construction of higher-point amplitudes proceeds in a similar manner. However, unlike the four-particle case, we can encounter amplitudes that are all-line shift constructible but non-vanishing. This can occur because none of the non-zero four-point amplitudes are purely anti-holomorphic or purely holomorphic, so any higher-point amplitudes (when constructed via all-line shift recursion) that receive contributions from these amplitudes will also be non-vanishing. An example is the five-point all-plus amplitude $\mathcal{A}_5(1^+,2^+,3^+,4^+,5^+)$, which is all-line shift constructible but has a term involving the product of two non-zero amplitudes $\mathcal{A}_3(1^+,2^+,3^+)\times\mathcal{A}_4(1^-,2^+,3^+,4^+)$, the second

[4]The apparent asymmetry between holomorphic and anti-holomorphic in our discussion arises from our choice of using the holomorphic all-line shift in Appendix 6.5. Of course, all conclusions hold for parity conjugate amplitudes as well, and could be manifested by using an anti-holomorphic all-line shift instead. In constructing higher-point amplitudes recursively, one has the freedom to independently choose the holomorphic or anti-holomorphic shift term-by-term and in various levels of the recursion.

of which includes both holomorphic and anti-holomorphic vertices. However, constructible higher-point amplitudes will be vanishing at tree level if they do not receive contributions from any channels other than those involving only purely holomorphic or anti-holomorphic vertices as building blocks.

6.4 Discussion

The constraints (6.4), (6.5), (6.7), (6.8) and (6.10)–(6.12) are incredibly restrictive. Most apparently sensible theories fail to satisfy them. Heterotic string theory (compactified on a torus to 4D) ostensibly fails to satisfy them due to the presence of $R^2\phi$ terms and the absence of an R^3 term.[5] However, the four-positive helicity graviton amplitude vanishes in this theory as can be seen from the double copy construction [234]. This is because $\kappa_{2,2,2}$ vanishes and the two scalars (axion and dilaton) give contributions to the left-hand side of (6.5) that vanish when summed. While the vanishing of the four-positive helicity amplitude does not guarantee associativity, it serves as an easy (particularly when the spectrum involves multiple particles with the same helicity) but powerful check on OPE associativity. It is intriguing to wonder about other contributions (massive particles, bound states, resonances, extended objects) to the OPE of massless particles, see for e.g. [235]. If some or all of these contributions are indeed present, this suggests that the OPE in (6.1) is incomplete and these additional contributions might modify the analysis in this paper. Alternatively, theories which fail to satisfy these constraints simply do not have celestial duals.

Interestingly, one other example of a theory which does satisfy the constraints is the chiral higher-spin theory studied in [236, 237, 238]. Working in the light-cone approach, they derived the following solution for the coupling constants after requiring Poincaré symmetry:

$$\kappa_{s_1,s_2,s_3} \sim \frac{(l_P)^{s_1+s_2+s_3-1}}{\Gamma(s_1+s_2+s_3)} \qquad s_1+s_2+s_3>0\,, \tag{6.32}$$

where l_P is a parameter with dimension of length. One can easily check that (6.32) satisfies all the constraints in (6.4), (6.5), (6.7), (6.8) and (6.10)–(6.12).

In light of [239, 230] it is natural to speculate about the prospect of a self-dual theory on the support of the associativity constraints, generalizing self-dual Yang-Mills and self-dual gravity with some higher derivative corrections. The key property of self-dual Yang-Mills and self-dual gravity is that only the anti-holomorphic three-point vertices are nonzero, and all higher-point amplitudes vanish at tree level. After including the higher-derivative interactions, if we continue to keep only the anti-holomorphic three-point vertices and set the holomorphic three-point vertices to zero, then all higher-point tree-level amplitudes will be vanishing only when the constraints are satisfied as we have shown. We leave the study of such possibilities for future work.

6.5 Appendix: All-line shift recursion relations

In this appendix we will review the all-line shift recursion relations following [231].

[5] We thank Mina Himwich for pointing this out.

The all-line shift recursion relations are based on shifting all of the external momenta. For the purpose this appendix, we treat $\lambda, \tilde{\lambda}$ (consequently $z, \bar{z}$) as independent complex variables. We will refer to them as holomorphic and anti-holomorphic respectively. We denote a scattering amplitude involving n massless particles (all considered outgoing) with momenta $p_1 = \lambda_1\tilde{\lambda}_1, \ldots, p_n = \lambda_n\tilde{\lambda}_n$ and helicities $s_1, \ldots, s_n$ by $\mathcal{A}_n\left(\left\{\lambda_1, \tilde{\lambda}_1\right\}^{s_1}, \ldots, \left\{\lambda_n, \tilde{\lambda}_n\right\}^{s_n}\right)$. Consider an all-line holomorphic shift

$$\hat{\lambda}_i = \lambda_i + \alpha\, w_i X \qquad i = 1, \ldots, n \tag{6.33}$$

where X is an arbitrary reference spinor, α is the deformation parameter and the w_i are chosen to satisfy momentum conservation

$$\sum_{i=1}^{n} w_i \tilde{\lambda}_i = 0\,. \tag{6.34}$$

The deformed amplitude has the following large α behavior [231]

$$\hat{\mathcal{A}}_n(\alpha) \to \alpha^a \qquad \text{as} \qquad \alpha \to \infty \qquad \text{with} \qquad 2a = 4 - n - c - \sum_{i=1}^{n} s_i\,, \tag{6.35}$$

where c is the mass dimension of the product of couplings in the amplitude. The undeformed amplitude can be related to its residues at non-zero values of α via the residue theorem

$$\mathcal{A}_n(\alpha = 0) = \oint_{\alpha=0} \frac{\mathrm{d}\alpha}{\alpha}\, \mathcal{A}_n(\alpha) = -\sum_j \operatorname*{Res}_{\alpha=\alpha_j}\left[\frac{1}{\alpha}\mathcal{A}_n\right]. \tag{6.36}$$

In order to use the all-line shift recursion to compute amplitudes recursively, it is crucial that there be no contribution to (6.36) from a residue at infinity. From (6.35) we see that this will be the case as long as

$$4 - n - c - \sum_{i=1}^{n} s_i < 0\,. \tag{6.37}$$

When this holds, then the tree-level deformed amplitude only has simple poles which occur when the sum of a subset of the external momenta goes on shell. The amplitude factorizes into lower-point subamplitudes on the residue of the pole.

In the paper, our main interest lies in the collinear channel where we have

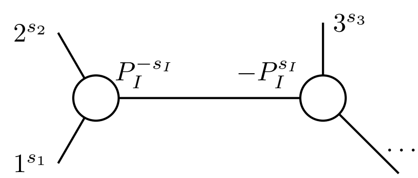

(6.38)

The value of α that corresponds to this channel is the one that makes the intermediate momentum P_I go on shell:

$$\hat{P}_I^2 = \langle\hat{1}\hat{2}\rangle\,[12] = 0 \qquad \Longrightarrow \qquad \alpha = -\frac{\langle 12\rangle}{w_1\langle X2\rangle - w_2\langle X1\rangle}\,, \tag{6.39}$$

and we can write

$$\hat{\lambda}_1 = \frac{\langle X1\rangle}{w_1\langle X2\rangle - w_2\langle X1\rangle}\,(w_1\lambda_2 - w_2\lambda_1)\,, \qquad \hat{\lambda}_2 = \frac{\langle X2\rangle}{w_1\langle X2\rangle - w_2\langle X1\rangle}\,(w_1\lambda_2 - w_2\lambda_1)\,, \tag{6.40}$$

$$\hat{\lambda}_I = w_1\lambda_2 - w_2\lambda_1\,, \qquad \hat{\tilde{\lambda}}_I = \frac{\langle X1\rangle\,\tilde{\lambda}_1 + \langle X2\rangle\,\tilde{\lambda}_2}{w_1\langle X2\rangle - w_2\langle X1\rangle}\,. \tag{6.41}$$

We therefore have

$$\begin{aligned}&\mathcal{A}_n\left(\left\{\lambda_1,\tilde{\lambda}_1\right\}^{s_1},\left\{\lambda_2,\tilde{\lambda}_2\right\}^{s_2},\ldots,\left\{\lambda_n,\tilde{\lambda}_n\right\}^{s_n}\right) \qquad (6.42)\\ =&\sum_{s_I}\hat{\mathcal{A}}_3\left(\left\{\hat{\lambda}_1,\tilde{\lambda}_1\right\}^{s_1},\left\{\hat{\lambda}_2,\tilde{\lambda}_2\right\}^{s_2},\left\{\hat{\lambda}_I,\hat{\tilde{\lambda}}_I\right\}^{-s_I}\right)\frac{1}{\langle 12\rangle\,[12]}\hat{\mathcal{A}}_{n-1}\left(\left\{\hat{\lambda}_I,\hat{\tilde{\lambda}}_I\right\}^{s_I},\ldots,\left\{\hat{\lambda}_n,\tilde{\lambda}_n\right\}^{s_n}\right)\\ &\qquad + \{\text{other channels}\}\end{aligned}$$

The other channels may include other collinear (for e.g. 34 collinear) as well as multiparticle poles.

The recursive computation of amplitudes is seeded by three-point amplitudes, which are completely fixed by Lorentz invariance and little group scaling to be[6]

$$A(1^{s_1},2^{s_2},3^{s_3}) = \begin{cases}\kappa_{s_1,s_2,s_3}[12]^{s_1+s_2-s_3}[23]^{s_2+s_3-s_1}[31]^{s_3+s_1-s_2}, & \text{if } s_1+s_2+s_3>0\,,\\ \kappa_{s_1,s_2,s_3}\langle 12\rangle^{s_3-s_1-s_2}\langle 23\rangle^{s_1-s_2-s_3}\langle 31\rangle^{s_2-s_1-s_3}, & \text{if } s_1+s_2+s_3<0\,.\end{cases} \tag{6.43}$$

A crucial aspect of the holomorphic shift is that the holomorphic three-point amplitudes vanish. This follows from the proportionality of the three holomorphic spinors $\hat{\lambda}_1$, $\hat{\lambda}_2$ and $\hat{\lambda}_I$ in (6.40), (6.41). Thus, only anti-holomorphic three-point amplitudes contribute in the collinear limit.

[6]In (6.6) and (6.9) we define certain κ's with different overall normalizations compared to this standard.

Chapter 7

All-order celestial OPE from on-shell recursion

This chapter is based on [47].

Holography in asymptotically flat spacetimes has grown into a vividly active field of research in recent years. An emerging candidate for such dualities is the idea of celestial holography [240]. According to its tenets, quantum gravity in zero cosmological constant spacetimes is proposed to be dual to *celestial conformal field theories* (CCFT) living on lightcone cuts like the celestial sphere in Lorentzian signature [43, 182] or the celestial torus in split signature [172]. Scattering amplitudes in the bulk are expected to equal correlators of local operators in such CCFTs. A top-down toy model realizing some of these expectations has also been put forward in [241].

A key observation made in [144] was that collinear limits of flat space scattering amplitudes map to operator product expansions (OPEs) in the dual CFT. In subsequent work [166], their observation was generalized to compute such *celestial OPEs* in a wide variety of theories like Yang-Mills and Einstein gravity. They determined the singular terms in celestial OPEs by using universal collinear limits that hold for all gluon and graviton amplitudes. In this paper, we will be concerned with completing the program of computing these OPEs to all orders (singular as well as regular) in the collinear expansion at tree level.

At this stage in the subject, due to open issues regarding locality and associativity of the celestial OPE [44, 45, 215], this computation is only accessible in a specific scattering configuration called the maximally helicity violating (MHV) sector. This corresponds to scattering two negative helicity massless particles against multiple positive helicity massless particles. It is this configuration that we will restrict attention to. At tree level in the MHV sector, we will show that the all-order celestial OPE of gluons and gravitons can be very easily extracted purely from the inverse soft recursion relations that their amplitudes satisfy.

This method bypasses a number of computational hurdles encountered in past work. In the original works [163, 165, 242, 164] that started the study of subleading terms in celestial OPEs, the authors were restricted to working order-by-order in a non-systematic fashion. They only studied regular terms at the first and second subleading orders in the collinear limit, and were also restricted to low multiplicity amplitudes. This was because they worked with explicit expressions for the MHV amplitudes like the Parke-Taylor or Hodges' formulae. Mellin transforms of these formulae tend to be highly nontrivial generalized hypergeometric functions [243]. We will show that it is incredibly more judicious to work directly with the recursion relations. In fact, the lesson one learns this way is that the inverse soft recursion for MHV amplitudes is *equivalent* to the OPE recursion in celestial CFT. In this sense, on-shell recursion takes the guise of an emergent phenomenon. This point has already been hinted at by other works like [244] for CSW rules or [245] for BCFW recursion.

The most powerful application of subleading terms in celestial OPEs has been to the discovery of infinite chiral symmetries. In a beautiful series of works [149, 170, 168, 196, 207], it was gradually realized that celestial duals of gravity and gauge theory possess symmetries generated by the loop algebras of $\mathrm{Ham}(\mathbb{C}^2)$ and $\mathrm{Maps}(\mathbb{C}^2, \mathfrak{g})$ respectively, with $\mathfrak{g}$ being the gauge group's Lie algebra. Our results for the all-order celestial OPE will be adapted to their representation theory. Crucially, the only descendants that appear in our OPEs will be the descendants associated to these symmetries, along with antiholomorphic conformal descendants. There won't be any holomorphic conformal descendant in sight! The reason this does not shriek inconsistency is that holomorphic conformal descendants happen to be expressible in terms of such current algebra descendants due to null state relations [164, 165] (see also [246, 247, 248]).

In the case of MHV gluon scattering, our all-order OPE has been previously obtained from a concrete vertex algebra realization in [249]. This specific realization was constructed by studying twistor string theory in the MHV sector. Twistor and ambitwistor strings are a class of topological string theories that give rise to remarkably compact worldsheet formulae for gluon and graviton tree amplitudes in all N^kMHV sectors (i.e., amplitudes involving $k+2$ negative helicity particles) [250, 251, 252, 253, 254]. As such, the algebra of their vertex operators can be systematically matched to the celestial OPE algebra (see also [255, 256]). However, calculating celestial OPEs from such vertex operators becomes cumbersome rather quickly. For example, it has proven much trickier to repeat such a calculation for the all-order MHV graviton OPE. In contrast, our recursion relation based approach will display no such shortcomings.

In the rest of this work, we provide more details of this approach. In Section 7.1, we review inverse soft recursion relations in the MHV sector. In Sections 7.2 and 7.3, we turn them into all-order collinear expansions for gluon and graviton scattering respectively. These are recast as all-order celestial OPEs both in momentum space and in the space of boost eigenstates. In Section 7.4, we close with a discussion of possible applications and generalizations.

Appendix 7.5 discusses the behavior of soft-hard correlators at infinity, which feeds into certain contour integral manipulations used to obtain correlators with descendant insertions. Appendix 7.6 contains the computation of the all-order OPE of soft gluon and graviton currents, again valid within the MHV sector. Appendix 7.7 provides further details of the Mellin transforms that convert momentum eigenstate celestial OPEs to those of boost eigenstates.

7.1 Inverse soft recursion

In this section, we review the inverse soft recursion relations for MHV amplitudes. Brief definitions of concepts of celestial holography will also be provided as and when required in later sections. Many reviews of celestial holography are by now available in the literature, see for instance [184, 257].

Gluons. A tree level gluon amplitude in gauge theory can be decomposed as

$$A(1^{a_1}\,2^{a_2}\,3^{a_3}\cdots n^{a_n}) = \sum_{\sigma\in S_{n-2}} C^{a_1 a_2 a_{\sigma_3}\cdots a_{\sigma_n}}\,A[1\,2\,\sigma_3\cdots\sigma_n]\,. \tag{7.1}$$

Here, the a_i are Lie algebra indices for the gauge group. $A[1\,2\,\sigma_3\cdots\sigma_n]$ denotes a color-ordered amplitude in the ordering associated to a permutation σ over $n-2$ legs. It carries a factor of the momentum conserving delta function $\delta^4(p_1+p_2+\cdots+p_n)$. The coefficients $C^{a_1 a_2 a_{\sigma_3}\cdots a_{\sigma_n}}$ are color factors that can be written in a variety of bases. To make contact with a CFT interpretation, it is convenient to work in the Del Duca-Dixon-Maltoni (DDM) basis [258]. DDM take the color factors to be

$$C^{a_1 a_2 a_3\ldots a_n} = f^{a_2 a_3}{}_{b_1} f^{b_1 a_4}{}_{b_2}\cdots f^{b_{n-4}a_{n-1}}{}_{b_{n-3}} f^{b_{n-3}a_n a_1}\,, \tag{7.2}$$

where $f^{ab}{}_c$ are the gauge group's structure constants, and Lie algebra indices are raised using the Killing form as usual.

Inverse soft recursion constructs n-point MHV amplitudes by attaching soft factors to lower multiplicity MHV amplitudes. For color-ordered gluon amplitudes $A[1\,2\,3\cdots n]$, this recurses over smaller color-ordered amplitudes while preserving the ordering of the labels. For concreteness, we will take gluon 1 to be positive helicity. The two negative helicity gluons need not be explicitly specified for the recursion to work, but the reader may feel free to take them to be gluons r and s.

Let $p_i^{\alpha\dot\alpha} = \lambda_i^\alpha\tilde\lambda_i^{\dot\alpha}$, $\alpha = 1,2, \dot\alpha = \dot 1,\dot 2$, denote the null momenta of the gluons, expressed in terms of standard spinor-helicity variables [224]. The inverse soft recursion for the color-ordered MHV amplitude only involves a single term on its right hand side:

$$A[1_+\,2\,3\cdots n] = \frac{\langle n2\rangle}{\langle n1\rangle\langle 12\rangle}\,A[\hat 2\cdots n-1\,\hat n]\,, \tag{7.3}$$

where the subscript on 1_+ singles it out as a positive helicity particle for clarity. The hatted particles have momenta $\hat p_2^{\alpha\dot\alpha} = \lambda_2^\alpha\hat{\tilde\lambda}_2^{\dot\alpha}$ and $\hat p_n^{\alpha\dot\alpha} = \lambda_n^\alpha\hat{\tilde\lambda}_n^{\dot\alpha}$, with the hatted spinor-helicity variables taking the deformed values

$$\hat{\tilde\lambda}_2 = \tilde\lambda_2 + \frac{\langle n1\rangle}{\langle n2\rangle}\,\tilde\lambda_1\,, \qquad \hat{\tilde\lambda}_n = \tilde\lambda_n + \frac{\langle 12\rangle}{\langle n2\rangle}\,\tilde\lambda_1\,. \tag{7.4}$$

Here and in what follows, $\langle ij\rangle := \epsilon_{\beta\alpha}\lambda_i^\alpha\lambda_j^\beta$ and $[ij] := \epsilon_{\dot\beta\dot\alpha}\tilde\lambda_i^{\dot\alpha}\tilde\lambda_j^{\dot\beta}$ denote Lorentz invariant spinor contractions built out of the $\mathrm{SL}(2,\mathbb{C})$ invariant Levi Civita symbols $\epsilon_{\alpha\beta}, \epsilon_{\dot\alpha\dot\beta}$. An application of Schouten's identity shows that $\hat p_2 + p_3 + \cdots + \hat p_n = p_1 + p_2 + \cdots + p_n$, so that $A[\hat 2\cdots n-1\,\hat n]$ also automatically contains the correct $(n-1)$-point momentum conserving delta functions $\delta^4(\hat p_2 + p_3 + \cdots + \hat p_n)$.

This recursion can be derived from BCFW recursion [259]. In the past, it has been used for obtaining the subleading soft gluon theorem [223]. To extend it to the color-dressed amplitude (7.1), relabel the index $\sigma_n \equiv i$ and break the sum over $\sigma \in S_{n-2}$ into a sum over i times a sum over permutations $\pi \in S_{n-3}$ of the remaining $n-3$ gluons:

$$A(1^{a_1}\, 2^{a_2}\, 3^{a_3} \cdots n^{a_n}) = \sum_{i=3}^{n} \sum_{\pi \in S_{n-3}[i]} C^{a_1 a_2 a_{\pi_3} \cdots a_{\pi_n} a_i} A[1\, 2\, \pi_3 \cdots \pi_n\, i]\,, \tag{7.5}$$

where $S_{n-3}[i]$ denotes permutations of the set $\{3, \ldots, n\} - \{i\}$, so that the subscript on π_a runs over $a \in \{3, \ldots, n\} - \{i\}$ in the i^{th} summand of the first sum. Inverse soft recursions for the summands are found by permuting the particle labels in (7.3):

$$A[1_+\, 2\, \pi_3 \cdots \pi_n\, i] = \frac{\langle i2 \rangle}{\langle i1 \rangle \langle 12 \rangle} A[\hat{2}\, \pi_3 \cdots \pi_n\, \hat{i}]\,. \tag{7.6}$$

From (7.2), we also find a recursion for the DDM color factor,

$$C^{a_1 a_2 a_{\pi_3} \cdots a_{\pi_n} a_i} = -f^{a_1 a_i}{}_b\, C^{b a_2 a_{\pi_3} \cdots a_{\pi_n}}\,, \tag{7.7}$$

where $C^{b a_2 a_{\sigma_3} \cdots a_{\sigma_{n-1}}}$ is an $(n-1)$-gluon color factor.

Plugging these into (7.1) and using cyclic symmetry $A[\hat{2}\, \pi_3 \cdots \pi_n\, \hat{i}] = A[\hat{i}\, \hat{2}\, \pi_3 \cdots \pi_n]$ gives a recursion for the color-dressed MHV amplitude[1]

$$A(1_+^{a_1}\, 2^{a_2} \cdots n^{a_n}) = -\sum_{i=3}^{n} \frac{\langle i2 \rangle}{\langle i1 \rangle \langle 12 \rangle} T_i^{a_1} A(\hat{2}^{a_2} \cdots \hat{i}^{a_i} \cdots n^{a_n})\,, \tag{7.8}$$

where, for clarity, we repeat the definitions of the hatted particles' spinor-helicity data:

$$\begin{aligned} \hat{\lambda}_2 &= \lambda_2\,, & \hat{\tilde{\lambda}}_2 &= \tilde{\lambda}_2 + \frac{\langle i1 \rangle}{\langle i2 \rangle} \tilde{\lambda}_1, \\ \hat{\lambda}_i &= \lambda_i\,, & \hat{\tilde{\lambda}}_i &= \tilde{\lambda}_i + \frac{\langle 12 \rangle}{\langle i2 \rangle} \tilde{\lambda}_1\,. \end{aligned} \tag{7.9}$$

The momenta of the other particles remain undeformed. We have also introduced an operator T_i^a that rotates the Lie algebra indices as

$$T_i^{a_1} A(\hat{2}^{a_2} \cdots \hat{i}^{a_i} \cdots n^{a_n}) := f^{a_1 a_i}{}_b\, A(\hat{2}^{a_2} \cdots \hat{i}^{b} \cdots n^{a_n})\,. \tag{7.10}$$

This is just a transformation in the adjoint representation.

Gravitons. The inverse soft recursion for graviton amplitudes can also be derived from BCFW recursion. It was used in [261] to derive the subleading and sub-subleading soft graviton theorems.

Let $M(1\,2 \cdots n)$ denote an n-graviton amplitude. Take it to be an MHV amplitude with graviton 1 being positive helicity. Then it satisfies the inverse soft recursion

$$M(1_+\, 2 \cdots n) = \sum_{i=3}^{n} \frac{[1i]}{\langle 1i \rangle} \frac{\langle i2 \rangle^2}{\langle 12 \rangle^2} M(\hat{2} \cdots \hat{i} \cdots n)\,. \tag{7.11}$$

[1]See [260] for a similar treatment of tree level BCFW recursion in full generality.

The hatted gravitons have the same spinor-helicity variables (7.9) as the hatted gluons. There is no color-ordering to be dealt with in this case. The color factors $f^{a_1 a_i}{}_b$ are instead replaced by kinematic factors $[1i]/\langle 1i\rangle$, reflecting color-kinematics duality. This fact is also known to translate to a color-kinematics duality at the level of celestial OPEs [262].

If one goes beyond the MHV sector, such recursion relations involve further terms on their right hand sides [224]. These terms generally contain multiparticle factorization poles. They cannot be interpreted as poles in the correlators of a local vertex algebra and also break the usual notions of associativity of the celestial OPE [215]. We leave the study of these more involved terms to the future, which might very well require a generalization like non-local vertex algebras [263].

7.2 MHV Gluon OPE

7.2.1 Collinear expansion

Spinor-helicity variables $\lambda_i^\alpha, \tilde{\lambda}_i^{\dot\alpha}$ are only defined up to the scalings $(\lambda_i, \tilde\lambda_i) \sim (t_i\lambda_i, t_i^{-1}\tilde\lambda_i)$ for $t_i \in \mathbb{C}^*$. This is known as little group scaling. Using this freedom, we choose to fix

$$\lambda_i^\alpha = \begin{pmatrix} 1 \\ z_i \end{pmatrix}, \qquad \tilde\lambda_i^{\dot\alpha} = \omega_i \begin{pmatrix} 1 \\ \bar z_i \end{pmatrix}, \qquad z_i, \bar z_i \in \mathbb{C}\,,\ \omega_i \in \mathbb{C}^*\,. \tag{7.12}$$

$z_i, \bar z_i$ are generally taken to be complex and independent of each other. They are complex conjugates only in Lorentzian signature where they act as coordinates on the celestial sphere. With this fixing of the scalings, one finds

$$\langle ij\rangle = z_{ij}\,, \qquad [ij] = \omega_i\omega_j \bar z_{ij}\,, \tag{7.13}$$

where $z_{ij} \equiv z_i - z_j$ and $\bar z_{ij} \equiv \bar z_i - \bar z_j$. This choice of little group fixing is the most efficient when working with a holomorphic collinear expansion, i.e., an expansion in small z_{ij} while keeping $[ij]$ arbitrary. While studying the twistorial origin of celestial OPEs, it was applied by Costello and Paquette to great success in [244, 230].

Let us now return to the recursion relations. The main observation underpinning our derivation of the celestial OPE is that the hatted spinor-helicity variables (7.9) can be written in the suggestive form

$$\begin{aligned} \hat{\tilde\lambda}_2 &= \tilde\lambda_2 + \frac{z_{i1}}{z_{i2}}\tilde\lambda_1 = \tilde\lambda_1 + \tilde\lambda_2 - \frac{z_{12}}{z_{i2}}\,\tilde\lambda_1\,, \\ \hat{\tilde\lambda}_i &= \tilde\lambda_i + \frac{z_{12}}{z_{i2}}\,\tilde\lambda_1\,. \end{aligned} \tag{7.14}$$

As a result, the inverse soft recursion (7.8) for the gluon MHV amplitude can be recast in terms of exponentiations of linear shifts of $\tilde\lambda_2$ and $\tilde\lambda_i$:

$$A(1_+^{a_1}\, 2^{a_2}\cdots n^{a_n}) = -\sum_{i=3}^{n} \frac{1}{z_{12}}\left(1 - \frac{z_{12}}{z_{i2}}\right)^{-1} \exp\left\{\frac{z_{12}}{z_{i2}}\big([1\partial_i] - [1\partial_2]\big)\right\} T_i^{a_1} A(\mathbf{2}^{a_2}\cdots n^{a_n}) \tag{7.15}$$

where we have introduced the abbreviation

$$[i\partial_j] \equiv \tilde\lambda_i^{\dot\alpha}\,\frac{\partial}{\partial\tilde\lambda_j^{\dot\alpha}} = \frac{\omega_i}{\omega_j}\left(\bar z_{ij}\,\frac{\partial}{\partial\bar z_j} + \omega_j\,\frac{\partial}{\partial\omega_j}\right) . \tag{7.16}$$

On the right hand side of (7.15), particles $3,\dots,n$ now carry the original undeformed momenta $p_3,\dots,p_n$. On the other hand, particle 2 is depicted in bold to signify that it carries the "effective" momentum

$$\mathbf{p}_2^{\alpha\dot\alpha} = \lambda_2^\alpha(\tilde\lambda_1+\tilde\lambda_2)^{\dot\alpha}\,. \tag{7.17}$$

Because $\lambda_j^1 = 1\ \forall\ j=1,\dots,n$ in our little group fixing, if needed, $\mathbf{p}_2^{\alpha\dot\alpha}$ can also be written in a little group invariant form by replacing $\tilde\lambda_1^{\dot\alpha}\mapsto(\lambda_1^1/\lambda_2^1)\tilde\lambda_1^{\dot\alpha}$.

These steps have brought the recursion to a form that is ripe for holomorphic collinear expansion. Taylor expanding (7.15) around $z_{12}=0$ yields

$$A(1_+^{a_1}\,2^{a_2}\cdots n^{a_n}) = -\sum_{i=3}^n\sum_{p=0}^\infty\frac{z_{12}^{p-1}}{z_{i2}^p}\sum_{q=0}^p\frac{([1\partial_i]-[1\partial_2])^q}{q!}\,T_i^{a_1}A(\mathbf{2}^{a_2}\cdots n^{a_n})\,. \tag{7.18}$$

Further expanding the factors of $([1\partial_i]-[1\partial_2])^q$ using the binomial theorem, one finds the all-order collinear expansion of the tree level MHV gluon amplitude,

$$\boxed{A(1_+^{a_1}\,2^{a_2}\cdots n^{a_n}) = -\sum_{p=0}^\infty z_{12}^{p-1}\sum_{q=0}^p\sum_{r=0}^q\frac{(-[1\partial_2])^{q-r}}{r!(q-r)!}\sum_{i=3}^n\frac{[1\partial_i]^r}{z_{i2}^p}\,T_i^{a_1}A(\mathbf{2}^{a_2}\cdots n^{a_n})\,.} \tag{7.19}$$

This holds regardless of the helicity of gluon 2.

7.2.2 Celestial OPE of momentum eigenstates

Celestial holography posits the existence of two dimensional operators $O_{s_i}^{a_i}(z_i,\tilde\lambda_i)$ in the celestial CFT that are dual to gluon momentum eigenstates. The subscripts denote helicities $s_i\in\{\pm1\}$. Correlators of such operators are conjectured to reproduce scattering amplitudes in the bulk,

$$A(1^{a_1}\,2^{a_2}\cdots n^{a_n}) = \left\langle O_{s_1}^{a_1}(z_1,\tilde\lambda_1)\,O_{s_2}^{a_2}(z_2,\tilde\lambda_2)\cdots O_{s_n}^{a_n}(z_n,\tilde\lambda_n)\right\rangle\,. \tag{7.20}$$

In particular, one reads off conjectural operator product expansions of the dual operators by demanding that the OPE expansions of the correlators reproduce collinear limits of scattering amplitudes. The resulting operator products are known as *celestial OPEs*.

Soft gluon currents. In the MHV sector, we can use this logic to read off gluon celestial OPEs to all orders from (7.19). To do so, we need to introduce positive helicity soft gluon currents. The soft expansion of a positive helicity hard gluon $O_+^a(z,\tilde\lambda)$ with $\tilde\lambda^{\dot\alpha}=\omega(1,\bar z)$ is a Taylor expansion in the energy ω.[2] Equivalently, it can be represented as a double Taylor expansion in $\tilde\lambda^{\dot 1},\tilde\lambda^{\dot 2}$,

$$O_+^a(z,\tilde\lambda) = \sum_{k,\ell=0}^\infty\frac{(\tilde\lambda^{\dot 1})^k(\tilde\lambda^{\dot 2})^\ell}{k!\,\ell!}\,J^a[k,\ell](z)\,. \tag{7.21}$$

[2]Our soft expansion starts at ω^0 in this little group fixing instead of with the usual Weinberg soft pole ω^{-1} that one encounters for the choice $\lambda^\alpha=\sqrt{\omega}(1,z)$, $\tilde\lambda^{\dot\alpha}=\sqrt{\omega}(1,\bar z)$. This is just a convenient convention.

The Taylor coefficients $J^a[k,\ell](z)$ are chiral currents known as *soft gluon currents*. Under Möbius transformations of z, they transform as chiral conformal primaries with conformal weights $h = 1 - \frac{k+\ell}{2}$. Similarly, under $\mathrm{SL}(2,\mathbb{C})$ rotations of $\tilde\lambda^{\dot\alpha}$, the currents at fixed $k+\ell$ span a spin $\frac{k+\ell}{2}$ representation of $\mathrm{SL}(2,\mathbb{C})$.

Celestial OPEs of these soft currents were determined in [170, 168]. Strominger further recognized in [168] that their modes generate the loop algebra of holomorphic maps $\mathbb{C}^2 \to \mathfrak{g}$, where $\mathfrak{g}$ is the gauge group's Lie algebra. Hence, this loop algebra was established to be a symmetry algebra of the celestial CFT dual to gauge theory. For the purposes of this work, we are adopting the simplifying notation of [244] for these currents.[3]

The leading singularity in (7.19) allows us to extract the singular part of the OPE. To see this, begin by truncating (7.19) to the singular order,

$$A(1_+^{a_1}\,2^{a_2}\cdots n^{a_n}) = -\frac{1}{z_{12}}\sum_{i=3}^{n} T_i^{a_1}\,A(\mathbf{2}^{a_2}\cdots n^{a_n}) + \mathrm{O}(z_{12}^0)\,. \tag{7.22}$$

Global color conservation for the $(n-1)$-point amplitude $A(\mathbf{2}^{a_2}\cdots n^{a_n})$ gives the identity

$$\sum_{i=3}^{n} T_i^{a_1}\,A(\mathbf{2}^{a_2}\cdots n^{a_n}) = -T_2^{a_1}\,A(\mathbf{2}^{a_2}\cdots n^{a_n}) = -f^{a_1a_2}{}_b\,A(\mathbf{2}^{b}\cdots n^{a_n})\,. \tag{7.23}$$

This is the conservation law associated to the leading soft gluon theorem [135]. Using this, we obtain the singular part of the collinear expansion,

$$A(1_+^{a_1}\,2^{a_2}\cdots n^{a_n}) = \frac{f^{a_1a_2}{}_b}{z_{12}}\,A(\mathbf{2}^{b}\cdots n^{a_n}) + \mathrm{O}(z_{12}^0)\,. \tag{7.24}$$

This provides the standard conjecture for the holomorphic hard gluon celestial OPE at order $1/z_{12}$ and all orders in $\bar z_{12}$ [144, 166, 170, 196]

$$O_+^{a_1}(z_1,\tilde\lambda_1)\,O_{s_2}^{a_2}(z_2,\tilde\lambda_2) \sim \frac{f^{a_1a_2}{}_b}{z_{12}}\,O_{s_2}^{b}(z_2,\tilde\lambda_1+\tilde\lambda_2)\,,\qquad s_2\in\{\pm1\}\,. \tag{7.25}$$

Thankfully, singularities in $\bar z_{12}$ do not come into play as long as we stay within the MHV sector, giving us a perfect toy model to work with.

Choosing $s_2 = +1$ and expanding in $\tilde\lambda_1^{\dot\alpha}, \tilde\lambda_2^{\dot\alpha}$, one can read off the current algebra of soft gluons,

$$J^a[k,\ell](z)\,J^b[m,n](w) \sim \frac{f^{ab}{}_c}{z-w}\,J^c[k+m,\ell+n](w)\,. \tag{7.26}$$

This has vanishing level (at least at tree level in the bulk). As mentioned before, this is the loop algebra of $\mathrm{Maps}(\mathbb{C}^2,\mathfrak{g})$ found in [168].[4] It originates in the symmetries of the Penrose-Ward transform as elaborated in [244].

[3] Our currents are related to Strominger's S-algebra currents as $S^{p,a}_m(z) = J^a[p-1+m, p-1-m](z)$, where $p \in \{1, \frac{3}{2}, 2, \frac{5}{2}, \dots\}$ and $|m| \le p-1$.

[4] Holomorphic maps $\mathbb{C}^2 \to \mathfrak{g}$ are generated by the monomials $v_1^k v_2^\ell \mathfrak{t}^a$, where v_1, v_2 are complex coordinates on $\mathbb{C}^2$ and $\mathfrak{t}^a$ are generators of $\mathfrak{g}$ with Lie bracket $[\mathfrak{t}^a,\mathfrak{t}^b] = f^{ab}{}_c\mathfrak{t}^c$. The set of such holomorphic maps has the natural Lie algebra structure $[v_1^k v_2^\ell \mathfrak{t}^a, v_1^m v_2^n \mathfrak{t}^b] = v_1^{k+m} v_2^{\ell+n} f^{ab}{}_c \mathfrak{t}^c$. The soft gluon OPE is seen to be the loop algebra based on this Lie algebra.

It is also useful to define certain currents that fall between the hard and soft gluons:

$$J^a[r](z,\tilde\lambda) = \sum_{k=0}^{r} \frac{(\tilde\lambda^{\dot 1})^k(\tilde\lambda^{\dot 2})^{r-k}}{k!(r-k)!}\, J^a[k,r-k](z)\,, \qquad r\in\mathbb{Z}_{\geq 0}\,. \tag{7.27}$$

These act as generating functions of the soft gluon currents. In terms of these, the positive helicity hard gluons admit the clean decomposition

$$O^a_+(z,\tilde\lambda) = \sum_{r=0}^{\infty} J^a[r](z,\tilde\lambda)\,. \tag{7.28}$$

Because $J^a[r](z,\tilde\lambda)$ is homogeneous of weight r in $\tilde\lambda^{\dot\alpha} = \omega(1,\bar z)$, the r^{th} term of this expansion is just ω^r times the r^{th} subleading soft gluon.

The OPE between soft and hard gluons can be compactly expressed as

$$J^{a_1}[r](z_1,\tilde\lambda_1)\, O^{a_i}_{s_i}(z_i,\tilde\lambda_i) \sim \frac{f^{a_1a_i}{}_b}{z_{1i}}\,\frac{[1\partial_i]^r}{r!}\, O^b_{s_i}(z_i,\tilde\lambda_i)\,. \tag{7.29}$$

This is a momentum space version of the boost eigenstate soft-hard OPEs found in [196]. It is obtained by relabeling $2\mapsto i$ in (7.25), expanding $O^b_{s_i}(z_i,\tilde\lambda_1+\tilde\lambda_i) = \epsilon^{[1\partial_i]}O^b_{s_i}(z_i,\tilde\lambda_i)$ in powers of $[1\partial_i]$, then comparing terms of homogeneity r in $\tilde\lambda_1^{\dot\alpha}$ on both sides. The operator $[1\partial_i]\equiv\tilde\lambda_1\cdot\partial_{\tilde\lambda_i}$ differentiates the $\tilde\lambda_i^{\dot\alpha}$ dependence of the hard gluon. The simple expression (7.29) is the main upshot of using the generating functions $J^a[r]$. OPEs between soft gluon currents $J^{a_1}[k,\ell](z_1)$ and hard gluon operators can be extracted by equating the coefficients of $(\tilde\lambda_1^{\dot 1})^k(\tilde\lambda_1^{\dot 2})^\ell$.

Soft gluon descendants. In the MHV sector, one does not encounter singularities in $\bar z_{12}$. Complexifying $z_i,\bar z_i$ (or working in split signature), one can therefore continue to treat the soft gluons $J^a[r](z,\tilde\lambda)$ as chiral currents living on the sphere coordinatized by z. That is, we are treating $\tilde\lambda^{\dot\alpha}$ as an operator label rather than a coordinate on the Riemann sphere on which the CCFT is defined. In particular, we can define $J^a[r]$ descendants as the $\tilde\lambda$-dependent operators

$$J^{a_1}_{-p}[r](\tilde\lambda_1)O^{a_2}_{s_2}(z_2,\tilde\lambda_2) := \oint_{|z_{12}|=\varepsilon}\frac{\mathrm{d}z_1}{2\pi\mathrm{i}}\,\frac{1}{z_{12}^p}\,J^{a_1}[r](z_1,\tilde\lambda_1)\,O^{a_2}_{s_2}(z_2,\tilde\lambda_2), \tag{7.30}$$

where $\varepsilon\ll 1$ and $p\geq 0$. The integrand of the contour integral is to be understood as the radially ordered operator product as is standard in 2d CFT.

Suppose one inserts such a descendant in a correlation function of hard gluon operators,

$$\begin{aligned}&\left\langle J^{a_1}_{-p}[r](\tilde\lambda_1)O^{a_2}_{s_2}(z_2,\tilde\lambda_2)\prod_{i=3}^n O^{a_i}_{s_i}(z_i,\tilde\lambda_i)\right\rangle\\ &\qquad = \oint_{|z_{12}|=\varepsilon}\frac{\mathrm{d}z_1}{2\pi\mathrm{i}}\,\frac{1}{z_{12}^p}\left\langle J^{a_1}[r](z_1,\tilde\lambda_1)\,O^{a_2}_{s_2}(z_2,\tilde\lambda_2)\prod_{i=3}^n O^{a_i}_{s_i}(z_i,\tilde\lambda_i)\right\rangle\,.\end{aligned} \tag{7.31}$$

Since the current $J^a[r](z,\tilde\lambda)$ transforms as a primary of weight $h=1-r/2$ under Möbius transformations of z, it has a pole of order $r-2$ at $z=\infty$. Because of this, the correlator on the right can also a priori have a pole of order $r-2$ at $z_1=\infty$.[5]

[5] We thank Elizabeth Himwich as well as one of the referees of this paper for emphasizing this subtlety.

In a garden variety CFT, we would have expected such a pole to drop out entirely and only two-particle singularities at $z_{ij} = 0$ to survive. We prove in appendix 7.5 the weaker result that the soft-hard amplitude that is supposed to equal the correlator on the right of (7.31) contains a pole at infinity that is indeed of order at most $r - 2$. This is all we need for what follows. It might still be the case that the residue at this pole vanishes, so that the pole may be spurious, but we leave this analysis to the future. In fact, such poles are expected to be related to the absence of universal soft theorems beyond the subleading order.

All in all, because correlators of $J^{a_1}[r](z_1, \tilde\lambda_1)$ only have a pole of order $r-2$ or less at $z_1 = \infty$, the integrand of the contour integral in (7.31) definitely has no singularities at $z_1 = \infty$ for $0 \le r \le p$.[6] In this range of r, the contour of integration can be deformed to surround all the other poles at $z_1 = z_i$, $i = 3, \dots, n$, instead of the original pole at $z_1 = z_2$. This converts the right hand side to

$$-\sum_{i=3}^{n} \oint_{|z_{1i}|=\varepsilon} \frac{\mathrm{d}z_1}{2\pi\mathrm{i}}\, \frac{1}{z_{12}^{p}} \left\langle J^{a_1}[r](z_1, \tilde\lambda_1)\, O^{a_2}_{s_2}(z_2, \tilde\lambda_2) \prod_{j=3}^{n} O^{a_j}_{s_j}(z_j, \tilde\lambda_j) \right\rangle . \tag{7.32}$$

The pole at $z_{1i} = 0$ is a simple pole with residue fixed by the soft-hard OPE (7.29). Hence, for $r \le p$, the descendant correlator can be expressed purely in terms of hard gluon correlators:

$$\begin{aligned} \left\langle J^{a_1}_{-p}[r](\tilde\lambda_1) O^{a_2}_{s_2}(z_2, \tilde\lambda_2) \prod_{i=3}^{n} O^{a_i}_{s_i}(z_i, \tilde\lambda_i) \right\rangle &= -\frac{1}{r!} \sum_{i=3}^{n} \frac{f^{a_1 a_i}{}_b}{z_{i2}^{p}} \left\langle [1\partial_i]^r O^b_{s_i}(z_i, \tilde\lambda_i) \prod_{\substack{j=2\\ j\neq i}}^{n} O^{a_j}_{s_j}(z_j, \tilde\lambda_j) \right\rangle \\ &= -\frac{1}{r!} \sum_{i=3}^{n} \frac{[1\partial_i]^r}{z_{i2}^{p}}\, T^{a_1}_i A(2^{a_2}\, 3^{a_3} \cdots n^{a_n})\,. \end{aligned} \tag{7.33}$$

To get the second line, we have used the duality statement (7.20) as well as the definition (7.10) of the adjoint action $T_i^{a_1}$. Luckily, we will only require descendant correlators for the range $r \le p$ when extracting the OPE.

All-order gluon OPE. Having defined the soft gluon descendants and their correlators, it becomes straightforward to extract the all-order celestial OPE from the all-order collinear expansion (7.19).

Using the duality statement (7.20) and the descendant correlator (7.33) – taken after a shift $\tilde\lambda_2 \mapsto \tilde\lambda_1 + \tilde\lambda_2$ – we get the all-order OPE expansion for CCFT correlators in the MHV sector,

$$\begin{aligned} &\left\langle O^{a_1}_{+}(z_1, \tilde\lambda_1)\, O^{a_2}_{s_2}(z_2, \tilde\lambda_2) \prod_{i=3}^{n} O^{a_i}_{s_i}(z_i, \tilde\lambda_i) \right\rangle \\ &\qquad = \sum_{p=0}^{\infty} z_{12}^{p-1} \sum_{q=0}^{p} \sum_{r=0}^{q} \frac{(-[1\partial_2])^{q-r}}{(q-r)!} \left\langle J^{a_1}_{-p}[r](\tilde\lambda_1) O^{a_2}_{s_2}(z_2, \tilde\lambda_1 + \tilde\lambda_2) \prod_{i=3}^{n} O^{a_i}_{s_i}(z_i, \tilde\lambda_i) \right\rangle . \end{aligned} \tag{7.34}$$

As foreshadowed, the index r only runs up to p. So we are happily in the range in which the contour deformation used to obtain (7.32) holds.

[6] Keep in mind that $\mathrm{d}z_1$ itself has a pole of order 2 while z_{12}^{-p} has a zero of order p at infinity.

This relation is equivalent to giving the following OPE to gluons 1 and 2:

$$O_+^{a_1}(z_1,\tilde\lambda_1)\,O_{s_2}^{a_2}(z_2,\tilde\lambda_2)=\sum_{p=0}^{\infty}z_{12}^{p-1}\sum_{q=0}^{p}\sum_{r=0}^{q}\frac{(-[1\partial_2])^{q-r}}{(q-r)!}\,J_{-p}^{a_1}[r](\tilde\lambda_1)O_{s_2}^{a_2}(z_2,\tilde\lambda_1+\tilde\lambda_2)\,. \tag{7.35}$$

It can be further cleaned up by exchanging the sums over q and r,

$$\boxed{O_+^{a_1}(z_1,\tilde\lambda_1)\,O_{s_2}^{a_2}(z_2,\tilde\lambda_2)=\sum_{p=0}^{\infty}z_{12}^{p-1}\sum_{r=0}^{p}\sum_{q=0}^{p-r}\frac{(-[1\partial_2])^{q}}{q!}\,J_{-p}^{a_1}[r](\tilde\lambda_1)O_{s_2}^{a_2}(z_2,\tilde\lambda_1+\tilde\lambda_2)\,.} \tag{7.36}$$

This is our result for the momentum space all-order celestial OPE of two gluons participating in an MHV amplitude. It holds for either value $s_2=\pm1$ of the helicity of the second gluon. To get a feel for this, it is useful to write out the first few terms of the sum explicitly,

$$\begin{aligned}
&O_+^{a_1}(z_1,\tilde\lambda_1)\,O_{s_2}^{a_2}(z_2,\tilde\lambda_2)\\
=&\frac{1}{z_{12}}\,J_0^{a_1}[0](\tilde\lambda_1)O_{s_2}^{a_2}(z_2,\tilde\lambda_1+\tilde\lambda_2)+\Big\{\big(1-[1\partial_2]\big)\,J_{-1}^{a_1}[0](\tilde\lambda_1)+J_{-1}^{a_1}[1](\tilde\lambda_1)\Big\}\,O_{s_2}^{a_2}(z_2,\tilde\lambda_1+\tilde\lambda_2)\\
&+z_{12}\left\{\left(1-[1\partial_2]+\frac{[1\partial_2]^2}{2!}\right)J_{-2}^{a_1}[0](\tilde\lambda_1)+\big(1-[1\partial_2]\big)\,J_{-2}^{a_1}[1](\tilde\lambda_1)+J_{-2}^{a_1}[2](\tilde\lambda_1)\right\}O_{s_2}^{a_2}(z_2,\tilde\lambda_1+\tilde\lambda_2)\\
&+\mathrm{O}(z_{12}^2)\,.
\end{aligned} \tag{7.37}$$

The leading term is of course just the leading "descendant" $J_0^{a_1}[0](\tilde\lambda_1)O_{s_2}^{a_2}(z_2,\tilde\lambda_1+\tilde\lambda_2)=f^{a_1a_2}{}_b\,O_{s_2}^{a_2}(z_2,\tilde\lambda_1+\tilde\lambda_2)$. The first subleading term receives contributions from descendants of both the leading and subleading soft gluon symmetries. Further terms receive contributions from soft gluons that sit at higher orders in the soft expansion.

As expected, (7.36) matches the all-order OPE obtained from the explicit vertex algebra realization coming from twistor string theory [249]. But even though finding such realizations is the ultimate goal of the celestial holography program, computations using explicit vertex operators can be cumbersome and depend intimately on the specific vertex algebra being studied. On the other hand, our bottom-up derivation of the OPE from on-shell recursion is more transparent and relatively more universal.

It also allows us to conclude that *inverse soft recursion for MHV amplitudes is dual to OPE recursion for CCFT correlators.* In this sense, on-shell recursion relations can potentially emerge from flat space holography. Since inverse soft recursion is just BCFW recursion in disguise, we hope that a similar statement might hold for BCFW recursion beyond the MHV sector, but this is left to future work.

7.2.3 Celestial OPE of boost eigenstates

The celestial OPE of boost eigenstates can be found by Mellin transforming the momentum space OPE. This calculation was already performed in [249], so we only repeat the main ideas.

Suppose we restrict to split signature kinematics following the lines of [169]. Decompose the dotted spinor helicity variable associated to a momentum eigenstate operator $O^a_s(z,\tilde\lambda)$ as

$$\tilde\lambda^{\dot\alpha} = \varepsilon\,\omega \begin{pmatrix} 1 \\ \bar z \end{pmatrix}, \quad \varepsilon \in \{\pm 1\}\,,\ \omega \in (0,\infty)\,, \tag{7.38}$$

with $z, \bar z$ now being real and independent. Let $\Delta \in \mathbb{C}$ and $h = (\Delta + s)/2$, $\bar h = (\Delta - s)/2$. Celestial operators dual to boost eigenstates of weight Δ and spin s are found by Mellin transforming the momentum eigenstate operators,

$$O^{\varepsilon,a}_{\Delta,s}(z,\bar z) = \int_0^\infty \frac{\mathrm{d}\omega}{\omega}\,\omega^{2\bar h}\,O^a_s(z,\tilde\lambda)\,. \tag{7.39}$$

Under $\mathrm{SL}(2,\mathbb{R})\times\mathrm{SL}(2,\mathbb{R})$ transformations of $z, \bar z$, these operators transform as conformal primaries of weights $(h,\bar h)$. So the basis of boost eigenstates is also known as a conformal basis, first constructed in [182].

Define the conformal primary positive helicity soft gluons

$$J^a[r](z,\bar z) := \frac{J^a[r](z,\tilde\lambda)}{(\varepsilon\omega)^r} = \sum_{k=0}^{r} \frac{\bar z^{r-k} J^a[k, r-k](z)}{k!(r-k)!}\,. \tag{7.40}$$

Equivalently, one can define $J^a[r]$ through residues of the conformal primary gluon operators [170]. The descendants appearing in their OPE with boost eigenstates are also defined by the usual contour integrals

$$J^a_{-p}[r](\bar z) O^{\varepsilon,b}_{\Delta,s}(w,\bar w) = \oint \frac{\mathrm{d}z}{2\pi\mathrm{i}}\,\frac{1}{(z-w)^p}\,J^a[r](z,\bar z)\,O^{\varepsilon,b}_{\Delta,s}(w,\bar w)\,, \tag{7.41}$$

where the contour surrounds the pole at $z = w$. Let's see how to express the celestial OPE of boost eigenstates in terms of these descendants.

Mellin transforming both sides of (7.36) leads to the following set of integrals:

$$\begin{aligned} &O^{\varepsilon_1,a_1}_{\Delta_1,+}(z_1,\bar z_1)\,O^{\varepsilon_2,a_2}_{\Delta_2,s_2}(z_2,\bar z_2) \\ &= \sum_{p=0}^{\infty} z_{12}^{p-1} \sum_{r=0}^{p}\sum_{q=0}^{p-r}\sum_{m=0}^{\infty} \frac{(-1)^q}{q!m!} \int_0^\infty \mathrm{d}\omega_1\,\omega_1^{2\bar h_1 - 1} \int_0^\infty \mathrm{d}\omega_2\,\omega_2^{2\bar h_2 - 1} (\varepsilon_1\omega_1)^{r+m} \\ &\quad\times \left(\frac{\varepsilon_1\omega_1}{\varepsilon_2\omega_2}\big(\bar z_{12}\bar\partial_2 + \omega_2\partial_{\omega_2}\big)\right)^q \bar z_{12}^m \bar\partial_2^m J^{a_1}_{-p}[r](\bar z_1) O^{a_2}_{s_2}\left(z_2, \frac{(\varepsilon_1\omega_1 + \varepsilon_2\omega_2)}{\varepsilon_2\omega_2}\tilde\lambda_2\right), \end{aligned} \tag{7.42}$$

where $(h_i,\bar h_i) = (\frac{\Delta_i+s_i}{2}, \frac{\Delta_i-s_i}{2})$, and $\bar\partial_i \equiv \partial/\partial\bar z_i$. The sum over m is just the Taylor expansion in $\bar z_{12}$ of the momentum eigenstate on the right of (7.36).

$\varepsilon_1 = \varepsilon_2$. In this case, we can introduce the change of integration variables

$$\omega_1 = t\omega\,, \quad \omega_2 = (1-t)\omega\,, \quad t \in (0,1)\,, \quad \omega \in (0,\infty)\,, \tag{7.43}$$

under which the integral (7.42) turns into (after some math):

$$
\begin{aligned}
&O^{\varepsilon_1,a_1}_{\Delta_1,+}(z_1,\bar z_1)\,O^{\varepsilon_2,a_2}_{\Delta_2,s_2}(z_2,\bar z_2) \\
&= \sum_{p,m=0}^{\infty} z_{12}^{p-1}\sum_{r=0}^{p}\sum_{q=0}^{p-r}\sum_{q'=0}^{q}\sum_{s=0}^{q'}\int_0^\infty \mathrm{d}\omega\,\omega^{2\bar h_1+2\bar h_2-1+r}\int_0^1 \mathrm{d}t\,t^{2\bar h_1-1+r+q+m}(1-t)^{2\bar h_2-q-1} \\
&\quad\times \frac{\varepsilon_1^r(-1)^{q-s}\,\Gamma(-2\bar h_2+q-q'+1)\,\bar z_{12}^{q'+m-s}}{(q-q')!\,s!\,(q'-s)!(m-s)!\,\Gamma(-2\bar h_2+1)}\bar\partial_2^{q'+m-s}J^{a_1}_{-p}[r](\bar z_1)O^{a_2}_{s_2}\left(z_2,\frac{(\varepsilon_1\omega_1+\varepsilon_2\omega_2)}{\varepsilon_2\omega_2}\tilde\lambda_2\right).
\end{aligned}
\tag{7.44}
$$

Performing the Mellin transform as well as the summation we finally get:

$$
\boxed{
\begin{aligned}
O^{\varepsilon_1,a_1}_{\Delta_1,+}(z_1,\bar z_1)\,O^{\varepsilon_2,a_2}_{\Delta_2,s_2}(z_2,\bar z_2) &= \sum_{p,\bar m=0}^{\infty}\sum_{r=0}^{p}\frac{\varepsilon_1^r}{\bar m!}B(2\bar h_1+r+\bar m,2\bar h_2)\frac{\Gamma(2\bar h_1+p+1)}{(p-r)!\,\Gamma(2\bar h_1+r+1)} \\
&\quad\times z_{12}^{p-1}\,\bar z_{12}^{\bar m}\bar\partial_2^{\bar m}\,J^{a_1}_{-p}[r](\bar z_1)O^{\varepsilon_1,a_2}_{\Delta_1+\Delta_2+r-1,s_2}(z_2,\bar z_2).
\end{aligned}}
\tag{7.45}
$$

We have put the derivation details in Appendix 7.7.

$\varepsilon_1=-\varepsilon_2$**.** The OPE when $\varepsilon_1=-\varepsilon_2$ gives a similar formula only that there are two terms produced corresponding to different ingoing/outgoing directions:

$$
\boxed{
\begin{aligned}
&O^{\varepsilon_1,a_1}_{\Delta_1,+}(z_1,\bar z_1)\,O^{\varepsilon_2,a_2}_{\Delta_2,s_2}(z_2,\bar z_2) \\
&= \sum_{p,\bar m=0}^{\infty}\sum_{r=0}^{p}\frac{\varepsilon_2^r}{\bar m!}(-1)^{r+\bar m}B(2\bar h_1+r+\bar m,-2\bar h_1-2\bar h_2-r-\bar m+1)\,\frac{\Gamma(2\bar h_1+p+1)}{(p-r)!\,\Gamma(2\bar h_1+r+1)} \\
&\qquad\qquad\times z_{12}^{p-1}\,\bar z_{12}^{\bar m}\bar\partial_2^{\bar m}\,J^{a_1}_{-p}[r](\bar z_1)O^{\varepsilon_2,a_2}_{\Delta_1+\Delta_2+r-1,s_2}(z_2,\bar z_2) \\
&\quad+\sum_{p,\bar m=0}^{\infty}\sum_{r=0}^{p}\frac{\varepsilon_1^r}{\bar m!}B(-2\bar h_1-2\bar h_2-r-\bar m+1,2\bar h_2)\,\frac{\Gamma(2\bar h_1+p+1)}{(p-r)!\,\Gamma(2\bar h_1+r+1)} \\
&\qquad\qquad\times z_{12}^{p-1}\,\bar z_{12}^{\bar m}\bar\partial_2^{\bar m}\,J^{a_1}_{-p}[r](\bar z_1)O^{\varepsilon_2,a_2}_{\Delta_1+\Delta_2+r-1,s_2}(z_1,\bar z_2)\,.
\end{aligned}}
\tag{7.46}
$$

7.3 MHV Graviton OPE

7.3.1 Collinear expansion

A similar story holds for MHV graviton scattering. In the choice of little group fixing $\lambda_i^\alpha=(1,z_i)$, the inverse soft recursion (7.11) for graviton MHV amplitudes takes the form

$$
M(1_+\,2\cdots n)=\sum_{i=3}^{n}\frac{[1i]}{z_{1i}}\frac{z_{i2}^2}{z_{12}^2}\,M(\hat 2\cdots\hat i\cdots n)\,,
\tag{7.47}
$$

wherein the hatted spinor-helicity variables read

$$
\hat{\tilde\lambda}_2=\tilde\lambda_1+\tilde\lambda_2-\frac{z_{12}}{z_{i2}}\,\tilde\lambda_1\,,\qquad \hat{\tilde\lambda}_i=\tilde\lambda_i+\frac{z_{12}}{z_{i2}}\,\tilde\lambda_1\,.
\tag{7.48}
$$

These are the same as for the gluon case.

Once again, we can expand the $(n-1)$-graviton amplitude on the right in small z_{12} by writing it in terms of exponentiations of linear shifts:

$$M(1_+\,2\cdots n) = -\sum_{i=3}^{n}\frac{z_{i2}[1i]}{z_{12}^2}\left(1-\frac{z_{12}}{z_{i2}}\right)^{-1}\exp\left\{\frac{z_{12}}{z_{i2}}\big([1\partial_i]-[1\partial_2]\big)\right\}M(\mathbf{2}\cdots n)\,. \tag{7.49}$$

On the right, gravitons $3,\dots,n$ carry the undeformed null momenta $p_3,\dots,p_n$, whereas the graviton 2 in bold carries the deformed null momentum $\mathbf{p}_2^{\alpha\dot\alpha} = \lambda_2^\alpha(\tilde\lambda_1+\tilde\lambda_2)^{\dot\alpha}$. Expanding this in z_{12}, one finds the all-order collinear expansion

$$M(1_+\,2\cdots n) = -\sum_{p=0}^{\infty} z_{12}^{p-2}\sum_{q=0}^{p}\sum_{r=0}^{q}\frac{(-[1\partial_2])^{q-r}}{r!(q-r)!}\sum_{i=3}^{n}\frac{[1i][1\partial_i]^r}{z_{i2}^{p-1}}\,M(\mathbf{2}\cdots n)\,. \tag{7.50}$$

Naively, it appears that this expansion starts at order $1/z_{12}^2$ instead of the universal collinear pole $1/z_{12}$ expected in a (tree level) holomorphic collinear limit. This is actually a spurious pole that drops out due to momentum conservation.

To see this, recall that our $(n-1)$-point amplitude $M(\mathbf{2}\,3\cdots n)$ comes equipped with delta functions imposing the momentum conservation

$$\mathbf{p}_2^{\alpha\dot\alpha} + p_3^{\alpha\dot\alpha} + \cdots + p_n^{\alpha\dot\alpha} = 0\,. \tag{7.51}$$

Contracting this with $\lambda_2^\alpha\tilde\lambda_1^{\dot\alpha}$ and using the fact that $\langle i2\rangle = z_{i2}$, we get the conservation law

$$\sum_{i=3}^{n}\langle i2\rangle[1i] \equiv \sum_{i=3}^{n} z_{i2}[1i] = 0\,. \tag{7.52}$$

Hence, if we write out the term of order $1/z_{12}^2$ in the expansion (7.50), we find that it vanishes:

$$-\frac{1}{z_{12}^2}\sum_{i=3}^{n} z_{i2}[1i]\,M(\mathbf{2}\cdots n) = 0\,. \tag{7.53}$$

This confirms that the collinear limit starts at order $1/z_{12}$.

So, dropping the $p=0$ term in the sum (7.50), we can shift the summation index $p\mapsto p+1$ to find the collinear expansion

$$\boxed{M(1_+\,2\cdots n) = -\sum_{p=0}^{\infty} z_{12}^{p-1}\sum_{q=0}^{p+1}\sum_{r=0}^{q}\frac{(-[1\partial_2])^{q-r}}{r!(q-r)!}\sum_{i=3}^{n}\frac{[1i][1\partial_i]^r}{z_{i2}^{p}}\,M(\mathbf{2}\cdots n)\,.} \tag{7.54}$$

This is our result for the all-order collinear expansion of the tree level graviton MHV amplitude. Next let us turn this into OPE expansions.

7.3.2 Celestial OPE of momentum eigenstates

Like in gauge theory, it is expected that there exist local operators $G_{s_i}(z_i,\tilde\lambda_i)$ dual to graviton momentum eigenstates of helicity $s_i\in\{\pm2\}$ and spinor-helicity data $\lambda_i^\alpha = (1,z_i)$, $\tilde\lambda_i^{\dot\alpha} = \omega_i(1,\bar z_i)$. Their correlators should compute graviton amplitudes in the bulk,

$$M(1\,2\cdots n) = \left\langle G_{s_1}(z_1,\tilde\lambda_1)\,G_{s_2}(z_2,\tilde\lambda_2)\cdots G_{s_n}(z_n,\tilde\lambda_n)\right\rangle\,. \tag{7.55}$$

Combining this with the collinear expansion (7.54), we can once again extract the all-order OPE in the MHV sector. Let us begin by recalling the notion of soft graviton currents.

Soft graviton currents. The soft expansion of a positive helicity graviton operator – as valid at least within an MHV correlator – is given by the double Taylor expansion[7]

$$G_+(z,\tilde\lambda) = \sum_{k,\ell=0}^{\infty} \frac{(\tilde\lambda^{\dot 1})^k(\tilde\lambda^{\dot 2})^\ell}{k!\,\ell!}\,\mathrm{w}[k,\ell](z)\,. \tag{7.56}$$

The chiral operators $\mathrm{w}[k,\ell](z)$ are currents with weights $h = 2 - \frac{k+\ell}{2}$ with respect to the conformal transformations of z. The currents at fixed $k+\ell$ also transform in a spin $\frac{k+\ell}{2}$ representation of the $\mathrm{SL}(2,\mathbb{C})$ that rotates $\tilde\lambda^{\dot\alpha}$. As shown by Strominger [168], the celestial OPEs of these currents form the loop algebra of $\mathrm{Ham}(\mathbb{C}^2)$, the holomorphic symplectomorphisms of $\mathbb{C}^2$. In the celestial holography literature, $\mathrm{Ham}(\mathbb{C}^2)$ is also referred to as the wedge subalgebra of $w_{1+\infty}$, which motivated the notation $\mathrm{w}[k,\ell]$ for the currents. The weight $h=2$ current $\mathrm{w}[0,0]$ actually turns out to be central, and its insertions in celestial correlators do not give rise to a nontrivial soft theorem. But it is usually left in for completeness.

The first step in deriving the celestial OPE is again to extract the singular terms in the OPE. The singular parts of the MHV collinear expansion are read off from (7.54),

$$M(1_+\,2\cdots n) = -\frac{1}{z_{12}}\left(\sum_{i=3}^{n}[1i] - \sum_{i=3}^{n}[1i][1\partial_2] + \sum_{i=3}^{n}[1i][1\partial_i]\right) M(\mathbf{2}\cdots n) + \mathrm{O}(z_{12}^0)\,. \tag{7.57}$$

Since $\lambda_i^1 = 1$ in our choice of little group fixing, specific components of the $(n-1)$-point momentum and angular momentum conservation laws give the constraints

$$\sum_{i=3}^{n}[1i]\,M(\mathbf{2}\cdots n) = -[12]\,M(\mathbf{2}\cdots n)\,, \tag{7.58}$$

$$\sum_{i=3}^{n}[1i][1\partial_i]M(\mathbf{2}\cdots n) = -[12][1\partial_2]M(\mathbf{2}\cdots n)\,, \tag{7.59}$$

thereby reducing the collinear limit to

$$M(1_+\,2\cdots n) = \frac{[12]}{z_{12}}\,M(\mathbf{2}\cdots n) + \mathrm{O}(z_{12}^0)\,. \tag{7.60}$$

Applying the duality dictionary (7.55), the singular part of the hard graviton OPE is found to be

$$G_+(z_1,\tilde\lambda_1)\,G_{s_2}(z_2,\tilde\lambda_2) \sim \frac{[12]}{z_{12}}\,G_{s_2}(z_2,\tilde\lambda_1+\tilde\lambda_2)\,. \tag{7.61}$$

This is the graviton celestial OPE of [166, 170] written in momentum space. It is leading order in z_{12} and all-order exact in $\bar z_{12}$.

Setting $s_2 = +2$, Taylor expanding both sides in $\tilde\lambda_1^{\dot\alpha}$ and $\tilde\lambda_2^{\dot\alpha}$, and equating coefficients of $(\tilde\lambda_1^{\dot 1})^k(\tilde\lambda_1^{\dot 2})^\ell(\tilde\lambda_2^{\dot 1})^m(\tilde\lambda_2^{\dot 2})^n$ yields the soft graviton current algebra (see Appendix 7.6 for details)

$$\mathrm{w}[k,\ell](z)\,\mathrm{w}[m,n](w) \sim \frac{kn-\ell m}{z-w}\,\mathrm{w}[k+m-1,\ell+n-1](w)\,. \tag{7.62}$$

[7] Again, this starts at order ω^0 instead of the usual soft graviton pole ω^{-1} due to our choice of little group fixing.

As mentioned above, this is the loop algebra of $\mathrm{Ham}(\mathbb{C}^2)$.[8] It provides an infinite dimensional enhancement of the holographic symmetries of quantum gravity in flat space whose implications are still being fervently investigated. The origin of these symmetries is again found in the twistor theory of Penrose's nonlinear graviton construction [207].

For our purposes, we will again be interested in working with their generating functions

$$\mathrm{w}[r](z,\tilde\lambda) = \sum_{k=0}^{r} \frac{(\tilde\lambda^{\dot 1})^k(\tilde\lambda^{\dot 2})^{r-k}}{k!(r-k)!}\,\mathrm{w}[k,r-k](z)\,, \qquad r\in\mathbb{Z}_{\geq 0}\,. \tag{7.63}$$

The hard gravitons can be expanded upon these as

$$G_+(z,\tilde\lambda) = \sum_{r=0}^{\infty}\mathrm{w}[r](z,\tilde\lambda)\,, \tag{7.64}$$

where the r^{th} term is essentially ω^r times the r^{th} order soft graviton. From (7.61), one finds a compact expression for the OPE of soft gravitons with hard gravitons,

$$\mathrm{w}[r](z_1,\tilde\lambda_1)\,G_{s_i}(z_i,\tilde\lambda_i) \sim \frac{[1i]}{z_{1i}}\,\frac{[1\partial_i]^{r-1}}{(r-1)!}\,G_{s_i}(z_i,\tilde\lambda_i)\,. \tag{7.65}$$

The boost eigenbasis version of these soft-hard OPEs were found in [196]. The central current $\mathrm{w}[0](z,\tilde\lambda)\equiv\mathrm{w}[0,0](z)$ of course has a regular OPE with all hard gravitons. The $r=1$ OPE is the supertranslation action. The $r=2$ OPE corresponds to superrotations. And the $r=3$ OPE corresponds to the sub-subleading soft graviton theorem of [261].

Soft graviton descendants. Viewing $\mathrm{w}[r](z,\tilde\lambda)$ as chiral currents on the sphere with coordinate z, we define the soft graviton descendants of a hard graviton by the contour integral

$$\mathrm{w}_{-p}[r](\tilde\lambda_1)G_{s_2}(z_2,\tilde\lambda_2) := \oint_{|z_{12}|=\varepsilon}\frac{\mathrm{d}z_1}{2\pi\mathrm{i}}\,\frac{1}{z_{12}^p}\,\mathrm{w}[r](z_1,\tilde\lambda_1)\,G_{s_2}(z_2,\tilde\lambda_2) \tag{7.66}$$

with $\varepsilon\ll 1$ and $p\geq 0$. The $p=0$ term is just meant to be the primary occurring on the right of (7.65), while the $p\geq 1$ descendants correspond to regular terms in the soft-hard OPE.

The current $\mathrm{w}[r](z,\tilde\lambda)$ has weight $h=2-r/2$ under conformal transformations of z, so correlators involving it can have a pole of order at most $r-4$ at $z=\infty$. Using (7.55), (7.65) and a contour-pulling argument that is identical to the gluon case, we then find that for $0\leq r\leq p+2$, an insertion of such a descendant in a correlator of hard gravitons can be expressed purely in terms of hard graviton amplitudes with one fewer particle:

$$\left\langle \mathrm{w}_{-p}[r](\tilde\lambda_1)G_{s_2}(z_2,\tilde\lambda_2)\prod_{i=3}^{n}G_{s_i}(z_i,\tilde\lambda_i)\right\rangle = -\frac{1}{(r-1)!}\sum_{i=3}^{n}\frac{[1i][1\partial_i]^{r-1}}{z_{i2}^p}\,M(2\,3\cdots n)\,. \tag{7.67}$$

After shifting $\tilde\lambda_2\mapsto\tilde\lambda_1+\tilde\lambda_2$ and $r\mapsto r+1$, these are immediately recognized to be the summands of the collinear expansion (7.54).

[8] Equip $\mathbb{C}^2$ with complex coordinates v_1, v_2 and a holomorphic Poisson structure

$$\{f,g\} = \partial_{v_1}f\,\partial_{v_2}g - \partial_{v_2}f\,\partial_{v_1}g\,, \qquad f,g\in\Omega^0(\mathbb{C}^2)\,.$$

Holomorphic symplectomorphisms of $\mathbb{C}^2$ are generated by the basis of holomorphic hamiltonians $v_1^k v_2^\ell$ with algebra $\{v_1^k v_2^\ell, v_1^m v_2^n\} = (kn-\ell m)\,v_1^{k+m-1}v_2^{\ell+n-1}$. The soft graviton currents span the loop algebra of this Poisson algebra.

All-order graviton OPE. Using the duality dictionary (7.55) for graviton scattering, we can rewrite the MHV collinear expansion (7.54) as the OPE expansion

$$\begin{aligned}&\left\langle G_+(z_1,\tilde\lambda_1)\,G_{s_2}(z_2,\tilde\lambda_2)\prod_{i=3}^n G_{s_i}(z_i,\tilde\lambda_i)\right\rangle\\&\quad=\sum_{p=0}^\infty z_{12}^{p-1}\sum_{q=0}^{p+1}\sum_{r=0}^{q}\frac{(-[1\partial_2])^{q-r}}{(q-r)!}\left\langle \mathrm{w}_{-p}[r+1](\tilde\lambda_1)O^{a_2}_{s_2}(z_2,\tilde\lambda_1+\tilde\lambda_2)\prod_{i=3}^n O^{a_i}_{s_i}(z_i,\tilde\lambda_i)\right\rangle\,.\end{aligned}\tag{7.68}$$

Again, $r+1\le p+2$ so our contour manipulations work. This can be further simplified by exchanging the sums over q and r, then shifting $r\mapsto r-1$. When the dust settles, one finds the following all-order OPE for two gravitons in the MHV sector:

$$\boxed{G_+(z_1,\tilde\lambda_1)\,G_{s_2}(z_2,\tilde\lambda_2)=\sum_{p=0}^\infty z_{12}^{p-1}\sum_{r=1}^{p+2}\sum_{q=0}^{p+2-r}\frac{(-[1\partial_2])^q}{q!}\,\mathrm{w}_{-p}[r](\tilde\lambda_1)G_{s_2}(z_2,\tilde\lambda_1+\tilde\lambda_2)\,.}\tag{7.69}$$

For the reader's benefit, we write out the first few terms of this OPE explicitly

$$\begin{aligned}&G_+(z_1,\tilde\lambda_1)\,G_{s_2}(z_2,\tilde\lambda_2)\\=&\frac{1}{z_{12}}\left\{\big(1-[1\partial_2]\big)\,\mathrm{w}_0[1](\tilde\lambda_1)+\mathrm{w}_0[2](\tilde\lambda_1)\right\}G_{s_2}(z_2,\tilde\lambda_1+\tilde\lambda_2)\\&+\left\{\left(1-[1\partial_2]+\frac{[1\partial_2]^2}{2!}\right)\mathrm{w}_{-1}[1](\tilde\lambda_1)+\big(1-[1\partial_2]\big)\,\mathrm{w}_{-1}[2](\tilde\lambda_1)+\mathrm{w}_{-1}[3](\tilde\lambda_1)\right\}G_{s_2}(z_2,\tilde\lambda_1+\tilde\lambda_2)\\&+z_{12}\left\{\left(1-[1\partial_2]+\frac{[1\partial_2]^2}{2!}-\frac{[1\partial_2]^3}{3!}\right)\mathrm{w}_{-2}[1](\tilde\lambda_1)+\left(1-[1\partial_2]+\frac{[1\partial_2]^2}{2!}\right)\mathrm{w}_{-2}[2](\tilde\lambda_1)\right.\\&\qquad\left.+\big(1-[1\partial_2]\big)\,\mathrm{w}_{-2}[3](\tilde\lambda_1)+\mathrm{w}_{-2}[4](\tilde\lambda_1)\right\}G_{s_2}(z_2,\tilde\lambda_1+\tilde\lambda_2)+\mathrm{O}(z_{12}^2)\,.\end{aligned}\tag{7.70}$$

This helps illuminate the pattern of the sums. The first term looks different from (7.61), but can be matched if one remembers from (7.65) that the leading "descendants" are given by $\mathrm{w}_0[r](\tilde\lambda_1)G_{s_2}(z_2,\tilde\lambda_1+\tilde\lambda_2)=[12][1\partial_2]^{r-1}G_{s_2}(z_2,\tilde\lambda_1+\tilde\lambda_2)/(r-1)!$. The remaining terms display the various orders of soft gravitons whose descendants enter the OPE. At the first subleading order, one finds supertranslation, superrotation as well as the sub-subleading soft graviton descendants. At order z_{12}^{p-1}, one only needs to use descendants of soft gravitons up to order $p+2$.

We find it remarkable that this can be expressed purely in terms of the soft graviton descendants (and $\bar L_{-1}=\partial_{\bar z_2}$ descendants if expanded in small $\bar z_{12}$). It does not really require an expansion in holomorphic conformal (or Virasoro) descendants. Moreover, explicit vertex algebra realizations of this OPE (like the ones for the gluon OPE coming from twistor strings [249]) have not been constructed as of the writing of this work. It would be very interesting to see if Skinner's gravitational twistor string [252] could fill in this gap.

7.3.3 Celestial OPE of boost eigenstates

In a similar manner to that of Section 7.2.3, we can study the celestial OPE of graviton boost eigenstates via Mellin transforming the OPE of momentum eigenstates. The boost eigenstates of gravitons are defined in the same way as (7.39). Similar to (7.40), we define the conformal primary positive helicity soft gravitons

$$\mathrm{w}(z,\bar{z}) := \frac{\mathrm{w}(z,\tilde{\lambda})}{(\varepsilon\omega)^r} = \sum_{k=0}^{r} \frac{\bar{z}^{r-k}\mathrm{w}[k,r-k](z)}{k!(r-k)!}\,. \tag{7.71}$$

One can then perform mode expansion over z on $\mathrm{w}(z,\bar{z})$, whose OPE with the boost eigenstates can be obtained by contour integrals

$$\mathrm{w}_{-p}[r](\bar{z})G^{\varepsilon}_{\Delta,s}(w,\bar{w}) = \oint \frac{\mathrm{d}z}{2\pi\mathrm{i}} \frac{1}{(z-w)^p}\, \mathrm{w}[r](z,\bar{z})\, O^{\varepsilon}_{\Delta,s}(w,\bar{w})\,, \tag{7.72}$$

The modes $\mathrm{w}_{-p}[r](\bar{z})$ can be regarded as the generators of soft descendant states. Mellin transforming (7.69) one can get the OPE of boost eigenstates of gravitons in terms of the following integral

$$\begin{aligned}
&G^{\varepsilon_1}_{\Delta_1,+}(z_1,\bar{z}_1)\, G^{\varepsilon_2}_{\Delta_2,s_2}(z_2,\bar{z}_2)\\
&= \sum_{p=0}^{\infty} z_{12}^{p-1} \sum_{r=0}^{p+1}\sum_{q=0}^{p+1-r}\sum_{m=0}^{\infty} \frac{(-1)^q}{q!m!} \int_0^\infty \mathrm{d}\omega_1\, \omega_1^{2\bar{h}_1-1} \int_0^\infty \mathrm{d}\omega_2\, \omega_2^{2\bar{h}_2-1} (\varepsilon_1\omega_1)^{r+m+1}\\
&\quad\times \left(\frac{\varepsilon_1\omega_1}{\varepsilon_2\omega_2}\left(\bar{z}_{12}\bar{\partial}_2 + \omega_2\partial_{\omega_2}\right)\right)^q \bar{z}_{12}^m \bar{\partial}_2^m \mathrm{w}_{-p}[r+1](\bar{z}_1) G^{\varepsilon_1}_{s_2}\left(z_2, \frac{(\varepsilon_1\omega_1+\varepsilon_2\omega_2)}{\varepsilon_2\omega_2}\tilde{\lambda}_2\right).
\end{aligned} \tag{7.73}$$

After some math similar to Appendix 7.7, the final OPE is

$$\boxed{\begin{aligned}
G^{\varepsilon_1}_{\Delta_1,+}(z_1,\bar{z}_1)\, G^{\varepsilon_2}_{\Delta_2,s_2}(z_2,\bar{z}_2) = &\sum_{p,\bar{m}=0}^{\infty}\sum_{r=0}^{p+1} \frac{\varepsilon_1^{r+1}}{\bar{m}!} \frac{B(2\bar{h}_1+r+\bar{m}+1, 2\bar{h}_2)\,\Gamma(2\bar{h}_1+p+3)}{(p-r+1)!\,\Gamma(2\bar{h}_1+r+2)}\\
&\times z_{12}^{p-1}\, \bar{z}_{12}^{\bar{m}}\bar{\partial}_2^{\bar{m}}\, \mathrm{w}_{-p}[r+1](\bar{z}_1) G^{\varepsilon_1}_{\Delta_1+\Delta_2+r-1,s_2}(z_2,\bar{z}_2).
\end{aligned}} \tag{7.74}$$

The boost eigenstate OPE when $\varepsilon_1 = -\varepsilon_2$ is similar only that there are two terms produced corresponding to different ingoing/outgoing directions:

$$\boxed{\begin{aligned}
&G^{\varepsilon_1}_{\Delta_1,+}(z_1,\bar{z}_1)\, G^{\varepsilon_2}_{\Delta_2,s_2}(z_2,\bar{z}_2)\\
&= \sum_{p,\bar{m}=0}^{\infty}\sum_{r=0}^{p+1} \frac{\varepsilon_2^{r+1}}{\bar{m}!}(-1)^{r+\bar{m}+1} \frac{B(2\bar{h}_1+r+\bar{m}+1, -2\bar{h}_1-2\bar{h}_2-r-\bar{m})\,\Gamma(2\bar{h}_1+p+3)}{(p-r+1)!\,\Gamma(2\bar{h}_1+r+2)}\\
&\qquad\times z_{12}^{p-1}\, \bar{z}_{12}^{\bar{m}}\bar{\partial}_2^{\bar{m}}\, \mathrm{w}_{-p}[r+1](\bar{z}_1) G^{\varepsilon_2}_{\Delta_1+\Delta_2+r-1,s_2}(z_2,\bar{z}_2)\\
&\quad+ \sum_{p,\bar{m}=0}^{\infty}\sum_{r=0}^{p+1} \frac{\varepsilon_1^{r+1}}{\bar{m}!} \frac{B(-2\bar{h}_1-2\bar{h}_2-r-\bar{m}, 2\bar{h}_2)\,\Gamma(2\bar{h}_1+p+3)}{(p-r+1)!\,\Gamma(2\bar{h}_1+r+2)}\\
&\qquad\times z_{12}^{p-1}\, \bar{z}_{12}^{\bar{m}}\bar{\partial}_2^{\bar{m}}\, \mathrm{w}_{-p}[r+1](\bar{z}_1) G^{\varepsilon_1}_{\Delta_1+\Delta_2+r-1,s_2}(z_2,\bar{z}_2)\,.
\end{aligned}} \tag{7.75}$$

7.4 Discussion

Regular terms have proven useful for extracting differential equations satisfied by MHV amplitudes from null state decoupling relations in CCFT [165, 164]. Remarkably, these differential equations were already shown to be equivalent to a linearized version of tree level BCFW recursion in [134].

Our calculation confirms that, indeed, the all-order celestial OPE is just a nonlinear extension of this idea that reproduces the exact recursion relation.

One intriguing shortcoming of our analysis is that the recursion relation does not allow us to obtain 3-point amplitudes from 2-point amplitudes. The latter are just meant to be the identity parts of the S-matrix, so that the corresponding 2-point celestial amplitudes tend to take the distributional form $\delta(z_{12})\delta(\bar{z}_{12})$ [139]. This means we do not yet know how to apply our OPE to a 2-point CCFT correlator and obtain the 3- and higher-point correlators. This is an important issue that needs to be resolved before any CCFT interpretation of 4d gauge theory or gravity may be taken seriously. A promising approach to this lies in the use of light and shadow transforms that may be cleverly used to make the 2- and 3-point functions non-distributional [171, 167, 264, 265, 266, 267, 268, 269, 270, 271]. It would be interesting to see if our all-order OPE can be used to build higher-point MHV amplitudes directly starting from a 2-point amplitude made non-distributional in this manner.

Another important issue facing celestial holography is to compute analogues of celestial OPE beyond the MHV sector. The singular part of the OPE is universal and valid for all scattering amplitudes, so it remains the same in N^kMHV amplitudes. At tree level, one expects that only the regular part may be nontrivially deformed.[9] Our calculation of regular terms in the MHV OPE is meant to provide an accessible test case to develop methods for obtaining regular terms in more involved celestial OPEs. In this way, we hope that our results bring us one step closer to bootstrapping flat space amplitudes from constraints imposed by the existence of a celestial dual. Going beyond pure Yang-Mills, along the lines of e.g. [272, 273], or beyond tree level, along the lines of e.g. [274, 153], would also be interesting.

At the first few orders, the gluon OPE was worked out in [242, 164] and the graviton OPE in [165], where holomorphic conformal descendants were found. However, at those orders, due the existence of null states [164, 165, 246], they can be fully converted to soft current descendants and antiholomorphic conformal descendants, consistent with our expressions (see for example [249]). Beyond the first few orders, consistency of our results with the appearance of holomorphic conformal descendants at arbitrarily high orders in z and $\bar{z}$ [242] would require the existence of sufficiently many null states at each order. We leave this as an interesting question for the future. If the exact set of null states can be written down at each order, it would also allow one to write down the OPEs in alternative bases, with different forms useful for different situations.

Perhaps most ambitiously, if one found a way to reverse the logic of our paper and bootstrapped the all-order celestial OPE by other means, it would provide the means of bootstrapping BCFW recursion for MHV tree amplitudes directly from celestial CFT. Now, it turns out that MHV amplitudes as well as celestial OPEs have also been explored at loop level in [239, 275, 46] and in self-dual curved backgrounds in [276, 241, 277]. These works discover that infinite dimensional symmetries like the $\mathrm{w}_{1+\infty}$ algebra persist in a wide range of scenarios, showing the robustness of the formalism of celestial holography. It may be possible to construct regular terms in the associated celestial

[9] Here, one includes terms that are regular in the holomorphic collinear limit but singular in the antiholomorphic one, and vice versa. It is standard to treat these limits as independent limits by complexifying momenta.

OPEs, possibly using symmetry constraints, and derive novel recursion relations for (at least rational parts of) amplitudes at loop level or on curved backgrounds. Perhaps the best success story in this direction is the recent work by Costello on two-loop amplitudes in QCD-like theories [278], wherein we expect the choice of regular terms in the OPE to translate into a choice of conformal block.

7.5 Appendix: Poles at infinity

In going from (7.31) to (7.32), we deformed the contour and dropped the contribution from $z_1 = \infty$. To justify this, we need to check whether the 1-form

$$\frac{\mathrm{d}z_1}{z_{12}^p} \left\langle J^{a_1}[r](z_1, \tilde{\lambda}_1) \prod_{i=2}^{n} O_{s_i}^{a_i}(z_i, \tilde{\lambda}_i) \right\rangle \tag{7.76}$$

has a pole at $z_1 = \infty$ when viewed as a bulk scattering amplitude. We will show that this has no pole at $z_1 = \infty$ precisely for the range

$$0 \leq r \leq p \tag{7.77}$$

that is suggested by the expected behavior of $J^{a_1}[r](z_1, \tilde{\lambda}_1)$ as a current of weight $h = 1 - r/2$.

This is precisely what we will need for extracting the celestial OPE. We only show this explicitly in the gluon case. The corresponding proof in the graviton case involves identical steps taken using Hodges' formula [279] for the MHV graviton amplitude (with rows and columns corresponding to graviton 1 and the two negative helicity gravitons removed, and both reference spinors chosen to be λ_1^α). We will avoid speculating what happens for $r > p$ (or $r > p + 2$ in the graviton case), but this may be related to the residue of MHV amplitudes at infinity as obtained for instance in equation (35) of [280].

To begin with the proof, we postulate as usual that there exist operators $O_{s_i}^{a_i}(z_i, \tilde{\lambda}_i)$ whose correlation function is the gluon MHV amplitude

$$\left\langle \prod_{i=1}^{n} O_{s_i}^{a_i}(z_i, \tilde{\lambda}_i) \right\rangle = \sum_{\sigma \in S_{n-2}} C^{a_1 a_2 a_{\sigma_3} \cdots a_{\sigma_n}} A[1\, 2\, \sigma_3 \cdots \sigma_n]\,, \tag{7.78}$$

where $A[1\,2\,3 \cdots n]$ is the Parke-Taylor color-stripped amplitude

$$A[1\,2\,3 \cdots n] = \frac{z_{kl}^4}{z_{12} z_{23} \cdots z_{n1}}\, \delta^4(p_1 + p_2 + \cdots + p_n) \tag{7.79}$$

written for the configuration in which particles k, l are negative helicity. For sake of simplicity, we are setting $\lambda_i^\alpha = (1, z_i), \tilde{\lambda}_i^{\dot{\alpha}} = \omega_i(1, \bar{z}_i)$ from the start.

As before, take particle 1 to be positive helicity without loss of generality. The soft-hard correlator

$$\left\langle J^{a_1}[r](z_1, \tilde{\lambda}_1) \prod_{i=2}^{n} O_{s_i}^{a_i}(z_i, \tilde{\lambda}_i) \right\rangle \tag{7.80}$$

is obtained by expanding the MHV amplitude as a series in $\tilde{\lambda}_1^{\dot{\alpha}}$. At the level of the Parke-Taylor amplitude, one finds the series expansion

$$A[1_+\,2\,3\cdots n] = \frac{z_{n2}}{z_{12}z_{n1}}\sum_{r=0}^{\infty}\frac{1}{r!}\,\mathcal{D}^r A[2\,3\cdots n]\,, \tag{7.81}$$

where $\mathcal{D}$ is the differential operator

$$\mathcal{D} = \frac{1}{z_{kl}}\left(z_{1l}[1\partial_k] - z_{1k}[1\partial_l]\right)\,. \tag{7.82}$$

This expansion may be obtained by using a Fourier representation of the momentum conserving delta functions,

$$\delta^4(p_1+p_2+\cdots+p_n) = \int \mathrm{d}^4x\sum_{r=0}^{\infty}\frac{(\mathrm{i}p_1\cdot x)^r}{r!}\,\epsilon^{\mathrm{i}(p_2+\cdots+p_n)\cdot x}\,, \tag{7.83}$$

and applying the identity

$$x^{\alpha\dot{\alpha}}\,\epsilon^{\mathrm{i}(p_k+p_l)\cdot x} = \frac{-\mathrm{i}}{\langle kl\rangle}\left(\lambda_k^{\alpha}\frac{\partial}{\partial\tilde{\lambda}_{l\dot{\alpha}}} - \lambda_l^{\alpha}\frac{\partial}{\partial\tilde{\lambda}_{k\dot{\alpha}}}\right)\epsilon^{\mathrm{i}(p_k+p_l)\cdot x} \tag{7.84}$$

to replace the factors of $(\mathrm{i}p_1\cdot x)^r$ by derivatives in the external data.

Since $\mathcal{D}$ is homogeneous of degree 1 in $\tilde{\lambda}_1^{\dot{\alpha}}$ (and thereby also in ω_1), (7.80) gets contributions only from terms of order $\mathcal{D}^r$ in each color order. This allows us to obtain the r^{th} soft-limit

$$\left\langle J^{a_1}[r](z_1,\tilde{\lambda}_1)\prod_{i=2}^{n}O_{s_i}^{a_i}(z_i,\tilde{\lambda}_i)\right\rangle = \sum_{\sigma\in S_{n-2}} C^{a_1a_2a_{\sigma_3}\cdots a_{\sigma_n}}\frac{z_{\sigma_n2}}{z_{12}z_{\sigma_n1}}\frac{1}{r!}\,\mathcal{D}^r A[2\,\sigma_3\cdots\sigma_n] \tag{7.85}$$

which has weight r in ω_1 as needed. (The actual soft limit is then obtained by dividing out the factor of ω_1^r, but it is innocuous here so we leave it be.)

To complete the proof, we observe from (7.82) that $\mathcal{D}$ has a pole of order 1 at $z_1=\infty$. So $\mathcal{D}^r$ has a pole of order r. Because the extra factors of $z_{\sigma_n2}/z_{12}z_{\sigma_n1}$ have a second order zero, each summand in the net soft-hard correlator (7.85) has a pole of order $r-2$ at $z_1=\infty$. On the other hand, the 1-form $\mathrm{d}z_1$ has a pole of order 2 at infinity, while the prefactor z_{12}^{-p} has a zero of order p. In total, (7.76) behaves like

$$z_1^{r-2+2-p} = z_1^{r-p} \tag{7.86}$$

at large z_1. And as we wished to prove, this is regular at infinity for $r\leq p$.

As an aside, notice that although the hard amplitude depended on z_1 in a distributional manner via its momentum conserving delta functions, the soft-hard amplitude only depends on z_1 rationally! So it makes sense to study its contour integrals as a function of z_1.

7.6 Appendix: Soft current OPEs

In this appendix, we obtain all-order OPEs between soft currents of both gluons and gravitons from momentum eigenstate hard-hard OPEs. Incidentally, the same results can be obtained from Mellin-transformed (boost eigenstate) OPEs.

7.6.1 All-order soft gluon OPE

Consider gluons first. From the definition (7.21), the soft currents are given by its inverse form

$$J^a[m,n](z) = \oint \frac{\mathrm{d}\tilde{\lambda}^{\dot{1}}}{2\pi\mathrm{i}\tilde{\lambda}^{\dot{1}}} \frac{\mathrm{d}\tilde{\lambda}^{\dot{2}}}{2\pi\mathrm{i}\tilde{\lambda}^{\dot{2}}} (\tilde{\lambda}^{\dot{1}})^{-m} (\tilde{\lambda}^{\dot{2}})^{-n}\; m!\, n!\; O^a_+[z,\tilde{\lambda}]. \tag{7.87}$$

Then the current OPE can be extracted by performing the integral

$$\begin{aligned} &J^a[k,l](z) J^b[m,n](w) \\ &= \oint \frac{\mathrm{d}\tilde{\lambda}^{\dot{1}}}{2\pi\mathrm{i}\tilde{\lambda}^{\dot{1}}} \frac{\mathrm{d}\tilde{\lambda}^{\dot{2}}}{2\pi\mathrm{i}\tilde{\lambda}^{\dot{2}}} \frac{\mathrm{d}\tilde{\kappa}^{\dot{1}}}{2\pi\mathrm{i}\tilde{\kappa}^{\dot{1}}} \frac{\mathrm{d}\tilde{\kappa}^{\dot{2}}}{2\pi\mathrm{i}\tilde{\kappa}^{\dot{2}}} \frac{k!\, l!\, m!\, n!}{(\tilde{\lambda}^{\dot{1}})^k (\tilde{\lambda}^{\dot{2}})^l (\tilde{\kappa}^{\dot{1}})^m (\tilde{\kappa}^{\dot{2}})^n} O^a_+[z,\tilde{\lambda}] O^b_+[w,\tilde{\kappa}]. \end{aligned} \tag{7.88}$$

Let us first look at the leading order calculation (in $z-w$), which already contains the main conceptual steps. The all-order calculation is analogous and will be presented afterwards. At leading order, the OPE between two positive-helicity hard gluons is given in (7.25) with s_2 set to $+1$:

$$O^a_+(z,\tilde{\lambda})\, O^b_+(w,\tilde{\kappa}) \sim \frac{f^{ab}{}_c}{z-w}\; O^c_+(w,\tilde{\lambda}+\tilde{\kappa}). \tag{7.89}$$

The hard gluon $O^c_+(w,\tilde{\lambda}+\tilde{\kappa})$ has the soft expansion

$$O^c_+(w,\tilde{\lambda}+\tilde{\kappa}) = \sum_{u,v=0}^{\infty} \frac{(\tilde{\lambda}^{\dot{1}}+\tilde{\kappa}^{\dot{1}})^u (\tilde{\lambda}^{\dot{2}}+\tilde{\kappa}^{\dot{2}})^v}{u!\, v!}\; J^c[u,v](w)\,, \tag{7.90}$$

which after binomial expansions becomes

$$O^c_+(w,\tilde{\lambda}+\tilde{\kappa}) = \sum_{u,v}^{\infty} \sum_{i=0}^{u} \sum_{j=0}^{v} \binom{u}{i}\binom{v}{j} (\tilde{\lambda}^{\dot{1}})^i (\tilde{\kappa}^{\dot{1}})^{u-i} (\tilde{\lambda}^{\dot{2}})^j (\tilde{\kappa}^{\dot{2}})^{v-j} \frac{J^c[u,v](w)}{u!v!}. \tag{7.91}$$

This can now be substituted into (7.88) to obtain

$$\begin{aligned} &J^a[k,l](z) J^b[m,n](w) \\ &\sim \frac{f^{ab}{}_c}{z-w} \binom{k+m}{k}\binom{l+n}{m} k!l!m!n! \frac{1}{(k+m)!(l+n)!} J^c[k+m,l+n](w) \\ &= \frac{f^{ab}{}_c}{z-w} J^c[k+m,l+n](w), \end{aligned} \tag{7.92}$$

where we have used the fact that only the term with $i=k$, $u-i=m$, $j=l$ and $v-j=n$ gets picked up by the contour integrals.

Now repeat the steps while keeping to all orders. The all-order hard-hard gluon OPE was given in (7.36). Since $J^a_{-p}[r](\tilde{\lambda})$ appears in the OPE and depends on $\tilde{\lambda}$, we need to expand it out to perform the explicit contour integrations. Combining (7.27) and (7.30) leads to the expansion

$$J^a_{-p}[r](\tilde{\lambda}) = \sum_{s=0}^{r} \frac{(\tilde{\lambda}^{\dot{1}})^s (\tilde{\lambda}^{\dot{2}})^{r-s}}{s!\,(r-s)!}\; J^a_{-p}[s,r-s]. \tag{7.93}$$

Another object in (7.36) that needs expansion is

$$[\tilde{\lambda}\partial_{\tilde{\kappa}}]^q = \sum_{t=0}^{q} \binom{q}{t} \left(\tilde{\lambda}^{\dot{1}} \frac{\partial}{\partial\tilde{\kappa}^{\dot{1}}}\right)^t \left(\tilde{\lambda}^{\dot{2}} \frac{\partial}{\partial\tilde{\kappa}^{\dot{2}}}\right)^{q-t}. \tag{7.94}$$

With that, the soft current OPE can now be easily obtained. Substituting (7.30), (7.94) and (7.91) into (7.36), and then the resulting expression into (7.88), we obtain

$$\begin{aligned} &J^a[k,l](z)J^b[m,n](w) \\ &=\sum_{p=0}^{\infty}(z-w)^{p-1}\sum_{r=0}^{p}\sum_{q=0}^{p-r}\sum_{s=0}^{r}\sum_{t=0}^{q}(-1)^q\binom{k}{s}\binom{l}{r-s}\binom{k-s}{t}\binom{l-(r-s)}{q-t} \\ &\times J^a_{-p}[s,r-s]J^b[k+m-s,l+n-(r-s)](w). \end{aligned} \tag{7.95}$$

Similar to before, to arrive at this expression, we have performed the contour integrals which picked up terms satisfying

$$s+i+t=k, \quad u-i-t=m, \quad r-s+j+q-t=l, \quad v-j-q+t=n. \tag{7.96}$$

Not all terms in the sums necessarily contribute. In fact, during the derivation, one has to be careful with two types of conditions. One arises from the fact that taking too many derivatives (with respect to $\tilde{\kappa}^{\dot{1}}$ and $\tilde{\kappa}^{\dot{2}}$ in our case) would result in zero, and this requires $t \leq u-i$ and $q-t \leq v-j$. The other type of conditions comes from the ranges of u, v, i and j in (7.91). After carefully treating them, we find that only terms with

$$s \leq k+m, \quad r-s \leq l+n, \quad s+t \leq k, \quad r-s+q-t \leq l \tag{7.97}$$

contribute to the sum. The formula written above is, however, still correct, owning to the fact that $J^a[m,n]=0$ when either m or n is negative and that $\binom{m}{n}=0$ when $m<n$.

Performing the summations over q and t leads to

$$\boxed{\begin{aligned} J^a[k,l](z)J^b[m,n](w) = &\sum_{p=0}^{\infty}(z-w)^{p-1}\sum_{r=0}^{p}\sum_{s=0}^{r}\binom{k}{s}\binom{l}{r-s}\binom{p-k-l}{p-r} \\ &\times J^a_{-p}[s,r-s]J^b[k+m-s,l+n-(r-s)](w). \end{aligned}} \tag{7.98}$$

If desired, this can be written in an alternative form by swapping the order of summations and relabeling, leading to

$$\begin{aligned} J^a[k,l](z)J^b[m,n](w) = &\sum_{p=0}^{\infty}(z-w)^{p-1}\sum_{s=0}^{p}\sum_{r=0}^{p-s}\binom{k}{s}\binom{l}{r}\binom{p-k-l}{p-r-s} \\ &\times J^a_{-p}[s,r]J^b[k+m-s,l+n-r](w). \end{aligned} \tag{7.99}$$

7.6.2 All-order soft graviton OPE

The soft graviton current OPE can be derived in exactly the same way, with the analogue of (7.95) being

$$\begin{aligned} &\mathrm{w}[k,l](z)\mathrm{w}[m,n](w) \\ &=\sum_{p=0}^{\infty}(z-w)^{p-1}\sum_{r=1}^{p+2}\sum_{q=0}^{p+2-r}\sum_{s=0}^{r}\sum_{t=0}^{q}(-1)^q\binom{k}{s}\binom{l}{r-s}\binom{k-s}{t}\binom{l-(r-s)}{q-t} \\ &\times \mathrm{w}_{-p}[s,r-s]\mathrm{w}[k+m-s,l+n-(r-s)](w). \end{aligned} \tag{7.100}$$

Performing the summations over q and t gives

$$\boxed{\begin{aligned}\mathrm{w}[k,l](z)\mathrm{w}[m,n](w) = &\sum_{p=0}^{\infty}(z-w)^{p-1}\sum_{r=1}^{p+2}\sum_{s=0}^{r}\binom{k}{s}\binom{l}{r-s}\binom{p+2-k-l}{p+2-r} \\ &\times \mathrm{w}_{-p}[s,r-s]\mathrm{w}[k+m-s,l+n-(r-s)](w).\end{aligned}} \tag{7.101}$$

Unlike the gluon case, the r and s sums cannot be swapped to give a simpler expression.

7.7 Appendix: Mellin transforms of momentum space OPEs

In this section we provide the computation details for the OPE of boost eigenstates when $\varepsilon_1 = \varepsilon_2$. Starting from (7.42), we first use the identity:

$$\begin{aligned}&\left(\frac{\varepsilon_1\omega_1}{\varepsilon_2\omega_2}\left(\bar{z}_{12}\bar{\partial}_2 + \omega_2\partial_{\omega_2}\right)\right)^q \\ &= \sum_{q'=0}^{q}\frac{q!}{q'!\,(q-q')!}\left(\frac{\varepsilon_1\omega_1}{\varepsilon_2\omega_2}\omega_2\partial_{\omega_2}\right)^{q-q'}\left(\frac{\varepsilon_1\omega_1}{\varepsilon_2\omega_2}\right)^{q'}\bar{z}_{12}^{q'}\bar{\partial}_2^{q'} \\ &= \sum_{q'=0}^{q}\frac{q!}{q'!\,(q-q')!}\left(\frac{\varepsilon_1\omega_1}{\varepsilon_2\omega_2}\right)^{q}\Big(\omega_2\partial_{\omega_2}-q+1\Big)\cdots\Big(\omega_2\partial_{\omega_2}-q'\Big)\,\bar{z}_{12}^{q'}\bar{\partial}_2^{q'}\,.\end{aligned} \tag{7.102}$$

Now we can see there are two contributions of $\bar{\partial}_2$: one is from $\bar{z}_{12}^{q'}\bar{\partial}_2^{q'}$ above, the other is from $\bar{z}_{12}^{m}\bar{\partial}_2^{m}$ in (7.42). We prefer to merge them together:

$$\begin{aligned}\left(\bar{z}_{12}^{q'}\bar{\partial}_2^{q'}\right)\left(\bar{z}_{12}^{m}\bar{\partial}_2^{m}\right) &= \sum_{s=0}^{q'}\binom{q'}{s}(-1)^s m\cdots(m-s+1)\bar{z}_{12}^{q'}\,\bar{z}_{12}^{m-s}\,\bar{\partial}_2^{q'-s}\,\bar{\partial}_2^{m} \\ &= \sum_{s=0}^{q'}(-1)^s\frac{q'!\,m!}{s!(q'-s)!(m-s)!}\bar{z}_{12}^{m-s}\,\bar{\partial}_2^{q_2-s}\,.\end{aligned} \tag{7.103}$$

Plugging (7.102) and (7.103) into (7.42), we get

$$\begin{aligned}&O^{\varepsilon_1,a_1}_{\Delta_1,+}(z_1,\bar{z}_1)\,O^{\varepsilon_2,a_2}_{\Delta_2,s_2}(z_2,\bar{z}_2) \\ &= \sum_{p=0}^{\infty}z_{12}^{p-1}\sum_{r=0}^{p}\sum_{q=0}^{p-r}\sum_{m=0}^{\infty}\sum_{q'=0}^{q}\sum_{s=0}^{q'}\int_0^\infty \mathrm{d}\omega_1\,\omega_1^{2\bar{h}_1-1}\int_0^\infty \mathrm{d}\omega_2\,\omega_2^{2\bar{h}_2-1} \\ &\quad\times\frac{(-1)^{q-s}}{q'!\,s!(q'-s)!(m-s)!}\frac{(\varepsilon_1\omega_1)^{q+r}}{(\varepsilon_2\omega_2)^q}\left(\omega_2\partial_{\omega_2}+1\right)\cdots\left(\omega_2\partial_{\omega_2}-q'\right) \\ &\quad\times\left(\frac{\varepsilon_1\omega_1}{\varepsilon_1\omega_1+\varepsilon_2\omega_2}\right)^m\bar{z}_{12}^{q'+m-s}\bar{\partial}_2^{q'+m-s}J^{a_1}_{-p}[r](\bar{z}_1)O^{a_2}_{s_2}\left(z_2,\frac{(\varepsilon_1\omega_1+\varepsilon_2\omega_2)}{\varepsilon_2\omega_2}\tilde{\lambda}_2\right) \\ &= \sum_{p=0}^{\infty}z_{12}^{p-1}\sum_{r=0}^{p}\sum_{q=0}^{p-r}\sum_{m=0}^{\infty}\sum_{q'=0}^{q}\sum_{s=0}^{q'}\int_0^\infty \mathrm{d}\omega_1\,\omega_1^{2\bar{h}_1-1}\int_0^\infty \mathrm{d}\omega_2\,\omega_2^{2\bar{h}_2-1} \\ &\quad\times\frac{(-1)^{q-s}}{q'!\,s!(q'-s)!(m-s)!}\frac{(\varepsilon_1\omega_1)^{q+r}}{(\varepsilon_2\omega_2)^q}\left(-2\bar{h}_2+1\right)\cdots\left(-2\bar{h}_2+q'\right)\end{aligned}$$

$$\times \left(\frac{\varepsilon_1\omega_1}{\varepsilon_1\omega_1+\varepsilon_2\omega_2}\right)^m \bar{z}_{12}^{q'+m-s}\bar{\partial}_2^{q'+m-s} J^{a_1}_{-p}[r](\bar{z}_1) O^{a_2}_{s_2}\left(z_2, \frac{(\varepsilon_1\omega_1+\varepsilon_2\omega_2)}{\varepsilon_2\omega_2}\tilde{\lambda}_2\right). \tag{7.104}$$

Taking $\varepsilon_1 = \varepsilon_2$ and use the change of integration variables

$$\omega_1 = t\omega\,, \quad \omega_2 = (1-t)\omega\,, \quad t\in(0,1)\,, \quad \omega\in(0,\infty)\,, \tag{7.105}$$

the OPE (7.104) turns into:

$$\begin{aligned}
&O^{\varepsilon_1,a_1}_{\Delta_1,+}(z_1,\bar{z}_1)\, O^{\varepsilon_2,a_2}_{\Delta_2,s_2}(z_2,\bar{z}_2)\\
&=\sum_{p=0}^{\infty} z_{12}^{p-1}\sum_{r=0}^{p}\sum_{q=0}^{p-r}\sum_{m=0}^{\infty}\sum_{q'=0}^{q}\sum_{s=0}^{q'}\int_0^\infty \mathrm{d}\omega\ \omega^{2\bar{h}_1+2\bar{h}_2-1+r}\int_0^1 \mathrm{d}t\ t^{2\bar{h}_1-1+r+q+m}\,(1-t)^{2\bar{h}_2-1-q}\\
&\quad\times \frac{\varepsilon_1^r\,(-1)^{q-s}(-2\bar{h}_2+q-q')!}{(q-q')!s!\,(q'-s)!(m-s)!(-2\bar{h}_2)!}\bar{z}_{12}^{q'+m-s}\bar{\partial}_2^{q'+m-s}J^{a_1}_{-p}[r](\bar{z}_1)O^{a_2}_{s_2}\left(z_2,\frac{(\varepsilon_1\omega_1+\varepsilon_2\omega_2)}{\varepsilon_2\omega_2}\tilde{\lambda}_2\right),
\end{aligned} \tag{7.106}$$

which equals (7.44). The t-integral produces an Euler-Beta function:

$$\begin{aligned}
&O^{\varepsilon_1,a_1}_{\Delta_1,+}(z_1,\bar{z}_1)\, O^{\varepsilon_2,a_2}_{\Delta_2,s_2}(z_2,\bar{z}_2)\\
&=\sum_{p=0}^{\infty} z_{12}^{p-1}\sum_{r=0}^{p}\sum_{q=0}^{p-r}\sum_{m=0}^{\infty}\sum_{q'=0}^{q}\sum_{s=0}^{q'}\int_0^\infty \mathrm{d}\omega\ \omega^{2\bar{h}_1+2\bar{h}_2-1+r}\,\frac{\Gamma(2\bar{h}_2-q)\Gamma(2\bar{h}_1+r+q+m)}{\Gamma(2\bar{h}_1+2\bar{h}_2+r+m)}\\
&\quad\times \frac{\varepsilon_1^r\,(-1)^{q-s}(-2\bar{h}_2+q-q')!}{(q-q')!s!\,(q'-s)!(m-s)!(-2\bar{h}_2)!}\bar{z}_{12}^{q'+m-s}\bar{\partial}_2^{q'+m-s}J^{a_1}_{-p}[r](\bar{z}_1)O^{a_2}_{s_2}\left(z_2,\frac{(\varepsilon_1\omega_1+\varepsilon_2\omega_2)}{\varepsilon_2\omega_2}\tilde{\lambda}_2\right).
\end{aligned} \tag{7.107}$$

Since the total power of $\bar{z}_{12}$ and $\bar{\partial}_2$ in the summand is equal to $q'+m-s$, we replace the index m by $\bar{m} := q'+m-s$. Furthermore, we also consider changing $q\to b := q-q'$, $q'\to a := q'-s$. Therefore the regions of summation above become

$$\begin{aligned}
&O^{\varepsilon_1,a_1}_{\Delta_1,+}(z_1,\bar{z}_1)\, O^{\varepsilon_2,a_2}_{\Delta_2,s_2}(z_2,\bar{z}_2)\\
&=\sum_{p=0}^{\infty} z_{12}^{p-1}\sum_{r=0}^{p}\sum_{\bar{m}=0}^{\infty}\sum_{a=0}^{\min(\bar{m},p-r)}\sum_{s=0}^{p-r-a}\sum_{b=0}^{p-r-a-s}\int_0^\infty \mathrm{d}\omega\ \omega^{2\bar{h}_1+2\bar{h}_2-1+r}\\
&\quad\times(-1)^{a+b}\varepsilon_1^r\,\frac{\Gamma(2\bar{h}_2-a-b-s)\Gamma(2\bar{h}_1+r+b+s+\bar{m})\,\Gamma(-2\bar{h}_2+b+1)}{\Gamma(2\bar{h}_1+2\bar{h}_2+r+\bar{m}-a)\,b!\,s!\,a!\,(\bar{m}-a-s)!\,\Gamma(-2\bar{h}_2+1)}\\
&\quad\times \bar{z}_{12}^{\bar{m}}\bar{\partial}_2^{\bar{m}}J^{a_1}_{-p}[r](\bar{z}_1)O^{a_2}_{s_2}\left(z_2,\frac{(\varepsilon_1\omega_1+\varepsilon_2\omega_2)}{\varepsilon_2\omega_2}\tilde{\lambda}_2\right).
\end{aligned} \tag{7.108}$$

To perform the summation on a, b, s, we use the identity

$$\begin{aligned}
&\sum_{a=0}^{\min(\bar{m},p-r)}\sum_{s=0}^{p-r-a}\sum_{b=0}^{p-r-a-s}(-1)^{a+b}\frac{\Gamma(2\bar{h}_2-a-b-s)\Gamma(2\bar{h}_1+r+b+s+\bar{m})\,\Gamma(-2\bar{h}_2+b+1)}{\Gamma(2\bar{h}_1+2\bar{h}_2+r+\bar{m}-a)\,b!\,s!\,a!\,(\bar{m}-a-s)!\,\Gamma(-2\bar{h}_2+1)}\\
&=\frac{1}{\bar{m}!}B(2\bar{h}_1+r+\bar{m},2\bar{h}_2)\frac{\Gamma(2\bar{h}_1+p+1)}{(p-r)!\,\Gamma(2\bar{h}_1+r+1)}\,.
\end{aligned} \tag{7.109}$$

Plugging (7.109) into (7.108), we obtain the final answer (7.45). In a similar manner, we can also obtain the Mellin-transformed graviton OPE (7.74).

Bibliography

[1] S. Fomin and A. Zelevinsky, "Cluster algebras i: foundations," *Journal of the American Mathematical Society* **15** (2002), no. 2 497–529, math/0104151.

[2] G. Kuperberg, "Spiders for rank 2 lie algebras," *Communications in mathematical physics* **180** (1996), no. 1 109–151, q-alg/9712003.

[3] S. Fomin and P. Pylyavskyy, "Tensor diagrams and cluster algebras," *Advances in Mathematics* **300** (2016) 717–787, 1210.1888.

[4] M. Gekhtman, M. Shapiro, and A. Vainshtein, *Cluster algebras and Poisson geometry.* American Mathematical Soc., 2010.

[5] B. Keller, "Cluster algebras, quiver representations and triangulated categories," 0807.1960.

[6] W. Chang, B. Duan, C. Fraser, and J.-R. Li, "Quantum affine algebras and grassmannians," *Mathematische Zeitschrift* **296** (2020), no. 3 1539–1583, 1907.13575.

[7] R. Feynman, "Space-time approach to quantum electrodynamics," *Physical Review* **76** (1949), no. 6 769.

[8] S. J. Parke and T. R. Taylor, "An Amplitude for n Gluon Scattering," *Phys. Rev. Lett.* **56** (1986) 2459.

[9] R. Britto, F. Cachazo, and B. Feng, "New recursion relations for tree amplitudes of gluons," *Nucl. Phys. B* **715** (2005) 499–522, hep-th/0412308.

[10] R. Britto, F. Cachazo, B. Feng, and E. Witten, "Direct proof of tree-level recursion relation in Yang-Mills theory," *Phys. Rev. Lett.* **94** (2005) 181602, hep-th/0501052.

[11] H. Elvang, D. Z. Freedman, and M. Kiermaier, "Proof of the MHV vertex expansion for all tree amplitudes in N=4 SYM theory," *JHEP* **06** (2009) 068, 0811.3624.

[12] F. Cachazo, P. Svrcek, and E. Witten, "MHV vertices and tree amplitudes in gauge theory," *JHEP* **09** (2004) 006, hep-th/0403047.

[13] A. Hodges, "Eliminating spurious poles from gauge-theoretic amplitudes," *JHEP* **05** (2013) 135, 0905.1473.

[14] J. M. Drummond, J. Henn, G. P. Korchemsky, and E. Sokatchev, "Dual superconformal symmetry of scattering amplitudes in N=4 super-Yang-Mills theory," *Nucl. Phys. B* **828** (2010) 317–374, 0807.1095.

[15] J. M. Drummond, J. M. Henn, and J. Plefka, "Yangian symmetry of scattering amplitudes in N=4 super Yang-Mills theory," *JHEP* **05** (2009) 046, 0902.2987.

[16] Z. Bern, L. J. Dixon, and V. A. Smirnov, "Iteration of planar amplitudes in maximally supersymmetric Yang-Mills theory at three loops and beyond," *Phys. Rev. D* **72** (2005) 085001, hep-th/0505205.

[17] N. Arkani-Hamed, J. L. Bourjaily, F. Cachazo, A. B. Goncharov, A. Postnikov, and J. Trnka, *Grassmannian Geometry of Scattering Amplitudes.* Cambridge University Press, 4, 2016.

[18] J. M. Drummond and L. Ferro, "The Yangian origin of the Grassmannian integral," *JHEP* **12** (2010) 010, 1002.4622.

[19] A. Goncharov, "Volumes of hyperbolic manifolds and mixed tate motives," *Journal of the American Mathematical Society* **12** (1999), no. 2 569–618.

[20] V. Del Duca, C. Duhr, and V. A. Smirnov, "The massless hexagon integral in D = 6 dimensions," *Phys. Lett. B* **703** (2011) 363–365, 1104.2781.

[21] A. B. Goncharov, M. Spradlin, C. Vergu, and A. Volovich, "Classical Polylogarithms for Amplitudes and Wilson Loops," *Phys. Rev. Lett.* **105** (2010) 151605, 1006.5703.

[22] S. Caron-Huot, "Superconformal symmetry and two-loop amplitudes in planar N=4 super Yang-Mills," *JHEP* **12** (2011) 066, 1105.5606.

[23] S. Caron-Huot and S. He, "Jumpstarting the All-Loop S-Matrix of Planar N=4 Super Yang-Mills," *JHEP* **07** (2012) 174, 1112.1060.

[24] S. He, Z. Li, and C. Zhang, "Two-loop octagons, algebraic letters and $\bar{Q}$ equations," *Phys. Rev. D* **101** (2020), no. 6 061701, 1911.01290.

[25] S. He, Z. Li, and C. Zhang, "The symbol and alphabet of two-loop NMHV amplitudes from $\bar{Q}$ equations," *JHEP* **03** (2021) 278, 2009.11471.

[26] Z. Li and C. Zhang, "The three-loop MHV octagon from $\overline{Q}$ equations," *JHEP* **12** (2021) 113, 2110.00350.

[27] S. Caron-Huot, L. J. Dixon, J. M. Drummond, F. Dulat, J. Foster, O. Gürdoğan, M. von Hippel, A. J. McLeod, and G. Papathanasiou, "The Steinmann Cluster Bootstrap for $N = 4$ Super Yang-Mills Amplitudes," *PoS* **CORFU2019** (2020) 003, 2005.06735.

[28] J. Golden, A. B. Goncharov, M. Spradlin, C. Vergu, and A. Volovich, "Motivic Amplitudes and Cluster Coordinates," *JHEP* **01** (2014) 091, 1305.1617.

[29] I. Prlina, M. Spradlin, J. Stankowicz, S. Stanojevic, and A. Volovich, "All-Helicity Symbol Alphabets from Unwound Amplituhedra," *JHEP* **05** (2018) 159, 1711.11507.

[30] I. Prlina, M. Spradlin, J. Stankowicz, and S. Stanojevic, "Boundaries of Amplituhedra and NMHV Symbol Alphabets at Two Loops," *JHEP* **04** (2018) 049, 1712.08049.

[31] J. Drummond, J. Foster, O. Gürdoğan, and C. Kalousios, "Algebraic singularities of scattering amplitudes from tropical geometry," *JHEP* **04** (2021) 002, 1912.08217.

[32] N. Henke and G. Papathanasiou, "How tropical are seven- and eight-particle amplitudes?," *JHEP* **08** (2020) 005, 1912.08254.

[33] N. Henke and G. Papathanasiou, "Singularities of eight- and nine-particle amplitudes from cluster algebras and tropical geometry," 2106.01392.

[34] Q. Yang, "Schubert problems, positivity and symbol letters," *JHEP* **08** (2022) 168, 2203.16112.

[35] L. Ren, M. Spradlin, and A. Volovich, "Symbol alphabets from tensor diagrams," *JHEP* **12** (2021) 079, 2106.01405.

[36] L. Ren, M. Spradlin, C. Vergu, and A. Volovich, "One-loop Integrals from Volumes of Orthoschemes," 2306.04630.

[37] O. Schnetz, "The geometry of one-loop amplitudes," 1010.5334.

[38] A. Bernig and L. Bröcker, "Courbures intrinseques dans les catégories analytico-géométriques," *Annales de l'institut Fourier* **53** (2003), no. 6 1897–1924.

[39] A. I. Davydychev and R. Delbourgo, "A Geometrical angle on Feynman integrals," *J. Math. Phys.* **39** (1998) 4299–4334, hep-th/9709216.

[40] L. Mason and D. Skinner, "Amplitudes at Weak Coupling as Polytopes in AdS_5," *J. Phys. A* **44** (2011) 135401, 1004.3498.

[41] D. Rudenko, "On the goncharov depth conjecture and a formula for volumes of orthoschemes," *arXiv preprint arXiv:2012.05599* (2020).

[42] J. M. Maldacena, "The Large N limit of superconformal field theories and supergravity," *Adv. Theor. Math. Phys.* **2** (1998) 231–252, hep-th/9711200.

[43] S. Pasterski, S.-H. Shao, and A. Strominger, "Flat Space Amplitudes and Conformal Symmetry of the Celestial Sphere," *Phys. Rev. D* **96** (2017), no. 6 065026, 1701.00049.

[44] J. Mago, L. Ren, A. Y. Srikant, and A. Volovich, "Deformed $w_{1+\infty}$ Algebras in the Celestial CFT," *SIGMA* **19** (2023) 044, 2111.11356.

[45] L. Ren, M. Spradlin, A. Yelleshpur Srikant, and A. Volovich, "On effective field theories with celestial duals," *JHEP* **08** (2022) 251, 2206.08322.

[46] R. Bhardwaj, L. Lippstreu, L. Ren, M. Spradlin, A. Yelleshpur Srikant, and A. Volovich, "Loop-level gluon OPEs in celestial holography," *JHEP* **11** (2022) 171, 2208.14416.

[47] L. Ren, A. Schreiber, A. Sharma, and D. Wang, "All-order celestial OPE from on-shell recursion," *JHEP* **10** (2023) 080, 2305.11851.

[48] D. Chicherin, J. M. Henn, and G. Papathanasiou, "Cluster algebras for Feynman integrals," *Phys. Rev. Lett.* **126** (2021), no. 9 091603, 2012.12285.

[49] S. He, Z. Li, and Q. Yang, "Notes on cluster algebras and some all-loop Feynman integrals," 2103.02796.

[50] N. Arkani-Hamed, T. Lam, and M. Spradlin, "Non-perturbative geometries for planar $\mathcal{N} = 4$ SYM amplitudes," *JHEP* **03** (2021) 065, 1912.08222.

[51] A. Herderschee, "Algebraic branch points at all loop orders from positive kinematics and wall crossing," 2102.03611.

[52] D. Speyer and L. Williams, "The tropical totally positive grassmannian," *Journal of Algebraic Combinatorics* **22** (2005), no. 2 189–210, math/0312297.

[53] N. Arkani-Hamed, S. He, and T. Lam, "Stringy canonical forms," *JHEP* **02** (2021) 069, 1912.08707.

[54] F. Cachazo, N. Early, A. Guevara, and S. Mizera, "Scattering Equations: From Projective Spaces to Tropical Grassmannians," *JHEP* **06** (2019) 039, 1903.08904.

[55] F. Cachazo and J. M. Rojas, "Notes on Biadjoint Amplitudes, Trop $G(3,7)$ and $X(3,7)$ Scattering Equations," *JHEP* **04** (2020) 176, 1906.05979.

[56] J. Drummond, J. Foster, O. Gürdoğan, and C. Kalousios, "Tropical Grassmannians, cluster algebras and scattering amplitudes," *JHEP* **04** (2020) 146, 1907.01053.

[57] F. Cachazo and N. Early, "Minimal Kinematics: An all k and n peek into Trop$^+G(k,n)$," 2003.07958.

[58] S. Fomin and A. Zelevinsky, "Y-systems and generalized associahedra," *Annals of Mathematics* **158** (2003), no. 3 977–1018, hep-th/0111053.

[59] J. Drummond, J. Foster, O. Gürdoğan, and C. Kalousios, "Tropical fans, scattering equations and amplitudes," 2002.04624.

[60] I. Prlina, M. Spradlin, and S. Stanojevic, "All-loop singularities of scattering amplitudes in massless planar theories," *Phys. Rev. Lett.* **121** (2018), no. 8 081601, 1805.11617.

[61] S. Caron-Huot and K. J. Larsen, "Uniqueness of two-loop master contours," *JHEP* **10** (2012) 026, 1205.0801.

[62] J. L. Bourjaily, A. J. McLeod, M. Spradlin, M. von Hippel, and M. Wilhelm, "Elliptic Double-Box Integrals: Massless Scattering Amplitudes beyond Polylogarithms," *Phys. Rev. Lett.* **120** (2018), no. 12 121603, 1712.02785.

[63] J. Mago, A. Schreiber, M. Spradlin, and A. Volovich, "Symbol alphabets from plabic graphs," *JHEP* **10** (2020) 128, 2007.00646.

[64] S. He and Z. Li, "A note on letters of Yangian invariants," *JHEP* **02** (2021) 155, 2007.01574.

[65] J. Mago, A. Schreiber, M. Spradlin, A. Yelleshpur Srikant, and A. Volovich, "Symbol alphabets from plabic graphs II: rational letters," *JHEP* **04** (2021) 056, 2012.15812.

[66] J. Mago, A. Schreiber, M. Spradlin, A. Yelleshpur Srikant, and A. Volovich, "Symbol Alphabets from plabic graphs III: $n = 9$," 2106.01406.

[67] A. Postnikov, "Total positivity, grassmannians, and networks," math/0609764.

[68] N. Arkani-Hamed, J. L. Bourjaily, F. Cachazo, A. B. Goncharov, A. Postnikov, and J. Trnka, *Grassmannian Geometry of Scattering Amplitudes.* Cambridge University Press, 4, 2016.

[69] C. Fraser, T. Lam, and I. Le, "From dimers to webs," *Transactions of the American Mathematical Society* **371** (2019), no. 9 6087–6124, 1705.09424.

[70] L. Lamberti, "Tensor diagrams and chebyshev polynomials," *International Mathematics Research Notices* **2020** (2020), no. 20 7218–7278, 1609.03501.

[71] J. D. Stasheff, "Homotopy associativity of h-spaces. i," *Transactions of the American Mathematical Society* **108** (1963), no. 2 275–292.

[72] J. D. Stasheff, "Homotopy associativity of h-spaces. ii," *Transactions of the American Mathematical Society* **108** (1963), no. 2 293–312.

[73] N. Arkani-Hamed, Y. Bai, S. He, and G. Yan, "Scattering Forms and the Positive Geometry of Kinematics, Color and the Worldsheet," *JHEP* **05** (2018) 096, 1711.09102.

[74] S. Fomin and A. Zelevinsky, "Cluster algebras iv: coefficients," *Compositio Mathematica* **143** (2007), no. 1 112–164, math/0602259.

[75] J. S. Scott, "Grassmannians and cluster algebras," *Proceedings of the London Mathematical Society* **92** (2006), no. 2 345–380.

[76] C. Fraser, "Braid group symmetries of grassmannian cluster algebras," *Selecta Mathematica* **26** (2020), no. 2 1–51, 1702.00385.

[77] G. Lusztig, "Canonical bases arising from quantized enveloping algebras," *Journal of the American Mathematical Society* **3** (1990), no. 2 447–498.

[78] S. Cautis, J. Kamnitzer, and S. Morrison, "Webs and quantum skew howe duality," *Mathematische Annalen* **360** (2014), no. 1 351–390, 1210.6437.

[79] D. Kim, "Graphical calculus on representations of quantum lie algebras," math/0310143.

[80] N. Early, "Weighted blade arrangements and the positive tropical Grassmannian," 2005.12305.

[81] S. Herrmann, A. Jensen, M. Joswig, and B. Sturmfels, "How to draw tropical planes," 0808.2383.

[82] F. Cachazo, A. Guevara, B. Umbert, and Y. Zhang, "Planar Matrices and Arrays of Feynman Diagrams," 1912.09422.

[83] S. He, L. Ren, and Y. Zhang, "Notes on polytopes, amplitudes and boundary configurations for Grassmannian string integrals," *JHEP* **04** (2020) 140, 2001.09603.

[84] A. Felikson, M. Shapiro, and P. Tumarkin, "Skew-symmetric cluster algebras of finite mutation type," *Journal of the European Mathematical Society* **14** (2012), no. 4 1135–1180, 0811.1703.

[85] Z. Bern, L. J. Dixon, D. C. Dunbar, and D. A. Kosower, "One loop n point gauge theory amplitudes, unitarity and collinear limits," *Nucl. Phys. B* **425** (1994) 217–260, hep-ph/9403226.

[86] Z. Bern, L. J. Dixon, D. C. Dunbar, and D. A. Kosower, "Fusing gauge theory tree amplitudes into loop amplitudes," *Nucl. Phys. B* **435** (1995) 59–101, hep-ph/9409265.

[87] L. J. Dixon, J. M. Drummond, and J. M. Henn, "Bootstrapping the three-loop hexagon," *JHEP* **11** (2011) 023, 1108.4461.

[88] L. J. Dixon, J. M. Drummond, and J. M. Henn, "Analytic result for the two-loop six-point NMHV amplitude in N=4 super Yang-Mills theory," *JHEP* **01** (2012) 024, 1111.1704.

[89] S. Caron-Huot and S. He, "Jumpstarting the All-Loop S-Matrix of Planar N=4 Super Yang-Mills," *JHEP* **07** (2012) 174, 1112.1060.

[90] Z. Bern, V. Del Duca, L. J. Dixon, and D. A. Kosower, "All non-maximally-helicity-violating one-loop seven-gluon amplitudes in N=4 super-yang-Mills theory," *Phys. Rev. D* **71** (2005) 045006, hep-th/0410224.

[91] S. Caron-Huot, "Superconformal symmetry and two-loop amplitudes in planar N=4 super Yang-Mills," *JHEP* **12** (2011) 066, 1105.5606.

[92] J. M. Drummond, G. Papathanasiou, and M. Spradlin, "A Symbol of Uniqueness: The Cluster Bootstrap for the 3-Loop MHV Heptagon," *JHEP* **03** (2015) 072, 1412.3763.

[93] L. J. Dixon, J. Drummond, T. Harrington, A. J. McLeod, G. Papathanasiou, and M. Spradlin, "Heptagons from the Steinmann Cluster Bootstrap," *JHEP* **02** (2017) 137, 1612.08976.

[94] J. Drummond, J. Foster, O. Gürdoğan, and G. Papathanasiou, "Cluster adjacency and the four-loop NMHV heptagon," *JHEP* **03** (2019) 087, 1812.04640.

[95] R. Britto, F. Cachazo, and B. Feng, "Generalized unitarity and one-loop amplitudes in N=4 super-Yang-Mills," *Nucl. Phys. B* **725** (2005) 275–305, hep-th/0412103.

[96] Z. Bern, L. J. Dixon, and D. A. Kosower, "All Next-to-maximally-helicity-violating one-loop gluon amplitudes in N=4 super-Yang-Mills theory," *Phys. Rev. D* **72** (2005) 045014, hep-th/0412210.

[97] S. He, Z. Li, and C. Zhang, "Two-loop Octagons, Algebraic Letters and $\bar{Q}$ Equations," *Phys. Rev. D* **101** (2020), no. 6 061701, 1911.01290.

[98] A. C.-T. Wu, "On the analytic properties of the 4-point function in perturbation theory," *Matematisk-fysiske Meddelelser udgivet af Det Kongelige Dnaske Videnskabernes Selskab* **33** (1961) no. 3, 1–88, PhD Thesis.

[99] G. 't Hooft and M. J. G. Veltman, "Scalar One Loop Integrals," *Nucl. Phys. B* **153** (1979) 365–401.

[100] A. Denner, U. Nierste, and R. Scharf, "A compact expression for the scalar one-loop four-point function," *Nuclear Physics B* **367** (1991), no. 3 637–656.

[101] A. Hodges, "The Box Integrals in Momentum-Twistor Geometry," *JHEP* **08** (2013) 051, 1004.3323.

[102] D. Nandan, M. F. Paulos, M. Spradlin, and A. Volovich, "Star Integrals, Convolutions and Simplices," *JHEP* **05** (2013) 105, 1301.2500.

[103] J. L. Bourjaily, E. Gardi, A. J. McLeod, and C. Vergu, "All-mass n-gon integrals in n dimensions," *JHEP* **08** (2020), no. 08 029, 1912.11067.

[104] J. Murakami and M. Yano, "On the volume of a hyberbolic and spherical tertrahedron," *Communications in analysis and geometry* **13** (2005), no. 2 379–400.

[105] M. F. Paulos, "Loops, Polytopes and Splines," *JHEP* **06** (2013) 007, 1210.0578.

[106] N. Arkani-Hamed and E. Y. Yuan, "One-Loop Integrals from Spherical Projections of Planes and Quadrics," 1712.09991.

[107] A. I. Davydychev, "Four-point function in general kinematics through geometrical splitting and reduction," *J. Phys. Conf. Ser.* **1085** (2018), no. 5 052016, 1711.07351.

[108] M. F. Paulos, M. Spradlin, and A. Volovich, "Mellin Amplitudes for Dual Conformal Integrals," *JHEP* **08** (2012) 072, 1203.6362.

[109] L. J. Dixon, J. M. Drummond, and J. M. Henn, "The one-loop six-dimensional hexagon integral and its relation to MHV amplitudes in N=4 SYM," *JHEP* **06** (2011) 100, 1104.2787.

[110] V. Del Duca, C. Duhr, and V. A. Smirnov, "The One-Loop One-Mass Hexagon Integral in D=6 Dimensions," *JHEP* **07** (2011) 064, 1105.1333.

[111] V. Del Duca, L. J. Dixon, J. M. Drummond, C. Duhr, J. M. Henn, and V. A. Smirnov, "The one-loop six-dimensional hexagon integral with three massive corners," *Phys. Rev. D* **84** (2011) 045017, 1105.2011.

[112] M. Spradlin and A. Volovich, "Symbols of One-Loop Integrals From Mixed Tate Motives," *JHEP* **11** (2011) 084, 1105.2024.

[113] L. Adams, E. Chaubey, and S. Weinzierl, "Planar Double Box Integral for Top Pair Production with a Closed Top Loop to all orders in the Dimensional Regularization Parameter," *Phys. Rev. Lett.* **121** (2018), no. 14 142001, 1804.11144.

[114] L. Adams, E. Chaubey, and S. Weinzierl, "Analytic results for the planar double box integral relevant to top-pair production with a closed top loop," *JHEP* **10** (2018) 206, 1806.04981.

[115] B. Ananthanarayan, S. Banik, S. Friot, and S. Ghosh, "Double box and hexagon conformal Feynman integrals," *Phys. Rev. D* **102** (2020), no. 9 091901, 2007.08360.

[116] S. Bloch, "Double Box Motive," *SIGMA* **17** (2021) 048, 2105.06132.

[117] A. Kristensson, M. Wilhelm, and C. Zhang, "Elliptic Double Box and Symbology Beyond Polylogarithms," *Phys. Rev. Lett.* **127** (2021), no. 25 251603, 2106.14902.

[118] M. Wilhelm and C. Zhang, "Symbology for elliptic multiple polylogarithms and the symbol prime," *JHEP* **01** (2023) 089, 2206.08378.

[119] A. C. Pozo and M. von Hippel, "A Three-Parameter Elliptic Double-Box," 2209.03921.

[120] J. M. Henn, A. Matijašić, and J. Miczajka, "One-loop hexagon integral to higher orders in the dimensional regulator," *JHEP* **01** (2023) 096, 2210.13505.

[121] H. Coxeter, "The functions of schläfli and lobatschefsky," *The Quarterly Journal of Mathematics* (1935), no. 1 13–29.

[122] H. Coxeter, "On schläfli's generalization of napier's pentagramma mirificum," *Bull. Calcutta Math. Soc* **28** (1936) 125–144.

[123] J. Böhm, "Inhaltsmessung im r 5 konstanter krümmung," *Archiv der Mathematik* **11** (1960) 298–309.

[124] J. Böhm, "Zu coxeters integrationsmethode in gekrümmten räumen," *Mathematische Nachrichten* **27** (1964), no. 3-4 179–214.

[125] R. Kellerhals, "Volumes in hyperbolic 5-space," *Geometric & Functional Analysis GAFA* **5** (1995), no. 4 640–667.

[126] L. J. Dixon, O. Gurdogan, A. J. McLeod, and M. Wilhelm, "Folding Amplitudes into Form Factors: An Antipodal Duality," *Phys. Rev. Lett.* **128** (2022), no. 11 111602, 2112.06243.

[127] Y.-T. Liu, "Antipodal symmetry of two-loop MHV amplitudes," *JHEP* **09** (2022) 131, 2207.11815.

[128] F. Loebbert, D. Müller, and H. Münkler, "Yangian Bootstrap for Conformal Feynman Integrals," *Phys. Rev. D* **101** (2020), no. 6 066006, 1912.05561.

[129] L. Corcoran, F. Loebbert, J. Miczajka, and M. Staudacher, "Minkowski Box from Yangian Bootstrap," *JHEP* **04** (2021) 160, 2012.07852.

[130] C. Duhr and F. Dulat, "PolyLogTools — polylogs for the masses," *JHEP* **08** (2019) 135, 1904.07279.

[131] F. C. Brown, "Single-valued multiple polylogarithms in one variable," *Comptes Rendus Mathematique* **338** (2004), no. 7 527–532.

[132] V. Del Duca, S. Druc, J. Drummond, C. Duhr, F. Dulat, R. Marzucca, G. Papathanasiou, and B. Verbeek, "Multi-Regge kinematics and the moduli space of Riemann spheres with marked points," *JHEP* **08** (2016) 152, 1606.08807.

[133] R. Britto, S. Mizera, C. Rodriguez, and O. Schlotterer, "Coaction and double-copy properties of configuration-space integrals at genus zero," *JHEP* **05** (2021) 053, 2102.06206.

[134] Y. Hu, L. Ren, A. Y. Srikant, and A. Volovich, "Celestial dual superconformal symmetry, MHV amplitudes and differential equations," *JHEP* **12** (2021) 171, 2106.16111.

[135] T. He, P. Mitra, and A. Strominger, "2D Kac-Moody Symmetry of 4D Yang-Mills Theory," *JHEP* **10** (2016) 137, 1503.02663.

[136] D. Kapec, P. Mitra, A.-M. Raclariu, and A. Strominger, "2D Stress Tensor for 4D Gravity," *Phys. Rev. Lett.* **119** (2017), no. 12 121601, 1609.00282.

[137] A. Bagchi, R. Basu, A. Kakkar, and A. Mehra, "Flat Holography: Aspects of the dual field theory," *JHEP* **12** (2016) 147, 1609.06203.

[138] C. Cheung, A. de la Fuente, and R. Sundrum, “4D scattering amplitudes and asymptotic symmetries from 2D CFT,” *JHEP* **01** (2017) 112, 1609.00732.

[139] S. Pasterski, S.-H. Shao, and A. Strominger, “Gluon Amplitudes as 2d Conformal Correlators,” *Phys. Rev. D* **96** (2017), no. 8 085006, 1706.03917.

[140] C. Cardona and Y.-t. Huang, “S-matrix singularities and CFT correlation functions,” *JHEP* **08** (2017) 133, 1702.03283.

[141] A. Ball, E. Himwich, S. A. Narayanan, S. Pasterski, and A. Strominger, “Uplifting AdS_3/CFT_2 to flat space holography,” *JHEP* **08** (2019) 168, 1905.09809.

[142] L. Donnay, A. Puhm, and A. Strominger, “Conformally Soft Photons and Gravitons,” *JHEP* **01** (2019) 184, 1810.05219.

[143] E. Himwich and A. Strominger, “Celestial current algebra from Low’s subleading soft theorem,” *Phys. Rev. D* **100** (2019), no. 6 065001, 1901.01622.

[144] W. Fan, A. Fotopoulos, and T. R. Taylor, “Soft Limits of Yang-Mills Amplitudes and Conformal Correlators,” *JHEP* **05** (2019) 121, 1903.01676.

[145] M. Pate, A.-M. Raclariu, and A. Strominger, “Conformally Soft Theorem in Gauge Theory,” *Phys. Rev. D* **100** (2019), no. 8 085017, 1904.10831.

[146] T. Adamo, L. Mason, and A. Sharma, “Celestial amplitudes and conformal soft theorems,” *Class. Quant. Grav.* **36** (2019), no. 20 205018, 1905.09224.

[147] D. Nandan, A. Schreiber, A. Volovich, and M. Zlotnikov, “Celestial Amplitudes: Conformal Partial Waves and Soft Limits,” *JHEP* **10** (2019) 018, 1904.10940.

[148] A. Puhm, “Conformally Soft Theorem in Gravity,” *JHEP* **09** (2020) 130, 1905.09799.

[149] A. Guevara, “Notes on Conformal Soft Theorems and Recursion Relations in Gravity,” 1906.07810.

[150] A. Fotopoulos, S. Stieberger, T. R. Taylor, and B. Zhu, “Extended BMS Algebra of Celestial CFT,” *JHEP* **03** (2020) 130, 1912.10973.

[151] A. Fotopoulos, S. Stieberger, T. R. Taylor, and B. Zhu, “Extended Super BMS Algebra of Celestial CFT,” *JHEP* **09** (2020) 198, 2007.03785.

[152] E. Himwich, S. A. Narayanan, M. Pate, N. Paul, and A. Strominger, “The Soft $\mathcal{S}$-Matrix in Gravity,” *JHEP* **09** (2020) 129, 2005.13433.

[153] L. Magnea, “Non-abelian infrared divergences on the celestial sphere,” *JHEP* **05** (2021) 282, 2104.10254.

[154] H. A. González and F. Rojas, “The structure of IR divergences in celestial gluon amplitudes,” 2104.12979.

[155] N. Arkani-Hamed, M. Pate, A.-M. Raclariu, and A. Strominger, “Celestial Amplitudes from UV to IR,” 2012.04208.

[156] E. Casali and A. Sharma, “Celestial double copy from the worldsheet,” *JHEP* **05** (2021) 157, 2011.10052.

[157] E. Casali and A. Puhm, “Double Copy for Celestial Amplitudes,” *Phys. Rev. Lett.* **126** (2021), no. 10 101602, 2007.15027.

[158] A. Schreiber, A. Volovich, and M. Zlotnikov, “Tree-level gluon amplitudes on the celestial sphere,” *Phys. Lett. B* **781** (2018) 349–357, 1711.08435.

[159] N. Banerjee, S. Banerjee, S. Atul Bhatkar, and S. Jain, “Conformal Structure of Massless Scalar Amplitudes Beyond Tree level,” *JHEP* **04** (2018) 039, 1711.06690.

[160] S. Albayrak, C. Chowdhury, and S. Kharel, “On loop celestial amplitudes for gauge theory and gravity,” *Phys. Rev. D* **102** (2020) 126020, 2007.09338.

[161] H. A. González, A. Puhm, and F. Rojas, “Loop corrections to celestial amplitudes,” *Phys. Rev. D* **102** (2020), no. 12 126027, 2009.07290.

[162] S. Stieberger and T. R. Taylor, “Strings on Celestial Sphere,” *Nucl. Phys. B* **935** (2018) 388–411, 1806.05688.

[163] S. Banerjee, S. Ghosh, and R. Gonzo, “BMS symmetry of celestial OPE,” *JHEP* **04** (2020) 130, 2002.00975.

[164] S. Banerjee and S. Ghosh, “MHV Gluon Scattering Amplitudes from Celestial Current Algebras,” 2011.00017.

[165] S. Banerjee, S. Ghosh, and P. Paul, “MHV graviton scattering amplitudes and current algebra on the celestial sphere,” *JHEP* **02** (2021) 176, 2008.04330.

[166] M. Pate, A.-M. Raclariu, A. Strominger, and E. Y. Yuan, “Celestial Operator Products of Gluons and Gravitons,” 1910.07424.

[167] W. Fan, A. Fotopoulos, S. Stieberger, T. R. Taylor, and B. Zhu, “Conformal blocks from celestial gluon amplitudes,” *JHEP* **05** (2021) 170, 2103.04420.

[168] A. Strominger, “w(1+infinity) and the Celestial Sphere,” 2105.14346.

[169] A. Atanasov, W. Melton, A.-M. Raclariu, and A. Strominger, “Conformal Block Expansion in Celestial CFT,” 2104.13432.

[170] A. Guevara, E. Himwich, M. Pate, and A. Strominger, "Holographic Symmetry Algebras for Gauge Theory and Gravity," 2103.03961.

[171] E. Crawley, N. Miller, S. A. Narayanan, and A. Strominger, "State-Operator Correspondence in Celestial Conformal Field Theory," 2105.00331.

[172] A. Atanasov, A. Ball, W. Melton, A.-M. Raclariu, and A. Strominger, "$(2,2)$ Scattering and the Celestial Torus," 2101.09591.

[173] A. Brandhuber, G. R. Brown, J. Gowdy, B. Spence, and G. Travaglini, "Celestial Superamplitudes," 2105.10263.

[174] H. Jiang, "Celestial superamplitude in $\mathcal{N}=4$ SYM theory," 2105.10269.

[175] K. Aomoto and M. Kita, *Theory of Hypergeometric Functions.* Springer Japan, Reading, Massachusetts, 2011.

[176] Y. Hu, L. Ren, M. Spradlin, A. Yelleshpur Srikant, and A. Volovich, "The Celestiahedron," *work in progress* (2021) yymm.nnnnn.

[177] H. Elvang and Y.-t. Huang, *Scattering Amplitudes in Gauge Theory and Gravity.* Cambridge University Press, 4, 2015.

[178] J. M. Henn and J. C. Plefka, *Scattering Amplitudes in Gauge Theories*, vol. 883. Springer, Berlin, 2014.

[179] Y. T. A. Law and M. Zlotnikov, "Poincaré constraints on celestial amplitudes," *JHEP* **03** (2020) 085, 1910.04356. [Erratum: JHEP 04, 202 (2020)].

[180] S. Stieberger and T. R. Taylor, "Symmetries of Celestial Amplitudes," *Phys. Lett. B* **793** (2019) 141–143, 1812.01080.

[181] Y. Abe, "A note on generalized hypergeometric functions, kz solutions, and gluon amplitudes," *Nuclear Physics B* **907** (Jun, 2016) 107–153.

[182] S. Pasterski and S.-H. Shao, "Conformal basis for flat space amplitudes," *Phys. Rev. D* **96** (2017), no. 6 065022, 1705.01027.

[183] A.-M. Raclariu, "Lectures on Celestial Holography," 2107.02075.

[184] S. Pasterski, "Lectures on Celestial Amplitudes," 2108.04801.

[185] P. B. Aneesh, G. Compère, L. P. de Gioia, I. Mol, and B. Swidler, "Celestial Holography: Lectures on Asymptotic Symmetries," 2109.00997.

[186] A. Strominger, "Lectures on the Infrared Structure of Gravity and Gauge Theory," 1703.05448.

[187] M. Pate, A.-M. Raclariu, A. Strominger, and E. Y. Yuan, "Celestial operator products of gluons and gravitons," 1910.07424.

[188] L. Donnay, A. Puhm, and A. Strominger, "Conformally soft photons and gravitons," *Journal of High Energy Physics* **2019** (2019), no. 1 184.

[189] M. Pate, A.-M. Raclariu, and A. Strominger, "Conformally soft theorem in gauge theory," *Physical Review D* **100** (2019), no. 8 085017.

[190] T. Adamo, L. Mason, and A. Sharma, "Celestial amplitudes and conformal soft theorems," *Classical and Quantum Gravity* **36** (2019), no. 20 205018.

[191] D. Nandan, A. Schreiber, A. Volovich, and M. Zlotnikov, "Celestial amplitudes: conformal partial waves and soft limits," *Journal of High Energy Physics* **2019** (2019), no. 10 1–14.

[192] A. Puhm, "Conformally soft theorem in gravity," *Journal of High Energy Physics* **2020** (2020), no. 9 1–15.

[193] A. Guevara, "Notes on conformal soft theorems and recursion relations in gravity," *arXiv preprint arXiv:1906.07810* (2019).

[194] Y. Hamada and G. Shiu, "Infinite Set of Soft Theorems in Gauge-Gravity Theories as Ward-Takahashi Identities," *Phys. Rev. Lett.* **120** (2018), no. 20 201601, 1801.05528.

[195] Z.-Z. Li, H.-H. Lin, and S.-Q. Zhang, "Infinite Soft Theorems from Gauge Symmetry," *Phys. Rev. D* **98** (2018), no. 4 045004, 1802.03148.

[196] E. Himwich, M. Pate, and K. Singh, "Celestial Operator Product Expansions and $\mathrm{w}_{1+\infty}$ Symmetry for All Spins," 2108.07763.

[197] A. Guevara, E. Himwich, M. Pate, and A. Strominger, "Holographic symmetry algebras for gauge theory and gravity," *arXiv preprint arXiv:2103.03961* (2021).

[198] I. Bakas, "The Large n Limit of Extended Conformal Symmetries," *Phys. Lett. B* **228** (1989) 57.

[199] E. Bergshoeff, P. Howe, C. Pope, E. Sezgin, X. Shen, and K. Stelle, "Quantisation deforms w_∞ to w_∞ gravity," *Nuclear Physics B* **363** (1991), no. 1 163–184.

[200] C. N. Pope, L. J. Romans, and X. Shen, "The Complete Structure of W(Infinity)," *Phys. Lett. B* **236** (1990) 173–178.

[201] C. N. Pope, "Lectures on W algebras and W gravity," in *Summer School in High-energy Physics and Cosmology*, pp. 827–867, 12, 1991. hep-th/9112076.

[202] C. Pope, X. Shen, and L. Romans, "w_∞ and the racah-wigner algebra," *Nuclear Physics B* **339** (1990), no. 1 191–221.

[203] C. N. Pope, X. Shen, K. W. Xu, and K.-j. Yuan, "SL(infinity,R) symmetry of quantum W(infinity) gravity," *Nucl. Phys. B* **376** (1992) 52–74.

[204] S. Odake and T. Sano, "W(1) + infinity and superW(infinity) algebras with SU(N) symmetry," *Phys. Lett. B* **258** (1991) 369–374.

[205] H. Jiang, "Holographic Chiral Algebra: Supersymmetry, Infinite Ward Identities, and EFTs," 2108.08799.

[206] C. Ahn, "Towards A Supersymmetric $w_{1+\infty}$ Symmetry in the Celestial Conformal Field Theory," 2111.04268.

[207] T. Adamo, L. Mason, and A. Sharma, "Celestial $w_{1+\infty}$ symmetries from twistor space," 2110.06066.

[208] H. Jiang, "Celestial OPEs and $w_{1+\infty}$ algebra from worldsheet in string theory," 2110.04255.

[209] H. Elvang, C. R. T. Jones, and S. G. Naculich, "Soft Photon and Graviton Theorems in Effective Field Theory," *Phys. Rev. Lett.* **118** (2017), no. 23 231601, 1611.07534.

[210] Z. Bern, V. Del Duca, and C. R. Schmidt, "The infrared behavior of one-loop gluon amplitudes at next-to-next-to-leading order," *Physics Letters B* **445** (1998), no. 1-2 168–177.

[211] Z. Bern, V. Del Duca, W. B. Kilgore, and C. R. Schmidt, "Infrared behavior of one-loop qcd amplitudes at next-to-next-to-leading order," *Physical Review D* **60** (1999), no. 11 116001.

[212] S. He, Y.-t. Huang, and C. Wen, "Loop corrections to soft theorems in gauge theories and gravity," *Journal of High Energy Physics* **2014** (2014), no. 12 115.

[213] F. Cachazo and E. Y. Yuan, "Are Soft Theorems Renormalized?," 1405.3413.

[214] Z. Bern, S. Davies, and J. Nohle, "On Loop Corrections to Subleading Soft Behavior of Gluons and Gravitons," *Phys. Rev. D* **90** (2014), no. 8 085015, 1405.1015.

[215] A. Ball, "Celestial locality and the Jacobi identity," *JHEP* **01** (2023) 146, 2211.09151.

[216] D. B. Fairlie and J. Nuyts, "Deformations and Renormalizations of W(infinity)," *Commun. Math. Phys.* **134** (1990) 413–420.

[217] W. Bu, S. Heuveline, and D. Skinner, "Moyal deformations, $W_{1+\infty}$ and celestial holography," *JHEP* **12** (2022) 011, 2208.13750.

[218] Z. Bern, G. Chalmers, L. Dixon, and D. A. Kosower, "One-loop n-gluon amplitudes with maximal helicity violation via collinear limits," *Physical review letters* **72** (1994), no. 14 2134.

[219] G. Mahlon, "Multigluon helicity amplitudes involving a quark loop," *Physical Review D* **49** (1994), no. 9 4438.

[220] Z. Bern, L. Dixon, M. Perelstein, and J. S. Rozowsky, "One-Loop n-Point Helicity Amplitudes in (Self-Dual) Gravity," hep-th/9809160.

[221] G. Chalmers and W. Siegel, "The Selfdual sector of QCD amplitudes," *Phys. Rev. D* **54** (1996) 7628–7633, hep-th/9606061.

[222] S. Weinberg, "Infrared photons and gravitons," *Phys. Rev.* **140** (1965) B516–B524.

[223] E. Casali, "Soft sub-leading divergences in Yang-Mills amplitudes," *JHEP* **08** (2014) 077, 1404.5551.

[224] H. Elvang and Y.-t. Huang, "Scattering Amplitudes," 1308.1697.

[225] L. J. Dixon, E. W. N. Glover, and V. V. Khoze, "MHV rules for Higgs plus multi-gluon amplitudes," *JHEP* **12** (2004) 015, hep-th/0411092.

[226] T. Klose, T. McLoughlin, D. Nandan, J. Plefka, and G. Travaglini, "Double-soft limits of gluons and gravitons," *Journal of High Energy Physics* **2015** (2015), no. 7 1–30.

[227] A. Volovich, C. Wen, and M. Zlotnikov, "Double soft theorems in gauge and string theories," *Journal of High Energy Physics* **2015** (2015), no. 7 1–25.

[228] S. He, Y.-t. Huang, and C. Wen, "Loop Corrections to Soft Theorems in Gauge Theories and Gravity," *JHEP* **12** (2014) 115, 1405.1410.

[229] P. Di Vecchia, R. Marotta, and M. Mojaza, "Subsubleading soft theorems of gravitons and dilatons in the bosonic string," *JHEP* **06** (2016) 054, 1604.03355.

[230] K. Costello and N. M. Paquette, "On the associativity of one-loop corrections to the celestial OPE," 2204.05301.

[231] T. Cohen, H. Elvang, and M. Kiermaier, "On-shell constructibility of tree amplitudes in general field theories," *JHEP* **04** (2011) 053, 1010.0257.

[232] J. Broedel and L. J. Dixon, "Color-kinematics duality and double-copy construction for amplitudes from higher-dimension operators," *JHEP* **10** (2012) 091, 1208.0876.

[233] D. Bai and Y.-H. Xing, "Higher Derivative Theories for Interacting Massless Gravitons in Minkowski Spacetime," *Nucl. Phys. B* **932** (2018) 15–28, 1610.00241.

[234] T. Azevedo, M. Chiodaroli, H. Johansson, and O. Schlotterer, "Heterotic and bosonic string amplitudes via field theory," *JHEP* **10** (2018) 012, 1803.05452.

[235] D. García-Sepúlveda, A. Guevara, J. Kulp, and J. Wu, "Notes on Resonances and Unitarity from Celestial Amplitudes," 2205.14633.

[236] R. R. Metsaev, "S matrix approach to massless higher spins theory. 2: The Case of internal symmetry," *Mod. Phys. Lett. A* **6** (1991) 2411–2421.

[237] R. R. Metsaev, "Poincare invariant dynamics of massless higher spins: Fourth order analysis on mass shell," *Mod. Phys. Lett. A* **6** (1991) 359–367.

[238] D. Ponomarev and E. D. Skvortsov, "Light-Front Higher-Spin Theories in Flat Space," *J. Phys. A* **50** (2017), no. 9 095401, 1609.04655.

[239] A. Ball, S. A. Narayanan, J. Salzer, and A. Strominger, "Perturbatively exact $w_{1+\infty}$ asymptotic symmetry of quantum self-dual gravity," *JHEP* **01** (2022) 114, 2111.10392.

[240] S. Pasterski, M. Pate, and A.-M. Raclariu, "Celestial Holography," in *Snowmass 2021*, 11, 2021. 2111.11392.

[241] K. Costello, N. M. Paquette, and A. Sharma, "Top-Down Holography in an Asymptotically Flat Spacetime," *Phys. Rev. Lett.* **130** (2023), no. 6 061602, 2208.14233.

[242] S. Ebert, A. Sharma, and D. Wang, "Descendants in celestial CFT and emergent multi-collinear factorization," *JHEP* **03** (2021) 030, 2009.07881.

[243] A. Schreiber, A. Volovich, and M. Zlotnikov, "Tree-level gluon amplitudes on the celestial sphere," *Phys. Lett. B* **781** (2018) 349–357, 1711.08435.

[244] K. Costello and N. M. Paquette, "Celestial holography meets twisted holography: 4d amplitudes from chiral correlators," *JHEP* **10** (2022) 193, 2201.02595.

[245] Y. Hu and S. Pasterski, "Celestial recursion," *JHEP* **01** (2023) 151, 2208.11635.

[246] S. Banerjee, S. Ghosh, and S. S. Samal, "Subsubleading soft graviton symmetry and MHV graviton scattering amplitudes," *JHEP* **08** (2021) 067, 2104.02546.

[247] S. Banerjee, S. Ghosh, and P. Paul, "(Chiral) Virasoro invariance of the tree-level MHV graviton scattering amplitudes," 2108.04262.

[248] S. Banerjee, H. Kulkarni, and P. Paul, "An infinite family of $w_{1+\infty}$ invariant theories on the celestial sphere," *JHEP* **05** (2023) 063, 2301.13225.

[249] T. Adamo, W. Bu, E. Casali, and A. Sharma, "All-order celestial OPE in the MHV sector," 2211.17124.

[250] E. Witten, "Perturbative gauge theory as a string theory in twistor space," *Commun. Math. Phys.* **252** (2004) 189–258, hep-th/0312171.

[251] R. Roiban, M. Spradlin, and A. Volovich, "On the tree level S matrix of Yang-Mills theory," *Phys. Rev. D* **70** (2004) 026009, hep-th/0403190.

[252] D. Skinner, "Twistor strings for $\mathcal{N} = 8$ supergravity," *JHEP* **04** (2020) 047, 1301.0868.

[253] L. Mason and D. Skinner, "Ambitwistor strings and the scattering equations," *JHEP* **07** (2014) 048, 1311.2564.

[254] Y. Geyer, A. E. Lipstein, and L. J. Mason, "Ambitwistor Strings in Four Dimensions," *Phys. Rev. Lett.* **113** (2014), no. 8 081602, 1404.6219.

[255] T. Adamo, W. Bu, E. Casali, and A. Sharma, "Celestial operator products from the worldsheet," *JHEP* **06** (2022) 052, 2111.02279.

[256] W. Bu, "Supersymmetric celestial OPEs and soft algebras from the ambitwistor string worldsheet," *Phys. Rev. D* **105** (2022), no. 12 126029, 2111.15584.

[257] T. McLoughlin, A. Puhm, and A.-M. Raclariu, "The SAGEX review on scattering amplitudes chapter 11: soft theorems and celestial amplitudes," *J. Phys. A* **55** (2022), no. 44 443012, 2203.13022.

[258] V. Del Duca, L. J. Dixon, and F. Maltoni, "New color decompositions for gauge amplitudes at tree and loop level," *Nucl. Phys. B* **571** (2000) 51–70, hep-ph/9910563.

[259] C. Boucher-Veronneau and A. J. Larkoski, "Constructing Amplitudes from Their Soft Limits," *JHEP* **09** (2011) 130, 1108.5385.

[260] C. Duhr, S. Hoeche, and F. Maltoni, "Color-dressed recursive relations for multi-parton amplitudes," *JHEP* **08** (2006) 062, hep-ph/0607057.

[261] F. Cachazo and A. Strominger, "Evidence for a New Soft Graviton Theorem," 1404.4091.

[262] R. Monteiro, "Celestial chiral algebras, colour-kinematics duality and integrability," *JHEP* **01** (2023) 092, 2208.11179.

[263] B. Bakalov and V. G. Kac, "Field algebras," *International Mathematics Research Notices* **2003** (2003), no. 3 123–159.

[264] A. Sharma, "Ambidextrous light transforms for celestial amplitudes," *JHEP* **01** (2022) 031, 2107.06250.

[265] W. Fan, A. Fotopoulos, S. Stieberger, T. R. Taylor, and B. Zhu, "Conformal blocks from celestial gluon amplitudes. Part II. Single-valued correlators," *JHEP* **11** (2021) 179, 2108.10337.

[266] Y. Hu, L. Lippstreu, M. Spradlin, A. Y. Srikant, and A. Volovich, "Four-point correlators of light-ray operators in CCFT," *JHEP* **07** (2022) 104, 2203.04255.

[267] S. Banerjee, R. Basu, and S. Atul Bhatkar, "Light transformed gluon correlators in CCFT," *JHEP* **01** (2023) 075, 2203.06657.

[268] S. De, Y. Hu, A. Yelleshpur Srikant, and A. Volovich, "Correlators of four light-ray operators in CCFT," *JHEP* **10** (2022) 170, 2206.08875.

[269] C.-M. Chang, W. Cui, W.-J. Ma, H. Shu, and H. Zou, "Shadow celestial amplitudes," *JHEP* **02** (2023) 017, 2210.04725.

[270] C. Jorge-Diaz, S. Pasterski, and A. Sharma, "Celestial amplitudes in an ambidextrous basis," *JHEP* **02** (2023) 155, 2212.00962.

[271] G. R. Brown, J. Gowdy, and B. Spence, "Celestial Twistor Amplitudes," 2212.01327.

[272] H. Luo, P. Mastrolia, and W. J. Torres Bobadilla, "Subleading soft behavior of QCD amplitudes," *Phys. Rev. D* **91** (2015), no. 6 065018, 1411.1669.

[273] F. Cachazo, P. Cha, and S. Mizera, "Extensions of Theories from Soft Limits," *JHEP* **06** (2016) 170, 1604.03893.

[274] N. Kalyanapuram, "Soft Gravity by Squaring Soft QED on the Celestial Sphere," *Phys. Rev. D* **103** (2021), no. 8 085016, 2011.11412.

[275] R. Bittleston, "On the associativity of 1-loop corrections to the celestial operator product in gravity," *JHEP* **01** (2023) 018, 2211.06417.

[276] T. Adamo, L. Mason, and A. Sharma, "MHV scattering of gluons and gravitons in chiral strong fields," *Phys. Rev. Lett.* **125** (2020), no. 4 041602, 2003.13501.

[277] R. Bittleston, S. Heuveline, and D. Skinner, "The Celestial Chiral Algebra of Self-Dual Gravity on Eguchi-Hanson Space," 2305.09451.

[278] K. J. Costello, "Bootstrapping two-loop QCD amplitudes," 2302.00770.

[279] A. Hodges, "A simple formula for gravitational MHV amplitudes," 1204.1930.

[280] A. Guevara, "Towards Gravity From a Color Symmetry," 2209.00696.